

**INVESTIGATION OF THIRD-ORDER
NONLINEAR OPTICAL AND ALL-OPTICAL
SWITCHING PROPERTIES OF SOME
METAL-ORGANIC MATERIALS**

Thesis

**Submitted in partial fulfillment of the requirements for the degree of
DOCTOR OF PHILOSOPHY**

by

MANJUNATHA K. B.



**DEPARTMENT OF PHYSICS
NATIONAL INSTITUTE OF TECHNOLOGY KARNATAKA
SURATHKAL, MANGALORE - 575 025
FEBRUARY, 2014**

**INVESTIGATION OF THIRD-ORDER
NONLINEAR OPTICAL AND ALL-OPTICAL
SWITCHING PROPERTIES OF SOME
METAL-ORGANIC MATERIALS**

Thesis

**Submitted in partial fulfillment of the requirements for the degree of
DOCTOR OF PHILOSOPHY**

by

MANJUNATHA K. B.



DEPARTMENT OF PHYSICS

NATIONAL INSTITUTE OF TECHNOLOGY KARNATAKA

SURATHKAL, MANGALORE - 575 025

FEBRUARY , 2014

DECLARATION

by the Ph.D. Research Scholar

I hereby *declare* that the Research Thesis entitled “**Investigation of third-order nonlinear optical and all-optical switching properties of some metal-organic materials**” which is being submitted to the *National Institute of Technology Karnataka, Surathkal* in partial fulfilment of the requirements for the award of the Degree of *Doctor of Philosophy* in Physics is a *bonafide report of the research work carried out by me*. The material contained in this Research Thesis has not been submitted to any University or Institution for the award of any degree.

Manjunatha K. B.

(Reg.No: 070512PH07F01)

Department of Physics

Place: NITK-Surathkal

Date:

CERTIFICATE

This is to *certify* that the Research Thesis entitled “**Investigation of third-order nonlinear optical and all-optical switching properties of some metal-organic materials**” submitted by Manjunatha K. B. (Register Number: 070512PH07F01) as the record of the research work carried out by him, is accepted *as the Research Thesis submission* in partial fulfilment of the requirements for the award of degree of **Doctor of Philosophy**.

Prof. G. Umesh
(Research Guide)

Date:

Chairman - DRPC

Date:

This thesis is dedicated

...to all my family members for their encouragement and support

...to my teachers for their moral guidance

...and to my good friends who supported me in all ways

during work

Acknowledgements

I would like to express my sincere gratitude to my supervisor, Prof. G. Umesh for his expert guidance and continuous support in completing this work successfully. It was a valuable experience to learn many aspects from him both as a teacher and a human being. I'm very grateful to him for his constant motivation, fruitful suggestions, kind support, guidance and continuous encouragement in all aspects that made my candidature a truly enriching experience at NITK.

I am very grateful and sincerely thank Department of Physics, NITK, Surathkal and also the institute by awarding the full time institute research scholarship.

I sincerely thank Dr. M. N. Satyanarayan, Department of Physics, NITK for his valuable suggestions and fruitful discussions.

I would like to thank Prof. N. K. Udayashankar, Head, Department of Physics and Chairman RPAC and Members of the RPAC, Prof. G. K. Shivakumar, Department of Physics and Prof. K. V. Gangadharan, Department of Mechanical Engineering, for spending their precious time to attend my seminars, providing valuable suggestions and having fruitful discussions.

I thank Prof. Kasturi V. Bangera, Prof. H.D. Shashikala, Dr. H.S. Nagaraja and Dr. Ajith K.M. Department of Physics, NITK, Surathkal for their wishes, moral support and allowing me to use their lab facilities.

My sincere thanks to Prof. B. Ramachandra Bhat, Department of Chemistry, NITK and his research students Dr. Dileep R., Dr. Rudresha B.J. and Dr. Ravindra R., for providing interesting metal-organic complexes in time and for their valuable suggestions, help and support throughout the work.

I would express my wholehearted thanks to my colleagues in the lab, Mr. Vikas M. Shelar, Mr. Hidayath Ulla, Ms. Shourie Ranjana and Ms. Jean Maria Fernandes for their support, fruitful discussions and immense help provided throughout the period of my research work.

My sincere thanks to Dr. Sujaya, Dr. Yogesh S., Dr. Nagaraja K.K., Mr. Venkateshwar Rao G. Mr. Santhosh S. and Mr. Shashidhara for their suggestions and help during my work.

I would like to express my sincere wholehearted thanks to Dr. Seetharam Shettigar, Professor and H.O.D, Department of Physics, NMAM Institute of Technology, Nitte and Dr. Poornesh, Department of Physics, Manipal Institute Technology, Manipal for their valuable suggestions, support and their unforgettable timely help.

I thank Department of Chemistry, NITK for allowing me to use their lab facilities.

My sincere thanks to Prof. U. Sripathi, Department of E & C, Dr. Puneekar G. S. and Mr. Jora M. Gonda, Department of E & E, NITK and Mr. Morrison, Laser Spectra Physics, Bangalore for their help and valuable suggestions for setting up the all-optical switching experiment.

My sincere thanks to Prof. M. S. Bhat, Department of E&C for his moral support.

I extend my sincere thanks to Mr. A. Aravinda Rao, Mr. M. Chandranath, Mr. Sheshappa Naik, Mrs. Mohini, Mrs. Ashalatha, Mrs. Sarita Shetty, Ms. Usha and Mr. Dhanaraj, Department of Physics, NITK, for their help.

I am thankful to Dr.K. Chandrasekharan, and his students Dr. Sudheesh P. and Mr. Siji Narendran, NITC, Calicut for DFWM measurements and his valuable discussions.

I would thank Prof. V. P. N. Nampoori, Cochin University of Science and Technology (CUSAT), Kerala and Dr. Reji Philip, Raman Research Institute (RRI), Bangalore for their valuable suggestions.

I would like to convey my thanks to Mr. Piyush Bhatt, Indian Institute of Technology Bombay (IITB), Mumbai for his help.

I thank Mr. Chandracharya, Department of Mechanical Engineering and Mr. Sathish, Department of Metallurgical and Materials Engineering for their timely help.

My heartfelt thanks to Dr. Harish C. Barshilia, Scientist G and Joint-head, SED, National Aerospace Laboratories (CSIR) for his help and suggestions.

The inspiration and support given by the other fellow Research Scholars of the Department of Physics, Department of Chemistry and other Departments have also been much appreciated.

Special thanks to all my best friends for their motivation and continuous encouragement.

Most importantly, I feel a deep sense of gratitude to my father Balakrishna, my mother Shamala, my uncle Arun, my brothers Kiran, Kishore, Keerthan and Kishan and my sister Bhagyalakshmi for their continuous support, advice and encouragement since from childhood to till now. My heartfelt special thanks to my wife, Arya and family members Bangaramma, Jayanthi, Sridevi, Sumitra, Sindupriya, Kavyashree, Puneeth, Ganyashree, Hishikesh and all my cousins for their encouragement and inspiration, and also the affection shown to me.

I remain thankful to all those who helped me directly/indirectly in carrying out this work.

I remain thankful to all those who helped me directly/indirectly in carrying out this work. Finally, I salute and thank the Almighty for always being with us giving us the required strength, energy, patience, knowledge and resources leading to the success of this research work.

MANJUNATHA K. B.

ABSTRACT

Nonlinear optical (NLO) materials and their structural engineering have gained growing importance in the field of nonlinear optics due to their large diverse applications in optoelectronics and photonics. In our efforts to identify the structure dependent NLO properties, we have investigated three different classes of organometallic complexes, viz. (i) palladium complexes with Schiff base ligand containing triphenylphosphine, (ii) ruthenium complexes with 1,3-dithiole-2-thione-4,5-dithiolate (dmit) and triphenylarsine/ triphenylphosphine ligands and (iii) ruthenium complexes of salen/salophene ligands. The solutions of these complexes were prepared by dissolving them into dimethylformamide (DMF) solvent. Solid films were formed by first dispersing the complexes in Polymethylmethacrylate (PMMA) solution and then spin-coating them on glass substrates. For linear optical characterization, UV-Vis absorption spectra and linear refractive indexes were determined for both solution and film form. Third-order nonlinear optical properties of the complexes were determined using Z-scan and Degenerate four wave mixing (DFWM) techniques with laser pulses of 7 ns at the wavelength of 532 nm. Using energy dependent transmission technique, optical power limiting performance of the complexes were studied. Further, all-optical switching behavior of the complexes were investigated using two color pump-probe technique. All complexes exhibit negative nonlinear refractive index (self-defocusing) and nonlinear absorption due to reverse saturable absorption (RSA) which is explained using five-level model. All the complexes investigated by us have shown good optical power limiting as well as all-optical switching behavior. This thesis provides an insight on the role of electron acceptor and electron donor substituent and the effect of π -conjugation and electron delocalization on third-order nonlinear optical properties of the metal-organic complexes. Further, the suitability of such materials for devices such as optical power limiters and all-optical switches is also discussed.

Keywords: Third-order nonlinear optical susceptibility, Z-scan, Optical power limiting, All-optical switching, DFWM, pump-probe technique.

CONTENTS

CHAPTER 1		Page No.
Introduction		
1.1	Nonlinear optics.....	1
1.2	Theoretical principles of nonlinear optics.....	2
1.3	Theoretical framework for nonlinear light-matter interactions.....	5
1.4	Third-order nonlinear optical processes.....	6
1.4.1	Nonlinear refractive index.....	6
1.4.2	Nonlinear absorption.....	7
1.4.3	Two-photon absorption.....	8
1.4.4	Excited state absorption.....	9
1.4.5	Third-harmonic generation.....	10
1.4.6	Electric-field induced second-harmonic generation.....	10
1.4.7	Four-wave mixing.....	10
1.5	Molecular mechanisms of the third-order nonlinear response.....	10
1.5.1	Electronic polarization.....	10
1.5.2	Raman induced kerr effect.....	11
1.5.3	Molecular orientational effects.....	11
1.5.4	Electrostriction.....	11
1.5.5	Population redistribution.....	11
1.5.6	Thermal contributions.....	12
1.6	Summary of the literature review.....	12

1.7	Scope and objectives of this thesis work.....	22
CHAPTER 2		
Experimental details		
2.1	Z-scan technique.....	27
2.1.1	Introduction.....	27
2.1.2	Principle of Z-scan technique.....	28
	(a) Nonlinear refraction.....	28
	(b) Nonlinear absorption.....	29
2.1.3	Advantages and disadvantages of the Z-scan technique.	31
	(a) Advantages of the Z-scan technique.....	31
	(b) Disadvantages of the Z-scan Technique.....	32
2.1.4	Theoretical background of Z-scan technique.....	32
2.1.5	Z-Scan experimental setup and measurement.....	38
	(a) Laser used in the experiments.....	39
	(b) Energy meter used in the experiments	40
	(c) Detector used in the experiments	40
2.2	Degenerate four wave mixing technique (DFWM).....	41
2.2.1	Introduction to DFWM technique.....	41
2.2.2	Advantages of the DFWM technique.....	43
2.2.3	Disadvantages of the DFWM technique.....	43
2.2.4	Theoretical description of DFWM.....	43
2.2.5	Measuring $\chi^{(3)}$	47

2.2.6	DFWM experimental setup and measurement.....	48
2.3	Optical power limiting: energy dependent transmission.....	50
2.3.1	Introduction.....	50
2.3.2	Experimental setup.....	52
2.4	All-optical switching: pump-probe technique.....	52
2.4.1	Introduction.....	52
2.4.2	Experimental setup.....	54
2.5	Sample preparation.....	56
2.6	Linear optical characterization.....	57
2.6.1	UV-Vis Absorption Spectroscopy.....	57
2.6.2	Refractive index measurement.....	58
2.6.3	Thickness Measurement.....	58

CHAPTER 3

Third-order nonlinear optical studies of Schiff base containing palladium metal-organic complexes

3.1	Introduction.....	59
3.2	Synthesis and characterization of Pd complexes.....	61
3.2.1	Materials and methods.....	61
3.2.2	Synthesis of ligand L1-L4.....	62
3.2.3	Synthesis of PdCl ₂ (PPh ₃) ₂	63
3.2.4	Synthesis of Pd Complexes.....	63
3.3	Molecular structures and UV-visible spectra of palladium complexes.....	66
3.4	Z-scan studies of palladium complexes.....	70
3.4.1	Nonlinear absorption studies.....	70

3.4.2	Nonlinear refraction studies.....	74
3.5	Degenerate four wave mixing studies.....	97
3.5.1	Calibration.....	97
3.5.2	DFWM results.....	98
3.6	Structure-property relationship with third-order nonlinear optical parameters in palladium metal-organic complexes.....	101
3.7	Optical power limiting studies.....	102
3.8	Concentration dependence of third order nonlinearity.....	110
3.9	All-optical switching studies of palladium complexes.....	111
3.10	Conclusions.....	113

CHAPTER 4

Third-order nonlinear optical studies of ruthenium metal-organic complexes containing dmit ligand

4.1	Introduction.....	115
4.2	Synthesis and characterization of ruthenium complexes based dmit ligand.....	116
4.2.1	Materials and methods.....	116
4.2.2	Synthesis of $[\text{RuCl}(\text{C}_3\text{S}_5)(\text{H}_2\text{O})(\text{AsPh}_3)_2]$	117
4.2.3	Synthesis of $[\text{RuCl}(\text{C}_3\text{S}_5)(\text{H}_2\text{O})(\text{PPh}_3)_2]$	117
4.3	Molecular structures and UV-visible spectra of ruthenium complexes containing dmit ligand.....	118
4.4	Z-scan studies of ruthenium complexes containing dmit ligands...	121
4.5	Degenerate four wave mixing studies.....	133
4.6	Structure-property relationship with third-order nonlinear optical parameters in ruthenium metal-organic complexes.....	135
4.7	Optical power limiting studies.....	136
4.8	Concentration dependence of third order nonlinearity.....	140

4.9	All-optical switching studies of ruthenium complexes.....	142
4.10	Conclusions.....	145

CHAPTER 5

Third-order nonlinear optical studies of ruthenium complexes containing salen and salophene

5.1	Introduction.....	146
5.2	Synthesis and characterization of ruthenium complexes containing salen and salophene.....	147
5.2.1	Materials and methods.....	147
5.2.2	Synthesis of ligand.....	148
5.2.3	General procedure for synthesis of complexes	148
	(a) [Ru (salen) (H ₂ O) (Cl)].....	149
	(b) [Ru (salophene) (H ₂ O) (Cl)].....	149
5.3	Molecular structures and UV-visible spectra of ruthenium complexes containing salen and salophene ligand.....	149
5.4	Z-scan studies of ruthenium complexes containing salen and salophene ligands.....	152
5.5	DFWM studies of ruthenium complexes containing salen and salophene ligands.....	165
5.6	Structure-property relationship with third-order nonlinear optical parameters in ruthenium metal-organic complexes with salen and salophene.....	166
5.7	Optical power limiting studies.....	168
5.8	Concentration dependence of third-order nonlinearity	172
5.9	All-optical switching studies of ruthenium complexes.....	173
5.10	Conclusions.....	176

CHAPTER 6

Summary and conclusions

6.1	Summary and conclusions	177
6.1.1	Palladium metal-organic complexes	177

6.1.2 Ruthenium metal-organic complexes	178
6.2 Scope for future work	179
References.....	181
List of publications.....	212
Curriculum vitae	214

List of Abbreviations

μs	microsecond
3PA	Three-Photon Absorption
A-D-A	Acceptor Donor Acceptor
D-A	Donor Acceptor
D-A-D	Donor Acceptor Donor
D-D	Donor Donor
DFWM	Degenerate Four Wave Mixing
EFISH	Electric Field Induced Second Harmonic
EM	Electromagnet
ESA	Excited State Absorption
fs	femtosecond
FT-IR	Fourier Transform Infrared
FWM	Four Wave Mixing
ILCT	Intra Ligand Charge Transfer
ISC	Inter System Crossing
LIG	Laser Induced Grating
LMCT	Ligand Metal Charge Transfer
MLCT	Metal Ligand Charge Transfer
ms	millisecond
NLA	Nonlinear Absorption
NLO	Nonlinear Optics
NLR	Nonlinear Refraction

NMR	Nuclear Magnetic Resonance
ns	nanosecond
OPL	Optical Power Limiting
PC	Phase Conjugate
ps	picosecond
RSA	Reverse Saturable Absorption
SA	Saturable Absorption
SEM	Scanning Electron Microscopy
SHG	Second Harmonic Generation
TGA	Thermogravimetric Analysis
THG	Third Harmonic Generation
TPA	Two-Photon Absorption
UV-Vis	Ultraviolet Visible

Nomenclature

f	Frequency
k	wave vector
n_0	Linear refractive index
n_2	Nonlinear refractive index
$T(z)$	Sample transmittance when at position z
w_0	Beam waist radius at the focal spot
z_0	Rayleigh length
α_0	Linear absorption coefficient
β	Nonlinear absorption coefficient
γ	Nonlinear refractive index (in m^2/W)
γ_h	Second-order hyperpolarizability
Δn	Change in index of refraction
ΔT_{p-v}	Change in normalized transmittance between peak and valley, $ T_p - T_v $
ΔZ_{p-v}	Distance between the Z positions of the peak and valley
λ	Wavelength
σ_{exc}	Excited-state absorption cross section
σ_g	Ground-state absorption cross section
$\chi^{(2)}$	Second order nonlinear optical susceptibility
$\chi^{(3)}$	Third order nonlinear optical susceptibility
ω	Angular frequency

CHAPTER 1

CHAPTER 1

INTRODUCTION

1.1 NONLINEAR OPTICS

Photonics has emerged as a “Path Breaking Technology” for the 21st century on account of intense research efforts put in by the global optics community over the past five decades. In photonics, photons are employed to acquire, store, process and transmit information, just as electrons are in electronics. Photonics has several advantages over electronics since a photon travels much faster than an electron in any material medium and a light beam can carry data at much higher rates than a stream of electrons. Further, photons that are propagating in any medium, are generally not affected by any stray external electric or magnetic fields existing in the surroundings.

Nonlinear optics (NLO) is a branch of photonics dealing with the interaction of strong electromagnetic fields with material media. It also deals with the propagation of light in nonlinear media, i.e., media in which the dielectric polarization \mathbf{P} depends nonlinearly on the electric field \mathbf{E} of the incident light. Excitation of nonlinear-optical responses in materials generally requires use of high intensity radiation such as that produced by lasers. The interactions of applied electromagnetic fields with various materials may result in the generation of new electromagnetic fields differing in phase, frequency, amplitude and polarization.

The first experiment on nonlinear optics was the observation of second harmonic generation (SHG) by Franken (1961), shortly after the invention of the first laser in 1960 by Theodore H. Maiman. In this experiment, when a coherent, high intensity ruby laser light, having a wavelength of 694 nm, was passed through a piece of crystalline quartz, the laser was partly converted to light at twice the frequency (or half the wavelength, i.e., 347nm) of the incident radiation. The first theoretical

analyses of nonlinear optical phenomena were carried out by Bloembergen (1964) and by Akhmanov and Khokhlov (1972).

The field of NLO has emerged as a major field of research over the past five decades not only because of its applications to photonic devices, but also because of the insufficient understanding of the fundamental nature of light-matter interaction and its dependence on material properties such as molecular structure, nature of charge-transfer and dielectric polarization. The search for new materials capable of exhibiting large NLO responses is a major activity in the field of nonlinear optics. The understanding of various molecular parameters that influence the NLO properties of the molecules helps us identify novel materials for these applications. A variety of systems including organic materials, polymers, organometallics, inorganic materials, semiconductors, nanomaterials, etc., have been investigated for device applications (He et al. 2008, Bass et al. 2001, Nalwa and Miyata 1997). Amongst these, organic materials have received much attention because of their structural flexibility, easy synthesis, large nonlinearity, fast response, etc. Among various methods to enhance the third-order nonlinearity of organic materials, incorporation of metals into organic molecules adds a new dimension and provides many new options.

1.2 THEORETICAL PRINCIPLES OF NONLINEAR OPTICS

Nonlinear optics is a branch of optics that deals with the response of various material media to strong optical fields applied on the medium. NLO effects have a strong influence on the propagation characteristics of light through any medium. The applied electromagnetic radiation interacts with the dipoles of the media, setting the dipoles into oscillations. Such oscillating dipoles constitute new sources of electromagnetic radiation, differing from the incident fields in phase, frequency, amplitude or propagation characteristics.

When laser light interacts with a material medium, it induces dielectric polarization in the medium. In terms of the molecular dipole moment μ_i , the bulk polarization P given by

$$\mu_i = -er \tag{1.1}$$

$$P = -Ner \quad (1.2)$$

where e is the electron charge, r is the displacement of the electron with respect to ion core and N is the electron density (Prasad and Williams 1992).

For weak applied electromagnetic fields, the induced polarization \overline{P} is linearly proportional to the electric field \overline{E} of the wave and is given by

$$\overline{P} = \varepsilon_0 \chi^{(1)} \overline{E} = \overline{P}_L \quad (1.3)$$

where ε_0 is the permittivity of free space and $\chi^{(1)}$ is the linear susceptibility of the material and is a second-rank tensor responsible for linear optical properties of materials like refraction, dispersion, birefringence and absorption. The linear susceptibility is related to the dielectric constant ε_r , as

$$\varepsilon_r = (1 + \chi^{(1)}) \quad (1.4)$$

The dielectric constant $\varepsilon_r(\omega)$ is related to the linear refractive index, $n(\omega)$, of the material by the relation,

$$n^2(\omega) = \varepsilon_r(\omega) = 1 + \chi^{(1)}(\omega) \quad (1.5)$$

Refractive index is in general a complex quantity and may be formally expressed as

$$n = N + iK \quad (1.6)$$

where N is the real part of the refractive index which accounts for the refraction and K is the imaginary part of the refractive index which takes care of the absorption of light in the dielectric medium (Prasad and Williams 1992).

However, when laser beams are transmitted through any material medium, the wave electric field can be quite high and the induced polarization then acquires a nonlinear dependence on the applied field. In general, the polarization of the material medium, through which a laser beam is propagated, is given by,

$$\overline{P} = \varepsilon_0 (\chi^{(1)} \overline{E} + \chi^{(2)} \overline{E}\overline{E} + \chi^{(3)} \overline{E}\overline{E}\overline{E} + \dots) \quad (1.7)$$

We may formally separate out the linear and nonlinear term as follows

$$\overline{P} = \overline{P}_L + \overline{P}_{NL} \quad (1.8)$$

where,

$$\overline{P}_{NL} = \varepsilon_0 (\chi^{(2)} \overline{E}\overline{E} + \chi^{(3)} \overline{E}\overline{E}\overline{E} + \dots) \quad (1.9)$$

where $\chi^{(2)}$ is the second-order nonlinear susceptibility, present only in non centrosymmetric materials, i.e. materials that lack inversion symmetry; it is also zero in isotropic media. $\chi^{(2)}$ is a third-rank tensor which gives rise to second harmonic generation (SHG), sum and difference frequency generation, optical rectification and electro-optic effect. $\chi^{(3)}$ is the third-order nonlinear susceptibility, which has no symmetry restrictions, and is a fourth-rank tensor. It is responsible for third harmonic generation, stimulated Raman scattering, phase conjugation, nonlinear refractive index, nonlinear absorption and optical bi-stability. The magnitude of $\chi^{(2)}$ and $\chi^{(3)}$ respectively, describe the strength of the second order and third-order processes and in all cases $\chi^{(1)} \gg \chi^{(2)} \gg \chi^{(3)}$ (Prasad and Williams 1992 and Sutherland 2003).

In the simplest case, the electric field of the laser beam propagating in a material medium, may be expressed as (plane wave)

$$E = E_0 \cos(\omega t - kz) \quad (1.10)$$

where E_0 is the amplitude, wave vector $k = 2\pi/\lambda$ (λ is the wavelength) and ω is the frequency of the incident optical wave.

Again, for the sake of simplicity, we may ignore the tensor character of the susceptibility. Hence, substituting equation (1.10) into (1.7) and using trigonometric relations one can transform equation (1.7) to the form

$$P = \frac{1}{2} \varepsilon_0 \chi^{(2)} E_0^2 + \varepsilon_0 \left(\chi^{(1)} + \frac{3}{4} \chi^{(3)} E_0^2 \right) E_0 \cos(\omega t - kz) + \frac{1}{2} \varepsilon_0 \chi^{(2)} E_0^2 \cos(2\omega t - 2kz) + \frac{1}{4} \varepsilon_0 \chi^{(3)} E_0^3 \cos(3\omega t - 3kz) + \dots \quad (1.11)$$

As can be seen, the polarization contains not only components that oscillate at the wave frequency ω , but also new terms oscillating at harmonic frequencies 2ω , 3ω , etc. as well as a dc term, which gives rise to optical rectification. In particular, the polarization components oscillating at frequencies ω , 2ω and 3ω , respectively, may be expressed as

$$P(\omega) = \varepsilon_0 \left[\chi^{(1)} + \frac{3}{4} \chi^{(3)} E_0^2 \right] E_0 \cos(\omega t - kz) \quad (1.12a)$$

$$P(2\omega) = \varepsilon_0 \frac{1}{2} \chi^{(2)} E_0^2 \cos(2\omega t - 2kz) \quad (1.12b)$$

$$P(3\omega) = \varepsilon_0 \frac{1}{4} \chi^{(3)} E_0^3 \cos(3\omega t - 3kz) \quad (1.12c)$$

The first term in $P(\omega)$ is related to the linear refractive index and the second term leads to an intensity-dependent refractive index $n(I)$. The term $P(2\omega)$ gives rise to many important effects such as frequency doubling or second-harmonic generation (SHG), and sum- and difference-frequency generation. The term $P(3\omega)$ accounts for phenomena such as third-harmonic generation (THG).

1.3 THEORETICAL FRAMEWORK FOR NONLINEAR LIGHT-MATTER INTERACTIONS

All electromagnetic phenomena are described by Maxwell's equations, which may be written as

$$\begin{aligned} \nabla \cdot \vec{D} &= \bar{\rho} \\ \nabla \cdot \vec{B} &= 0 \\ \nabla \times \vec{E} &= -\frac{\partial \vec{B}}{\partial t} \\ \nabla \times \vec{H} &= \frac{\partial \vec{D}}{\partial t} + \vec{J} \end{aligned} \quad (1.13)$$

For optical field propagation in a dielectric media, we may assume

$$\rho = 0 \quad (1.14)$$

and

$$\vec{J} = 0 \quad (1.15)$$

Furthermore, we also assume that the material is nonmagnetic, so that

$$\vec{B} = \mu_0 \vec{H} \quad (1.16)$$

The field quantities \vec{D} and \vec{E} are related by,

$$\vec{D} = \epsilon_0 \vec{E} + \vec{P} \quad (1.17)$$

The propagation of an electromagnetic (EM) wave is governed by the wave equation, obtained from the Maxwell's equation, and is given by

$$\nabla \times \nabla \times \vec{E} + \frac{1}{c^2} \frac{\partial^2}{\partial t^2} \vec{E} = -\frac{1}{\epsilon_0 c^2} \frac{\partial^2 \vec{P}}{\partial t^2} \quad (1.18)$$

where the polarization $\vec{P} = \vec{P}_L + \vec{P}_{NL}$. Formally, the displacement vector D may be expressed as

$$D = D^{(1)} + P^{NL} \quad (1.19)$$

The nonlinear polarization, appearing on right side of the equation plays the role of a driving source, inducing electromagnetic waves at various new frequencies.

1.4 THIRD-ORDER NONLINEAR OPTICAL PROCESSES

The dominant nonlinear effect in all centro-symmetric materials is the third order optical nonlinearity. In all such materials, the nonlinear absorption coefficient (β) and nonlinear refractive index (n_2) are related to the imaginary and real parts of third-order nonlinear susceptibility ($\chi^{(3)}$). The third order nonlinear susceptibility is generally a complex quantity and is written as,

$$\chi^{(3)} = \chi_R^{(3)} + i\chi_I^{(3)} \quad (1.20)$$

where the imaginary part is related to NLA coefficient β through,

$$\chi_I^{(3)} = \frac{n_o^2 \epsilon_o c^2}{\omega} \beta \quad (1.21)$$

and the real part is related to n_2 through,

$$\chi_R^{(3)} = 2n_o^2 \epsilon_o c n_2 \quad (1.22)$$

The different mechanisms originating from this type of nonlinearity, among them, we have the following:

1.4.1 Nonlinear Refractive Index

The intensity dependent nonlinear refractive index can be expressed as,

$$n = n_0 + n_2 I \quad (1.23)$$

where n_0 is the linear refractive index, n_2 is the nonlinear refractive index and I is the intensity of the propagating laser beam.

The change in the refractive index induces an intensity dependent phase change given by

$$\Delta\phi_0 = \frac{2\pi}{\lambda} n_2 I L \quad (1.24)$$

where L is the length of nonlinear material and λ is the wavelength of the incident light. This intensity dependent phase change can change the geometrical properties of light propagation, leading to phenomena such as self-focusing (positive n_2) and self-defocusing (negative n_2).

The nonlinear refractive index (n_2) can be related to real part of $\chi^{(3)}(-\omega; \omega, \omega, -\omega)$ and written as (Hales and Perry 2008),

$$n_2 = \frac{3}{4\varepsilon_0 n_0(\omega)^2 c} \text{Re}[\chi^{(3)}(-\omega; \omega, \omega, -\omega)] \quad (1.25)$$

where $n_0(\omega)$ is linear refractive index at frequency ω , ε_0 is the free space permittivity and c is the speed of light in vacuum.

1.4.2 Nonlinear Absorption

The Beer-Lambert's law describes linear absorption of light in a material medium and is given by

$$I(z) = I_0 e^{-\alpha_0(\omega)z} \quad (1.26)$$

where I_0 is the incident intensity, $\alpha_0(\omega)$ is the linear absorption coefficient, z is the propagation distance in the absorbing medium and $I(z)$ is the intensity at distance z . The differential form of Beer-Lambert's law describes how light intensity decreases with propagation distance in a medium when α_0 is constant,

$$\frac{\partial I}{\partial z} = -\alpha_0(\omega) I \quad (1.27)$$

In the case of nonlinear absorption, higher order intensity terms have to be included. The above differential equation then gets modified to

$$\frac{\partial I}{\partial z} = -\alpha_0(\omega)I - \beta(\omega)I^2 - \gamma(\omega)I^3 \quad (1.28)$$

where $\beta(\omega)$ is the two-photon absorption (TPA) coefficient, $\gamma(\omega)$ is the three-photon absorption (3PA) coefficient; the higher order absorption terms are neglected for the present investigations.

For materials possessing negligible linear absorption, the dominating term is TPA and other terms can be ignored and the above equation reduces to

$$\frac{\partial I}{\partial z} = -\beta(\omega)I^2 \quad (1.29)$$

The above equation is solved by separation of variables which yields

$$I(z) = \frac{I_0}{1 + \beta I_0 z} \quad (1.30)$$

where I_0 is the incident intensity, β is the two-photon absorption coefficient and z is the distance that light has travelled in the sample.

1.4.3 Two-Photon Absorption

The two-photon absorption is a basic radiation-matter interaction mechanism. The TPA coefficient β is a macroscopic parameter characterizing the material. TPA is the process in which simultaneous absorption of two photons causes electronic transition from ground state to an excited state of the molecule. The theory of TPA was first developed by Goeppert-Mayer in 1931 and was experimentally observed for the first time by Kaiser and Garret in 1961.

The intensity of the beam as it propagates through the medium is given by (Sutherland 2003),

$$\frac{\partial I}{\partial Z} = -\alpha_0 I + \beta I^2 \quad (1.31)$$

and the solution of this equation may be expressed as

$$T = \frac{I(L)}{I_0} = \frac{T_0}{1 + I_0 \beta(I) L_{eff}} \quad (1.32)$$

where $T_0 = \exp(-\alpha_0 L)$ is the linear transmission, L is the physical length of the sample and $L_{eff} = (1 - \exp(-\alpha_0 L))/\alpha_0$ is the effective sample length. Here, α_0 is the linear absorption coefficient and β is the two-photon absorption coefficient.

The TPA coefficient can be related to the imaginary part of third-order nonlinear optical susceptibility and is given by (Hales and Perry 2008),

$$\beta = \frac{3\omega}{2\varepsilon_0 n_0(\omega)^2 c^2} \text{Im}[\chi^{(3)}(-\omega; \omega, -\omega, \omega)] \quad (1.33)$$

where β (m/W) is the nonlinear absorption coefficient. Further, a total absorption coefficient can be defined, in terms of α_0 and β , as

$$\alpha(I) = \alpha_0 + \beta(I) \quad (1.34)$$

where α_0 is the linear absorption coefficient and I is the laser intensity.

1.4.4 Excited State Absorption (ESA)

When the input light intensity is strong and its pulse width is a few nanosecond, the excited states are generally strongly populated and the lifetime of the excited state is of the order of a nanosecond. These conditions induce the excited molecule to be excited to the even higher lying state with absorption of another photon from the incident light before it completely gets relaxed to the ground state. There are two ESA phenomenon that can occur. If excited state absorption cross section is smaller than the ground state absorption cross section, then the total absorption decreases as the population in excited state rises. This is known as saturable absorption (SA). In the other situation, when the excited state absorption cross section is larger than the ground state absorption cross section, it leads to increased absorption as the system is excited. This is known as Reverse saturable absorption (RSA). RSA was first observed by Giuliano and Hess (Giuliano and Hess 1967, Sutherland 2003 and Sutherland et al. 2005).

1.4.5 Third-Harmonic Generation through $\chi^{(3)}(-3\omega; \omega, \omega, \omega)$

Third-Harmonic Generation (THG) is one the basic nonlinear optical processes. THG is the process wherein three photons of the same frequency ω interact with the nonlinear medium and, hence, combine to create a new photon at a frequency 3ω . This leads to generation of a laser beam at third-harmonic of the fundamental wave.

1.4.6 Electric-field Induced Second-Harmonic Generation (EFISH) through $\chi^{(3)}(-2\omega; 0, \omega, \omega)$

In this phenomenon a static electric field is applied to the material medium and simultaneously, the laser beam interacts with the nonlinear material medium, resulting in the generation of second harmonic light even in the materials having inversion symmetry.

1.4.7 Four-Wave Mixing (FWM) Through $\chi^{(3)}(\omega_4; \omega_1, \omega_2, \omega_3)$:

In general four-wave mixing in a nonlinear medium is a third-order nonlinear optical process. The interaction of three laser beams with frequencies ω_1 , ω_2 , and ω_3 generates a fourth wave with a frequency $\omega_{FWM} = \omega_1 \pm \omega_2 \pm \omega_3$ via third-order nonlinear susceptibility $\chi^{(3)}$. If an FWM process involves wave fields of same frequency, then it is referred to as degenerate four-wave mixing (DFWM).

1.5 MOLECULAR MECHANISMS FOR THIRD-ORDER NONLINEARITY

1.5.1 Electronic Polarization

This mechanism refers to distortion of the electron cloud around the atom or molecule by the application of laser light. The observed nonlinearity is related to the microscopic second-order hyperpolarizability γ . The third-order nonlinear optical susceptibility $\chi^{(3)}$ and time response of the process in non-resonant condition is $\sim 10^{-14}$ esu and $\sim 10^{-15}$ s, respectively. This is the fastest non-resonant electronic process in molecules (Sutherland 2003).

1.5.2 Raman Induced Kerr Effect

This effect is related to the Stimulated Raman scattering process. The change in the refractive index occurs due to the interaction of a strong pump beam with the Raman active medium, resulting in the creation of a weak beam. The Raman susceptibility has a typical value of $|\text{Re}(\chi^{(3)})| \sim 10^{-14}$ esu, and the response time $\sim 10^{-15}$ s (Sutherland 2003).

1.5.3 Molecular Orientational Effects

Anisotropic molecules show optically isotropic behavior in the bulk when they are disordered and randomly oriented, as for instance, in solutions or liquid crystals above the transition temperature. On the application of strong electric field, the induced dipole moment of the molecules experiences a torque that tends to align the molecule in the direction of the applied field. The change in the refractive index is induced by the reorientation of the molecular dipoles. Typical nonlinearity associated with small anisotropic molecular systems is $\chi^{(3)} \sim 10^{-14}$ esu and the response time is $\sim 10^{-12}$ s. Liquid crystals in their isotropic phase exhibit larger nonlinearities, $\chi^{(3)} \sim 10^{-12}$ esu, with slow time responses $\sim 10^{-3} - 10^{-2}$ s (Shen 1984).

1.5.4 Electrostriction

Electrostriction is an effect that requires the presence of inhomogeneities in the intensity profile of the laser beam. Such an inhomogeneous field produces a force on the collection of molecules or atoms and is called the electrostrictive force. The typical value for susceptibility in this case is $\chi^{(3)} \sim 10^{-14}$ esu, and the response time $\sim 10^{-15}$ s (Sutherland 2003).

1.5.5 Population Redistribution

This effect occurs when the frequency of the incident beam is close to a transition resonance of the atom or molecule responsible for the nonlinear behavior. Near resonance the electrons occupy an excited state for a finite period of time. Since the optical polarization is determined by the total number of atoms or molecules in the ground electronic state (for low intensity light), this population redistribution results in a change of the index of refraction. This effect can be seen in atomic vapors,

molecular gases, organic molecules and semiconductors. The typical value for population redistribution susceptibility is $\chi^{(3)} \sim 10^{-8}$ esu, and the response time is $\sim 10^{-8}$ s (Sutherland 2003, Butcher and Cotter 1990 and Villaverde 1980).

1.5.6 Thermal Contributions

Change in the temperature of the material causes the changes in the refractive index. This phenomenon is called thermo-optic effect. In most of the materials the density changes with temperature. As the temperature increases the density of the material decreases. Refractive index is proportional to the molecular density and hence any change in the density reflects as a change in refractive index. The typical value for susceptibility is $\chi^{(3)} \sim 10^{-4}$ esu, and the response time is $\sim 10^{-3}$ s (Sutherland 2003).

1.6 SUMMARY OF THE LITERATURE REVIEW

The Nonlinear optical properties of the materials may be exploited to control and manipulate light for applications in the fields of optoelectronics, photonics, health monitoring, sensor networks, etc. Over the past three decades intensive efforts have been made to develop devices based on various nonlinear optical phenomena. Further progress in these areas requires synthesis of new materials possessing novel nonlinear optical characteristics. The research efforts focused on developing new materials has led to the new field of “Engineered Materials” wherein materials possessing specific nonlinear optical properties are being invented.

From the viewpoint of device applications, it has been a challenge to create a material with all the desired optical properties along with ease of synthesis on a large scale, compatibility for integration with other electronic devices on a chip scale and long device life-times after fabrication. Molecular engineering techniques are being used to synthesize and explore new materials possessing better performance characteristics for future photonics device applications.

All materials exhibit NLO phenomena. The mechanisms for optical nonlinearity are different in organic materials as compared to inorganic materials. In early 1970s NLO effects were observed in a variety of inorganic materials like quartz

crystal, potassium dihydrogen phosphate (KDP), lithium niobate (LiNbO_3), potassium titanyl phosphate (KTP), barium borate (BBO) and some semiconductor materials such as cadmium sulfide, gallium arsenide (Hutchings and Van Stryland 1992, Eimerl 1987 and Van Stryland et al. 1985), doped glasses, nanoparticles, carbon nanotubes, ferro fluids, liquid crystals, etc. (He et al. 2008, Bass et al. 2001, Nalwa and Miyata 1997, Chemla and Zyss 1987). Apart from these, large classes of organic and polymeric molecules have been studied because of their large NLO response over a broad wavelength range, fast response, ease of processing and integration into devices. Their conjugated molecular structure leads to large nonlinearity, design flexibility, low dielectric constants and high optical damage thresholds (Whittall et al. 1999). The disadvantages of organic materials are narrower optical transmittance and considerably smaller device life time compared to inorganics, which makes them less attractive for device applications. Among various methods to enhance the third-order nonlinearity, optical transmittance and stability of organic materials, incorporation of metals into organic molecules has turned out to be very attractive, thus creating new options for improving device characteristics. Organometallics have the advantage of a wide choice of organic materials as well as metals, thereby providing scope for creating materials having greater robustness and thermal stability. Organometallic and coordination compounds facilitate alteration of oxidation state, spin state and NLO properties of organics leading to good transmittance and temporal and thermal stability (Hiroyuki 2002). The central metal atom of organometallic and coordination complexes can readily coordinate with conjugated ligands and undergo metal-ligand orbital overlap, thereby facilitating effective electronic transitions between metal-ion and ligand. This leads to large changes in the electric dipole moment of the molecules (Nalwa 1991 and Whittall et al. 1999) and hence, also to large optical nonlinearity.

Insertion of metal atoms into conjugated ligands may significantly influence the π -electron behavior and the energy of the excited states due to low-lying $d-d$ transitions occurring in these systems (Nalwa 1991, Whittall et al. 1999, Whittall et al. 1998, Cifuentes and Humphrey 2004 and Vlcek 2000). The most common types of organometallics and coordination complexes are polysilanes, metal polyynes,

metallocenes, metal dithiolenes, MPP complexes, metal carbonyl complexes, and MPc complexes.

In the recent years, organometallic and coordination complexes possessing optimal characteristics have been explored for use in novel photonic devices. In view of the exciting promise of organics for novel optical devices we chose to investigate the third-order nonlinear optical properties of organometallics and coordination complexes with a view to use them for optical power limiting and all-optical switching devices. The correlation of molecular structure with the third-order nonlinear optical property of various organometallic and coordination compounds has attracted considerable interest in recent years (Green et al. 2011, Schwich et al. 2011, Samoc et al. 2012) due to their rich redox properties, efficient charge-transfer characteristics, and versatile molecular configurations. The metal atom may be placed at the center of the charge-transfer system, enabling the d electrons of the transition metal atom to take part in the conjugation of the organic ligand.

Ever since the NLO effect in organometallics was observed in ferrocenyl derivatives by Green et al. (1987), the interest in organometallics and coordination complexes has grown tremendously. The values of third order susceptibility $\chi^{(3)}$ and second hyperpolarizability (γ_h) of ferrocene in ethanol solution, using self-focusing of nano-second laser pulses at 1064nm wavelength, were determined by Winter et al. 1988. Later Perry et al. (1989) determined the $\chi^{(3)}$ values for symmetric ferrocene-capped diacetylene by Third Harmonic Generation and commented that nonlinearity may be enhanced by three-photon resonance. Polin et al. (1994) estimated $\chi^{(3)}$ values for ferrocenyl-substituted phenylacetylenes using DFWM and proposed that NLO properties get enhanced due to two-photon resonance. Ghosal et al. (1990) studied the NLO effect of ferrocene derivatives by changing the ligand environment in tetrahydrofuran (THF) solution using picoseconds DFWM technique at the wavelength of 1064 nm.

Frazier et al. (1987) investigated the third-order nonlinearities using THG of palladium polyynes complexes and determined the $\chi^{(3)}$ values. Blau et al. (1991) reported the third-order NLO properties of a series of metal polyynes and investigated

the role of the metal atom on the NLO properties. Yang et al. (1998) investigated the third-order nonlinear optical properties of Ni-polyynes copolymers containing various ligands, with PPh₃ and PBu₃, using DFWM technique, and also discussed the structure-property relationship for the complexes. Later Yang et al. (2003) reported NLO properties of three Pd-polyynes using DFWM and claimed that the Pd-polyynes possess larger NLO properties than reported earlier on Ni-polyynes. The NLO properties of a series of platinum metal complexes containing ter/bipyridyl polyphenylacetylide ligands has been investigated at 532 nm with nanosecond laser pulses by Sun et al. (2003). They also discussed the effect of ligand environment and length of conjugation on observed NLO properties due to RSA phenomena. The wavelength dependent cubic nonlinearity of platinum complexes containing Polyynediyl ligands has been investigated by femtosecond Z-scan technique and the frequency dependent cubic hyperpolarizability has been observed. Further, the experimental results have been compared with theoretical studies by Samoc et al. (2008).

Metallocenes is a class of organometallics complexes. Group 4 metallocene complexes are normally d⁰ and 16 electron complexes. Myers et al. (1992) have estimated the third-order nonlinear optical coefficients of group 4 metallocene halide and acetylide complexes of Ti, Zr and Hf using the THG technique. They observed that the second-order hyperpolarizability of halide containing complexes was relatively small due to weak charge transfer between ligand and the metallocenes. However, complexes containing acetylide possess larger second-order hyperpolarizability values than the halide. This is due to electron accepting character of acetylide group and also effective charge transfer between metal and acetylide. Consequent changes in second-order hyperpolarizability values for different metal ions are also discussed. The magnitudes of $\chi^{(3)}$ for a series of metallocenes have been determined using THG technique and the origin of nonlinearity under the influence of metal-ion on π -conjugated systems have been investigated by Kamata et al. (1995).

Powell et al. (2004) have reported the wavelength dependence of the imaginary and real part of second-order hyperpolarizability of organometallic dendrimer over a range of wavelength. For wavelength range of 700 – 850 nm the Z-

scan results show that the nonlinear absorption coefficient β was negative, which was attributed to saturable absorption. Outside this range, β was seen to be positive and, hence, TPA was the dominant mechanism. The real part of hyperpolarizability (γ_{real}) was negative over the measurement range, except around 1200 nm where γ_{real} is positive. Recently, Samoc et al. (2011) have studied the spectral dependence (520–1600 nm) of the hyperpolarizability of arylalkynylruthenium dendrimers by Z-scan technique using femtosecond laser. Their results reveal that all investigated complexes exhibit positive γ_{img} , implying occurrence of TPA, and negative γ_{real} , thereby suggesting the occurrence of self-defocusing. Recently the three-photon absorption behavior of platinum complexes in infrared region (850 – 1200 nm) was studied using Z-scan technique. The observed results were interpreted employing the sum-over states approach (Vivas et al. 2011).

The magnitude of quadratic and cubic NLO properties of organometallics depends strongly on the specific metal-ions present in the organic molecules. Feuvrie et al. (2007) studied this aspect using a series of octupolar Tris(bipyridyl)metal complexes with different metals [(Fe(II), Ru(II), Ni(II), Cu(II), Zn(II)] and performing harmonic light scattering (HLS) and Z-scan experiments (765 and 965 nm) measurements. The first hyperpolarizability coefficient (β) ranged from 211×10^{-30} to 340×10^{-30} esu and the TPA cross section values varied from 650 - 2200 GM (GM= Goeppert-Mayer, $1 \text{ GM} = 1 \times 10^{-50} \text{ cm}^4 \text{ s/photon}$). It was concluded that NLO properties can be tuned by modifying the metal ion. This report also revealed the role of π -conjugated donor group on observed NLO properties.

Espinoza et al. (2010) have studied the role of the number of ferrocenyl ended groups in porphyrin-containing dendrimers on the third-order NLO properties. The dendrimer containing 16 ferrocenyl groups has larger NLO value than that containing 8 ferrocenyl groups. The Authors claimed that the increased value is due to the presence of more ferrocenyl groups in the dendrimer. The structural dependence of the second-order hyperpolarizability of chromium complexes of NH_2 -substituted aryl ring and the unsubstituted ring has been studied using DFWM technique by YiZhong et al. (2008). To study the effect of electron donor on NLO properties of metal complexes, Qian et al. (2010) have carried out Z-scan experiments on Nickel

complexes with and without donor group of CH₂. Both complexes exhibit nonlinear refraction and the complex with donor group shows larger nonlinear absorption than the one without donor group. The authors attributed this to the increase in molecular conjugation (due to transition dipole moment) and effect of electrons present in the substituent.

The important classes of organometallics are metal phthalocyanines (MPC) and metal porphyrins (MPP). To study the role of the central metal-ion on third-order optical susceptibility, DFWM experiments are performed on complexes containing Pt and Pb, and also on metal-free tetrakis(cumylphenoxy)phthalocyanines. Metal substitution strongly enhances the off-resonant $\chi^{(3)}$. Thus, Pt - phthalocyanine has $\chi^{(3)}$ of 2×10^{-10} esu and Pb - phthalocyanine has $\chi^{(3)}$ of 2×10^{-11} esu which is much higher than that of metal free phthalocyanine. Garcia et al. (1996) have also carried out similar investigations on octasubstituted metallophthalocyanines. Using THG at wavelengths of 1064 nm and 1904 nm, the $\chi^{(3)}$ values of series of octasubstituted metallophthalocyanines were determined by varying the metal (Cu, Ni and Co). The enhancement of nonlinearity was observed in cobalt containing compound at the wavelength of 1904 nm and this was shown to be due to two-photon transitions. To study the effect of ligand environment with metal, Cheng et al. (2001) have theoretically calculated the electronic structure and spectra of the metal phthalocyanines of Zn, Ni and TiO. They also evaluated dynamic third-order susceptibilities employing third-harmonic generation, electric-field-induced second harmonic generation and degenerate four-wave mixing optical processes. Their results were compared with experimental results. The calculated susceptibility values increased in the order PcNi < PcZn < PcTiO as the distance between central metal atom and ligand plane was increased in the order PcNi < PcZn < PcTiO which was in tune with experimental results. The π - π^* transition is responsible for the observed third-order nonlinearity in PcM (M=Zn, Ni) and ligand metal charge transfer (LMCT) is responsible for third-order nonlinearity in PcTiO.

Terazima et al. (1997) have measured the real and imaginary parts of $\chi^{(3)}$ for porphyrin oligomers containing different numbers of repetition units using single beam Z-scan technique with laser pulses of width of 30 ps at the wavelength of 640

and 1064 nm. The real part of $\chi^{(3)}$ was seen to increase as the number of monomers were increased. The authors explained that higher nonlinearity was due to porphyrins attached to meso position and two photon resonance processes. Humphrey and Kuciauskas (2004) have investigated the wavelength dependent (760-1350 nm) third-order nonlinear optical susceptibilities of electropolymerized Fe(III) tetrakis(*p*-hydroxyphenyl) porphyrin films using DFWM technique. The $\chi^{(3)}$ values of the films were of the order of 10^{-12} esu. By applying sum-over-states theoretically, the values of $\chi^{(3)}$ and second order hyperpolarizability γ were also determined. Recently Krishna et al. (2012) have reported the nonlinear optical studies of covalently functionalized novel graphene oxide–[Cu, Zn, Sn, H₂ (metal free), VO] porphyrin composites. NLO properties of graphene–porphyrin composites were investigated using the Z-scan technique at 532 and 800 nm with nanosecond (ns) and femtosecond (fs) laser pulses. The composites showed strong TPA as well as ESA leading to RSA behavior in the ns regime and saturable absorption (SA) behavior was observed in fs regime. The authors also observed that the metal free porphyrin–graphene oxide (GO) composite exhibits stronger NLA behavior compared to other GO–porphyrin composites (Krishna et al. 2012).

The applications of these molecules for practical device require optically active compounds in solid state form. From this point of view, many researchers have studied the NLO properties of active molecules in film form. Rojo et al. (1999) reported the third-order nonlinear optical susceptibilities of organo-bi-metallic complexes of Mo/Fe in chloroform solutions (at $\lambda = 1907$ nm) and dispersed into spin-coated poly-methyl-methacrylate (PMMA) films (at $\lambda = 1907$ nm and $\lambda = 1064$ nm) using THG technique. Changes in the NLO properties based on the role of conjugation length, substituents in the bridge, and molecular structure (“straight” or “bent”) have been identified. The multilayer copper phthalocyanine films doped into PMMA were prepared using spin coating method and their NLO properties were investigated using Z-scan technique with nanosecond laser pulses. Kurum et al. (2009) reported that polymeric films show better intensity dependent absorption than the complex in chloroform solution. Using Z-scan technique and 4 ns laser pulses at a wavelength of 532 nm, Tekin et al. (2010) have investigated the nonlinear absorption

coefficient and optical power limiting behavior of zinc phthalocyanine complexes in solution and solid PMMA composite films. PMMA doped complexes exhibit larger nonlinear absorption than that of complexes in solution form.

All-optical switching behavior of many materials has been investigated. Some of them are listed below:

- Organic materials : Samoc et al. 1995, Xu et al. 1996, Kar 2000, Abdeldayem et al. 2003, Wang et al. 2011, Hales et al. 2006, Bahtiar et al. 2009, Hales et al. 2010, He et al. 2011, Jin et al. 2007
- Bacteriorhodopsin : Roy et al. 2004, Huang et al. 2004, Roy et al. 2010
- Organometallics : Henari 2001, Liu et al. 2004, Singh et al. 2005, Singh et al. 2006
- Liquid crystal materials : Ikeda et al. 1996, Lee et al. 2000, Khoo et al. 2007, Miroshnichenko et al. 2008, Sio et al. 2008, Hrozhyk et al. 2010
- Glasses : Friberg et al. 1987, Harbold et al. 2002
- Semiconductors : Piccione et al. 2012, Erlacher et al. 2004
- Nanoparticles : Padilha et al. 2005, Hu et al. 2008, Joseph et al. 2010
- Photonic crystals: Soto et al. 2004, Hu et al. 2004, Maksymov et al. 2007, Hache and Bougeois 2000
- Carbon nanotubes and graphene: Chen et al. 2002, Zhu et al. 2006, Wang et al. 2010.

A brief overview of all-optical switching behavior of organometallics is presented in what follows. Henari (2001) has demonstrated the reverse saturable absorption (RSA) based all-optical switching of Pt-phthalocyanine using pump-probe technique. It was shown that this material could be used for making optically inverted switch and NOR gate. The author also established that strong triplet state absorption is responsible for the observed switching behavior (Henari 2001). Liu et al. (2004) investigated the NLO properties of lanthanide bisphthalocyanines, using Z-scan technique, and showed that the nonlinearity was due to RSA and it could be utilized for making optical switches and NOT gate with two different laser beams, i.e. pump and probe beam, respectively. The effect of phthalocyanine ring on RSA was also

discussed. Singh et al. (2005) studied the all-optical switching in zinc and vanadium complexes using pump-probe method. The authors used cw He-Ne laser as probe beam and pulsed Nd: YAG laser (20 ns) as pump beam and obtained the response time of the complexes. Experimental results have been explained using rate equation model. By including nonlinear excited-state absorption in the rate equations, all-optical switching in Pt: ethynyl complex was theoretically analyzed. The effect of various parameters, such as pump pulse width, its peak intensity, transition times of $S_1 \rightarrow S_0$ and $S_1 \rightarrow T_1$ states and lifetime of triplet state on switching characteristic has been analyzed in detail. The authors also pointed out that one can design all-optical NOT and the universal NOR and NAND logic gates using multiple pump laser pulses. Recently Gatri et al. (2012) have investigated all-optical switching based on optical Kerr effect in organometallic complex of ruthenium (II) acetylides containing an azobenzene moiety as a photochromic group using picosecond pump - cw probe technique. The role of ruthenium in the dynamics of molecular motion has also been studied.

Metal complexes with Schiff base ligands have not been explored much for third-order nonlinear optical properties. Tian et al. (2005) investigated third-order nonlinear optical susceptibility ($\chi^{(3)}$), two-photon absorption (TPA) coefficient and TPA cross section of ruthenium complex with Schiff base ligand using Z-scan technique at 532 nm. In 2006 Das et al. studied TPA cross section of a Schiff base ligand with and without Zn(II) and Cu(I) as metal centers. Chandrasekhar et al. (2010) also studied the variation in NLO properties of Schiff bases by changing the metal ions. Third-order nonlinear optical properties of donor acceptor salen ligand based Schiff base complexes of Ni and Cu have been investigated by changing the electron accepting/donating groups and also the central metal ions in the complexes (Tedim et al. 2006). Our group has investigated the third-order nonlinear optical properties and optical power limiting of three different Schiff base complexes, with Ni, Zn and Fe as the metal ions, by using Z-scan technique (Sampath Kumar et al. 2010). There are very few reports on third-order NLO properties of palladium complexes and no reports on ruthenium complexes with salen and salophene based Schiff base ligands.

With this in mind we selected palladium and ruthenium Schiff base complexes for our experimental investigations.

A brief review on metal dithiolene complexes as NLO materials is presented below. Hursthouse et al. (1995) has reported the synthesis and third-order nonlinear optical coefficients of nickel complexes of unsymmetrical dithiolene ligand using DFWM technique. They also studied the effect of bulky substituent on NLO properties. The third-order nonlinearity of didodecyldimethylammonium – Au (dmit)₂ (dmit=1, 3 – dithiole – 2 – thione - 4, 5-dithiolate) was investigated by measuring optical Kerr effect at 830 nm wavelength on femtosecond time scale by Wang et al.(1999). They obtained the second-order hyperpolarizability to be 2.2×10^{-32} esu. Dai et al. (2000) have reported a new method to synthesize unsymmetrical dithiolene complex of Cadmium and Zinc and have determined their NLO properties at 532 nm. Wang et al. (2011) reported the synthesis, crystal growth, and NLO properties of the aurate complex of dmit ligand using Z-scan technique. In early 2012 Chen et al. investigated the third-order nonlinear optical properties of aurate dmit complexes in acetonitrile solution and doped PMMA thin film using the Z-scan technique at a wavelength 1064 nm with laser pulse duration of 20 ps. The complex, in acetonitrile solution, exhibits negative nonlinear refractive index of -1.9×10^{-18} m²/W and -8.9×10^{-15} m²/W in the polymer thin film form, but has negligible NLA in both forms. Based on the above results the authors suggested that the investigated complex has potential for the application in all-optical switching devices. Recently Hu et al. (2012) have synthesized and performed NLO characterizations for two Ni and two Au complexes containing the multi-sulfur dithiolene ligand in DMF solution at the concentration of 2×10^{-4} mol/L using Z-scan technique using 6.5 ns optical pulses at 532 nm wavelength. Further, only two Au complexes exhibited nonlinear absorption, calculated to be 2.223×10^{-10} m W⁻¹ and 1.673×10^{-10} m W⁻¹, respectively. The nonlinear absorption of Ni complex was seen to be negligible and all complexes exhibited negative nonlinear refractive index calculated to be -3.37×10^{-11} esu, -4.83×10^{-11} esu and -5.66×10^{-11} esu for Ni complex and two Au complexes, respectively. Third-order non-linear susceptibility $\chi^{(3)}$ of two Au complexes was estimated to be 7.3×10^{-13} and 7.4×10^{-13} esu, respectively. Following this line of

research we have synthesized new type of ruthenium complexes with dmit ligand containing triphenylphosphine/ triphenylarsine and investigated their NLO properties.

The third-order nonlinear optical parameters of large variety of molecules can be determined using different experimental techniques, such as Z-scan, Degenerate four wave mixing (DFWM), Third-Harmonic Generation (THG) and Electric field induced second harmonic generation (EFISH). The Z-scan technique was first developed by Bahae et al. (1989) it is highly sensitive, simple to implement and enables simultaneous measurement of both sign and magnitude of nonlinear absorption and refraction coefficients of various materials. Furthermore, to improve the sensitivity of Z-scan technique many research groups used laser beams with different intensity profiles, such as top-hat beam, trimmed Airy beam, Gaussian–Bessel beam , elliptic Gaussian-beam , Hermite – Gaussian-beam , Laguerre–Gaussian-beam , Gaussian Schell-model beam , and quasi-one-dimensional slit (QODS) beam (Zhao and Palffy-Muhoray 1993, Xia et al. 1994, Rhee et al. 1996, Hughes and Burzler 1997, Zang et al. 2003, Tsigaridas et al. 2003, Zhang and Kuzyk 2006, Liu et al. 2008 and Gu et al. 2004).

1.7 SCOPE AND OBJECTIVES OF THIS THESIS WORK

The design of novel NLO materials has become a focus of recent research because of rapid advancement in various photonic technologies. Therefore, the search for new type of NLO materials with desired NLO properties is of great interest currently. Among the variety of materials, organometallics have the advantage of combining organic materials (having structural flexibility, large nonlinearity and fast response) with metals, thereby enhancing the robustness and thermal stability of the materials. In addition to these, NLO properties can be tuned by changing the metal and ligand environment, oxidation state, coordination geometry etc. Due to this flexibility with organometallics, there is great scope for synthesizing materials with the good NLO properties. For device applications the molecules could be embedded in a suitable polymer (guest-host systems), because liquid materials are often not suitable for device applications. The host polymer should possess high laser damage threshold, good optical quality with high transparency, good thermal and

photochemical stability. It should also allow the fabrication of devices at low cost and in desired shape at low processing temperatures. Polymethylmethacrylate (PMMA) is often used as a host material because it is a hard, rigid and transparent polymer with glass transition temperature of 125 °C, and is a polar material having a larger dielectric constant than that of other thermoplastics.

In this thesis we present an investigation on the third order NLO properties of metal-organic materials. We have selected two types of metal complexes and their derivatives with palladium and ruthenium as metal ions. Solid samples in film form were prepared by dispersing them in PMMA matrix. Samples in solution form were also prepared by dissolving the organics in DMF liquid. The mechanisms responsible for third-order nonlinear optical properties of the complexes were also studied.

To study the role of incorporation of electron withdrawing and donating groups, at the terminus of the molecules, on third-order nonlinear optical properties of the metal-organic complexes, the following four metal-organic complexes of palladium were used:

1. Pd-N-(2-pyridyl)-N'-(5-nitro salicylidene)hydrazine triphenylphosphine **[PdL1]**
2. Pd-N-(2-pyridyl)-N'-(5-chloro salicylidene) hydrazine triphenylphosphine **[PdL2]**
3. Pd-N - (2 - pyridyl) - N' - (salicylidene)hydrazine triphenylphosphine **[PdL3]**
4. Pd-N-(2-pyridyl)-N'-(5-methoxy salicylidene) hydrazine triphenylphosphine **[PdL4]**

To study the effect of molecular structure on third-order nonlinear optical properties of the metal-organic complexes, the following two novel ruthenium metal-organic complexes containing 1, 3-dithiole-2-thione- 4, 5-dithiolate (dmit), triphenylarsine/triphenylphosphine ligands were chosen :

1. [Ru (dmit) (triphenylarsine) (H₂O) (Cl)] {dmit=1, 3 – dithiole – 2 – thione - 4, 5-dithiolate} **[RuL1]**.
2. [Ru (dmit) (triphenylphosphine) (H₂O) (Cl)] {dmit=1,3 – dithiole – 2 – thione - 4, 5-dithiolate} **[RuL2]**.

To study the effect of π -conjugation and delocalization on third-order nonlinear optical properties, the following two ruthenium metal-organic complexes containing salen / salophene ligands were selected:

1. [Ru (salen) (H₂O) (Cl)] salen = *N, N'*-disalicylidene - 1,2-ethylenediimine dianion **[RuL3]**
2. [Ru (salophene) (H₂O) (Cl)] salophene = *N, N'*-disalicylidene-1,2-ethylendiimine dianion **[RuL4]**.

The main research objectives were:

- To investigate the third-order nonlinear optical properties of palladium and ruthenium complexes with their derivatives in both solution and solid film form by dispersing the complexes in PMMA matrix.
- To fabricate metal complex doped PMMA films at different wt. % using spin coating method.
- To measure linear optical properties of metal complexes using UV-Visible fiber optic spectrometer, spectroscopic ellipsometer and abbe refractometer.
- To investigate third-order NLO properties of metal complexes using single beam Z-scan and DFWM techniques.
- To investigate the optical power limiting behavior of the metal complexes.
- To investigate the all-optical switching capability of the metal complexes using pump-probe technique.

The work presented in the thesis is broadly divided into six chapters. Detailed results of experimental investigations on third-order nonlinear optical properties by using Z-scan and DFWM techniques, optical power limiting and also all-optical switching behaviour using pump-probe method for three different classes of metal-organic complexes and their derivatives are presented.

Chapter 1 contains a general introduction to nonlinear optics, theoretical aspects of light-matter interaction in nonlinear regime and different nonlinear optical processes. Literature survey on the recent status of the research work on different types of NLO

materials used is presented. The scope and objectives of the present work are mentioned at the end of this chapter.

Chapter 2 presents the details of experimental techniques used in this study. The first section contains an introduction to Z-scan technique, its theoretical description along with formulae used for calculations and the experimental setup used in our laboratory. An introduction to degenerate four wave mixing technique, its theoretical description and the experimental arrangement used in this study are presented in second section. The third section provides an introduction to optical power limiting, various nonlinear optical processes leading to optical power limiting and describes the experimental method adopted. The fourth section of this chapter contains an introduction to all-optical switching and description of experimental setup used for this measurement. The last section gives details of sample preparation and its characterization in terms of UV-Visible absorption spectra, refractive indices and thickness determination.

Chapter 3 describes the results of Z-scan, DFWM, optical power limiting and all-optical switching studies on series of palladium metal-organic complexes. The nonlinear optical properties of the complexes with varying functional group were studied. A possible mechanism responsible for the third-order nonlinearity of the compounds has been discussed. An attempt has been made to establish the molecular structure-NLO property relationship. The study of concentration dependent third-order NLO and optical power limiting capabilities and intensity dependent all-optical switching studies of these metal-organic complexes have also been presented.

Chapter 4 This chapter reports the results of Z-scan, DFWM, optical power limiting and all-optical switching experiments on two ruthenium complexes containing dmit ligand. The effect of molecular structure on third-order nonlinear optical properties of the metal-organic complexes was studied. The concentration dependence of third-order nonlinear optical properties of these metal-organic complexes is also presented.

Chapter 5 This chapter focuses on the results of Z-scan, DFWM, optical power limiting and all-optical switching experiments on two ruthenium complexes containing salen and salophene ligands. The effect of π -conjugation and delocalization on third-order nonlinear optical properties is discussed. The structure-property

relation has been discussed. The concentration dependence of third-order nonlinear optical properties of these metal-organic complexes is also presented.

Chapter 6 summarizes the main results and conclusions of our research work. It concludes with suggestions for further research on this topic. The references, list of publications and bio-data are at the end of the thesis.

CHAPTER 2

CHAPTER 2

EXPERIMENTAL DETAILS

Abstract

This Chapter describes the experiments carried out to investigate third-order NLO properties, optical power limiting capability and all-optical switching behavior of the new metal-organic materials synthesized by us. The basic principles behind each experiment are discussed and the formulae used for the calculation of NLO coefficients are presented. The experimental set up used in this study is described in detail.

2.1 Z-SCAN TECHNIQUE

2.1.1 Introduction

Single beam Z-scan technique, developed by Bahae et al. (1989), is widely employed to determine third-order nonlinear optical properties. Compared to other techniques, this is a relatively simple technique to determine both nonlinear absorption (NLA) and nonlinear refraction (NLR) for solid and liquid samples. It provides a highly sensitive and straightforward method for determining the nonlinear refractive index, the sign and the magnitude of the real and the imaginary part of the third order nonlinear optical susceptibility and nonlinear absorption coefficient of nonlinear materials. Basically, the Z-scan method consists of translating a sample through the focus of a Gaussian beam and monitoring the changes in the far field intensity pattern. The beam propagation direction is taken to be Z-axis and, hence, the name Z-scan. The sample material acts like an intensity dependent thin lens. As the sample is translated along the beam path its effective focal length changes, depending on the intensity of the converging laser beam. This change will be reflected in the intensity distribution at the aperture kept in the far field. The transmitted intensity is first measured keeping an aperture in front of the detector, thus obtaining “closed aperture Z-scan data”. Next, the transmittance is measured without the aperture, as the sample is translated along the Z-direction in order to obtain the “open aperture Z-scan

data”. The sample itself behaves as a thin lens for the laser beam propagating through it. The change in the intensity distribution at the aperture kept in the far field zone, measured as closed aperture Z -scan data, is a measure of the nonlinear refraction due to the sample. In addition to this refraction due to nonlinearity, the medium also possesses nonlinear absorption, which is estimated using the open aperture Z -scan measurements. Thus, collectively, the closed aperture and the open aperture data enable us to calculate values of both n_2 and β .

2.1.2 Principle of Z-Scan Technique

(a) Nonlinear Refraction

A nonlinear optical material may exhibit either negative nonlinear refractive index or positive nonlinear refractive index. We first consider a material possessing positive nonlinear refractive index. The sample thickness is assumed to be smaller than the Rayleigh range of the focused laser beam, i.e. the sample is “thin”. This can be regarded as a thin lens having an optical intensity dependent focal length. In our experiments, nonlinear refraction measurement process involves translation of the sample from about $Z = -16$ mm to $Z = +16$ mm, $Z = 0$ being the focal point of the laser beam in the absence of the sample. At $Z = \pm 16$ mm, the intensity of the laser beam incident on the sample is quite low, and hence negligible nonlinear refraction occurs. Therefore the sample behaves as a linear medium. As the sample approaches the focal point, $Z = 0$, the beam intensity increases rapidly, leading to self-lensing in the sample. A negative self-lensing effect, also called self-defocusing, prior to the focus will tend to collimate the beam causing a beam narrowing at the aperture. The consequence of this nonlinear refraction on the laser beam propagation is a shift in the focal point of the beam from $Z = 0$ towards +ve Z -values, which results in an increase in the measured transmitted intensity. As the translation of the sample is continued further beyond $Z = 0$, the same self-defocusing effect occurs which increases the beam divergence, leading to beam broadening at the aperture. Consequently, the transmitted intensity of the laser beam decreases rapidly. Further translation towards $Z = +16$ leads to rapid reduction in the beam intensity in the sample and the nonlinearity disappears. Consequently, the transmittance returns to the linear value corresponding to the initial sample position $Z = -16$ mm. When the sample is close to the focal point $Z = 0$, the nonlinearity is very

strong. The measured transmitted intensity as a function of Z shows a pre-focal peak for $Z < 0$ followed by post-focal valley for $Z > 0$, which is the signature of negative refractive nonlinearity (i.e. $n_2 < 0$) in a given medium. Similarly, for a material having positive nonlinear refractive index (i.e. $n_2 > 0$), the measured transmitted intensity as a function of Z shows a pre-focal valley for $Z < 0$ followed by post-focal peak for $Z > 0$. A typical Z-scan plot of negative nonlinear refractive index is shown in the Figure 2.1.

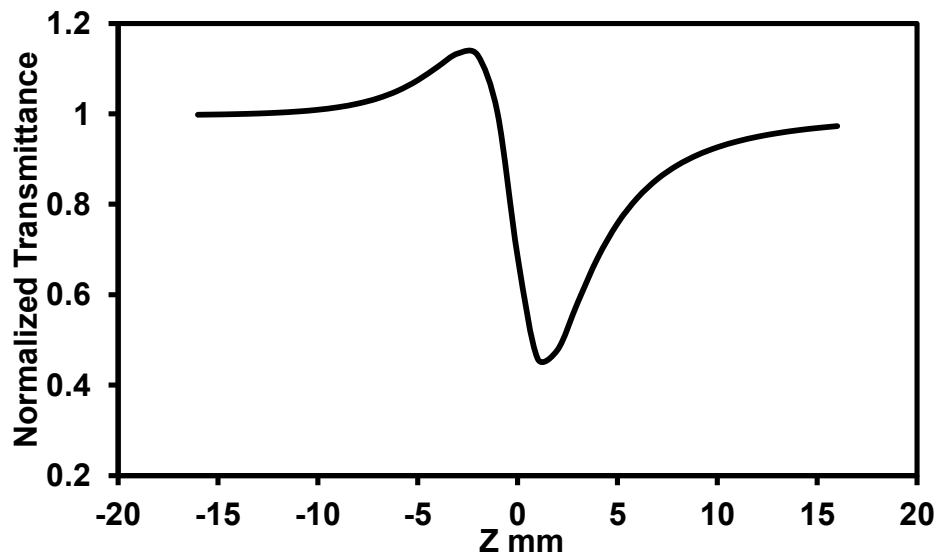


Figure 2.1 Typical plot of closed aperture Z-scan data

(b) Nonlinear Absorption

The nonlinear absorption coefficient of the sample can be calculated from the open aperture Z-scan data. The sensitivity of the measured data to nonlinear refraction is entirely due to the presence of the aperture kept in front of the detector. Removal of the aperture completely eliminates this effect. The open aperture Z-scan trace exhibits decrease in the transmittance close to the focus $Z = 0$ of the laser beam. A typical open aperture Z-scan plot is shown in the Figure 2.2.

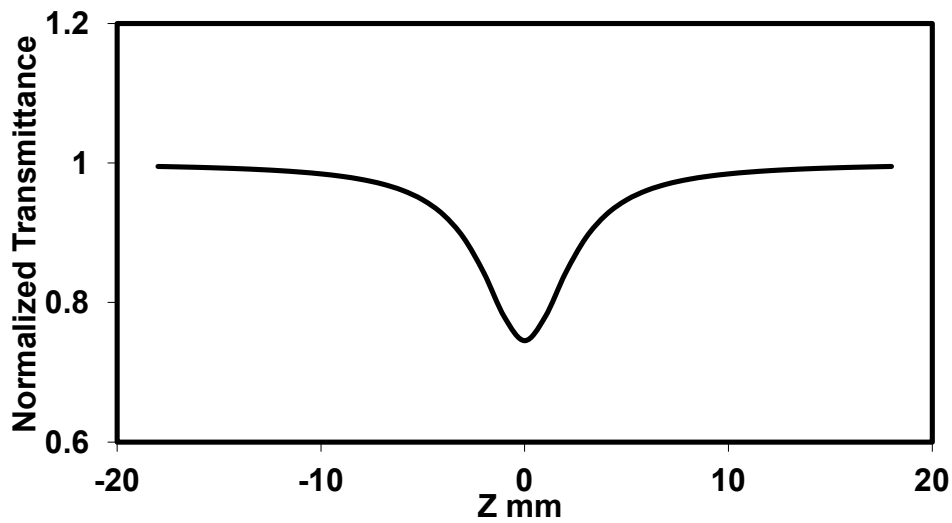


Figure 2.2 Typical plot of open aperture Z-scan data

The sample may possess absorptive nonlinearities due to mechanisms, such as multiphoton absorption and saturable absorption. Qualitatively, multiphoton absorption suppresses the peak and enhances the valley in the closed aperture z-scan plot. On the other hand, saturation effect does the opposite. Usually the nonlinear refraction is accompanied by nonlinear absorption. To estimate the pure refractive nonlinearity, the ratio of closed aperture Z-scan data by open aperture Z-scan data is calculated yielding the “normalized” Z-scan curve which is effectively free from nonlinear absorption. A typical normalized Z-scan plot, corresponding to pure nonlinear refraction, is shown in the Figure 2.3. One can calculate both nonlinear refractive index n_2 , and nonlinear absorption coefficient β , by utilizing graphs shown in Figures 2.2 and 2.3.

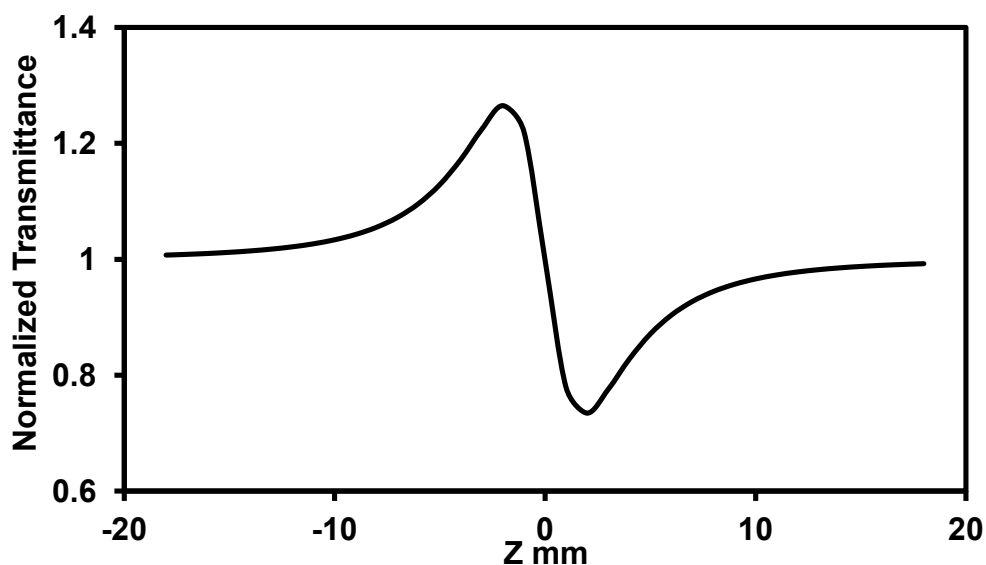


Figure 2.3 Typical normalized Z-scan plot

2.1.3 Advantages and disadvantages of the Z-Scan technique

(a) Advantages of the Z-scan technique

The Z-scan technique has several advantages:

- It is simple to carry out.
- It is a single beam technique and so laser beam alignment is easy.
- It can be used to determine both the sign and magnitude of the nonlinearity. The shape of the Z-scan curve determines the sign of optical nonlinearity.
- In this technique the contribution of nonlinear absorption and nonlinear refraction to nonlinear susceptibility $\chi^{(3)}$ can be separately estimated.
- The real and imaginary parts of third-order nonlinear susceptibility $\chi^{(3)}$ can be determined in this method.
- It is a good method for rapidly screening new nonlinear materials.
- The technique can also be modified to study nonlinearities on different time scales as well as to estimate higher order contributions.

(b) Disadvantages of the Z-scan technique

- The analysis assume the use of a laser beam with pure Gaussian intensity profile in the transverse plane of the beam for the measurements.

2.1.4 Theoretical background of Z-Scan technique

The theory for the Z-scan method was developed by Sheik-Bahae and others (Bahae et al. 1989). Schematic Z-scan experimental set up is given in Figure 2.4.

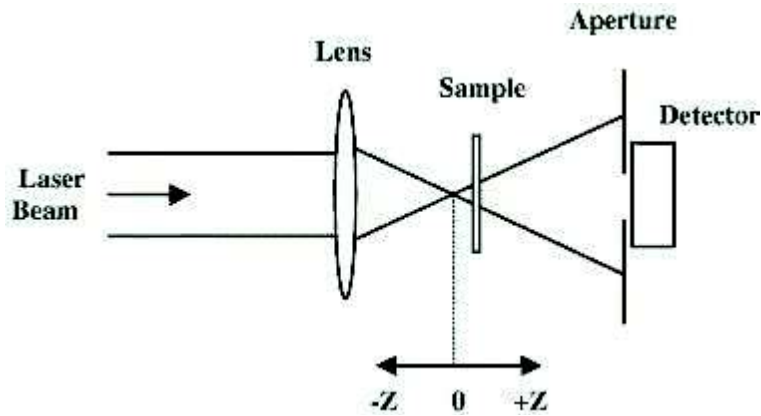


Figure 2.4 Schematic Z-scan experimental setup

The electric field $E(r, z, t)$ of a Gaussian laser beam of cylindrical shape, with beam waist radius w_0 , propagating along the z direction in free space, can be written as

$$E(r, t, z) = E_0(t) \frac{w_0}{w(z)} \exp\left(-\frac{r^2}{w^2(z)} - \frac{ikr^2}{2R(z)}\right) e^{-i\phi(z, t)} \quad (2.1)$$

where $w(z)$ is the beam waist at a distance z from the beam focal point and is given by $w^2(z) = w_0^2 \left(1 + z^2/z_0^2\right)$, the radius of curvature of the wave front at any position z is given by $R(z) = z \left(1 + z_0^2/z^2\right)$, $z_0 = kw_0^2/2$ is known as the diffraction length or Rayleigh range of the beam, $k = 2\pi/\lambda$ is the wave vector and λ is the laser wavelength in free space. $E_0(t)$ denotes the electric field of the laser at the beam focus. The term $e^{-i\phi(z, t)}$ contains phase variations independent of r .

For simplicity, we consider the case of a material having cubic nonlinearity. The index of refraction ‘ n ’ may be expressed as,

$$n = n_0 + \frac{n_2}{2}|E|^2 = n_0 + \gamma I \quad (2.2)$$

where n_0 is the linear index of refraction, n_2 (esu) or γ (m^2/W) are the nonlinear refractive index coefficients, E is the electric field, I is the intensity of the laser beam within the sample and $\Delta n = \gamma I$ is the nonlinear part of the refractive index of the material. The parameters n_2 and γ are related through the equation,

$$n_2(\text{esu}) = \frac{cn_0}{40\pi} \gamma(\text{m}^2/\text{W}) \quad (2.3)$$

The sample thickness is considered to be small enough, so that any changes in the beam diameter within the sample due to either diffraction or nonlinear refraction can be neglected. Generally, nonlinear medium could be considered as “thin” if its thickness L is less than the Rayleigh range, z_0 . In such a case the nonlinear self-refraction process is referred to as “self action” (Weaire et al. 1974).

For samples possessing weak nonlinearities, and within the limits of slowly varying envelope approximation (SVEA), the spatial variation of the radial phase and the intensity I of the propagating laser beam are governed by,

$$\frac{d\Delta\phi}{dz'} = \Delta n(I)k \quad (2.4)$$

$$\frac{dI}{dz'} = -\alpha(I)I \quad (2.5)$$

where z' is the propagation length in the sample, $\alpha(I)$ in general includes both linear and nonlinear absorption. For materials with cubic nonlinearity, but having weak nonlinear absorption, Equations (2.4) and (2.5) can be solved to obtain the phase shift $\Delta\phi$ at the exit surface of the sample. The solutions are,

$$\Delta\phi(r, t, z) = \Delta\phi_0(t, z, L) \exp\left(-\frac{2r^2}{w^2(z)}\right) \quad (2.6)$$

with

$$\Delta\phi_0(t, z) = \frac{\Delta\Phi_0(t, L)}{1 + \frac{z^2}{z_0^2}} \quad (2.7)$$

where $\Delta\Phi_0(t)$ is the on axis phase shift at the focus, and is given by,

$$\Delta\Phi_0(t) = k\Delta n_0(t)L_{eff} \quad (2.8)$$

Here $L_{eff} = 1 - e^{-\alpha_0 L} / \alpha_0$ is the effective thickness of the sample having physical thickness L and its linear absorption coefficient is α_0 . I_0 is the on axis irradiance at the focus ($z=0$). Further, $\Delta n_0(t) = \gamma I_0(t)$ with $I_0(t)$ given by,

$$I_0 = \frac{4\sqrt{\ln 2} I_{total}}{\sqrt{\pi^3} w_0^2 \tau} \quad (2.9)$$

where I_{total} is the energy incident on the sample and τ is the pulse width of the laser beam.

The complex electric field exiting the sample may now be expressed as (Bahae et al, 1990),

$$E_e(r, t, z) = E_i(r, t, z) e^{-\alpha_0 L/2} e^{i\Delta\phi(r, t, z)} \quad (2.10)$$

where $E_i(r, t, z)$ is the amplitude at the input face of the sample.

Employing Kirchoff's diffraction theory, the far field pattern of the beam at the aperture plane is expressed as the Fraunhofer diffraction pattern of $E_e(r, t, z)$, the electric field at the output face of the sample. For this purpose we may employ the Taylor series expansion of the nonlinear phase term, $e^{i\Delta\phi(z, r, t)}$ which is given by,

$$e^{i\Delta\phi(z, r, t)} = \sum_{m=0}^{\infty} \frac{[i\Delta\phi_o(z, t)]^m}{m!} e^{-2mr^2/w^2(z)} \quad (2.11)$$

Each component can now be simply propagated to the aperture plane where they can be superposed to reconstruct the full beam. Taking account of the initial curvature for the focused beam, the resultant electric field pattern at the aperture is,

$$E_a(r, t) = E(z, r=0, t) e^{-\alpha_0 L/2} \sum_{m=0}^{\infty} \frac{[i\Delta\phi_o(z, t)]^m}{m!} \frac{w_{m0}}{w_m} \cdot \exp\left(-\frac{r^2}{w_m^2} - \frac{ikr^2}{2R_m} + i\theta_m\right) \quad (2.12)$$

Defining d as the propagation distance in free space from the sample to the aperture plane and $g = 1 + d/R(z)$, the various parameters in the Equation (2.12) are expressed as (Bahae et al. 1990),

$$w_{m0}^2 = \frac{w^2(z)}{2m+1}, d_m = \frac{kw_{m0}^2}{2}, w_m^2 = w_{m0}^2 \left[g^2 + \frac{d^2}{d_m^2} \right], R_m = d \left[1 - \frac{g}{g^2 + \frac{d^2}{d_m^2}} \right]^{-1}$$

$$\theta_m = \tan^{-1} \left[\frac{d/d_m}{g} \right] \quad (2.12a)$$

The optical power transmitted through the aperture is obtained by spatially integrating $|E_a(r, t)|^2$ at the aperture as follows,

$$P_T(\Delta\Phi_0(t)) = c\varepsilon_0 n_0 \pi \int_0^{r_a} |E_a(r, t)|^2 r dr \quad (2.13)$$

where ε_0 is the permittivity of vacuum. Taking the temporal profile of the pulse into account, the normalized transmittance $T(z)$ can be calculated as ,

$$T(z) = \frac{\int_{-\infty}^{\infty} P_T(\Delta\Phi_0(t)) dt}{S \int_{-\infty}^{\infty} P_i(t) dt} \quad (2.14)$$

where $P_i(t) = \pi w_0^2 I_0(t)/2$ is the instantaneous input power on the sample, and S is the transmittance of the aperture placed in front of the detector and is given by,

$$S = 1 - \exp(-2r_a^2/w_a^2) \quad (2.15)$$

where w_a denotes the beam radius at the aperture after removing the sample from the beam path and r_a is the aperture radius.

For a given $\Delta\Phi_0$ the magnitude and profile of $T(z)$, i.e., Z-scan trace, does not depend on the wavelength as long as the field is measured in the far field zone. The aperture size S , however, is an important parameter since a larger aperture reduces the variation in $T(z)$. This reduction is more prominent at the peak of the Z-scan trace, where beam narrowing occurs. For very large aperture ($S=1$), the effect vanishes and $T(z)=1$ for all z and $\Delta\Phi_0$. For small $|\Delta\Phi_0|$ ($|\Delta\Phi_0| \ll 1$), the peak and valley occur at the same distance with respect to focus and for a cubic nonlinearity, this distance is found to be $\approx 0.86z_0$ (Bahae et al. 1990). For larger phase distortions $|\Delta\Phi_0| > 1$,

numerical evaluation of equations (2.12) – (2.15) shows that the peak and valley are no longer symmetrically located. The peak and valley both get shifted together towards +z or -z depending on the sign of nonlinearity ($\pm\Delta\Phi_0$) such that their separation remains nearly constant at $\Delta T_{p-v} \approx 1.7z_0$.

For small phase distortions and small aperture ($S \approx 0$),

$$\Delta T_{p-v} \approx 0.406 |\Delta\Phi_0| \quad (2.16)$$

where ΔT_{p-v} is the difference between the peak and valley of the normalized Z-scan plot and is easily measured from the graph.

Numerical calculations show that this relation is accurate to within 0.5% of the experimental value for $|\Delta\Phi_0| \leq \pi$. For larger aperture, the numerical coefficient becomes smaller than 0.406. For $S=0.5$, it becomes ≈ 0.34 and at $S=0.7$ it reduces to ≈ 0.29 . Based on the numerical curve fitting, the following relationship can be used to account for such variations within $\pm 2\%$ accuracy:

$$\Delta T_{p-v} \approx 0.406(1-S)^{0.25} |\Delta\Phi_0| \quad (2.17)$$

Equations (2.16) and (2.17) are used in our work to estimate the coefficient of nonlinear index (n_2) with good accuracy.

Z scan technique can also be used to determine the nonlinear absorption coefficient for materials that show both nonlinear refraction and absorption simultaneously (Bahae et al. 1990). Large refractive nonlinearity in materials is commonly associated with a resonant transitions which may be of single or multiphoton nature. The nonlinear absorption arises from either direct multiphoton absorption, saturation of the single photon absorption or dynamic free carrier absorption. In such cases, a Z-scan with a fully open aperture ($S=1$), is insensitive to nonlinear refraction (thin sample approximation). Such open aperture Z-scan traces, with no aperture, are usually symmetric with respect to the focus ($z=0$) where they have a minimum transmittance. The coefficient of nonlinear absorption can be easily calculated from such transmittance curves.

The intensity distribution of the laser beam exiting out of the sample may be expressed as,

$$I_e(z, r, t) = \frac{I(z, r, t)e^{-\alpha_0 L}}{1 + q(z, r, t)} \quad (2.18)$$

and the corresponding phase shift as,

$$\Delta\phi(z, r, t) = \frac{k\gamma}{\beta} \ln[1 + q(z, r, t)] \quad (2.19)$$

where $q(z, r, t) = \beta I(z, r, t)L_{eff}$

Combining above two Equations (2.18) and (2.19), we obtain the complex electric field at the exit surface of the sample to be (Herman 1984),

$$E_e = E(z, r, t)e^{-\alpha_0 L/2} (1 + q)^{(ik\gamma/\beta - 1/2)} \quad (2.20)$$

Equation (2.20) reduces to Equation (2.10) in the absence of nonlinear absorption.

The transmittance in the case of open aperture Z-scan ($S=1$) is obtained by spatially integrating Equation (2.18) at z over r and may be expressed as follows,

$$T(z) = \frac{\ln[1 + q_0(z)]}{q_0(z)} \text{ for } |q_0(z)| < 1 \quad (2.21)$$

where $q_0 = \beta I_0 L_{eff} / (1 + z^2/z_0^2)$.

For a cubic nonlinearity and small phase change, it can be shown that the normalized transmittance in the case of closed aperture Z-scan is (Liu et al. 2001, Chapple et al. 1997 and Yin et al. 2000)

$$T(z) = 1 - \frac{4x\Delta\Phi_0}{(x^2 + 9)(x^2 + 1)} - \frac{2(x^2 + 3)\Delta\Psi_0}{(x^2 + 9)(x^2 + 1)} \quad (2.22)$$

where $\Delta\Phi_0 = \frac{\Delta T_{p-v}}{0.406(1-S)^{0.25}}$ for $|\Delta\Phi_0| \leq \pi$ and $\Delta\Psi_0 = \frac{1}{2} \beta I_0 L_{eff}$, where $\Delta\Phi_0$ is the on-axis phase shift due to nonlinear refraction, $\Delta\Psi_0$ is the on-axis phase shift due to nonlinear absorption, ΔT_{p-v} is the peak to valley transmittance difference, S is transmittance of the aperture, which is equal to 0.5 in our experiments. I_0 is the irradiance at the beam waist ($z=0$), and $L_{eff} = (1 - e^{-\alpha_0 L})/\alpha_0$, $x = z/z_0$, z_0 is the Rayleigh range and for a pure nonlinear refraction curve, obtained by division of closed aperture scan by open aperture scan, the normalized transmittance is shown to be (Bahae et al. 1990)

$$T(z) = 1 - \frac{4\Delta\Phi_0 x}{(x^2 + 9)(x^2 + 1)} \quad (2.23)$$

Once $\Delta\Phi_0$ is calculated from Equation (2.17), one can readily calculate γ through

$$\gamma = \frac{\Delta\Phi_0 \lambda}{2\pi L_{eff} I_0}, \quad (2.24)$$

from which one can obtain n_2 through the conversion formula as given in Equation (2.3).

The third-order nonlinear susceptibility has real and imaginary parts. The real part of the third-order nonlinear susceptibility is related to n_2 through

$$\text{Re } \chi^{(3)} = 2n_0^2 \varepsilon_0 c n_2, \quad (2.25)$$

and imaginary part is related to the nonlinear absorption through

$$\text{Im } \chi^{(3)} = n_0^2 \varepsilon_0 c \beta / 2\pi \quad (2.26)$$

2.1.5 Z-Scan experimental setup and measurement

Z-scan method is a standard technique for nonlinear optical measurements and was used for all the work reported in this thesis because of the relative simplicity of its optical layout and the ease with which nonlinearities can be estimated from the acquired data (Bahae and Hasselbeck 2000, Blau et al. 2004, Van Stryland and Bahae 1998, Van Stryland and Bahae 1998).

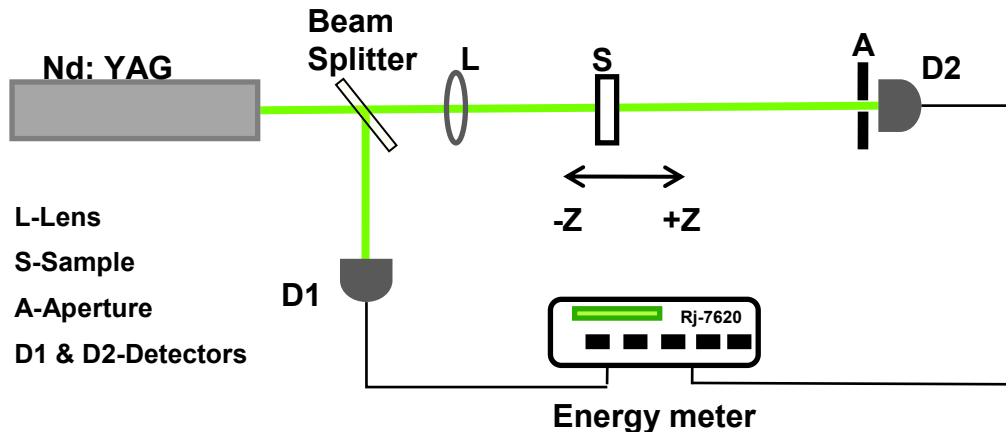


Figure 2.5 Layout of the experimental setup for Z-scan technique

The experimental set up for Z scan used in our laboratory is shown in Figure 2.5. The Gaussian laser beam from the Nd-YAG laser was focused by using a lens of 25 cm focal length. The resulting beam waist radius at the focal spot was calculated using the formula $w_0 = 1.22\lambda f / d$, where f is focal length of the lens and d is the diameter of the laser beam incident on the lens and was found to be 18.9 μm . The corresponding Rayleigh length, calculated using the formula $z_0 = \pi w_0^2 / \lambda$, was found to be 2.11 mm. For Z-scan measurements on liquid samples, a cuvette of 1 mm thickness was used. The sample was moved from one side of the focal spot to the other side along the laser beam axis using a computer controlled linear translation stage. The translation range (32 mm) was sufficient to cover the linear as well as the nonlinear regimes. The detector was placed at a distance of about 30 cm from the focal spot ($z=0$). A circular aperture of diameter 5 mm was placed in front of the detector and the detector output was monitored as the sample was translated along the laser beam axis from $Z = -16$ mm to $Z = +16$ mm. The set up was standardized using CS_2 as standard reference. The value of $\chi^{(3)}$ for CS_2 was obtained to be 3.81×10^{-3} esu, which agrees well with the value 4×10^{-3} esu, reported in the literature (Shirk et al. 1992 and Philip et al. 1999).

By performing closed aperture (with aperture in front of the detector) Z-scan, the nonlinear refractive index can be computed by measuring the difference in peak and valley transmittance ($\Delta T_{p-v} = T_p - T_v$) (Van Stryland and Bahae 1998).

(a) Laser used in the experiments

The details of the laser source used in our experiments are as follows:

1. Q-switched Nd-YAG laser; Model GCR -170 from Spectra – Physics, USA.
2. Available laser wavelengths: 1064 nm (fundamental), 532 nm (second harmonic) and 355 nm (third harmonic). We used the 532 nm laser in all our experiments.
3. Pulse width: 7 ns at 532 nm
4. Pulse repetition rate: 10 Hz
5. Divergence: <0.5 m rad, full angle

6. Line width: $<1 \text{ cm}^{-1}$
7. Maximum pulse energy: 750 mJ for 1064 nm and 400 mJ for 532 nm
8. Beam diameter: $\sim 10 \text{ mm}$
9. Transverse intensity distribution: nearly Gaussian

(b) Energy meter used in the experiments

1. Energy meter: Rj-7620 from Laser Probe Inc., USA.
2. Max. pulse rep rate: 40 Hz
3. Resolution: 0.03% of full scale.
4. Average Mode: 1, 10, or 100 pulses.
5. Ratio range: 10 to 1 (probe dependent).
6. Ratio accuracy: $\pm 2 \text{ LSD}$.
7. Trigger select: Internal, External.
8. Internal (auto) trigger: Channel A; Energy $> 7\%$ of F.S.
9. External trigger: TTL; within $\pm 20 \mu\text{s}$ of optical pulse.
10. Accuracy: $\pm 0.5\%$.
11. Analog (Ratio) output: 0 - 10 VDC.

(c) Detector probe used in the experiments

1. Probe: RjP-735 Cavity Pyroelectric Energy Probe
2. Spectral response: 0.18 - 20 μm
3. Maximum total energy: 1.0 J
4. Maximum energy density: 1.0 J/cm
5. Max. peak pulse power density: 1.0 MW/cm
6. Max. average power density :5.0 W/cm
7. Minimum detectable energy: 100 nJ

8. Maximum pulse rep rate: 40 Hz
9. Maximum pulse width: 1.0 msec
10. Calibration accuracy: $\pm 5\%$
11. Linearity: $\pm 0.5\%$
12. Detector exit port active area: 1.0 cm^2

2.2 DEGENERATE FOUR WAVE MIXING TECHNIQUE (DFWM)

2.2.1 Introduction to DFWM Technique

The interaction of four electromagnetic waves in a nonlinear optical medium via the third-order nonlinearity is termed as four wave mixing. Here, three coherent waves get mixed inside a nonlinear medium, thereby generating a fourth wave. When all the waves have the same frequency, the interaction is called Degenerate Four Wave Mixing (DFWM).

Depending on the choice of experimental conditions, the forward folded BOXCARS configurations (Laubereau et al. 1973, Bogdan et al. 1981, Kobayashi et al. 1988, Schmid et al. 1995, Williams et al. 1996 and Hauer et al. 2007) or the backward geometries (Caro and Gower 1982, Yariv 1978 and Pepper 1982) can be employed for the DFWM measurements. The forward DFWM method involves one pump beam (E_f) and one probe beam (E_p). The two beams are incident on the sample from the same side and they overlap with each other inside the sample. The output waves are the transmitted pump and probe, a conjugate wave (E_c) and a fourth wave called the auxiliary wave (E_a). In the backward DFWM geometry involves two pump beams, which are counter propagating. The probe beam is incident on the sample at a small angle to the direction of the forward pump beam. A fourth beam is generated, which is the signal beam. It is phase-conjugate to the probe beam, and propagates exactly opposite to the probe beam direction.

In forward folded BOXCARS configurations, the input laser beam is first expanded and then split into two pump beams and a probe beam using a plane mask with three holes; the holes are located at the corners of a square. These three beams emerge from the mask as beams parallel to each other such that they form three sides

of a parallelepiped of square cross section. These three separate beams are then focused by a lens onto a single spot on the sample as shown in the Figure 2.6. The diametrically opposite beams are the pump beams. The third beam is the probe. These three beams will interact nonlinearly when focused on to the sample to generate a fourth beam, called the signal beam. It will appear at the fourth corner (K_4) of the square on the output plane, as shown in Figure 2.6.

The interaction of three coherent waves in a nonlinear medium generates a fourth wave, i.e. the signal beam. The strength of this signal beam depends on a coupling constant that is proportional to third order susceptibility $\chi^{(3)}$. Hence, measurements on phase conjugate signal will yield information about the $\chi^{(3)}$ component for the medium (Walser et al. 1998, Zhao et al. 1991, Ghoshal et al. 1989, Zhao et al. 1988, Singh et al. 1990, Pang et al. 1991, Singh et al. 1988, Samoc and Prasad 1989, Cui et al. 1991 and Casstevens et al. 1990).

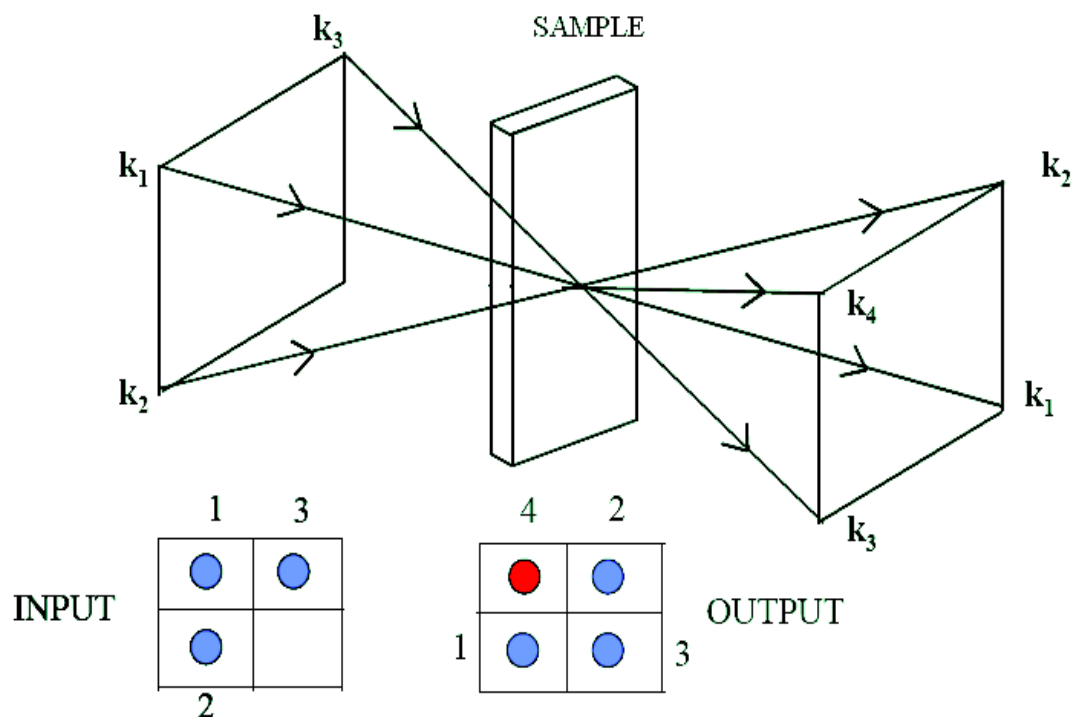


Figure 2.6 Forward folded boxcars DFWM configuration. The 4th spot in the output is the signal beam.

The two pump beams mix within the material medium forming an interference pattern. This interference pattern in turn creates a refractive index grating, due to the third order nonlinear optical property of the material, if the intensities of the probe beams is adequate. The probe beam passing through this grating creates the fourth beam. The intensity of the fourth, or signal beam, is proportional to the product of the intensities of the three input beams and to the square of the absolute value of the third-order susceptibility of the medium i.e. $I_4 = |\chi^{(3)}|^2 I_1 I_2 I_3$.

2.2.2 Advantages of the DFWM technique

1. The Phase Conjugate (PC) signal is distinguishable from other three beams since it is spatially separated and the signal strength has a characteristic dependence on the input intensities, which can be used for verification of the experiment.
2. Laser beams need not have Gaussian intensity profile.

2.2.3 Disadvantages of the DFWM technique

1. A reference material is required to quantify the $\chi^{(3)}$ values of the new materials.
2. It is not possible to separately estimate the real and imaginary parts of $\chi^{(3)}$
3. Sign of the nonlinearity cannot be determined.
4. The experiment is relatively complicate to set up (Hales and Perry 2008).

2.2.4 Theoretical description of DFWM

The DFWM phenomena can be understood on the basis of two commonly used theoretical approaches, the NLO description and laser induced grating (LIG) process. The NLO description exploits the phenomena of induced third-order polarizations due to the interaction of strong optical fields in the medium. DFWM signal is radiated as a fourth wave due to the induced nonlinear polarization. LIG mechanism involves generation of DFWM signal due to the diffraction from laser induced grating generated by the nonlinear mixing of two strong pump beams.

The DFWM experiments can be set up with different geometries such as phase conjugate (PC-DFWM) or backward geometry, BOXCARS or forward geometry and nearly counter-propagating (NCP-DFWM) geometry.

The detailed theoretical description of PC-DFWM configuration was developed by Yariv and Pepper in 1977 for non-absorbing materials. Later, linear absorption was included and theory was generalized by Caro and Gower in 1982. Through a steady-state theory they were able to relate the amplitude of DFWM signal parameters to the third order nonlinear optical susceptibility of the material. Their analysis can be applied to the forward geometry and also to other configurations.

Let us assume the angle between the three incident waves to be small so that these beams may be treated as collinear over the interaction length in the material sample. Each of the incident beams is further approximated to a monochromatic plane wave (steady-state approximation).

The incident applied fields induce a polarization $\vec{P}^{(3)}$ in the medium which is given by (Butcher and Cotter 1990)

$$P^{(3)}(r, t) = \varepsilon_0 \int_{-\infty}^{+\infty} d\tau_1 \int_{-\infty}^{+\infty} d\tau_2 \int_{-\infty}^{+\infty} d\tau_3 R^{(3)}(\tau_1, \tau_2, \tau_3) E(r, t - \tau_1) E(r, t - \tau_2) E(r, t - \tau_3) \quad (2.27)$$

$R^{(3)}$ is the time domain response function, a 4th rank tensor which relates the magnitude of the third-order polarization to the magnitude of the applied field.

The DFWM signal wave at frequency ω may be written as (Caro and Gower 1982, Shen 1986 and MacKenzie et al. 1986)

$$P^{(3)}(r, t) = \frac{1}{2} \left[P_{\omega}^{(3)}(r) \exp(-i\omega t) + c.c \right] \quad (2.28)$$

where

$$\left(P_{\omega}^{(3)}(r) \right)_i = \varepsilon_0 \frac{3}{4} \sum \left\{ \chi_{ijkl}^{(3)}(-\omega, \omega, \omega, -\omega) A_F(r)_j A_B(r)_k A_P^*(r)_l \times \exp \left[i(k_F + k_B - k_P^*) \cdot r \right] \right\} \quad (2.29)$$

The indices i, j, k, l represents Cartesian coordinates. The subscripts F, B and P represent the two pump beams (F and B) and a probe beam (P), respectively. A_i is scalar amplitude of the field along one of the axes. The approximation assumes that the nonlinear interaction is weak, and amplitudes of the incident fields are considered to be constant along the medium, implying no pump depletion. In the small incidence

angle limit the electric field polarization of the probe beam can be taken to be along one of the axes (x or y-polarized). Equation 2.29 can then be written as

$$\left(P_{\omega}^{(3)}(r)\right)_D = \varepsilon_0 \frac{3}{4} \chi_{DFBP}^{(3)}(-\omega, \omega, \omega, -\omega) A_F(r)_j A_B(r)_k A_P^*(r)_l \times \exp\left[i(k_F + k_B - k_P^*) \cdot r\right] \quad (2.30)$$

The interaction of two pump beams and a probe beam generates third-order nonlinear optical polarization $\left(P_{\omega}^{(3)}(r)\right)_D$ that radiates the DFWM signal wave (D-wave) whose amplitude and polarization is determined by $\chi_{DFBP}^{(3)}$ (Kühlke 1984, Eyring and Fayer 1984, Fourkas et al. 1992 and Fourkas et al. 1992). The role of nonlinear absorption and self-focusing/defocusing which are induced from incident fields are not considered for this analysis (Yariv 1989).

All nonlinear wave mixing phenomena involve energy transfer between the interacting waves. For efficient energy transfer between the waves, conservation of wave energy and wave momentum must be satisfied (Butcher and Cotter 1990 and Bloembergen 1980). Energy conservation in DFWM leads to the following equation for the frequency of the signal wave

$$\omega_D = \omega_F + \omega_B - \omega_P \quad (2.31)$$

Balancing the momentum for the four interacting waves leads to a phase mismatch Δk given by

$$\Delta \vec{k} = (\vec{k}_F + \vec{k}_B - \vec{k}_P) - \vec{k}_D \quad (2.32)$$

where $|\vec{k}| = \frac{2\pi n_0}{\lambda}$

Ideally, the phase mismatch must be zero. For forward folded BOXCARS configuration, by arranging the angles of the interacting beams to be small, the phase mismatch can be minimized.

Using Maxwell's equation the intensity of DFWM signal can be derived following the coupled wave theory (Butcher and Cotter 1990, Yariv 1989 and Fisher 1983). In the limit of weak nonlinearity and applying the slowly varying envelope approximation (Shen 1984, Yariv and Pepper 1977 and Butcher and Cotter 1990), the intensity of the signal wave as a function of Δk may be obtained as

$$I_4 = I_1 I_2 I_3 \frac{9\omega^2 |\chi^{(3)}|^2 T(1-T)^2}{16c^4 n_0^4 \epsilon_0^2 \alpha_0^2} \left[\frac{\sin(|\Delta k|L/2)}{|\Delta k|L/2} \right] \quad (2.33)$$

where T is the transmittance of the sample, n_0 is the linear refractive index, ϵ_0 is the dielectric constant, α_0 is the linear absorption coefficient and L is the sample thickness.

For perfectly phase matched DFWM process $\Delta k = 0$ and, hence, equation 2.33 reduces to

$$I_D = I_F I_B I_P \frac{9\omega^2 |\chi^{(3)}|^2 T(1-T)^2}{16c^4 n_0^4 \epsilon_0^2 \alpha_0^2} \quad (2.34)$$

If the sample is non-absorbing, the above equation becomes

$$I_D = I_F I_B I_P \frac{9\omega^2 |\chi^{(3)}|^2 L^2}{16c^4 n_0^4 \epsilon_0^2} \quad (2.35)$$

Equation 2.35 gives the intensity of DFWM signal which depends on the sample length L , third-order nonlinear optical susceptibility $|\chi^{(3)}|$ and the product of the intensities of the other three interacting beams.

The generation of DFWM signal wave in LIG process is described by two steps (Eichler et al. 1986). The first being the formation of a laser-induced grating by the interference of two pump beams in the nonlinear medium, and the second being the diffraction of the probe beam from the formed LIG. The intensity of the diffracted beam provides information on the grating amplitude and therefore the magnitude of the medium nonlinearity. Depending upon the nature of the grating more than one order can be generated during diffraction process (Eichler 1977, Wherrett et al. 1983, Trebino et al. 1986 and Fourkas et al. 1992).

The interference pattern due to the mixing of two plane waves may be expressed as

$$I(x) = I_1 + I_2 + 2\Delta I \cos\left(\left|\vec{q}_{21}\right|x\right) \quad (2.36)$$

where $\Delta I = \sqrt{I_1 I_2}$ and \vec{q}_{21} is the grating vector, determined by the wave vectors of the interfering waves

$$|\bar{q}_{21}| = |\bar{k}_2 - \bar{k}_1| \quad (2.37)$$

The grating period Λ is determined by the beam angle θ_w by

$$\Lambda = \frac{\lambda}{2n_0 \sin(\theta_w/2)} \quad (2.38)$$

The intensity modulation in the interference pattern causes periodic modulation in the complex refractive index n of the nonlinear medium. When the modulations are due to change in the real part of n , a *phase grating* is created, while changes in the imaginary part of n results in an *amplitude grating*. A mixed grating is obtained when both the real and imaginary part of n are modulated (Eichler et al. 1986).

2.2.5 Measuring $\chi^{(3)}$

Determining the value of $\chi^{(3)}$ requires the knowledge of interaction length of the beams inside the sample, their absolute energy, the pulse shape, etc. We have adopted the simpler procedure of measuring the relative value of $|\chi^{(3)}|$ for the new material with respect to that of a standard reference material such as CS₂. This procedure is seen to yield fairly accurate values. All measurements are conducted at 532 nm, CS₂ used as the reference, for which $|\chi^{(3)}|$ is taken to be 4×10^{-13} esu (Shirk et al. 1992).

The $|\chi^{(3)}|_{sample}$ can be measured relative to a reference $|\chi^{(3)}|_{ref}$. Maintaining the same experimental conditions, DFWM signal level is measured as a function of pump energy for the sample as well as the reference. The data obtained is fitted to the following cubic equation for both cases

$$S_D = v \cdot S_L^3 \quad (2.39)$$

For non absorbing materials the $|\chi^{(3)}|_{sample}$ can be calculated as

$$|\chi^{(3)}|_{sample} = |\chi^{(3)}|_{ref} \left(\frac{I_{sample}}{I_{ref}} \right)^{1/2} \left(\frac{n_{sample}}{n_{ref}} \right)^2 \left(\frac{l_{ref}}{l_{sample}} \right) \quad (2.40)$$

For samples that absorb the laser light, the above expression gets modified to

$$\left| \chi^{(3)} \right|_{sample} = \left| \chi^{(3)} \right|_{ref} \left(\frac{I_{sample}}{I_{ref}} \right)^{1/2} \left(\frac{n_{sample}}{n_{ref}} \right)^2 \left(\frac{l_{ref}}{l_{sample}} \right) \left(\frac{\alpha_0 l}{e^{-\alpha_0 l/2} (1 - e^{-\alpha_0 l})} \right) \quad (2.41)$$

where I_{sample} and I_{ref} are DFWM signal intensities, n_{sample} and n_{ref} are their linear refractive index, l_{ref} and l_{sample} is interaction length in the medium, and α_0 is the linear absorption coefficient at 532 nm.

The second-order hyperpolarizability (γ_h) of the complex was estimated using following relation (Gong et al. 1992).

$$\gamma_h = \chi^{(3)} / L^4 N \quad (2.42)$$

where, N is the density of molecules in the unit of molecules per cm^3 . The term L is the local field factor given by $L = (n^2 + 2)/3$ and n is refractive index.

2.2.6 DFWM experimental setup and measurement

The DFWM experiments were set up using forward folded BOXCARs configuration. In order to achieve “folded BOXCARs” the input laser beam is split into three beams and they are aligned such that they form spots on the three corners of a square in the input plane, as shown in Figure 2.7. A Q-Switched Nd: YAG laser (Spectra Physics GCR 170) of wavelength 532 nm producing pulses of width 7 ns at 10 Hz repetition rate was used as the excitation source. Intensity of the each beam was kept same. The input intensity is measured using pyroelectric detector (RjP735). The three beams are focused using a plano-convex lens (focal length =50 cm). The three beams need to be spatially and temporally overlapped in order to generate the signal. The DFWM signal is generated due to phase matched interaction ($k_4 = k_3 - k_2 + k_1$). A mask is placed just after the collimating lens to block beams 1, 2 and 3 as well as self-diffracted beams and scatter coming from the sample, allowing the DFWM signal to pass. The signal is detected using another pyroelectric detector (RjP-735). Both the detectors are connected to the energy meter (Rj-7620). The laser energy at the sample was varied by the combinations of neutral density filters. Measurements were done on each sample by recording the intensity of the generated signal verses the input intensity. The strength of this signal beam is proportional to the $\chi^{(3)}$. The output

signal will exhibit a cubic power-dependency on the incident intensity is shown Figure 2.8.

In a DFWM experiment, reference material with known values of $|\chi^{(3)}|_{ref}$ must be used to obtain the magnitude of $|\chi^{(3)}|_{sample}$ for a new sample by using Equation (2.41)

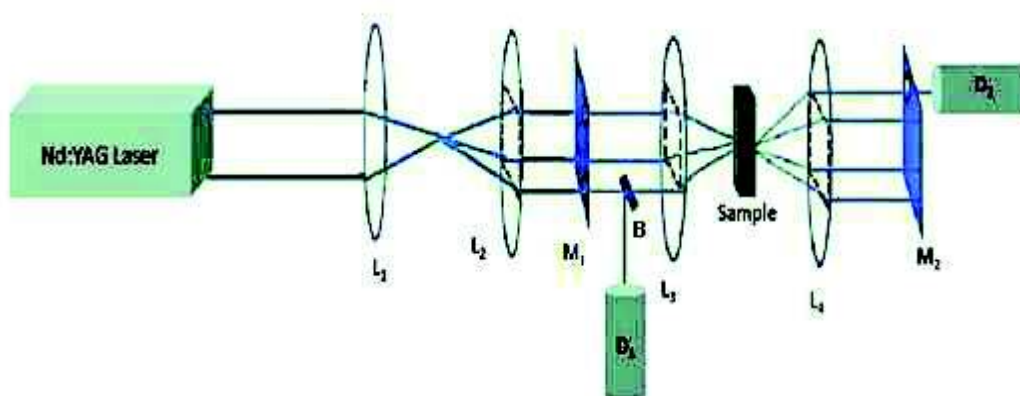


Figure 2.7 DFWM setup in the forward BOXCARS configuration

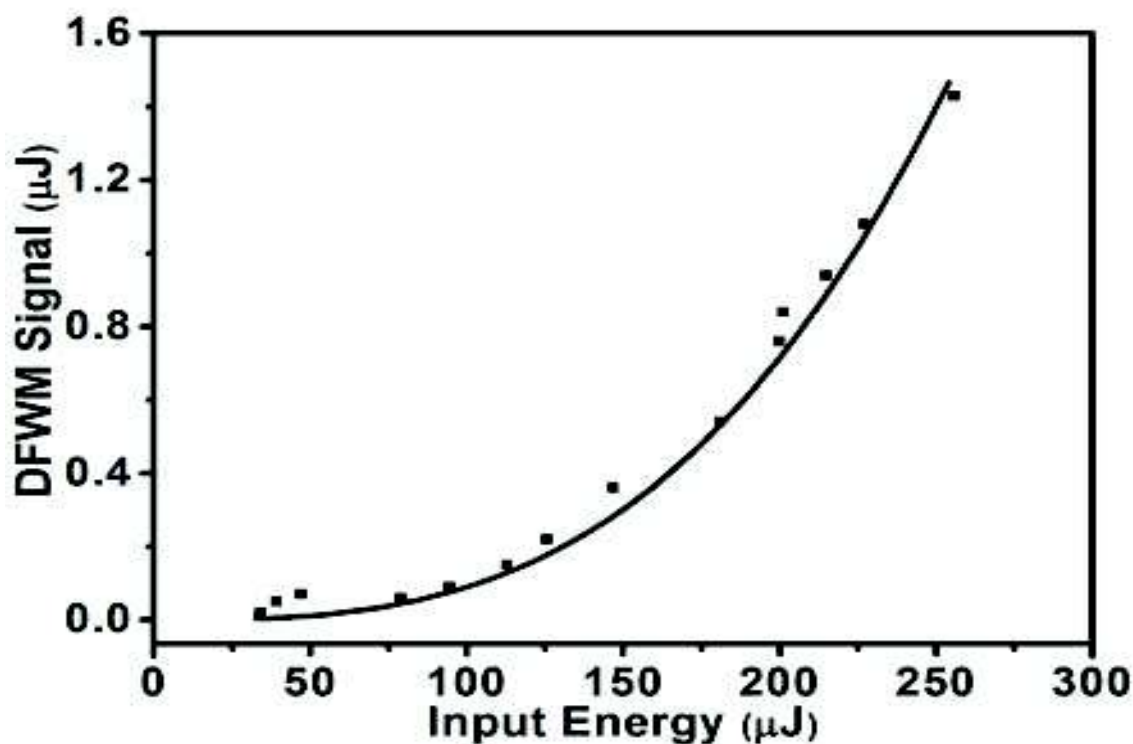


Figure 2.8 Typical Variation of the DFWM signal as a function of the input energy

2.3 OPTICAL POWER LIMITING: ENERGY DEPENDENT TRANSMISSION

2.3.1 Introduction

As the name implies, an optical power limiter (OPL) is a device designed to keep the power, irradiance, energy, or fluence transmitted by an optical system below a specified maximum value regardless of the input. The optical power limiter is one of the important devices to control the high intensity light. An ideal nonlinearly absorbing medium for optical power limiting should exhibit very high linear transmissivity for a weak input optical signal, but possess much lower nonlinear transmissivity for an intense optical signal. The input-output energy relationship of an ideal optical limiter is shown in Figure 2.9. The most important application of such a device is the protection of sensitive optical sensors and components from laser damage. It has also been demonstrated that optical power limiter can be used for pulse shaping and smoothing and pulse compression (Band et al. 1986 and He et al. 1998). The optical power limiters are broadly classified into two categories, active optical power limiter and passive optical power limiter (Tutt and Boggess 1993). In active optical power limiter the transmittance is actively controlled by external feedback mechanism, but it is usually a slow process and, hence, not fit for practical applications (Hagan 2001).

On the other hand, passive optical power limiting systems uses nonlinear optical material that acts as combined sensor, processor and modulator; on the other hand the transmittance reduces automatically above the threshold intensity level. The advantages of the passive OPL are high speed, simplicity, compactness and low cost.

For practical applications a good optical power limiter has to satisfy some of the following requirements,

1. Low input threshold
2. Fast response time (i.e. the response should be for pulses shorter than 10 μ s)
3. Broadband response
4. Low optical scattering
5. Must be robust and have long operating life

The physical mechanisms responsible for passive power limiting can be divided into two different classes of optical nonlinearities, i.e. instantaneous and

accumulative nonlinearities. In an instantaneous process the response of the nonlinearity to the applied optical field occurs immediately. Two-photon absorption and Kerr effect are the examples of instantaneous nonlinearity. The accumulative nonlinearities arise when the induced nonlinear polarization either develops or decays on a timescale comparable to or longer than the excitation duration. In other words, the instantaneous nonlinearity depends on the instantaneous intensity within the medium whereas the accumulative nonlinearity is based on energy transfer from the optical field to the material and is dependent on the energy density, fluence, deposited on the medium (Tutt and Boggess 1993). The most important instantaneous process associated with OPL is two-photon absorption (TPA) (Kershaw et al. 1998). The examples of accumulative nonlinearities in optical limiting are excited state absorption (Sun and Riggs 1999 and Perry 1997) and nonlinear refraction (Kamada et al. 1999).

The most important mechanisms involved in optical power limiting are two photon absorption (TPA) (Kershaw et al. 1998), reverse saturable absorption (RSA) (which translates into increased optical absorption with increased incident optical intensity) (Sun and Riggs 1999), nonlinear refraction (due to molecular reorientation, electronic Kerr effect, excitation of free carriers, photorefractive, optically induced heating in the material) (Perry et al. 1997) and induced scattering (optically induced heating or plasma generation in the medium).

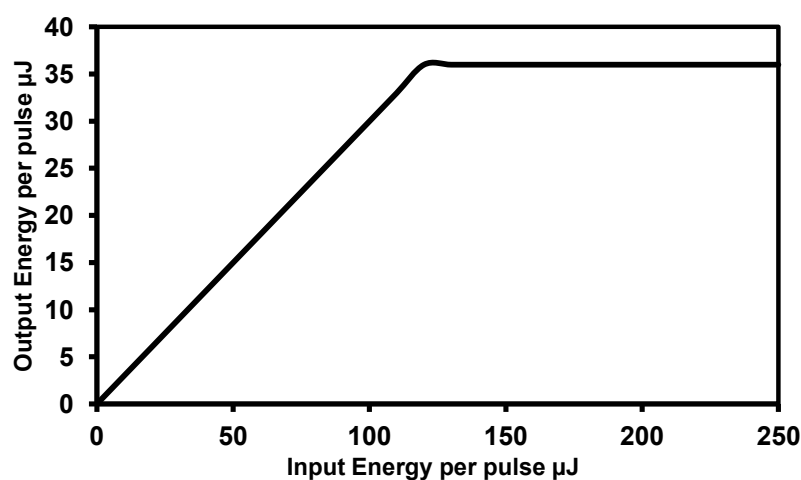


Figure 2.9 Typical response of an ideal optical limiter

The two-photon absorption is an instantaneous nonlinearity. In this case electron is promoted from ground state to an excited state through a virtual intermediate state by simultaneously absorbing two photons (Kershaw et al. 1998).

The reverse saturable absorption was first observed by Giuliano and Hess in 1967 (Giuliano and Hess 1967). There are two conditions required for RSA to occur: (1) Molecules in the ground state and in the excited state can absorb incident photons with the same frequency; (2) The absorption cross section of the excited states must be larger than that of the ground state.

2.3.2 Experimental Setup

For optical power limiting measurements, the laser beam (Nd: YAG 532 nm, 7 ns) was focused on the sample, by a convex lens of focal length 25 mm, giving a focussed spot radius of 18.9 μm . By varying the input laser energy, the change in transmitted energy is measured using the Pyroelectric detectors with Laser Probe Rj-7620 Energy meter. The experimental set up is as shown in Figure 2.10.

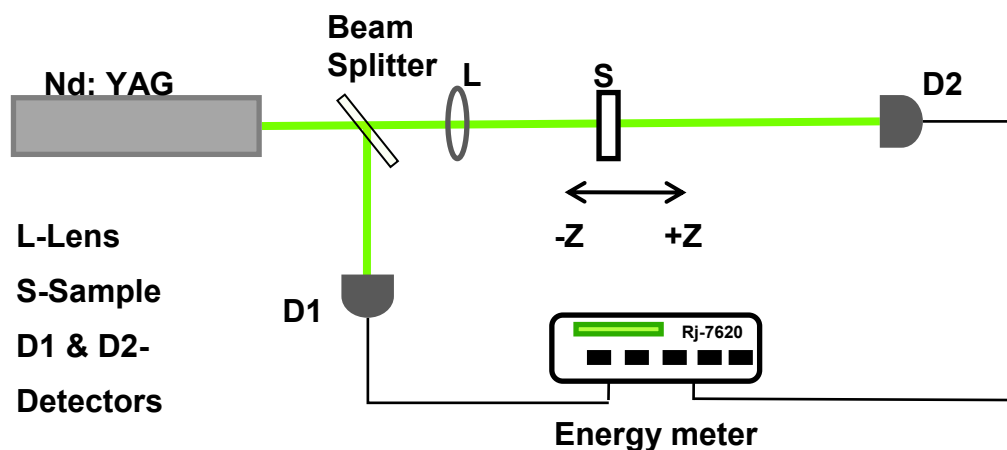


Figure 2.10 Experimental setup for optical power limiting

2.4 ALL-OPTICAL SWITCHING: PUMP-PROBE TECHNIQUE

2.4.1 Introduction

All-optical devices use light either in the form of the signal itself or as a separate control beam to influence some operating characteristics, typically the

transmission of light through the device. A switch is a basic building block of information processing systems. The key element in an all-optical switch is a material that exhibits large nonlinear optical response. High-Speed and high sensitivity optical devices play an important role in optical information processing, optical computation and optical communications. Therefore study of all-optical switching characteristics is of great importance. The optical switching property is closely linked to the NLO properties of the material used for making the device (Almeida et al. 2004, Haque and Nelson 2010, Mingaleev et al. 2006, Hu et al. 2008 and Hales et al. 2010).

The phenomenon of excited state absorption (ESA) is a promising mechanism of all-optical switching in which a pump beam excites the molecules from the ground to the excited-state that leads to modulation of the transmission of a probe beam. All-optical switching based on ESA, using a pump-probe configuration is a simple, flexible and convenient technique for practical applications compared to other methods, for instance those based on phase conjugation and interference phenomena (Abdeldayem et al. 2003, Li et al. 1994, Roy and Yadav 2011, Li et al. 1994, Wang et al. 2010, Henari and Cassidy 2012, Sharma et al. 2005, Singh et al. 2005 and Charas et al. 2011). The transmission of the cw probe beam gets modulated due to the intensity-induced changes in the population of the ground and excited states by a cw or pulsed pump beam depending on the kinetic and spectral response of the material (Sharma et al. 2005, Singh et al. 2005 and Charas et al. 2011). All-optical switching based on ESA using the pump-probe technique has been recently reported in a variety of organic and inorganic systems that include, polydiacetylene (Abdeldayem et al. 2003), metallophthalocyanine (Li et al. 1994 and Roy and Yadav 2011), C₆₀ (Li et al. 1994), graphene (Wang et al. 2010), organometallic phthalocyanine (Dasari et al. 2011), twisted π -system chromophores (He et al. 2011), congo red solution (Henari and Cassidy 2012), TiO₂ nanowires (Zhang et al. 2011), polymethine dyes (Sharma et al. 2005), metalloporphyrins (Singh et al. 2005), and Ter(9,9'-spirobifluorene)-co-methylmethacrylate copolymer (Charas et al. 2011) and aqueous silver nanoparticles (Hari et al. 2012).

2.4.2 Experimental setup

Pump-probe technique is used to study the all-optical switching capability of the metal-organic complexes. It is a popular technique to determine all-optical switching properties (Singh et al. 2005, Abdeldayem et al. 2003, Wu et al. 2004, Liu et al. 2004, Wang et al 2010, Wu et al. 2003, Wu et al. 2003, Xu et al. 2008, Luo et al. 2005 and Xu et al. 2008). This involves measuring the transmittance of a weak probe pulse when the sample is pumped by a strong pump beam. An all optical switching action can take place by transmitting both continuous probe beam and pulsed pump beam through the switching material. Interaction of these two beams will modify the intensity of the output probe beam. In our experiment the Q-Switched Nd: YAG laser pulses of wavelength 532 nm and 7 ns pulse width was used as the pump beam. The probe beam was a low-power (2 mW) continuous wave He-Ne laser beam of wavelength 633 nm. The pump and probe beams were focused on the sample using two convex lenses of focal length 25 and 30 cm respectively. The sample is placed in the path of Q-Switched Nd: YAG laser beam. The nonlinear optical properties of the samples induced by the pump beam will be monitored by detecting the probe beam. The transmitted time-dependent probe beam was detected using a photomultiplier tube (PMT) (R928P, Hamamatsu). The signal was analyzed using a Digital Storage Oscilloscope (500 MHz, HP 54616B), which was triggered by the Nd: YAG laser. The typical experimental set up is shown in Figure 2.11. When the sample is pumped by a strong beam of wavelength 532 nm, the output intensity of the probe beam from the sample is low (defined as ‘off state’). When pump beam is blocked from the sample the intensity of output probe beam is high (defined as ‘on state’). Thus the sample exhibits an all-optical switching effect. Figure 2.12 shows a typical optical switching curve as seen in the oscilloscope.

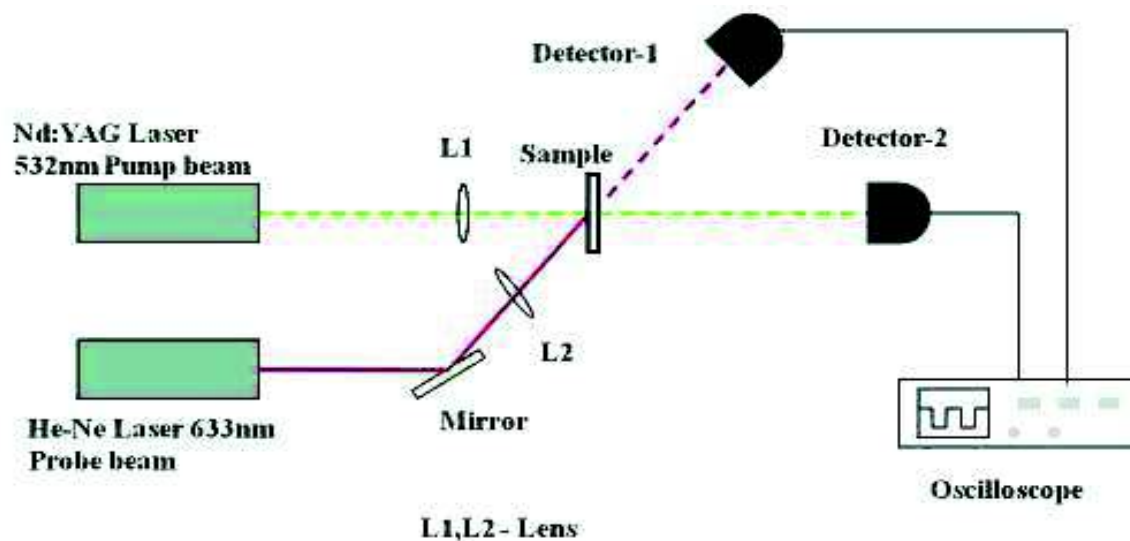


Figure 2.11 Experimental setup for studying the all-optical switching characteristics

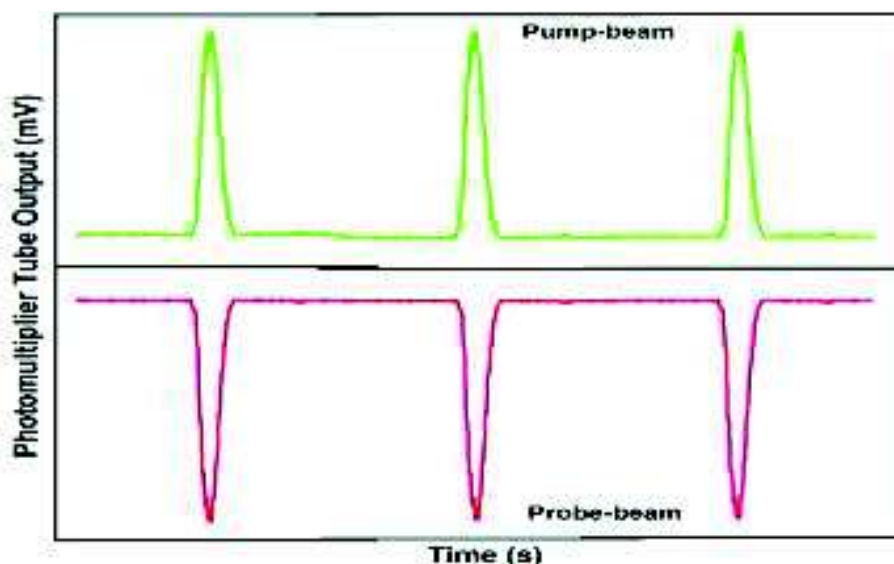


Figure 2.12 Typical all-optical switching waveforms as seen in the oscilloscope

In general, the intensity of the probe beam is considered to be very weak compared to the pump beam so that the probe beam does not affect the material response. The switching characteristics are not affected by the probe beam intensity, provided the absorption spectra of the ground and the excited-state do not match the wavelength of the probe light. Moreover, the switching time is limited ($\sim\mu\text{s}$ – ms) by the long lifetime of the triplet state in organic molecules (Roy and Yadav 2011).

2.5 SAMPLE PREPARATION

Palladium and ruthenium metal based metal-organic complexes were studied for our investigations. We have investigated the optical nonlinearities of these metal complexes in solution and as well as solid state form. To prepare the solution of these metal-organic complexes, research grade N,N-dimethylformamide (DMF) was used as the solvent. Solutions of different concentrations were taken in a quartz cuvette of path length 1 mm for the experiments. The metal-organic complexes were dispersed into Poly (methyl methacrylate) to fabricate the test samples in the solid state form.

Poly (methylmethacrylate) (PMMA) is often used as the host polymer because it is a hard, rigid and transparent polymer with a glass transition temperature of 125⁰C. It is mechanically tougher than polystyrene. It's molecular formula is (C₅H₈O₂)_n and the structure is as given below,

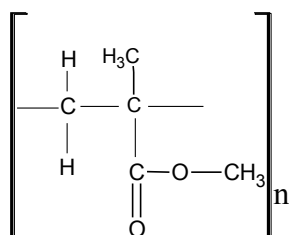


Figure 2.13 Structure of PMMA

PMMA is a polar (proton acceptor) material and has a large dielectric constant. PMMA is a thermoplastic and can be melted and moulded into any desired shape. PMMA's physical durability is far superior to that of other thermoplastics. Its resistance to environmental factors is markedly superior to that of other thermoplastics. It is the most commonly used polymeric material because of its optical transparency. Its laser damage threshold is far superior to that of other polymers (Zidan 2003). We have, therefore, selected PMMA as the polymer into which the NLO samples are doped.

For the preparation of the solid-state metal complex-polymer films, 1 g of PMMA (Sigma Aldrich, Mw. 1,00,000) was added to 4 ml of 1,2 – Dichlorobenzene (DCB) in a glass vial placed on a magnetic stirrer and stirred for about 6 h at room temperature to ensure that it is completely dissolved. A specific quantity of the metal

complex was added to the PMMA solution and stirred for about 40 h and also ultrasonicated for 2 h. As a result a homogeneous solution was obtained. A thin layer of this solution was deposited on circular glass slides, of diameter of 22 mm and thickness of 0.15 mm by Spin Coating technique. The glass substrates were cleaned prior to use adopting the following procedure:

- Dip the glass slide into 3:1 mixture of H₂SO₄ and H₂O₂ (pirana etch) solution for about 15 minutes.
- Clean with de ionized water for 5 minutes.
- Rinse with de ionized water for 1 minute.
- The glass slide is baked in open on a hot plate at about 100 °C.

The film samples were deposited using freshly prepared complex/polymer solution on cleaned glass substrate by using a Spin Coater (Milman, SPN 2000). A few drops of the solution were placed on the glass substrate using a glass syringe and the substrate is spun at a speed of 1200 rpm for 10 sec. The substrate was then kept on a Hot Plate at 60 °C for 10 h to facilitate the removal of residual solvent. The concentration of the dopant in the polymer matrix was calculated using the following relation

$$\text{Wt (\%)} \text{ of the dopant} = \frac{\text{Wt (gm) of the dopant}}{(\text{Wt (gm) of the dopant} + \text{PMMA})} \times 100$$

2.6 LINEAR OPTICAL CHARACTERIZATION

To determine the linear optical properties of the metal-organic complexes, the following techniques were employed in our investigations

2.6.1 UV-Vis Absorption Spectroscopy

Ultraviolet and Visible Absorption Spectroscopy was used to identify the electronic transitions occurring in the samples. This data is used to determine the strength of single photon absorption at the wavelength of the laser used for Z-scan. The UV –Vis spectra of all the samples were recorded at room temperature using a Fibre-optic Spectrometer (SD 2000, Ocean Optics Inc.) for the samples.

2.6.2 Refractive Index Measurement

The refractive index of the samples in solution form was measured using Abbe's Refractometer (Make: Advance Research Instruments, New Delhi) at desired wavelength. In the case of film samples, the refractive index was obtained using Spectroscopic Ellipsometry (Sentech SE 800).

2.6.3 Film Thickness Measurement

The thickness of the sample films was obtained by Spectroscopic Ellipsometry (Sentech SE 800) and was found to be $\approx 11 \mu\text{m}$. Cross sectional scanning electron microscope pictures confirmed this value of the thickness of the film.

CHAPTER 3

CHAPTER 3

THIRD-ORDER NONLINEAR OPTICAL STUDIES OF SCHIFF BASE CONTAINING PALLADIUM METAL-ORGANIC COMPLEXES

Abstract

This chapter describes the results of Z-scan, DFWM, optical power limiting and all-optical switching studies on series of palladium metal-organic complexes. A possible mechanism responsible for the third-order nonlinearity of the compounds has been discussed. An attempt has been made to establish the molecular structure-NLO property relationship. The study of concentration dependent third-order NLO and optical power limiting capabilities and intensity dependent all-optical switching studies of these metal-organic complexes have also been presented.

3.1 INTRODUCTION

Among various methods to enhance the third-order nonlinearity of organic materials, incorporating metals into organic molecules adds a new dimension to the search of new materials suitable for photonic devices. The insertion of a metal ion into a conjugated structure may significantly influence the π -electron behavior in the molecule. Organometallic and coordination compounds, with multi-dimensional π -conjugated systems, are amongst the most promising third-order nonlinear materials due to their generally high chemical and thermal stability (Nalwa and Miyata 1997). Compounds containing transition metals possess new properties due to the presence of various excited states on account of low-lying $d-d$ electronic transitions in these systems. Furthermore, the ligand-metal bonding results in large molecular hyperpolarizability due to the transfer of electron density between the metal atom and the ligand systems (Nalwa 1991). This transfer causes the electron orbitals of the ligands to overlap with the metal orbitals, thus leading to large intermolecular

interactions and excellent ultrafast non-resonant nonlinear response (Nalwa and Miyata 1997). Some organometallic and coordination compounds have shown significant frequency doubling responses in which the metal acts to reinforce planarity and to improve π -type mixing between donor and acceptor regions. The most common types of organometallics and coordination compounds are polysilanes, metal polyynes, metallocenes, metal dithiolenes, metal porphyrincomplexes, metal carbonyl complexes and metal phthalocyanine complexes.

Schiff bases are a class of organic compound which contain a carbon-nitrogen double bond with the nitrogen atom connected to an aryl or alkyl group but not hydrogen. Schiff bases can form stable complex with metals. The Schiff base transition metal complexes are very attractive due to their easy synthesis, chemical and thermal stability. In this class of materials, the NLO properties can be enhanced by adopting suitable design strategies such as donor- π -bridge-acceptor (D- π -A), donor- π -bridge-donor (D- π -D), acceptor- π -bridge-donor- π -bridge-acceptor (A- π -D- π -A), and donor- π -bridge-acceptor- π -bridge-donor (D- π -A- π -D) conjugated structures (Das et al. 2006). Introduction of a metal ion into these π -conjugated structures results in polarizable d orbital electrons and the charge transfer mechanism of metal to ligand contributes to the larger nonlinear activity of these materials (Huang et al. 2008, Benson et al. 1994, He et al. 2008 and Deng et al. 2000). Metal ions, being excellent templates, can gather many organic one dimensional dipolar chromophores to form two dimensional and three dimensional NLO-phores. Furthermore, metal centers insert more sublevels into the energy hierarchy which allows additional electronic transitions leading to the NLO response. Incorporation of a metal into the organic chromophores enhances the laser damage threshold, optical quality, thermal and photochemical stability (Das et al. 2006).

Polymethylmethacrylate (PMMA) is widely used as a host polymer because it is a sufficiently hard and rigid polymer, transparent in the visible spectral range, has fairly high laser damage threshold and a glass transition temperature of 125 °C. PMMA is also a polar material and has larger dielectric constant than any other thermoplastics (Zidan 2003).

In the search for new materials for NLO device applications, the incorporation of electron withdrawing and donating groups is seen to affect the third-order nonlinear optical properties of metal-organic complexes. With this in mind we synthesized a series of palladium containing triphenylphosphine and Schiff base ligands. These metal-organics exhibit interesting electronic and optical properties tunable by virtue of the coordinated metal ion in the centre of the molecule. In the UV–Vis spectral region, often two different transitions occur in metal-organic complexes, viz. a strong intra-ligand charge-transfer transition and a low-energy metal to ligand/ligand to metal charge-transfer transition. These transitions lead to enhanced NLO properties. A major advantage of palladium metal-organic complex is that it can be grown as a crystal or it can be incorporated into a suitable polymer matrix, thereby enhancing the chemical and physical stability of the organic materials while retaining strong NLO properties.

In this chapter we report the results of third-order nonlinear optical properties of palladium metal-organic complex measured by Z-scan and DFWM methods in the 532 nm wavelength region. The optical power limiting and all-optical switching ability of the complex were also experimentally revealed by performing energy dependent transmission and pump-probe experiments.

3.2 SYNTHESIS AND CHARACTERIZATION OF Pd COMPLEXES

3.2.1 Materials and Methods

Analytic grade chemicals were used for synthesizing all the samples. Solvents were purified and dried according to standard procedure (Vogel 1989). Salicylaldehyde, 2-hydrazinopyridine, and anhydrous PdCl₂ were purchased from Merck and were used without further purification. Detailed synthesis, characterization of ligand and complexes were reported in the literature (Dileep and Bhat 2010).

Electronic spectra of the complexes, dissolved into CH₃OH solvent, were measured on a GBC Cintra 101 UV-Vis double beam Spectrophotometer in the 200–800 nm wavelength range. FT-IR spectra of the complexes were recorded on a Thermo Nicolet Avatar FT-IR Spectrometer in the frequency range 400–4000 cm⁻¹.

The C, H and N contents were determined by Thermoflash EA1112 series elemental analyzer. ^1H and ^{13}C NMR spectra were recorded in Bruker AMX 400 instrument using TMS as internal standard. ^{31}P NMR spectra were recorded in Bruker AMX 400 instrument in CDCl_3 with H_3PO_4 as a reference. Magnetochemical measurements were recorded on a Sherwood UK magnetic balance.

3.2.2 Synthesis of ligand L1-L4

A solution of salicylaldehyde or 5-sub-salicylaldehydes (0.03 mmol) in methanol (10 cm^3) was added to a solution of 2-hydrazinopyridine (0.006 g, 0.03 mmol) in methanol (10 cm^3). The mixture was stirred for 15 minutes at room temperature. The yellow colored solid formed was filtered, washed with water and recrystallized using alcohol.

L1-- (N-(2-pyridyl)-N'-(5-nitrosalicylidene)hydrazine)

L2-- (N-(2-pyridyl)-N'-(5-chlorosalicylidene)hydrazine)

L3 -- (N-(2-pyridyl)-N'-(salicylidene)hydrazine)

L4 -- (N-(2-pyridyl)-N'-(5-methoxysalicylidene)hydrazine)

Table 3.1 Yield, CHN, IR and NMR data of the ligands L1 – L4

Ligand	CHN found (Calculated)	IR (KBr, cm^{-1})	^1H NMR (CDCl_3 , δ ppm)
L1 $\text{C}_{12}\text{H}_{10}\text{N}_4\text{O}_3$ Yield: 78%.	C: 55.59 (55.81) H: 3.68 (3.90), N: 21.34 (21.70)	3091, 1615, 1318, 602, 490	6.6-7.3 (m, 7H, Ar-H), δ 8.7 (1H, $-\text{CH}=\text{N}-$), δ 10.3 (Ar-OH).
L2 $\text{C}_{12}\text{H}_{10}\text{ClN}_3\text{O}$ Yield: 82%.	C: 58.05 (58.19), H: 3.98 (4.07) N: 16.77 (16.97)	3090, 1620, 1324, 605, 488	6.6-7.3 (m, 7H, Ar-H), δ 8.7 (1H, $-\text{CH}=\text{N}-$), δ 10.3 (Ar-OH).

L3 $C_{12}H_{11}N_3O$ Yield: 79%.	C: 67.30 (67.59), H: 5.09 (5.20), N: 19.57 (19.71)	3092, 1612, 1321, 609, 490	6.6-7.3 (m, 8H, Ar-H), δ 8.8 (1H, -CH=N-), δ 10.3 (Ar-OH).
L4 $C_{13}H_{13}N_3O_2$ Yield: 75%.	C: 63.98 (64.19), H: 5.21 (5.39), N: 17.05 (17.27)	3095, 1610, 1320, 614, 487	4.1 (Ar-OCH ₃) 6.6-7.3 (m, 7H, Ar-H), δ 8.7 (1H, -CH=N-), δ 10.3 (Ar-OH).

3.2.3 Synthesis of $PdCl_2(PPh_3)_2$

A 0.01 mol of $PdCl_2$ was added to a solution of triphenylphosphine (0.02 mol) in tetrahydrofuran. The mixture was refluxed for 5 hours with constant stirring. The dark yellow colored precipitate was filtered and washed (Asma et al. 2006).

3.2.4 Synthesis of Pd Complexes

Complexes **PdL1-PdL4** were prepared by stirring a mixture of [$PdCl_2(PPh_3)_2$] in 3 cm³ of 0.1M sodium acetate and the respective ligands (L1-L4) in 15 cc alcohol in a 1:1 ratio for 5 hours. The red colored solid was filtered off, washed with ethanol and dried in *vacuo*. The characterization data are given in Tables 3.2 and 3.3.



L: L1/L2/ L3/L4

Scheme: Synthetic scheme of palladium complexes

Complex	Abbreviation
$Pd(L1)PPh_3$	PdL1
$Pd(L2)PPh_3$	PdL2
$Pd(L3)PPh_3$	PdL3
$Pd(L4)PPh_3$	PdL4

Table 3.2 Yield, CHN and IR data of the palladium complexes (PdL1 – PdL4)

Palladium complex	CHN found (Calculated)	IR (KBr, cm ⁻¹)
PdL1 <i>C₃₀H₂₄N₄O₃PPd</i> Yield: 72%	C: 57.26(57.57), H: 3.67(3.86), N: 8.72(8.95) Pd: 16.83(17.00)	3099 (s), 619, 481 (m), 1595 (s), 1351 (w), 549 (m), 1429, 1087, 695.
PdL2 <i>C₃₀H₂₄ClN₃OPPd</i> Yield: 75%.	C: 58.25 (58.55), H: 3.68(3.93), N: 6.46(6.83), Pd: 17.19(17.29)	3110 (s), 620, 478 (m), 1597 (s), 1330 (w), 545 (m), 1435, 1101, 690.
PdL3 <i>C₃₀H₂₅N₃OPPd</i> Yield: 79%.	C: 61.84 (62.02), H: 4.21(4.34), N: 7.12(7.23), Pd: 18.15(18.32)	3105 (s), 623, 479 (m), 1592 (s), 1345 (w), 550 (m), 1446, 1095, 697.
PdL4 <i>C₃₁H₂₇N₃O₂PPd</i> Yield: 75%.	C: 60.41 (60.94), H: 4.28(4.45), N: 6.67(6.88), Pd: 17.34(17.42)	3109 (s), 618, 482 (m), 1586 (s), 1346 (w), 550 (m), 1428, 1105, 695

Table 3.3 NMR data of the palladium complexes (PdL1 - PdL4)

Palladium complex	¹ H NMR (CDCl ₃ , δ ppm)	¹³ C NMR (ppm)	³¹ P NMR (H ₃ PO ₄ , δ ppm)
PdL1	3.8 (s, 1H, N-H), 6.6-7.4(m, 15 H, Ar-H), 7.4-7.8 (m, 8 H, Ar-H), 8.6 (d, 1 H, -CH=N-)	166.18 (C-O), 153.39 (C=N), 144.42 (C-P), 161.61, 147.17, 137.01, 114.55, 105.97 (Carbon atoms in Pyridine), 119.03, 119.41, 129.81, 131.69, 140.73 (Carbon atoms in salicylaldehyde).	22.8

PdL2	3.8 (s, 1H, N-H), 6.6-7.3(m, 15 H, Ar-H), 7.4-7.8 (m, 8 H, Ar-H), 8.5 (d, 1 H, -CH=N-)	160.65 (C-O), 154.05 (C=N), 144.66 (C-P), 161.61, 147.17, 137.01, 114.55, 105.97 (Carbon atoms in Pyridine), 110.15, 118.99, 121.07, 133.51, 135.61 (Carbon atoms in salicylaldehyde)	22.3
PdL3	3.8 (s, 1H, N-H), 6.6-7.3 (m, 15H, Ar-H), 7.4-7.7 (m, 8H, Ar-H), 8.5 (d, 1H, -CH=N-).	163.98 (C-O), 154.51 (C=N), 143.98 (C-P), 161.46, 147.57, 137.41, 114.05, 106.97 (Carbon atoms in Pyridine), 117.55, 119.84, 133.73, 136.92 (Carbon atoms in salicylaldehyde).	23.4
PdL4	3.8 (s, 1H, N-H), 6.6- 7.3 (m, 15 H, Ar-H), 7.4-7.8 (m, 8 H, Ar-H), 8.5 (d, 1 H, -CH=N-)	156.06 (C-O), 154.11 (C=N), 143.61 (C-P), 161.21, 147.20, 137.86, 114.65, 106.27 (Carbon atoms in Pyridine), 115.24, 118.70, 120.10, 125.23, 152.78 (Carbon atoms in salicylaldehyde),	22.6

The complexes were soluble in common organic solvents such as CH₃OH, CH₃CN, C₆H₆, DMSO and DMF and were found to be thermally stable up to 300 °C.

3.3 MOLECULAR STRUCTURES AND UV-VISIBLE SPECTRA OF PALLADIUM COMPLEXES

The molecular structures of the palladium complexes are shown in Figures 3.1 to 3.4. The molecules PdL1 and PdL2 contain strong electron acceptor group (NO_2 and Cl) and PdL3 and PdL4 have electron donor group (H and OCH_3). The UV-Vis spectra of all four palladium complexes dissolved in solution as well as in film form are shown in Figures 3.5 to 3.8. The complex show large absorption in the region 230–500 nm. The bands appearing in the region 230–350 nm are assigned to intraligand charge transfer transitions (ILCT) and the less intense bands in the range 390–500 nm corresponds to the d-d forbidden transitions (Dileep and Bhat 2010). The small absorption tails at 532 nm give linear absorption coefficient (α_0) for all samples, which are tabulated in Table 3.8.

The following complexes were synthesized for our studies:

1. Pd-N-(2-pyridyl)-N'-(5-nitrosalicylidene)hydrazine triphenylphosphine [**PdL1**]
2. Pd-N-(2-pyridyl)-N'-(5-chlorosalicylidene)hydrazine triphenylphosphine [**PdL2**]
3. Pd-N-(2-pyridyl) - N' - (salicylidene)hydrazine triphenylphosphine [**PdL3**]
4. Pd-N-(2-pyridyl)-N'-(5-methoxysalicylidene)hydrazine triphenylphosphine [**PdL4**]

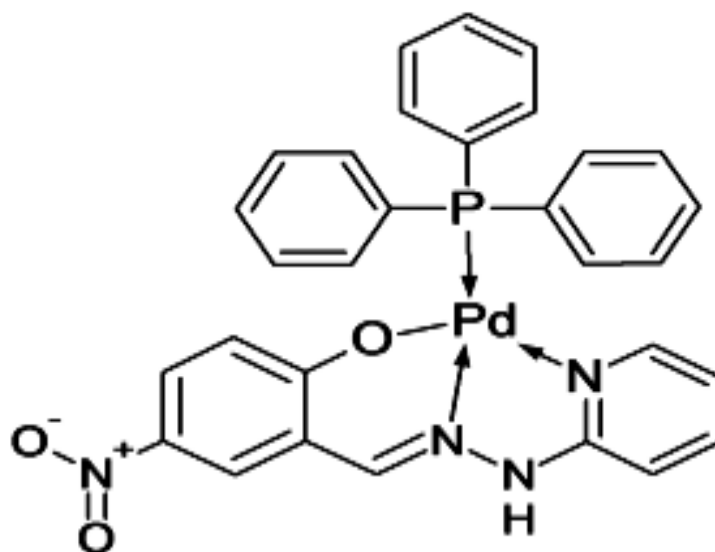


Figure 3.1 Molecular structure of Pd-N-(2-pyridyl)-N'-(5-nitro salicylidene)hydrazine triphenylphosphine [**PdL1**]

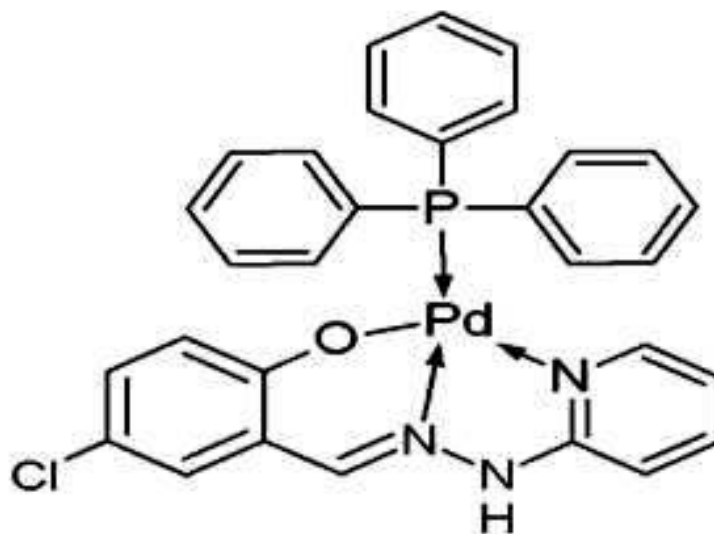


Figure 3.2 Molecular structure of Pd-N-(2-pyridyl)-N'-(5-chloro salicylidene) hydrazine triphenylphosphine [PdL2]

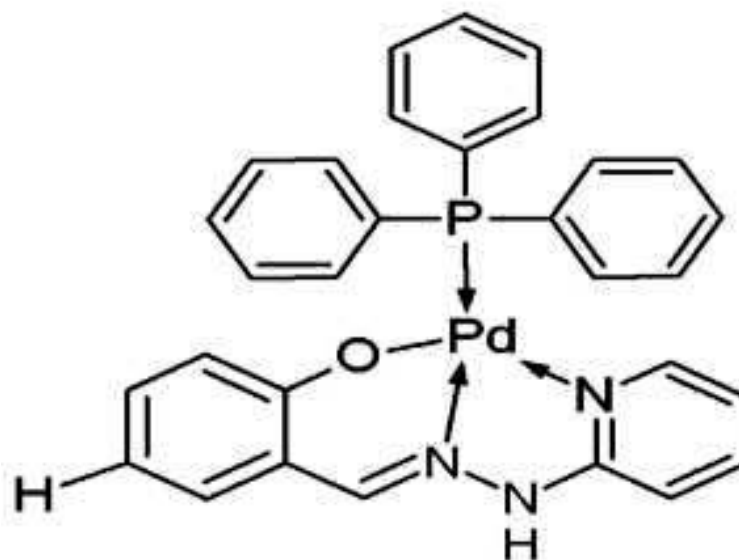


Figure 3.3 Molecular structure of Pd-N-(2-pyridyl)-N'-(salicylidene) hydrazine triphenylphosphine [PdL3]

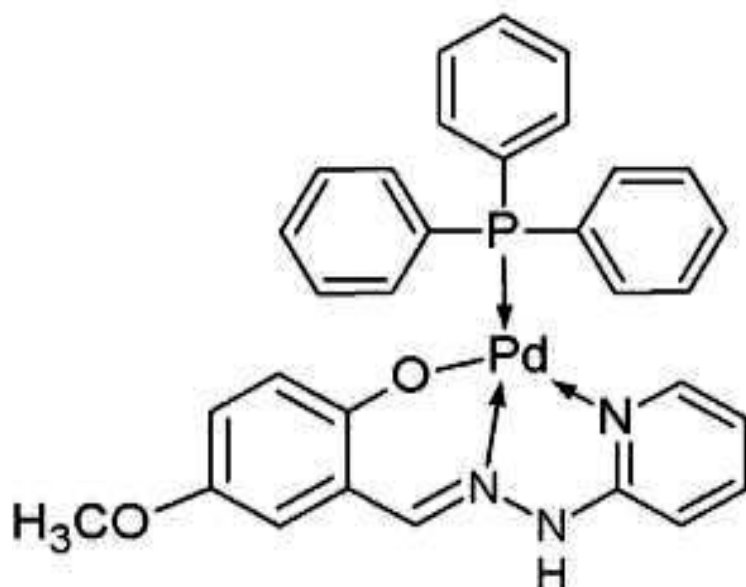


Figure 3.4 Molecular structure of Pd-N-(2-pyridyl)-N'-(5-methoxy salicylidene) hydrazine triphenylphosphine [PdL4]

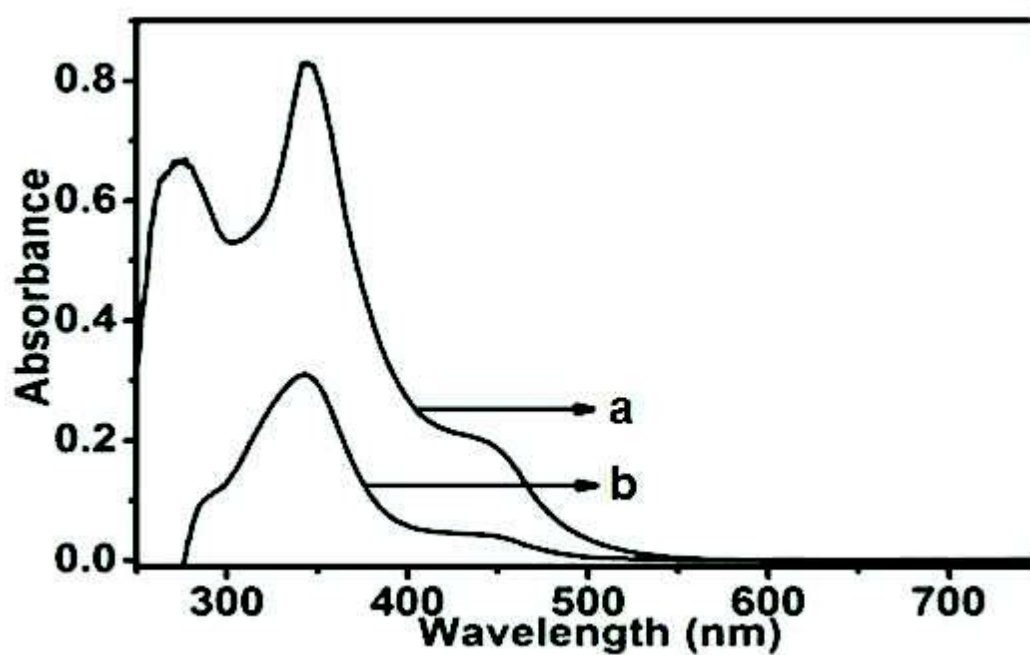


Figure 3.5 UV-Visible absorption spectrum of the palladium complex PdL1 in both solution (a) and film form (b), (Absorbance (A) = $-\ln(I/I_0)$, where I – transmitted intensity and I_0 – incident intensity)

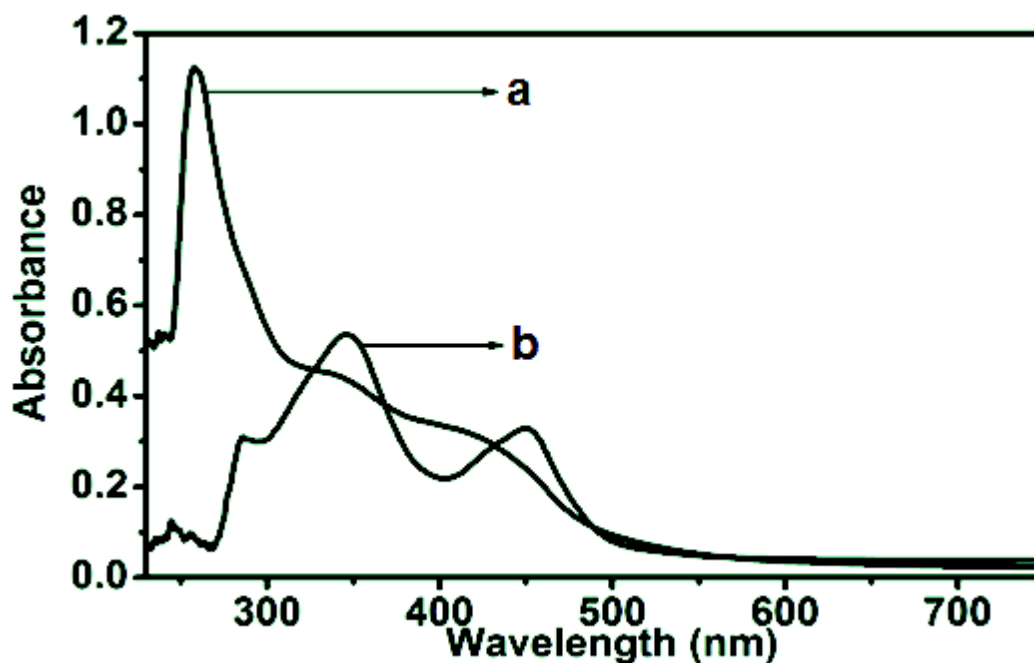


Figure 3.6 UV-Visible absorption spectrum of the palladium complex PdL2 in both solution (a) and film form (b), (Absorbance $(A) = -\ln(I/I_0)$, where I – transmitted intensity and I_0 – incident intensity)

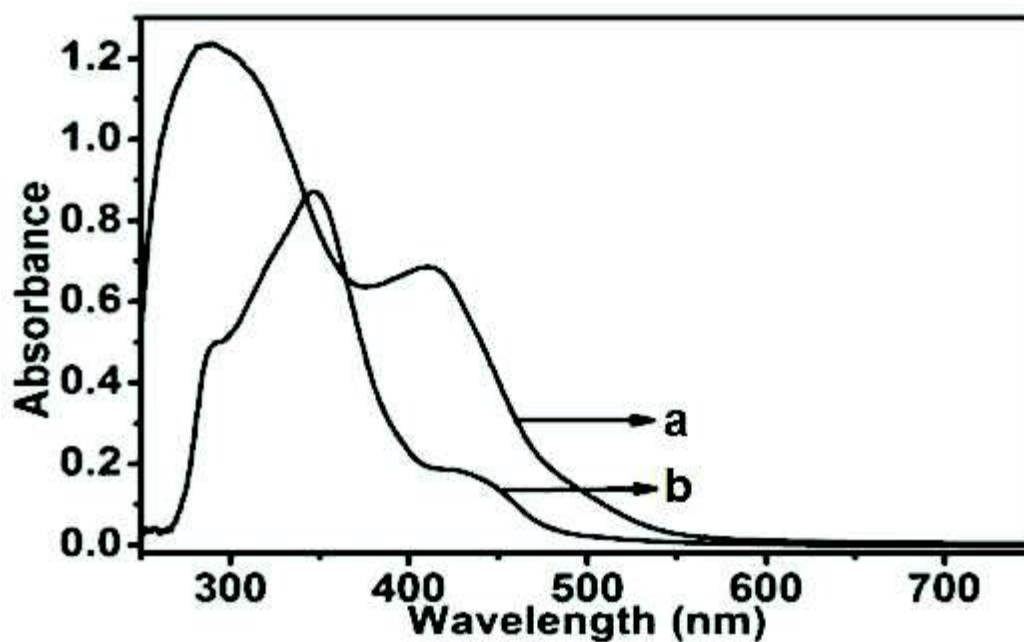


Figure 3.7 UV-Visible absorption spectrum of the palladium complex PdL3 in both solution (a) and film form (b), (Absorbance $(A) = -\ln(I/I_0)$, where I – transmitted intensity and I_0 – incident intensity)

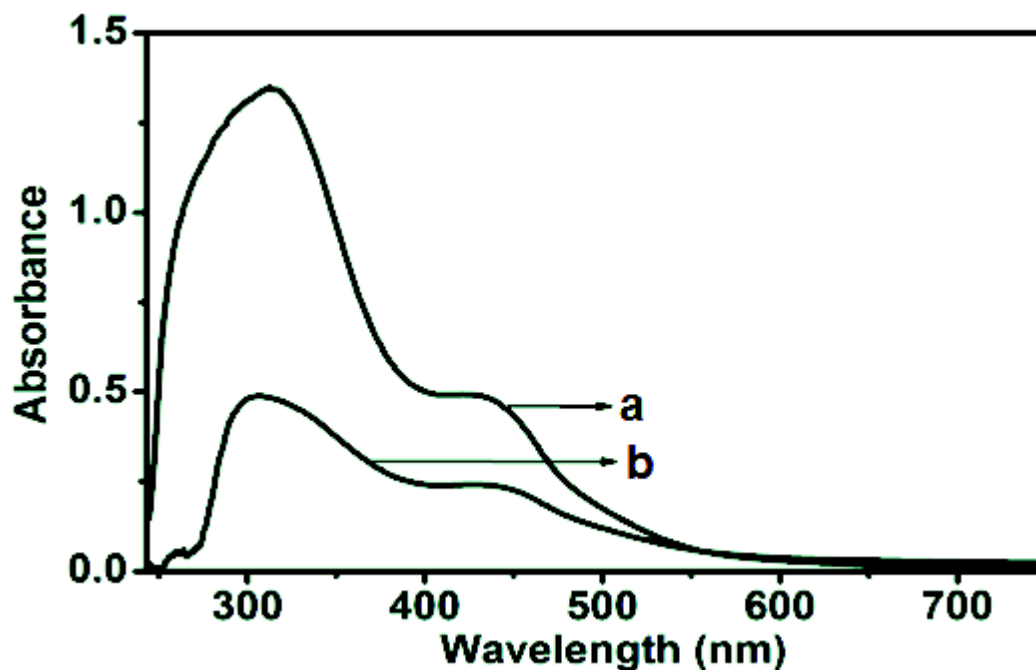


Figure 3.8 UV-Visible absorption spectrum of the palladium complex PdL4 in both solution (a) and film form (b), (Absorbance (A) = $-\ln(I/I_0)$, where I – transmitted intensity and I_0 – incident intensity)

3.4 Z-SCAN STUDIES OF PALLADIUM COMPLEXES

The experimental investigations of the third-order nonlinear optical parameters of palladium complexes in solution and film forms at different concentrations were carried out by Z-Scan technique using 7 ns laser pulses at 532 nm wavelength. The experiments were carried out using input pulse energy of 50 μJ , which corresponds to an on-axis peak irradiance of 1.2 GW/cm^2 . The experimental details of the Z-scan measurements are explained in section 2.1.5 of this thesis and sample preparations are described in section 2.5.

3.4.1 Nonlinear absorption studies

By performing open aperture Z-scan experiments the magnitude of effective nonlinear absorption coefficient (β_{eff}) of palladium complexes was estimated. It was necessary to perform a background scan using only the solvent and pure PMMA film in order to estimate the contribution of PMMA host. Figures 3.10 (a) and 3.11 (a)

show the open aperture Z-scan performed with DMF and pure PMMA samples. It clearly indicates that DMF and pure PMMA exhibit negligible nonlinear absorption. Figures 3.12 (a) to 3.15 (a) show open aperture Z-scan curves of PdL1, PdL2, PdL3 and PdL4 in solution form at the concentration of 1×10^{-3} mol/L. Figures 3.16 (a) to 3.23 (a) show open aperture Z-scan curves of PdL1, PdL2, PdL3 and PdL4 in film form at the dopant concentrations of 0.5 and 2.0 wt. %. The open aperture curves are symmetric with respect to the laser beam focus. The normalized transmittance valley indicates the presence of induced nonlinear absorption in both solution as well as film form. Similar open aperture Z-scan curves were also obtained for other concentrations of solutions and films. The corresponding normalized transmission as a function of sample position in open aperture condition is given by (Bahae et al. 1990 and O'Flaherty et al. 2003),

$$T(z) = 1 - (q_0 / 2\sqrt{2}) \quad \text{for } |q_0| < 1 \quad (3.1)$$

where q_0 is defined as,

$$q_0 = \beta_{eff} I_0 L_{eff} / (1 + z^2 / z_0^2) \quad (3.2)$$

where β_{eff} is the nonlinear absorption coefficient of the sample, I_0 is the intensity of the laser beam at the focus, z_0 is the Rayleigh range for the lens used for focusing the laser beam. $L_{eff} = [1 - \exp(-\alpha_0 L)] / \alpha_0$ is the effective sample thickness for a sample of actual thickness L and α_0 is the linear absorption coefficient. In general, induced nonlinear absorption can occur due to a variety of processes such as two photon absorption (TPA), excited state absorption (ESA), free carrier absorption and reverse saturable absorption (RSA). The nonlinear absorption of nanosecond pulses is generally explained by five-level model (Yim et al. 1998 and Poornesh et al. 2010). It consists of two energy level systems of singlet and triplet states in which singlet states have S_0 as the ground state, and S_1 and S_2 as the first and second excited states, respectively, and triplet states have T_1 and T_2 as the first and second excited states, respectively, as shown in Figure 3.9. Each electronic state has many vibrational levels. When the molecule is exposed to 532 nm, 7 ns laser pulses, it gets excited from ground state S_0 to the upper vibrational level of first excited singlet state S_1

$[S_1 \leftarrow S_0(\nu=0)]$ by absorbing two photons simultaneously. This is denoted as two-photon absorption (TPA) characterized by an absorption cross section of σ_0 . From the state S_1 the molecule can be further excited to the higher excited state $S_2[S_2 \leftarrow S_1]$ on a nanosecond time scale. In nanosecond time scale singlet transition does not deplete the population of S_1 level appreciably, since atoms excited to S_2 decay to S_1 itself within picoseconds. If the laser pulse is longer than few nanoseconds, there should be a significant amount of population transfer from S_1 to T_1 by non-radiative intersystem crossing and usually the lifetime for this is larger than ~ 1 ns. In the next step transitions can occur from T_1 to T_2 (Yim et al. 1998, Cassano et al. 2005 and Poornesh et al. 2010). The molecules in states S_1 and T_1 can be excited to the higher excited states S_2 and T_2 with absorption cross section of σ_S and σ_T respectively. The relaxation time from the states S_1 and T_1 is less than a ps. The excited-state absorption (ESA) occurs when molecules are excited from an already excited state to a higher excited state. When singlet excited state S_1 or triplet state T_1 or

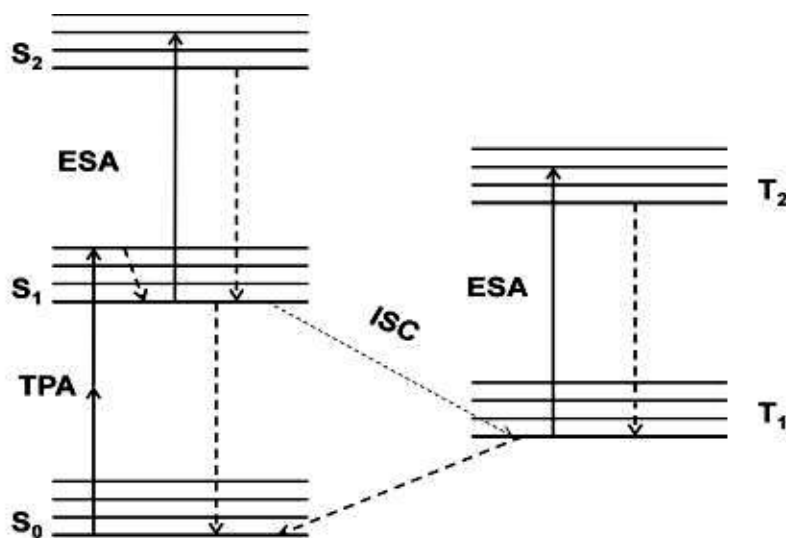


Figure 3.9 Five level model for nonlinear optical absorption. Here S_0 , S_1 and S_2 represent ground, first excited and second excited singlet states, T_1 and T_2 represent first excited and second excited triplet states, TPA, ESA and ISC represent two-photon absorption, excited state absorption and intersystem crossing, respectively.

both have larger absorption cross section than the ground state, reverse saturable absorption (RSA) is said to occur. In our case, nanosecond laser pulses were used,

and, hence, triplet–triplet transitions are expected to make significant contribution to the observed nonlinear absorption. Moreover, the positive nonlinear absorption coefficient implies that RSA is the operating mechanism (Zhang et al. 2007). The excited state absorption cross section (σ_{exc}) can be obtained from the open aperture Z-scan data (Henari et al. 1997, Sun et al. 1999 and Wood et al. 1995). Intensity of the laser beam changes as it propagates through the sample and is given by,

$$\frac{dI}{dz} = -\alpha_0 I - \sigma_{exc} N(t), \quad (3.3)$$

$$\frac{dN}{dt} = \frac{\alpha_0 I}{\hbar\omega}, \quad (3.4)$$

where I is the intensity, z is the sample position, N is the density of charges in the excited state, ω is the angular frequency of the laser and α_0 is the linear absorption. By combining Equations (3.3) and (3.4), we have

$$\frac{dI}{dz} = -\alpha_0 I - \frac{\sigma_{exc} \alpha_0 I}{\hbar\omega} \int_{-\infty}^t I(t') dt' \quad (3.5)$$

Solving the above equation for the fluence and integrating over the spatial extent of the beam, the normalized energy transmission for open aperture is obtained as (Wood et al. 1995),

$$T = \ln \left(1 + \frac{q_0}{1+x^2} \right) / \left(\frac{q_0}{1+x^2} \right) \quad (3.6)$$

where $x=z/z_0$, z is the distance of the sample from the focus, z_0 is the Rayleigh length given by the formula $z_0 = \pi w_0^2 / \lambda$ (λ is the wavelength and w_0 is the beam waist at the focus) and q_0 is given by the equation (Henari 2001, Huang et al. 2008 and Benson et al. 1994)

$$q_0 = \frac{\sigma_{exc} \alpha_0 F_0(r=0) L_{eff}}{2\hbar\omega}, \quad (3.7)$$

where α_0 is the linear absorption coefficient, $L_{eff} = [1 - \exp(-\alpha_0 L)] / \alpha_0$, ω is the angular frequency of the laser and F_0 is the on-axis fluence at the focus which is related to the incident energy I_{total} by

$$F_0 = \frac{2I_{total}}{\pi\omega_0^2}, \quad (3.8)$$

The values of effective excited-state absorption cross-section σ_{exc} of the complexes were obtained by fitting the open aperture data using the Equation (3.6). The ground-state absorption cross-section σ_g was calculated using the relation

$$\sigma_g = \frac{\alpha_0}{N_a C}, \quad (3.9)$$

where N_a is the Avogadro's number and C is the concentration in mol/L. The magnitude of σ_{exc} and σ_g of the complexes in solution and film form are given in Tables 3.4 and 3.5, respectively. The larger value of σ_{exc} compared to σ_g indicates that the observed nonlinear absorption is due to RSA (Henari 2001, Henari et al. 1997, Sun et al. 1999 and Przhonska et al. 1998). On the other hand, if the nonlinear absorption mechanism is TPA, β_{eff} should be constant independent of the on-axis input intensity I_0 (Guo et al. 2003; He et al. 1998). Figures 3.24 to 3.27 show that β_{eff} decreases with increasing on-axis intensity I_0 , thereby implying that RSA is the operating mechanism (Guo et al. 2003 and Auger et al. 2003). The calculated values of β_{eff} and $\text{Im } \chi^{(3)}$ using relation Equation 2.26 are given in Tables 3.6 and 3.7.

3.4.2 Nonlinear refraction studies

The closed aperture Z-scan was performed on the samples to determine the sign and magnitude of nonlinear refraction. In this case too, DMF and pure PMMA did not show nonlinear refraction behavior as indicated by Figure 3.10 (b) and 3.11 (b). Figure 3.12 (b) to 3.15 (b) show closed aperture Z-scan curves of PdL1, PdL2, PdL3 and PdL4 in solution form at the concentration of 1×10^{-3} mol/L. Figures 3.16 (b) to 3.23 (b) show closed aperture Z-scan curves of PdL1, PdL2, PdL3 and PdL4 in film form at the dopant concentrations of 0.5 and 2.0 wt.%. The complexes exhibit a pre-focal transmittance peak followed by a post-focal valley which is the signature of negative nonlinear refraction (self-defocusing), i.e. $n_2 < 0$. Closed aperture Z-scan measurements yield data on the combined action of both nonlinear absorption and nonlinear refraction, which is reflected in closed aperture Z-scan curves having a reduced peak and enhanced valley. Using the division method (Bahae et al. 1990), wherein the closed aperture data is divided by open aperture data, one can eliminate nonlinear absorption from the closed aperture data and, thereby, obtain pure nonlinear refraction curve. The pure nonlinear refraction curves of PdL1, PdL2, PdL3 and PdL4

in solution form, at the concentration of 1×10^{-3} mol/L, are shown in Figures 3.12 (c) to 3.15 (c) and in film form, at the dopant concentrations of 0.5 and 2.0 wt.%, in Figure 3.16 (c) to 3.23 (c). It is observed that the peak-to-valley difference in transmission for closed-aperture Z-scan satisfies the condition $\Delta Z_{p-v} \sim 1.7\Delta Z_0$, thus confirming that the third-order nonlinearity is due to electronic process (Bahae et al. 1990). The calculated values of nonlinear refractive index n_2 and real part of nonlinear optical susceptibility $\text{Re } \chi^{(3)}$ using relations given in Equations 2.24 and 2.25 are given in Tables 3.6 and 3.7.

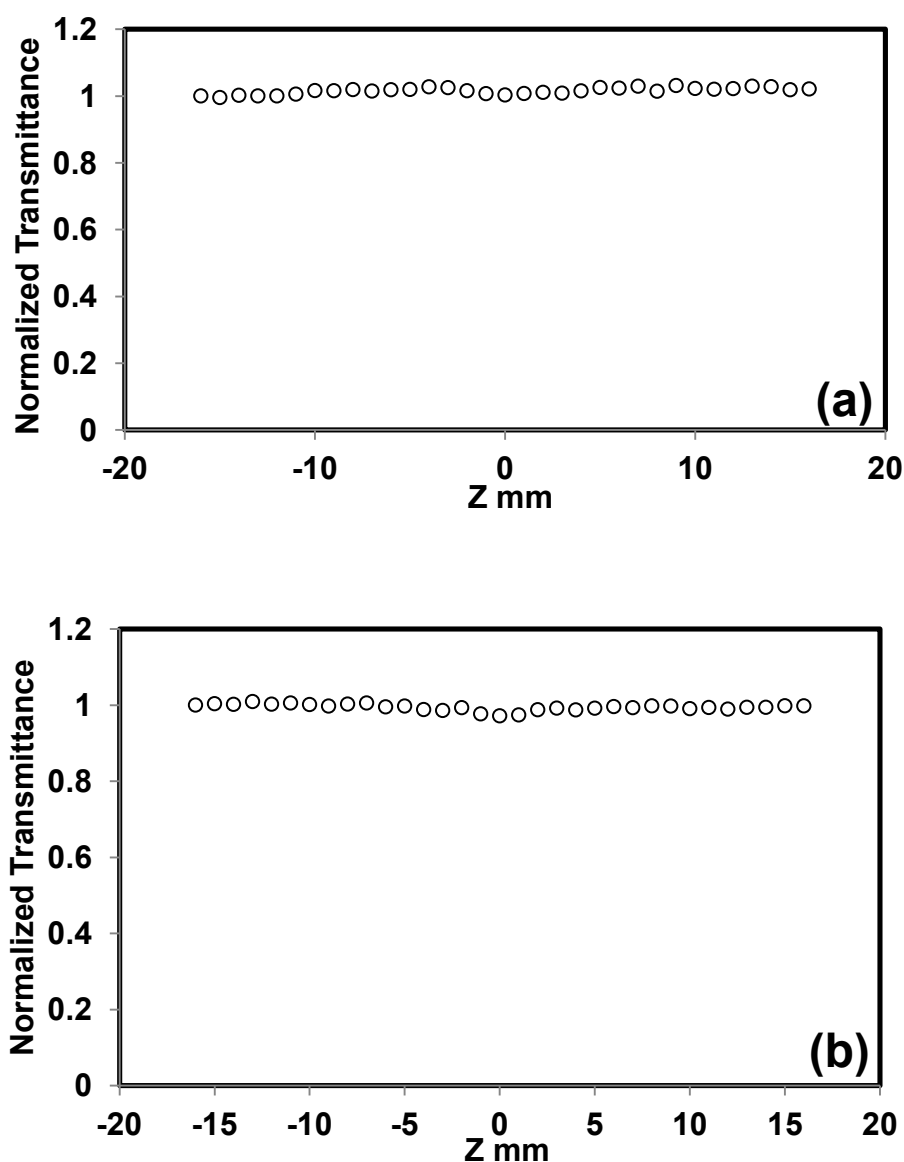


Figure 3.10 Plots of Open aperture (a) and Closed aperture (b) curves of pure DMF solution

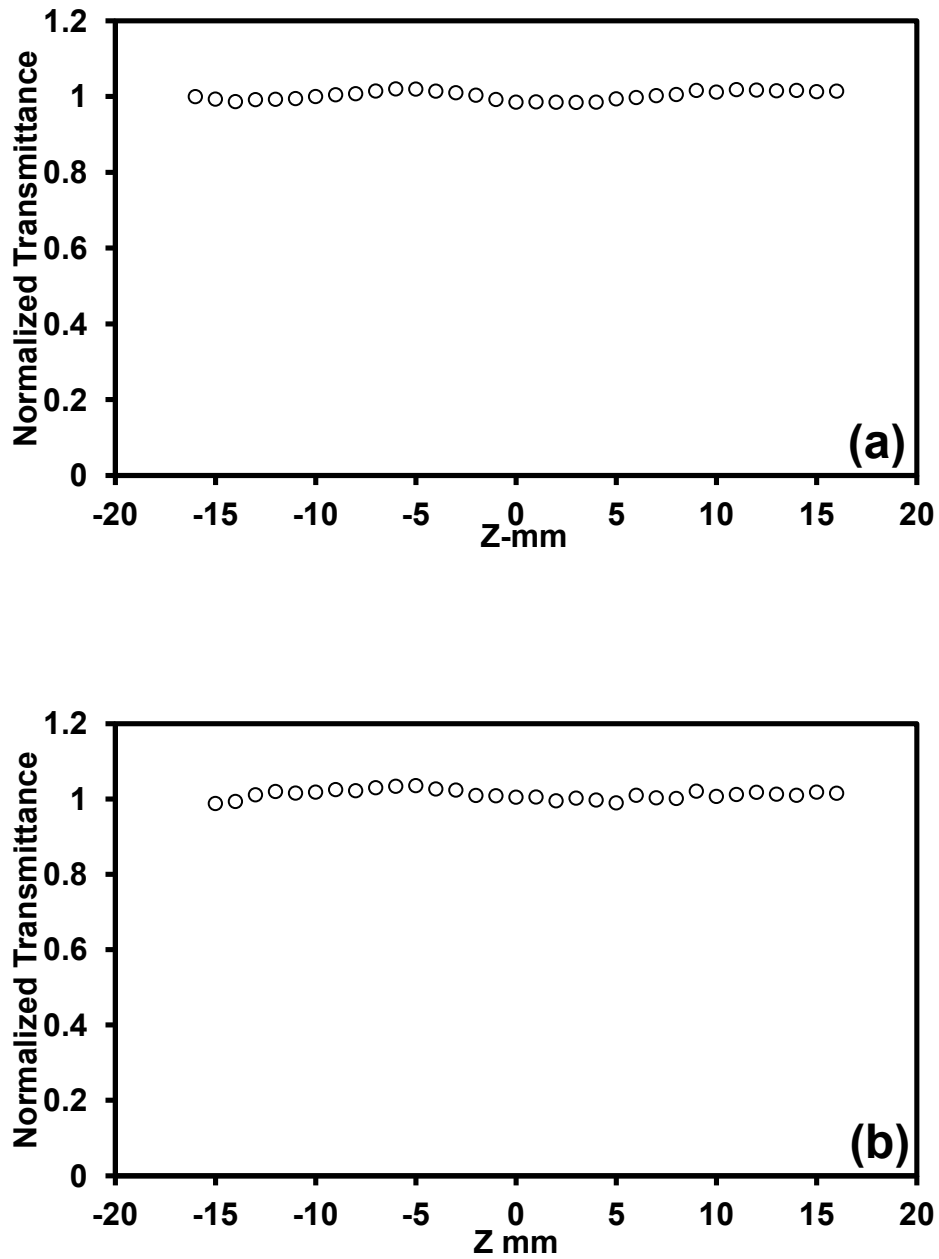


Figure 3.11 Plots of Open aperture (a) and Closed aperture (b) curves of pure PMMA

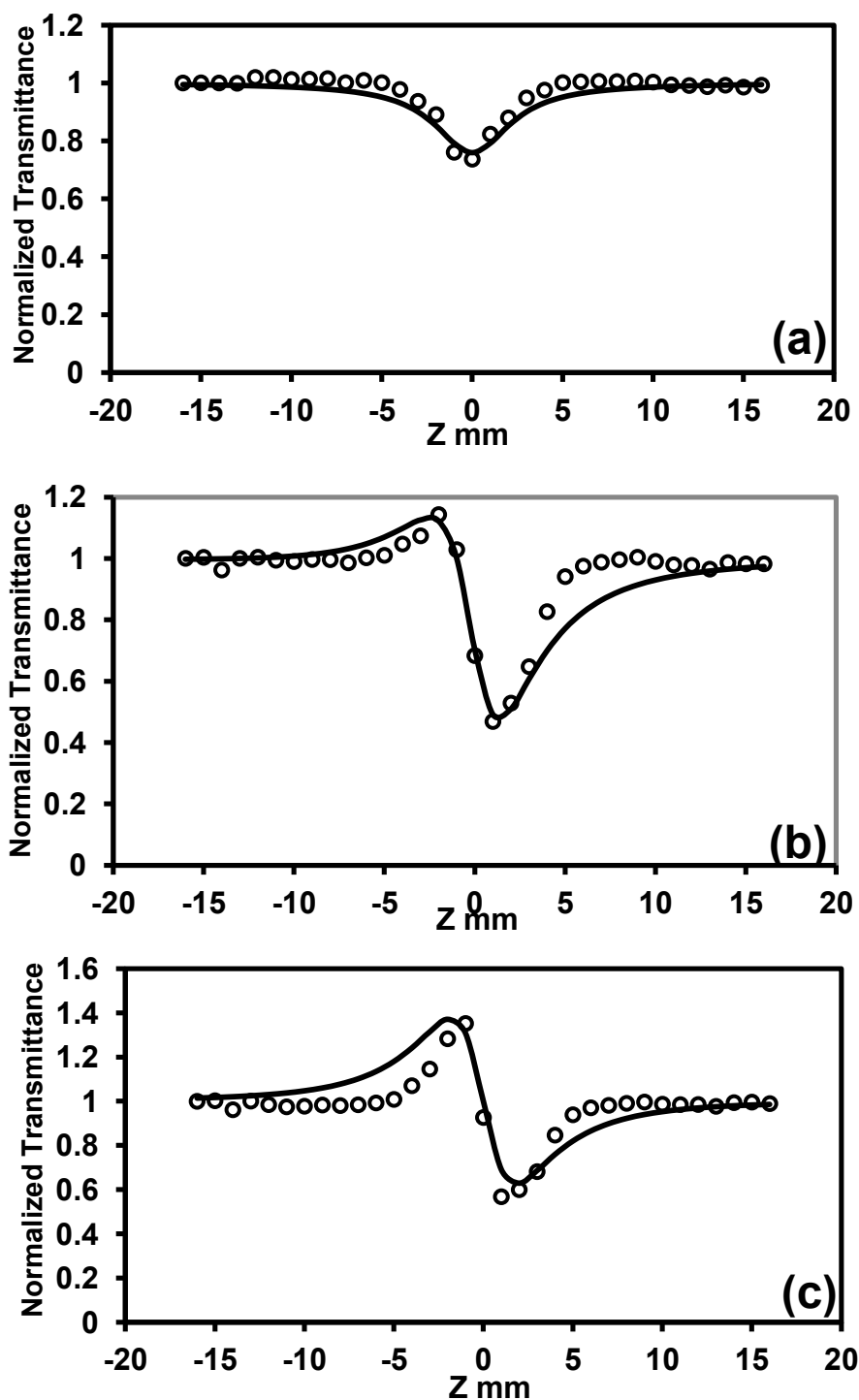


Figure 3.12 Plots of Open aperture (a), Closed aperture (b) and Pure nonlinear refraction (c) curves for PdL1 in solution form (1×10^{-3} mol/L). Solid line is a theoretical fit to the experimental data

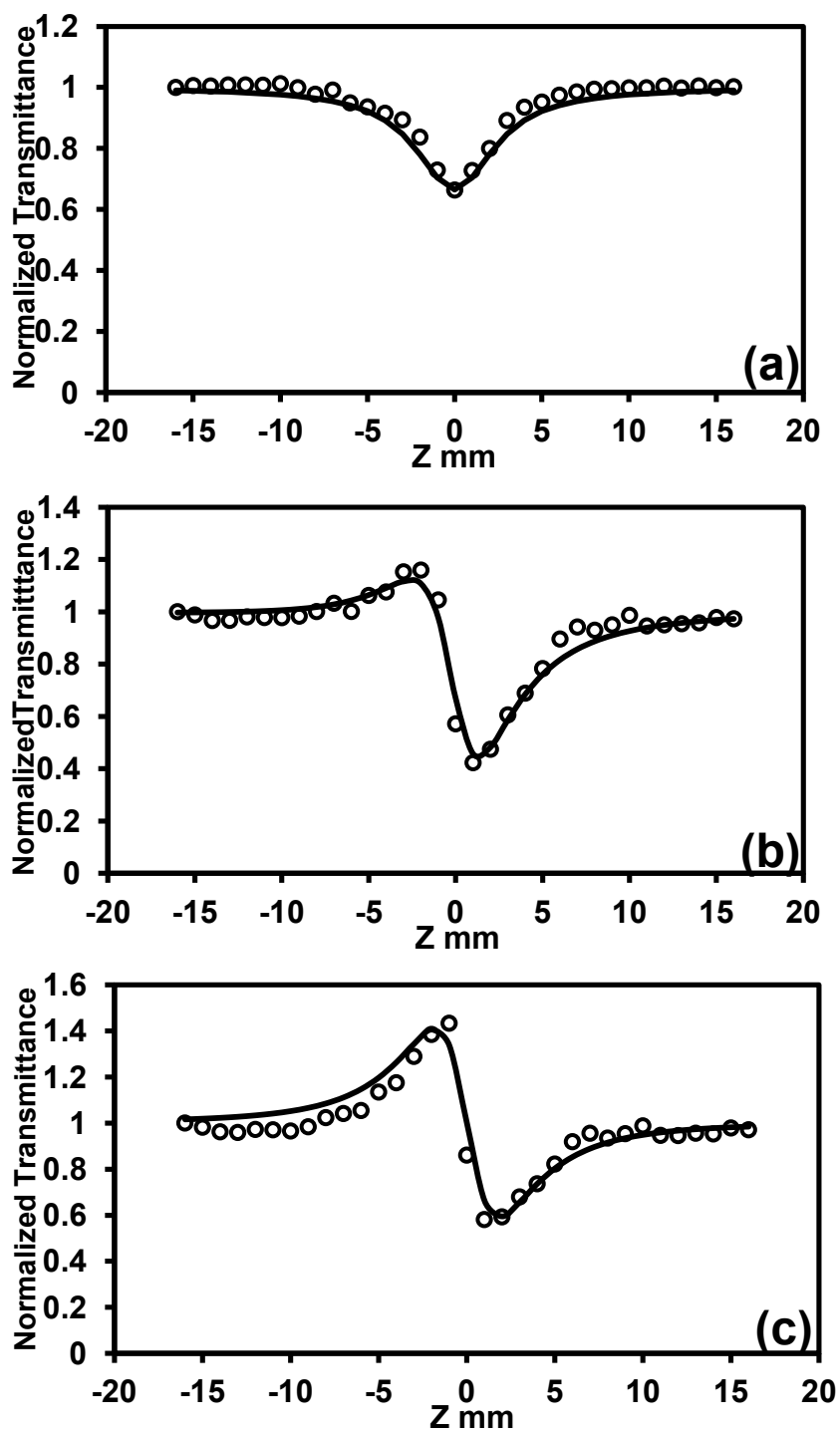


Figure 3.13 Plots of Open aperture (a), Closed aperture (b) and Pure nonlinear refraction (c) curves for PdL2 in solution form (1×10^{-3} mol/L). Solid line is a theoretical fit to the experimental data

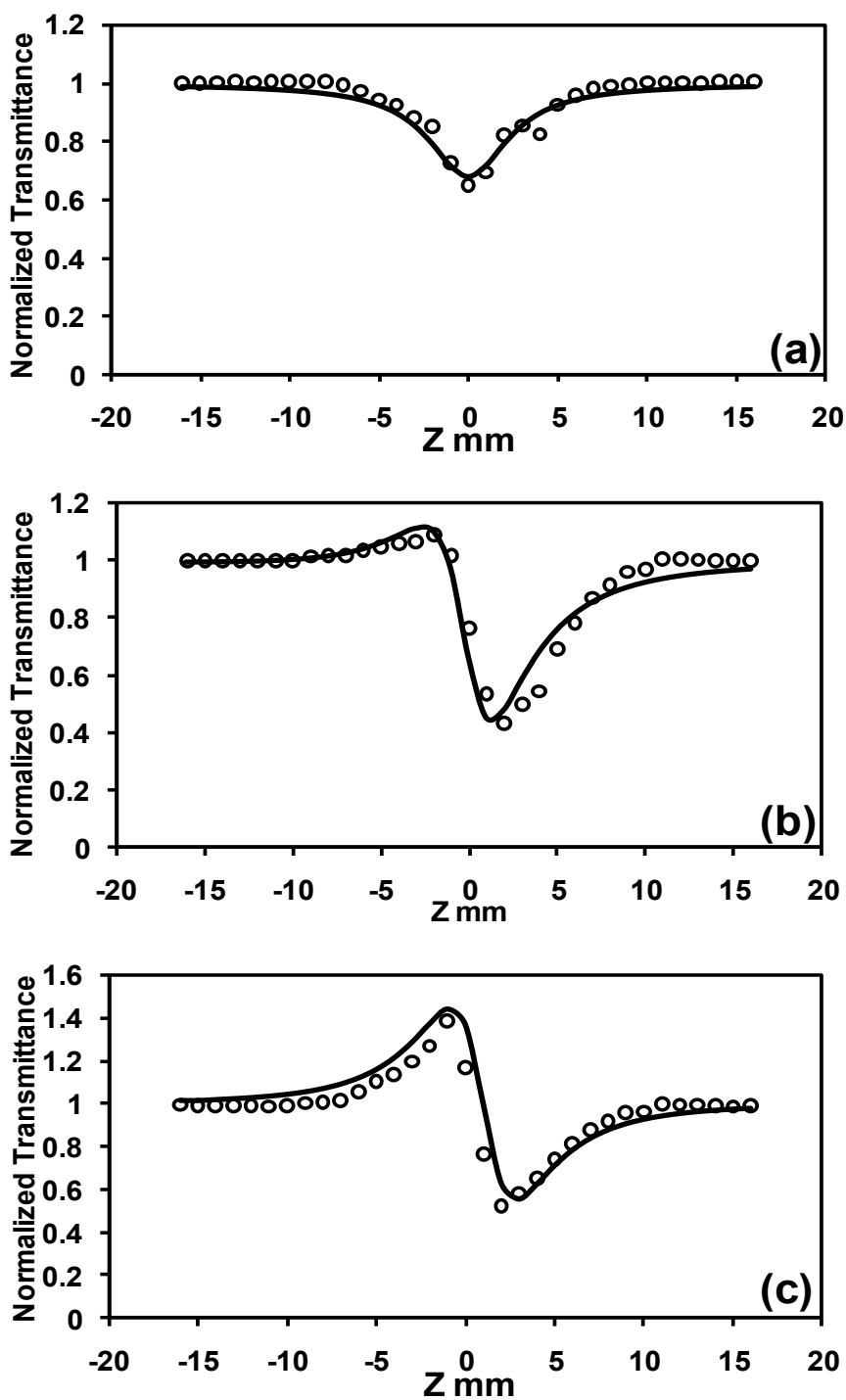


Figure 3.14 Plots of Open aperture (a), Closed aperture (b) and Pure nonlinear refraction (c) curves for PdL3 in solution form (1×10^{-3} mol/L). Solid line is a theoretical fit to the experimental data

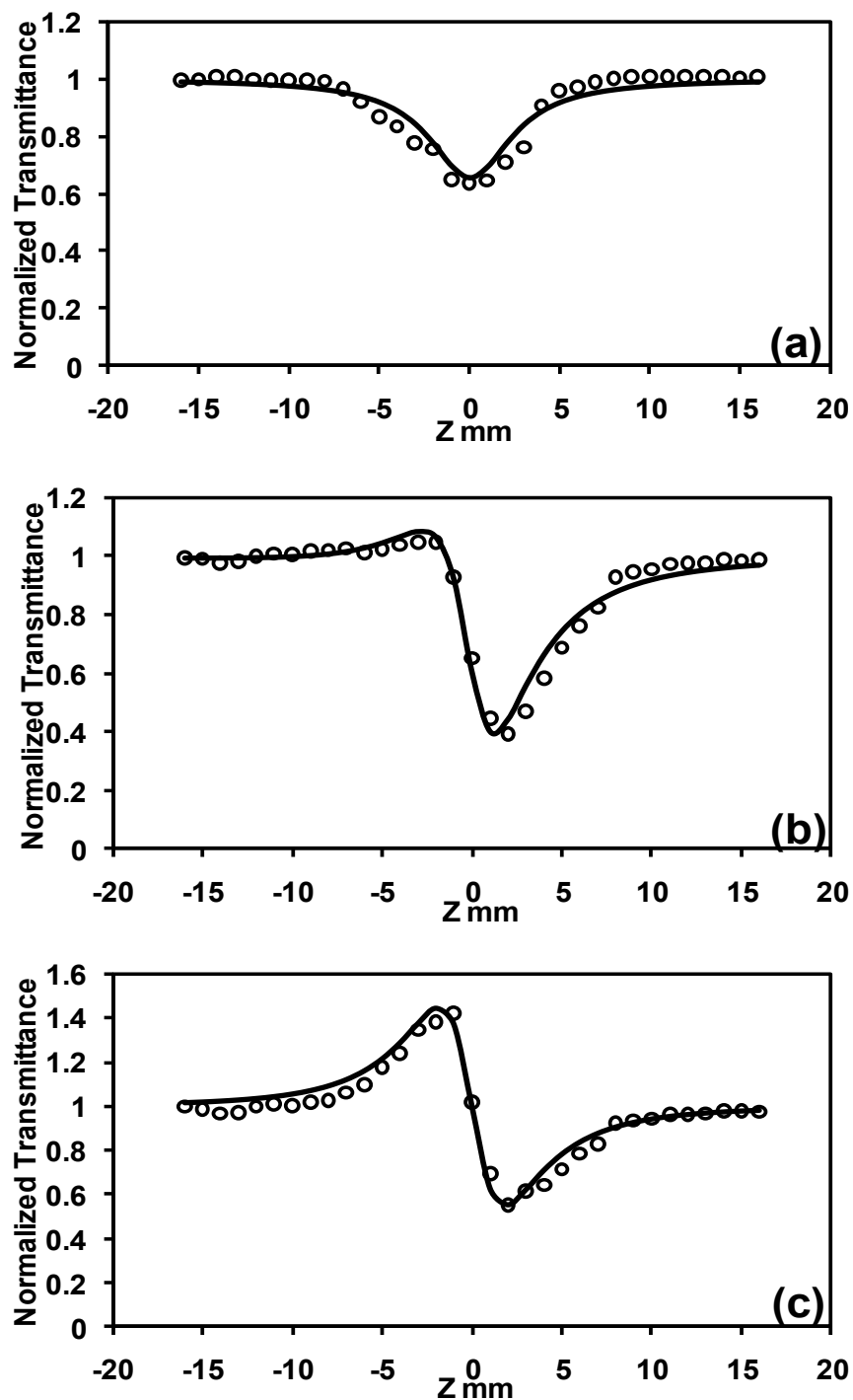


Figure 3.15 Plots of Open aperture (a), Closed aperture (b) and Pure nonlinear refraction (c) curves for PdL4 in solution form (1×10^{-3} mol/L). Solid line is a theoretical fit to the experimental data

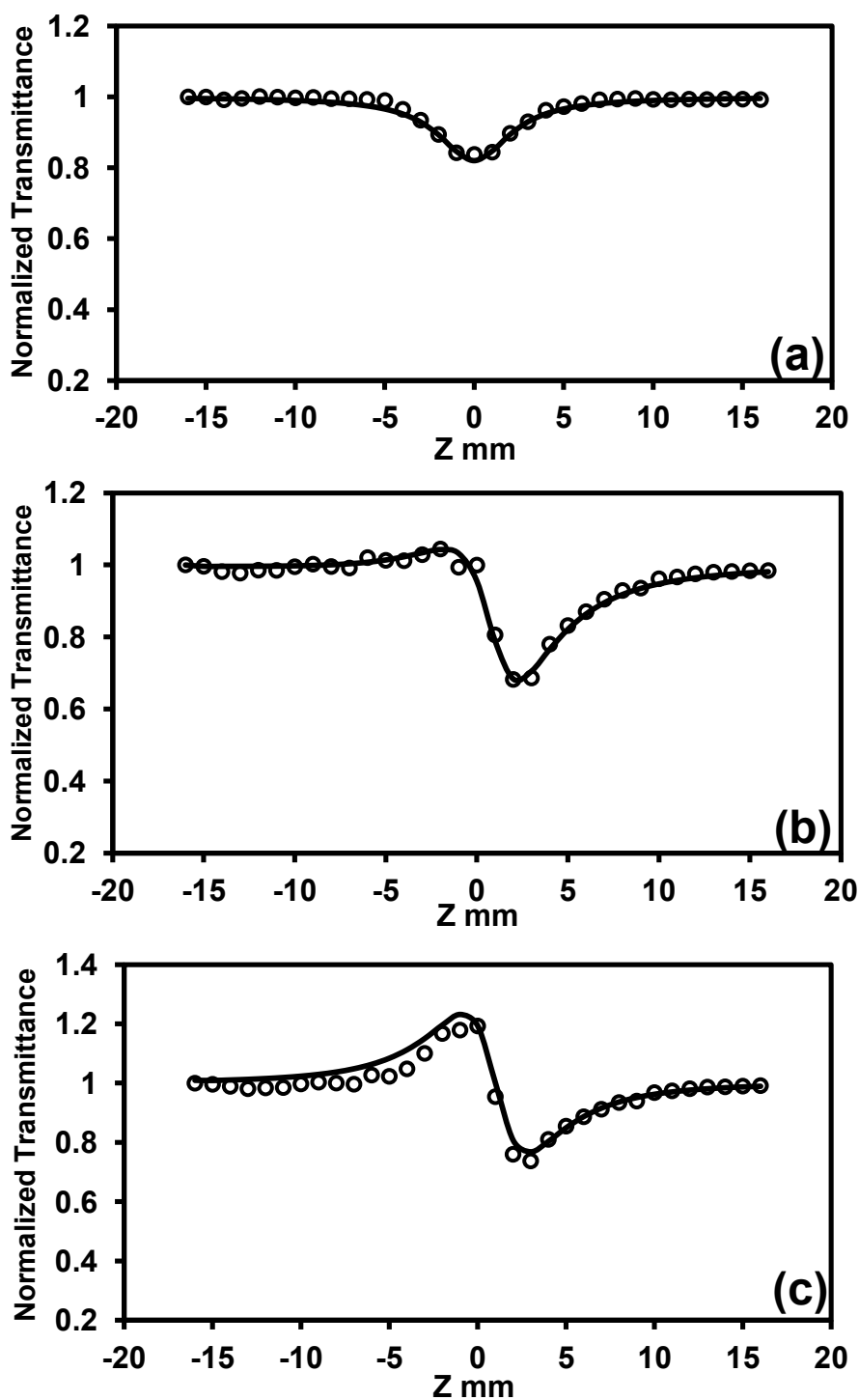


Figure 3.16 Plots of Open aperture (a), Closed aperture (b) and Pure nonlinear refraction (c) curves for PdL1 in film form (0.5 wt.%). Solid line is a theoretical fit to the experimental data

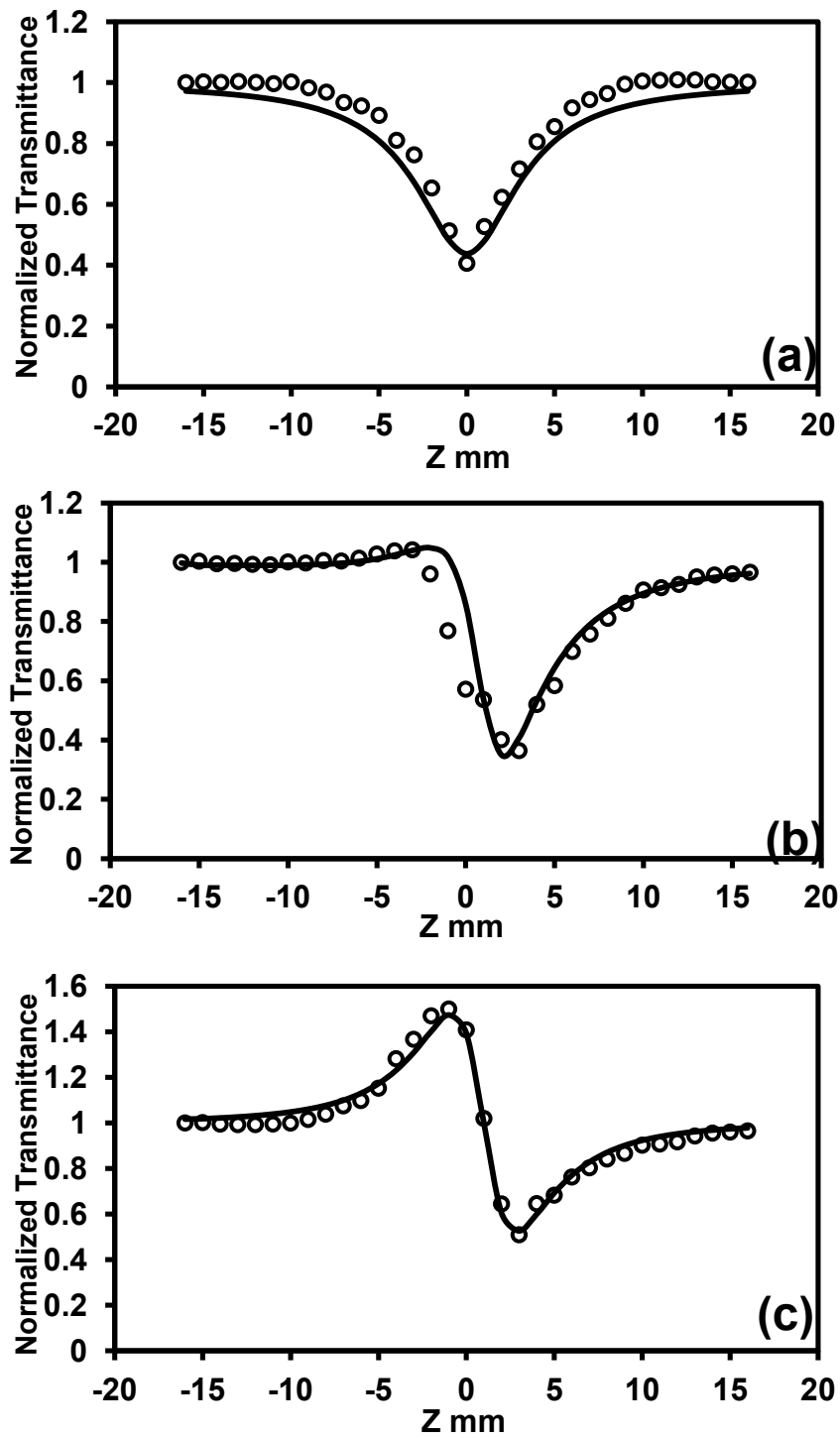


Figure 3.17 Plots of Open aperture (a), Closed aperture (b) and Pure nonlinear refraction (c) curves for PdL1 in film form (2.0 wt.%). Solid line is a theoretical fit to the experimental data

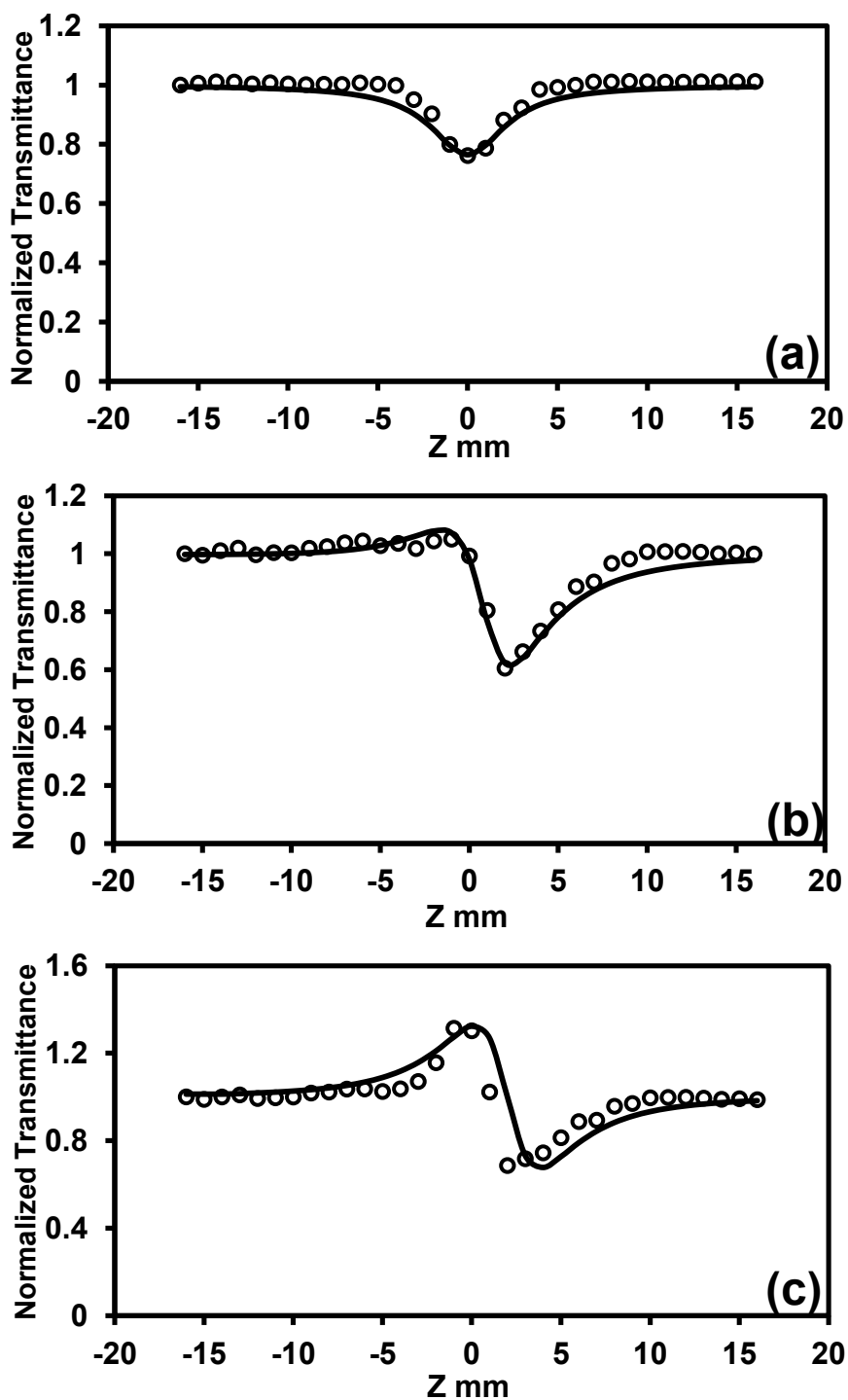


Figure 3.18 Plots of Open aperture (a), Closed aperture (b) and Pure nonlinear refraction (c) curves for PdL2 in film form (0.5 wt.%). Solid line is a theoretical fit to the experimental data

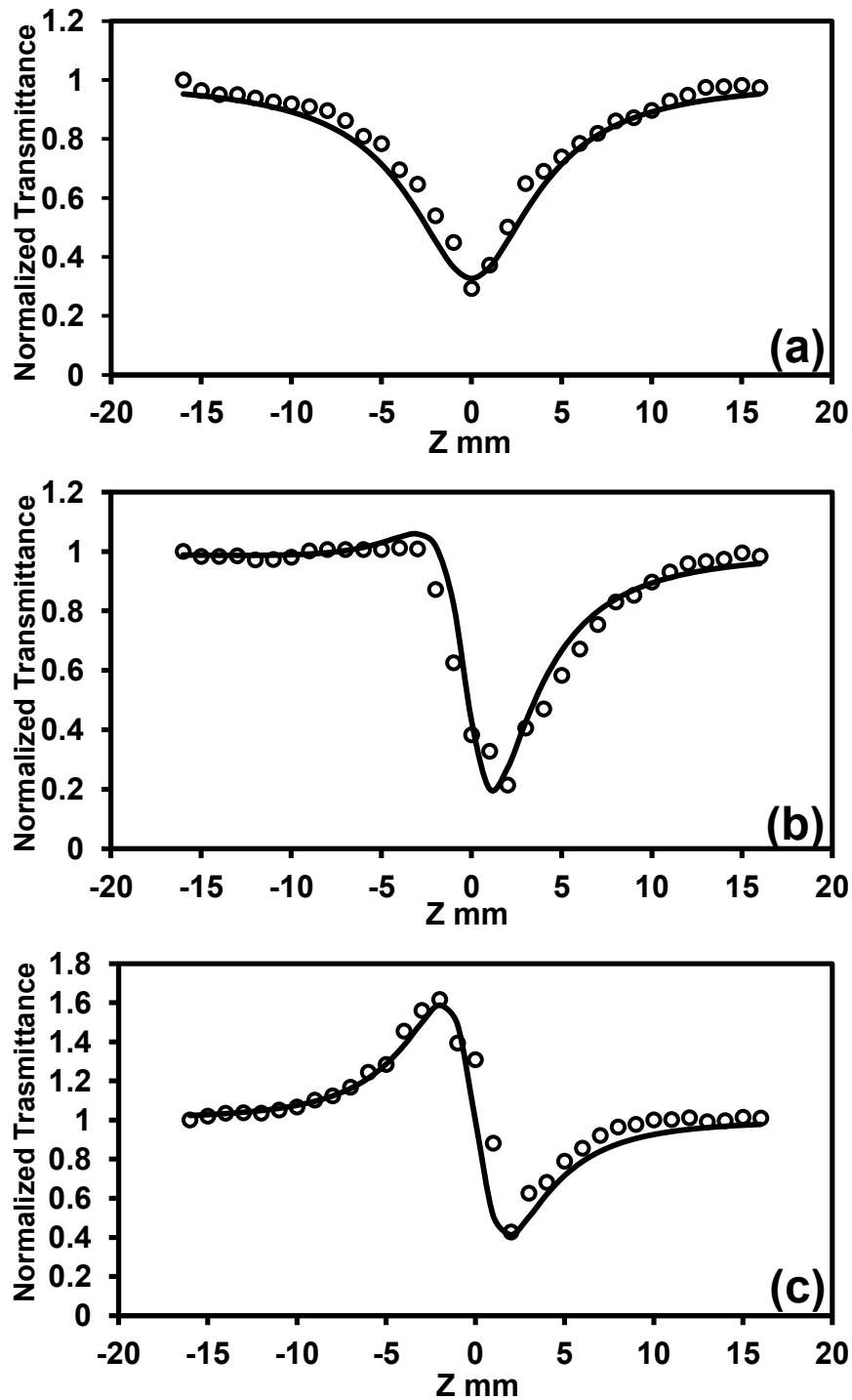


Figure 3.19 Plots of Open aperture (a), Closed aperture (b) and Pure nonlinear refraction (c) curves for PdL2 in film form (2.0 wt.%). Solid line is a theoretical fit to the experimental data

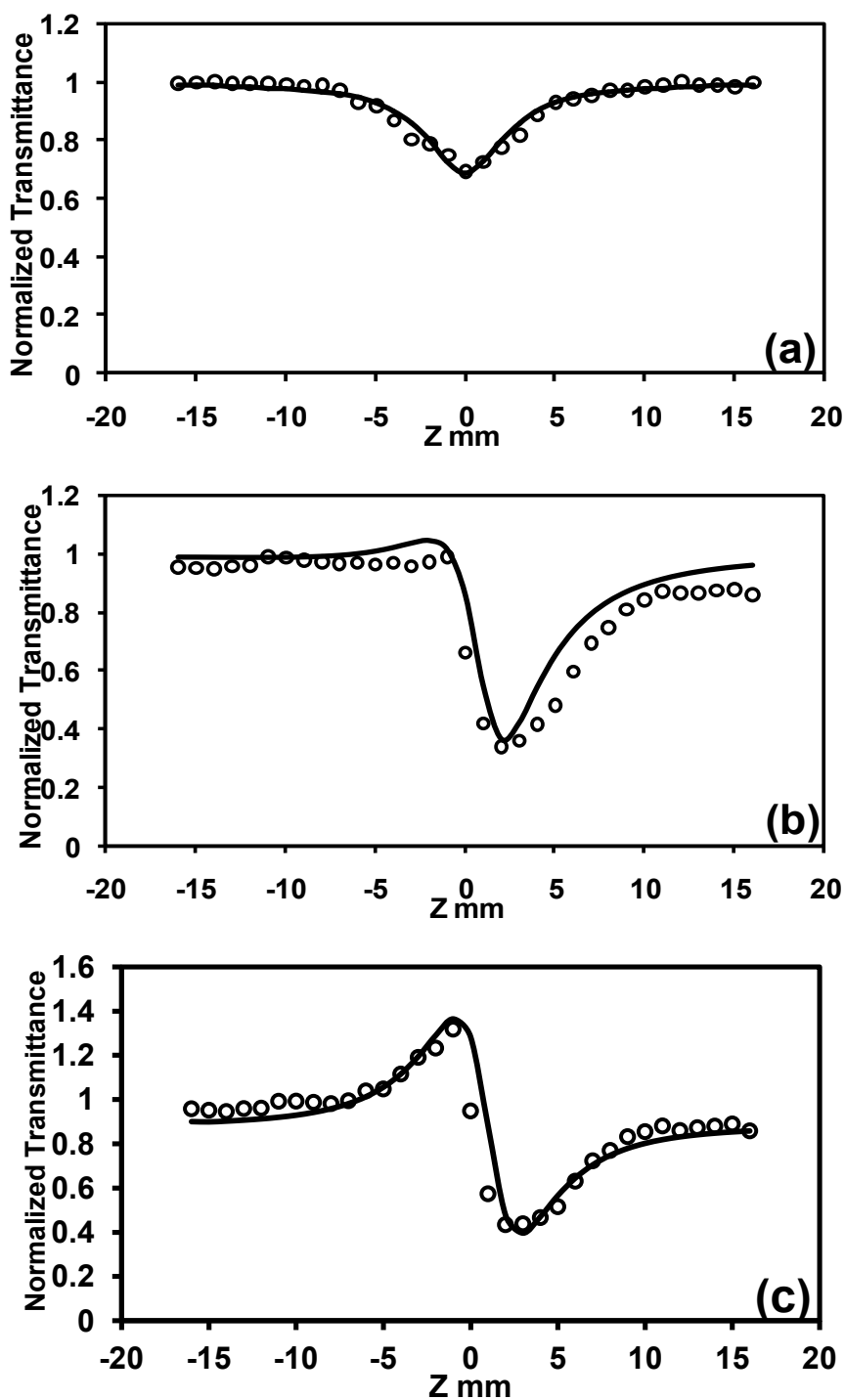


Figure 3.20 Plots of Open aperture (a), Closed aperture (b) and Pure nonlinear refraction (c) curves for PdL3 in film form (0.5 wt.%). Solid line is a theoretical fit to the experimental data

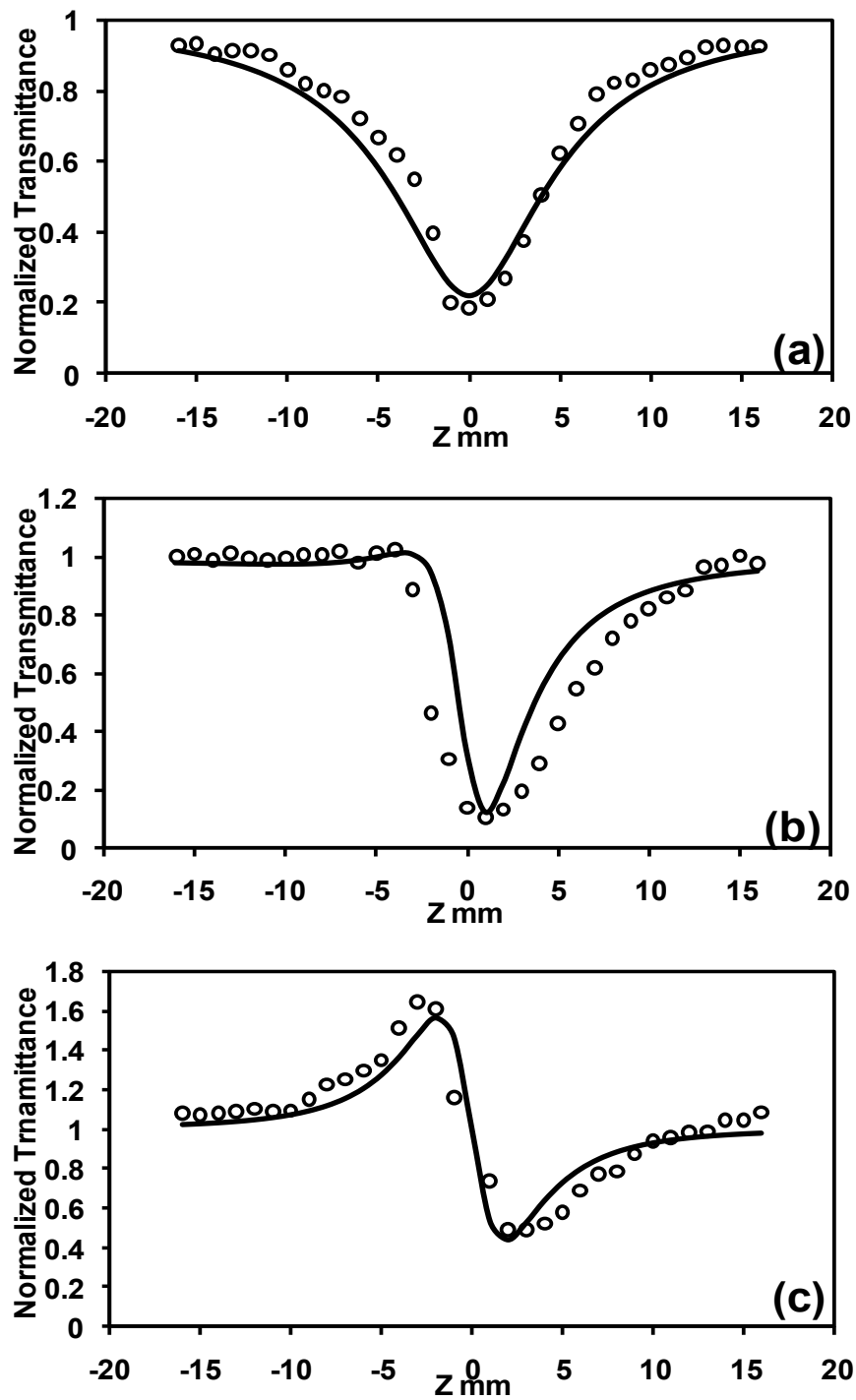


Figure 3.21 Plots of Open aperture (a), Closed aperture (b) and Pure nonlinear refraction (c) curves for PdL3 in film form (2.0 wt.%). Solid line is a theoretical fit to the experimental data

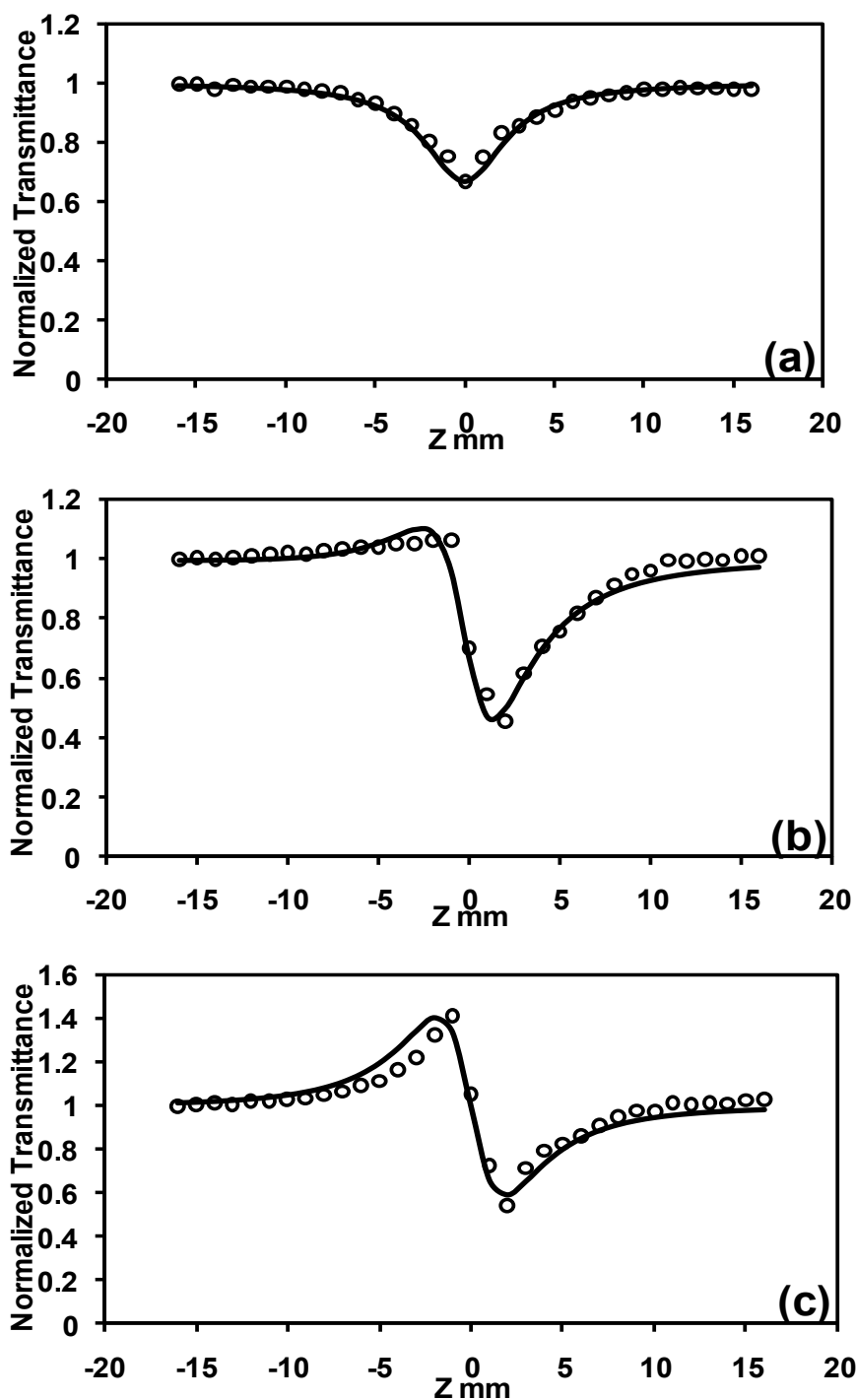


Figure 3.22 Plots of Open aperture (a), Closed aperture (b) and Pure nonlinear refraction (c) curves for PdL4 in film form (0.5 wt.%). Solid line is a theoretical fit to the experimental data

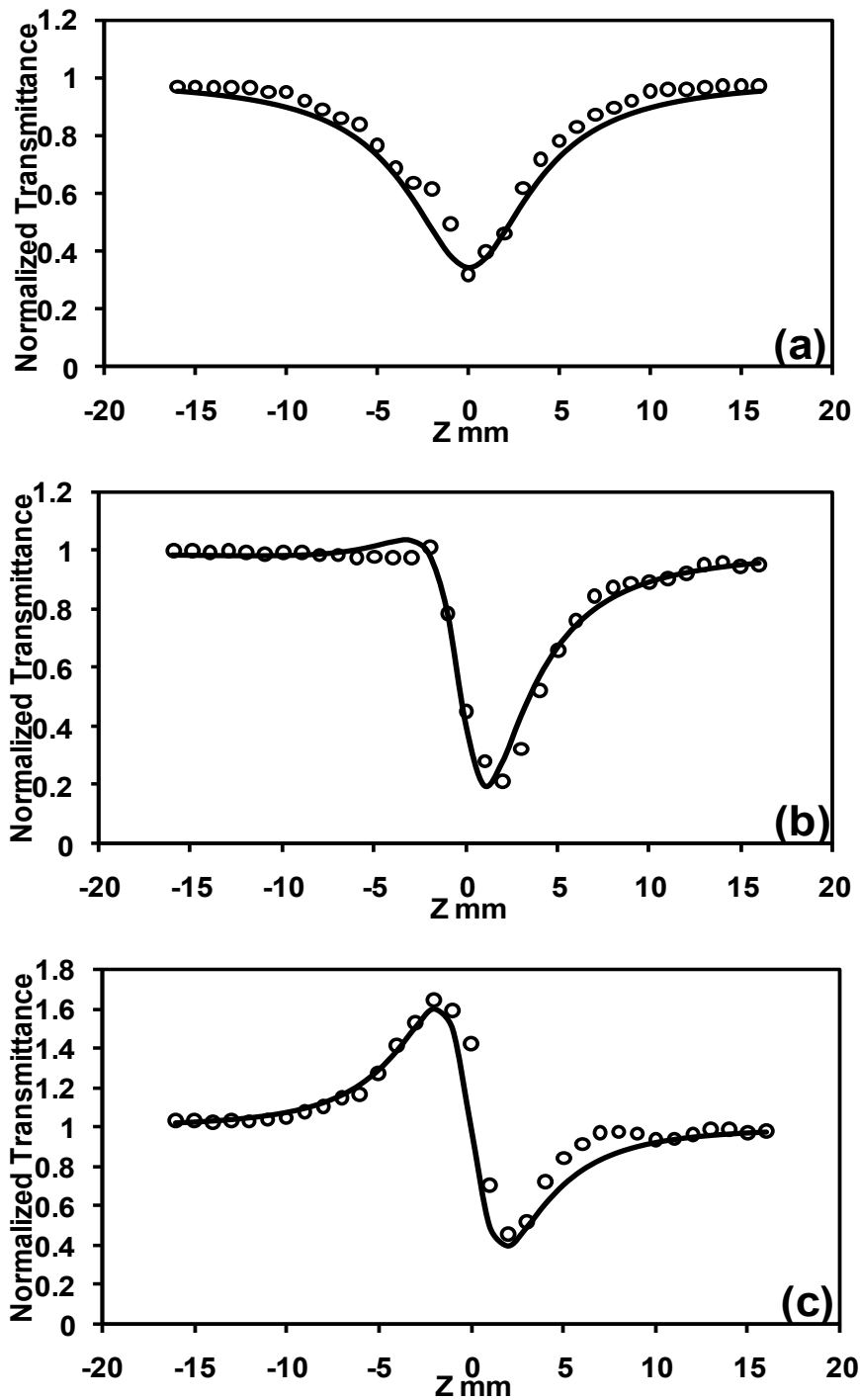


Figure 3.23 Plots of Open aperture (a), Closed aperture (b) and Pure nonlinear refraction (c) curves for PdL4 in film form (2.0 wt.%). Solid line is a theoretical fit to the experimental data

Table 3.4 Ground state absorption cross-section and excited state absorption cross-section of the palladium complexes in solution form at different concentrations

Sample	Concentrations (x 10 ⁻³ mol/L)	σ_g (x 10 ⁻¹⁹ cm ²)	σ_{exc} (x 10 ⁻¹⁸ cm ²)
PdL1	0.25	8.075	1.485
	0.5	7.468	1.765
	1	7.045	3.018
PdL2	0.25	8.368	1.606
	0.5	7.524	1.972
	1	7.116	3.427
PdL3	0.25	8.254	1.719
	0.5	7.625	2.018
	1	7.205	3.816
PdL4	0.25	8.515	1.826
	0.5	7.878	2.135
	1	7.345	4.065

Table 3.5 Ground state absorption cross-section and excited state absorption cross-section of the palladium complexes doped in film form at different dopant concentrations

Sample	Dopant Concentrations (wt.%)	σ_g ($\times 10^{-17} \text{ cm}^2$)	σ_{exc} ($\times 10^{-16} \text{ cm}^2$)
PdL1	0.5	4.376	2.371
	1.0	3.076	3.145
	1.5	2.478	3.486
	2.0	2.256	3.701
PdL2	0.5	4.741	2.498
	1.0	3.318	3.226
	1.5	2.865	3.540
	2.0	2.646	3.726
PdL3	0.5	5.016	2.677
	1.0	3.641	3.368
	1.5	3.129	3.672
	2.0	2.912	3.814
PdL4	0.5	5.426	2.819
	1.0	3.823	3.581
	1.5	3.493	3.818
	2.0	3.128	4.089

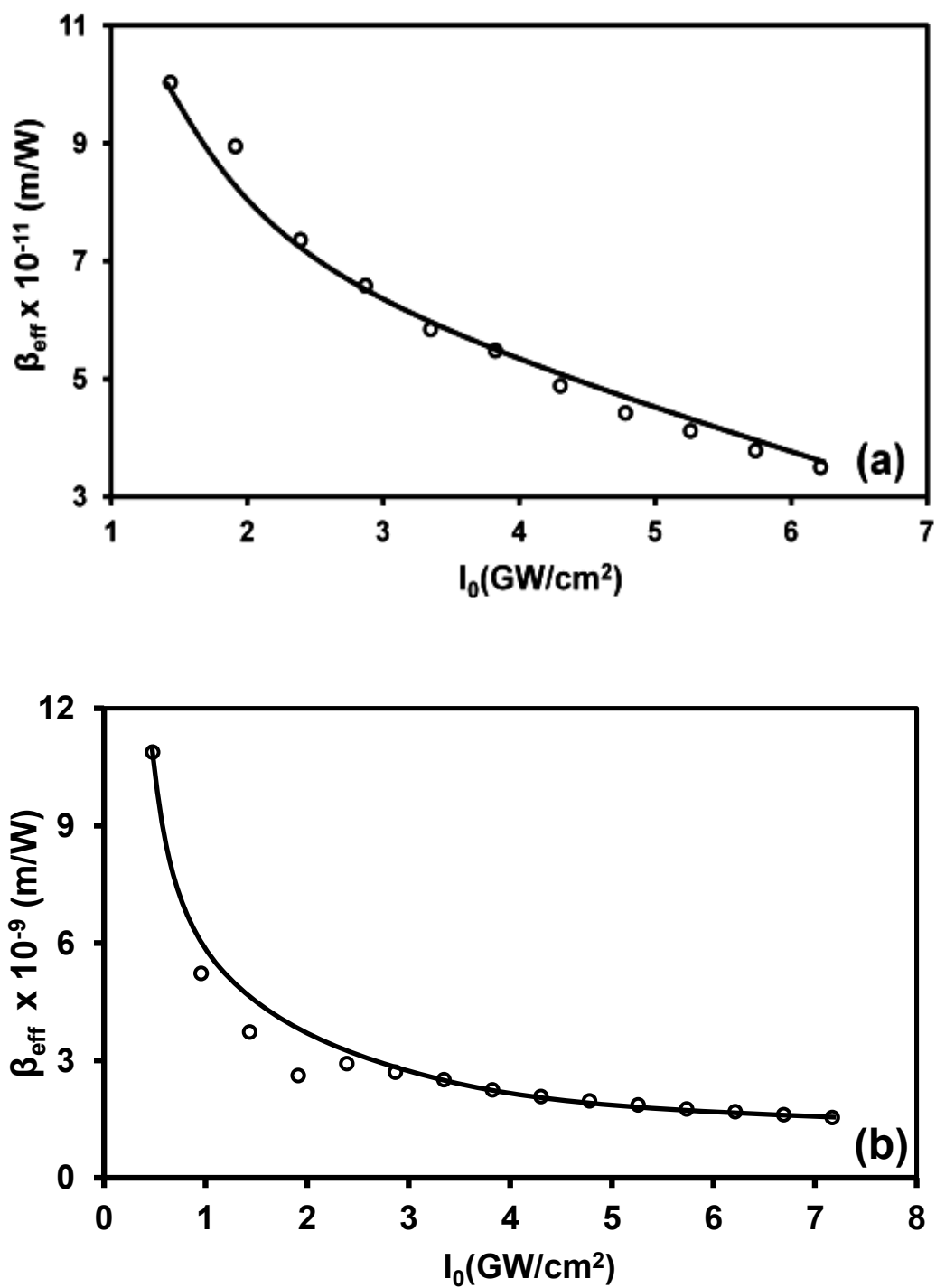


Figure 3.24 Nonlinear absorption coefficient (β_{eff}) versus on-axis input intensity I_0 for PdL1 in solution (1x10⁻³ mol/L) (a) and film form (1.0 wt.%) (b)

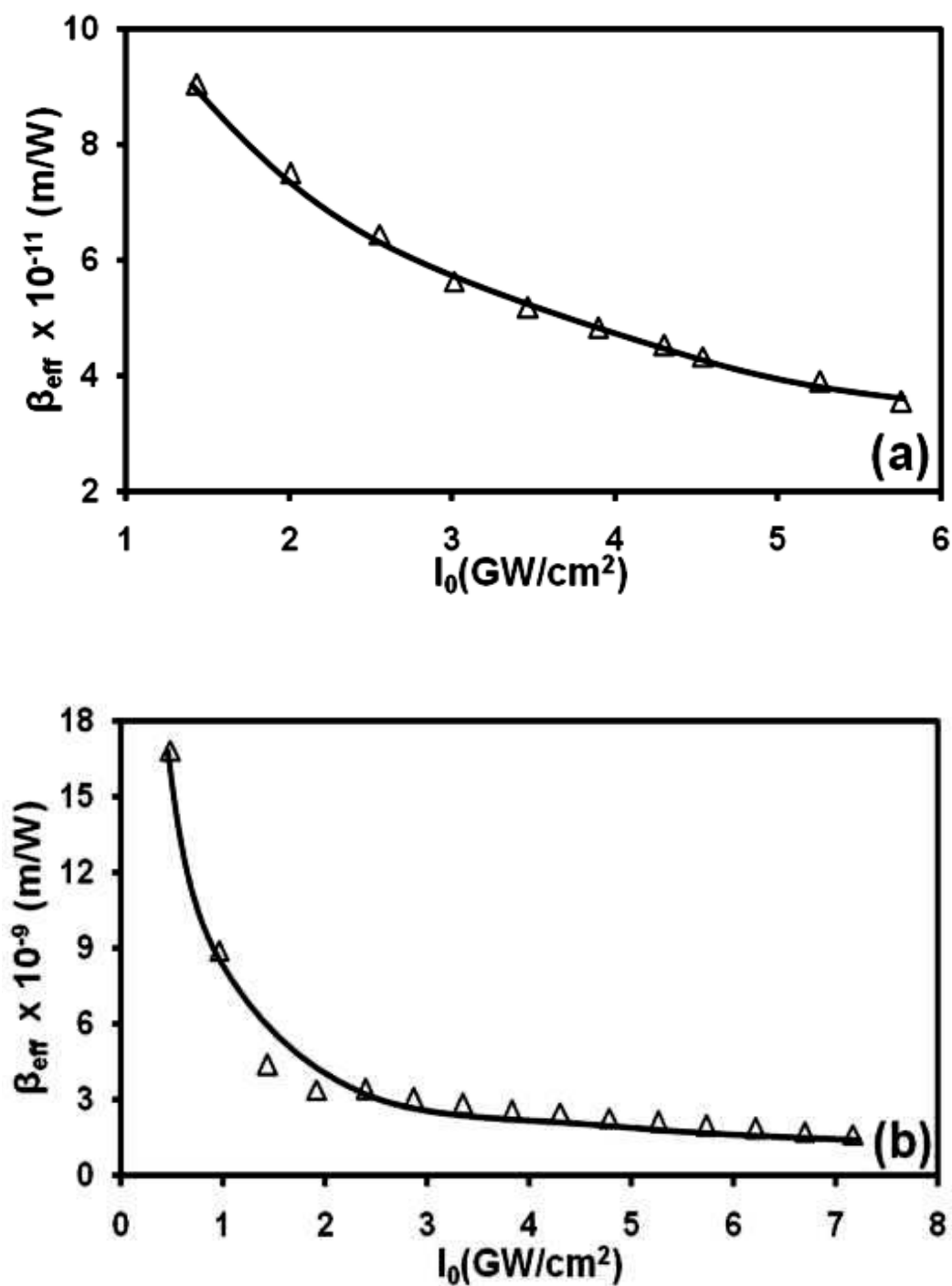


Figure 3.25 Nonlinear absorption coefficient (β_{eff}) versus on-axis input intensity I_0 for PdL2 in solution (1x10⁻³ mol/L) (a) and film form (1.0 wt.%) (b)

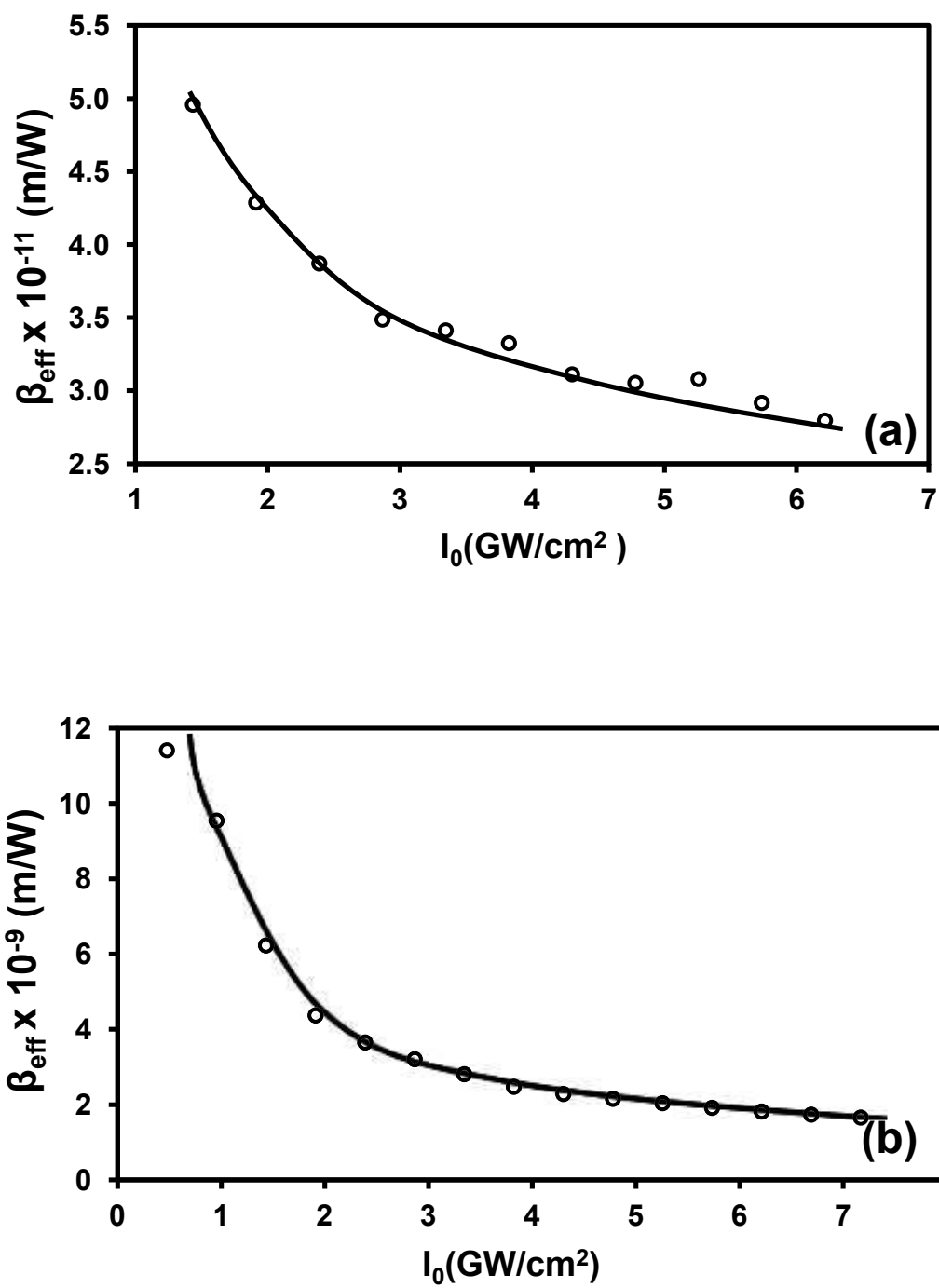


Figure 3.26 Nonlinear absorption coefficient (β_{eff}) versus on-axis input intensity I_0 for PdL3 in solution (1x10⁻³ mol/L) (a) and film form (1.0 wt.%) (b)

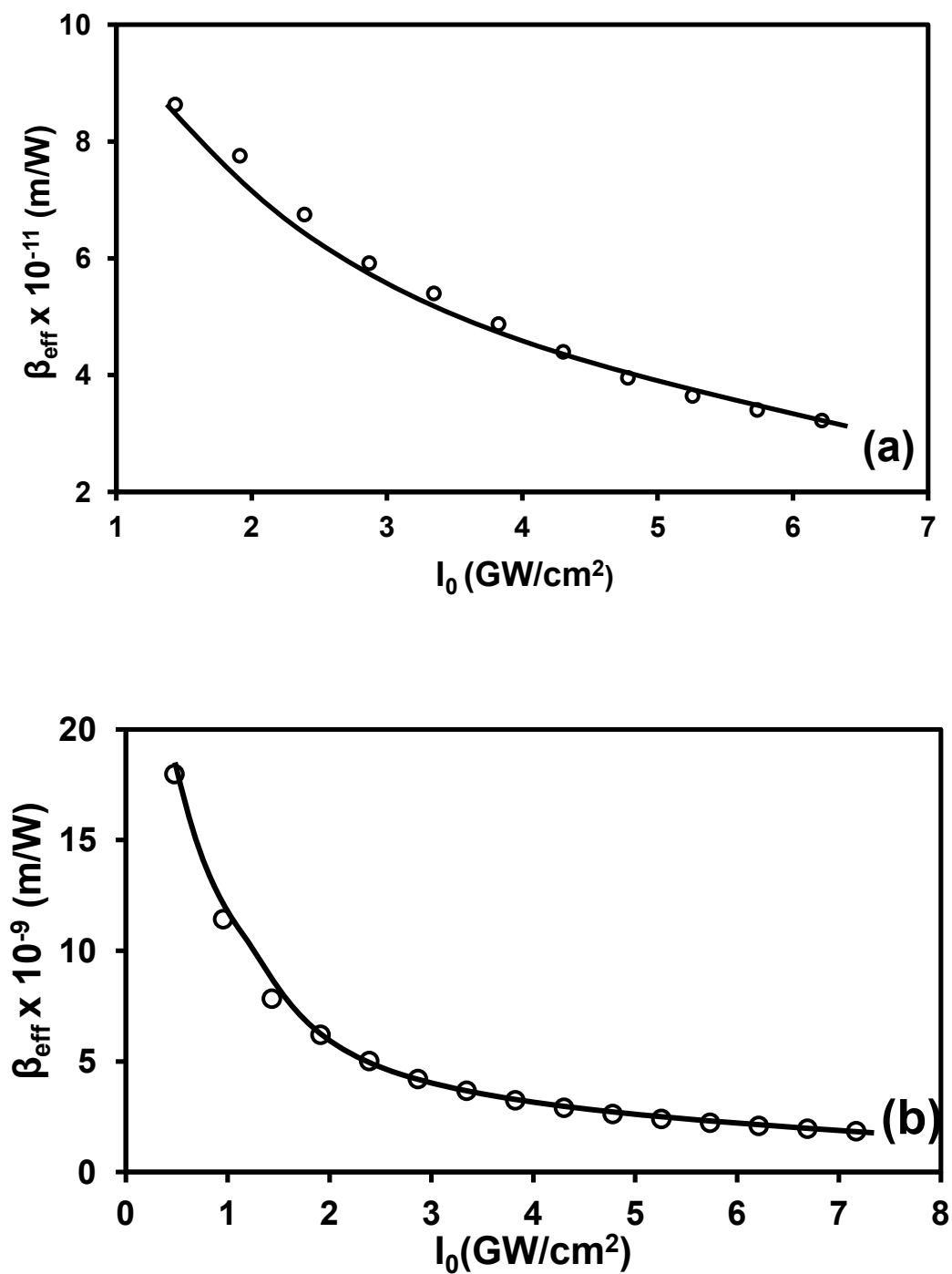


Figure 3.27 Nonlinear absorption coefficient (β_{eff}) versus on-axis input intensity I_0 for PdL4 in solution (1×10^{-3} mol/L) (a) and film form (1.0 wt.%) (b)

Table 3.6 Third-order nonlinear optical parameters of palladium complexes in solution form at different concentrations at the input laser intensity of 1.2 GW/cm².

Sample	Concentration (mol/L) x10 ⁻³	β_{eff} (m/W) x10 ⁻¹¹	$\text{Im } \chi^{(3)}$ (esu) x10 ⁻¹³	n_2 (esu) x10 ⁻¹¹	$\text{Re } \chi^{(3)}$ (esu) x10 ⁻¹³
PdL1	0.25	3.585	0.532	-2.617	-2.738
	0.5	4.511	0.670	-3.758	-3.932
	1	6.229	0.925	-4.605	-4.819
PdL2	0.25	4.077	0.616	-2.812	-2.974
	0.5	5.320	0.803	-4.037	-4.270
	1	8.067	1.218	-5.112	-5.407
PdL3	0.25	4.260	0.636	-2.855	-2.999
	0.5	5.881	0.879	-4.096	-4.303
	1	8.478	1.267	-5.228	-5.492
PdL4	0.25	4.994	0.747	-2.973	-3.126
	0.5	6.591	0.986	-4.331	-4.554
	1	8.887	1.329	-5.377	-5.653

Table 3.7 Third-order nonlinear optical parameters of the palladium complexes at different dopant concentrations in film form at the input laser intensity of 1.2 GW/cm².

Sample	Concentration (wt.%)	β_{eff} (m/W) x10 ⁻⁹	Im $\chi^{(3)}$ (esu) x10 ⁻¹¹	n_2 (esu) x10 ⁻⁹	Re $\chi^{(3)}$ (esu) x10 ⁻¹¹
PdL1	0.50	4.524	0.996	-3.593	-4.887
	1.00	10.820	2.381	-6.470	-8.799
	1.50	12.358	2.720	-7.184	-9.771
	2.00	17.739	3.905	-8.376	-11.392
PdL2	0.50	7.347	1.617	-5.468	-7.436
	1.00	14.075	3.098	-7.455	-10.139
	1.50	15.904	3.501	-7.727	-10.510
	2.00	20.742	4.566	-9.291	-12.635
PdL3	0.50	8.414	1.852	-5.896	-8.018
	1.00	15.181	3.342	-7.721	-10.501
	1.50	18.462	4.064	-8.579	-11.667
	2.00	23.861	5.252	-9.701	-13.194
PdL4	0.50	9.593	2.120	-6.449	-8.771
	1.00	17.171	3.780	-8.275	-11.255
	1.50	20.069	4.418	-9.476	-12.887
	2.00	25.704	5.658	-11.020	-14.986

Second order hyperpolarizability (γ_h) of a molecule is related to the third-order bulk susceptibility through Equation (2.42) as shown in chapter 2. The calculated values of γ_h for PdL1, PdL2, PdL3 and PdL4 are 1.390×10^{-30} esu, 1.591×10^{-30} esu, 1.561×10^{-30} esu and 1.768×10^{-30} esu, respectively.

3.5 DEGENERATE FOUR WAVE MIXING STUDIES

Q-Switched Nd:YAG laser producing of 7 ns pulses at 532 nm wavelength was used as the excitation source. The energy of the phase conjugate signal as well as the pump beams were measured by using Rjp-735 pyroelectric detectors which are connected to dual channel energy meter Rj-7620 (Laser Probe Inc., USA).

The magnitude of third-order nonlinear optical susceptibility $|\chi^{(3)}|$ (Caro and Gower 1982) of palladium complexes were estimated using the following relations:

$$\chi_{sample}^{(3)} = \chi_{ref}^{(3)} \left(\frac{I_{sample}}{I_{ref}} \right)^{1/2} \left(\frac{n_{sample}}{n_{ref}} \right)^2 \left(\frac{l_{ref}}{l_{sample}} \right) \left(\frac{\alpha_0 l}{e^{-\alpha_0 l/2} (1 - e^{-\alpha_0 l})} \right) \quad (3.10)$$

where I_{sample} and I_{ref} are DFWM signal intensities, n is the refractive index, l is the thickness of the medium, and α_0 is the linear absorption coefficient at 532 nm. We have used CS₂ as the reference material for which $|\chi_{ref}^{(3)}|$ is taken to be 4×10^{-13} esu (Shirk et al. 1992).

3.5.1 Calibration

In DFWM experiment, to measure $|\chi^{(3)}|$, the experimental setup has to be standardized using a well known reference nonlinear optical material. Carbon disulphide (CS₂) is used as the standard material because of its completely non-resonant Kerr nonlinearity due to orientational response. Figure 3.28 shows the DFWM signal as a function of input laser energy for CS₂, the solid curve is the theoretical fit to experimental data points.

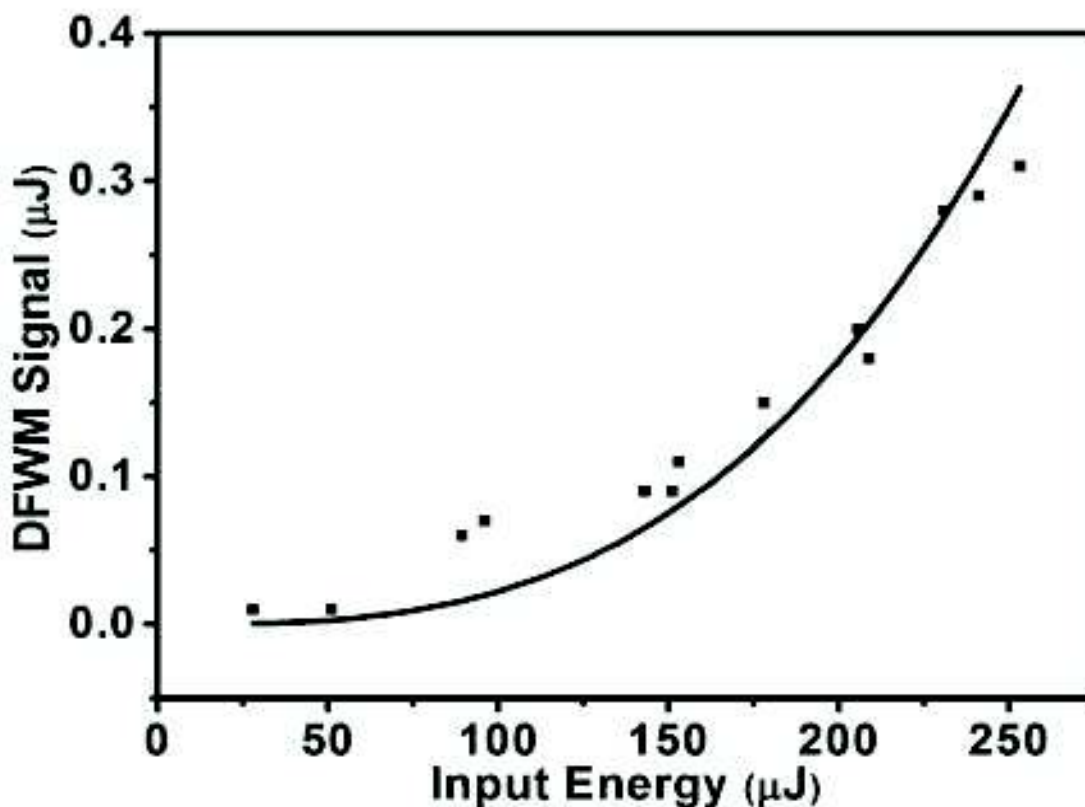


Figure 3.28 DFWM signal of CS₂. Squares are data points while the solid curve is a cubic fit to the data

3.5.2 DFWM results

Figures 3.29 to 3.32 shows the DFWM signal versus input energy graphs for palladium complexes at the concentrations of 1×10^{-3} mol/L. The cubic dependence of DFWM signal with respect to input energy is observed in all samples. The signal is proportional to the cubic power of the input intensity as given by the Equation 2.35. This behavior of the DFWM signal indicates the third-order nature of the nonlinear process involved.

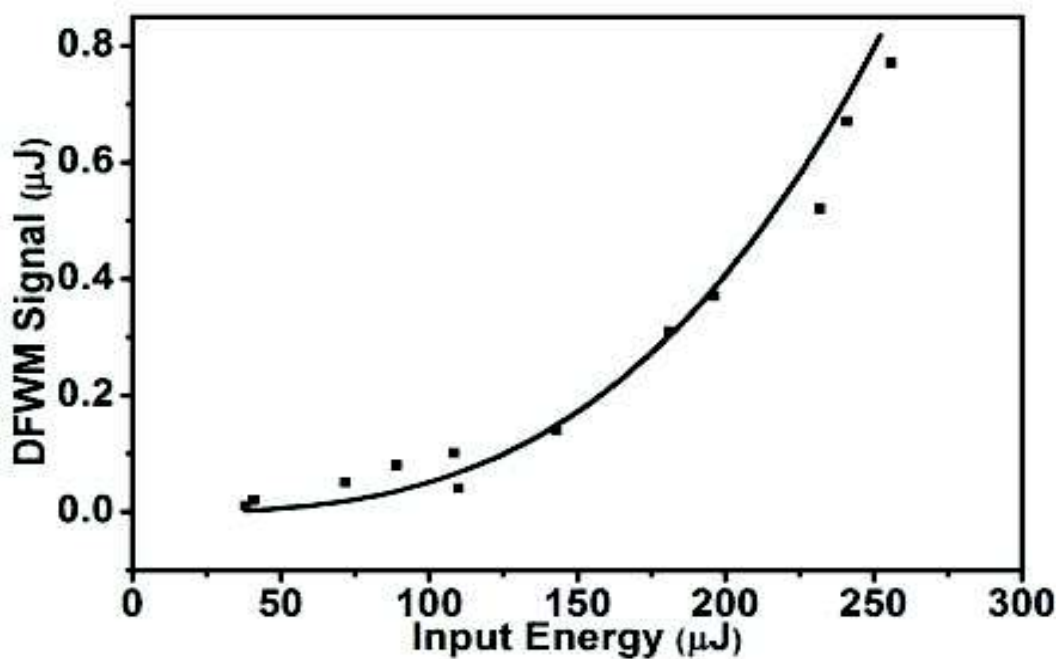


Figure 3.29 DFWM signal of PdL1 at the concentration of 1×10^{-3} mol/L. Squares are data points while the solid curve is a cubic fit to the data

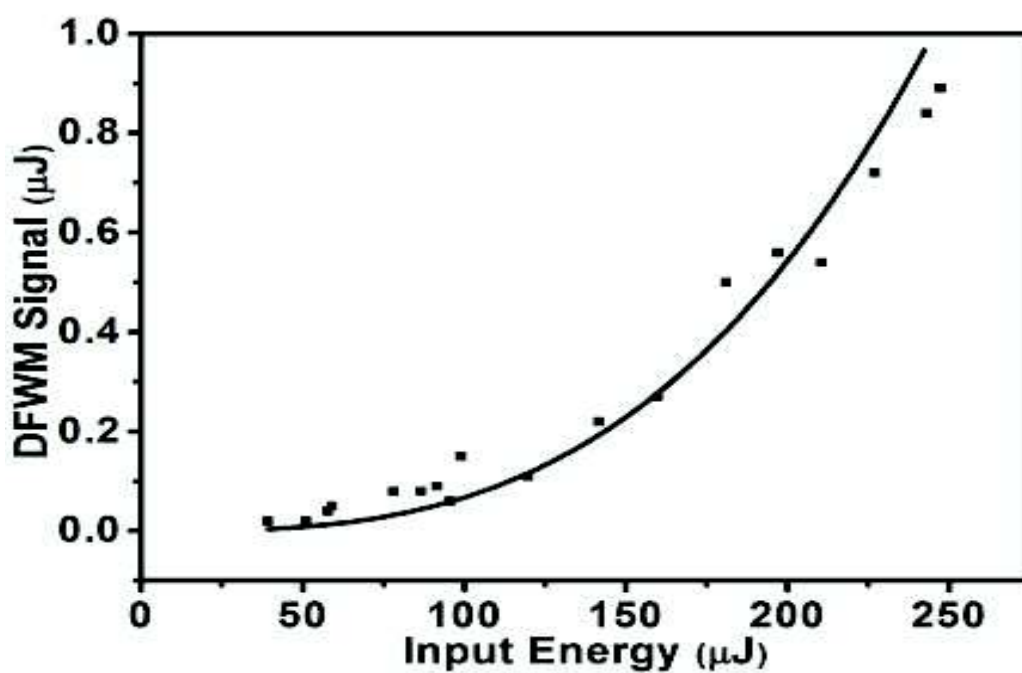


Figure 3.30 DFWM signal of PdL2 at the concentration of 1×10^{-3} mol/L. Squares are data points while the solid curve is a cubic fit to the data

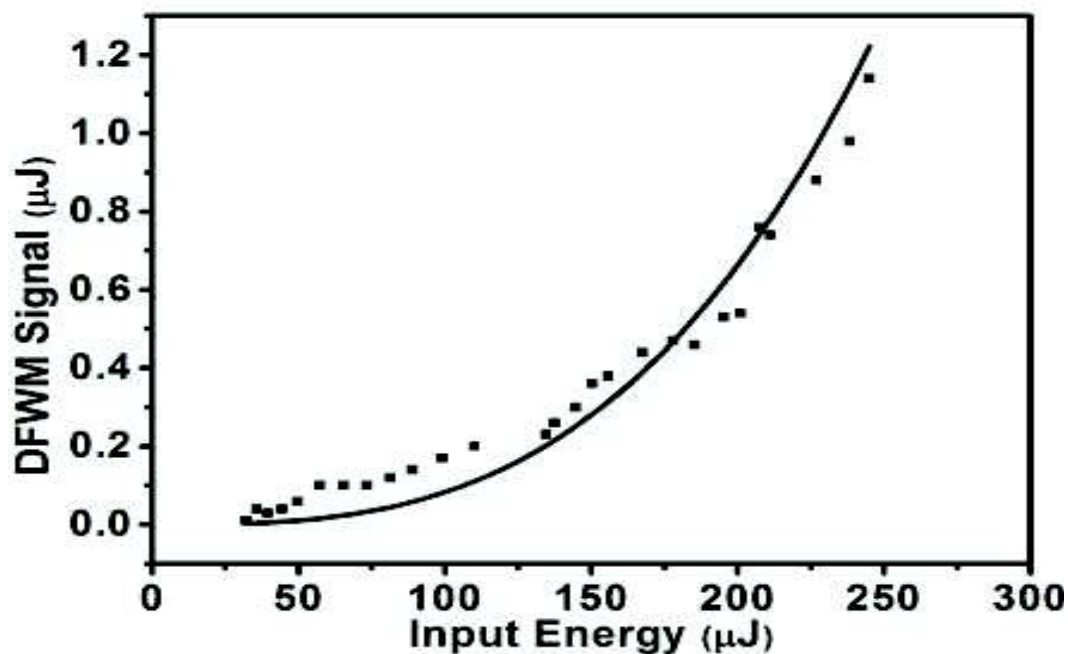


Figure 3.31 DFWM signal of PdL3 at the concentration of 1×10^{-3} mol/L. Squares are data points while the solid curve is a cubic fit to the data

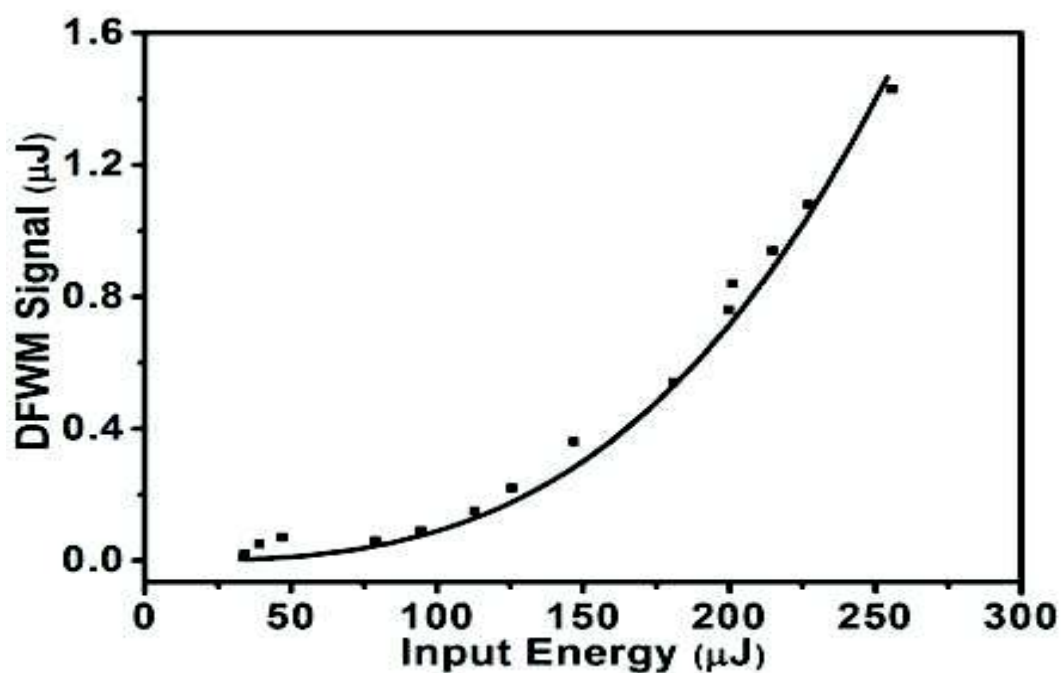


Figure 3.32 DFWM signal of PdL4 at the concentration of 1×10^{-3} mol/L. Squares are data points while the solid curve is a cubic fit to the data

The measured values of third-order nonlinear optical susceptibility $|\chi^{(3)}|$, second-order hyperpolarizability γ_h are given in the Table 3.8.

Table 3.8 Linear absorption coefficient α_0 , third-order nonlinear optical susceptibility $|\chi^{(3)}|$, second-order hyperpolarizability γ_h of different palladium complexes measured by DFWM technique.

Sample	α_0 (cm ⁻¹)	$ \chi^{(3)} $ (x 10 ⁻¹³ esu)	γ_h (x 10 ⁻³¹ esu)
PdL1	0.328	4.612	2.498
PdL2	0.262	5.208	2.763
PdL3	0.475	5.999	3.263
PdL4	0.731	6.080	3.308

3.6 STRUCTURE-PROPERTY RELATIONSHIP WITH THIRD-ORDER NONLINEAR OPTICAL PARAMETERS IN PALLADIUM METAL-ORGANIC COMPLEXES

The experimental results permit us to draw a number of interesting conclusions. The conjugated triphenylphosphine ligand with its electron accepting character (d to σ^*) (Orpen and Connelly 1985 and Pacchioni and Bagus 1992), facilitates effective electronic communication and CT transitions between metal (palladium) and ligands leading to large dipole moment changes between the excited states (Poornima et al. 2003). Several reports on complexes containing phosphine (Cheng et al. 1990, Whittal et al. 1997, Whittal et al. 1996 and McDonagh et al. 2000) and Schiff base (Tian et al. 2005, Bella and Fragala 2000 and Costes et al. 2005) ligands suggest large nonlinear absorption coefficient for those materials. The existence of strong intramolecular CT excitations in a molecular environment is the key to the NLO activity. The first criterion can be satisfied by considering a polarizable molecular system (e.g. π -conjugated pathway) having an uneven or asymmetric charge distribution. The simplest way to achieve this is to have a donor (D) – acceptor (A) system with a bridge (D– π –A), which can help the electronic transport between the donor and the acceptor. Most metal complexes can be envisaged within the above mentioned D– π –A system, in which donor and/or acceptor, or the bridge moieties are selectively replaced by an organometallic group.

This is because metal complexes possess intense, low energy MLCT, LMCT, or intraligand charge transfer (ILCT) excitations. Therefore, they can effectively behave as donor and/or acceptor groups of the D- π -A system, or as constituents of the polarizable bridge (Poornima et al. 2003). Metal ions make an important contribution to the NLO properties. The strength of the NLO properties can be altered by the π -back-donation capacity of the metal ions to the ligands. An increase in this π -back-donation capacity may enhance the extension of the electronic π system and improve the NLO properties (Chao et al. 1999). From these results it is clear that the resonance and structural effects, which determine the electronic polarization properties, will modulate the observed nonlinearity.

Among the four complexes studied, the methoxy substituted complex shows maximum nonlinearity, whereas nitro substituted complex shows least. This can be explained by, electron donation capacity of the substituent. The presence of methoxy group at para position in the Schiff base ligand increases the electron donation ability of ligand towards metal centre, whereas the presence of nitro group decreases the electron donation. Hydrogen and chloro substituted ligands are weak electron donors. This clearly explains the observed trend in the nonlinearity.

3.7 OPTICAL POWER LIMITING STUDIES

Materials with large nonlinear absorption exhibit strong optical power limiting behavior. These materials are recognized as potential materials for application in sensors and human eye protection. The essential requirements for optical power limiting materials are high linear transmittance and high damage threshold (Tutt and Boggess 1993). Reverse saturable absorption (RSA) based nonlinear optical materials have attracted significant interest as optical power limiters. The five level model describes the process responsible for the optical limiting effects of RSA. In the case of RSA, the absorption cross section of the excited state, σ_{exc} , should exceed the ground state cross section, σ_g . An efficient optical limiter should therefore have:

- i) A triplet state absorption cross section that is larger than the ground state ($\sigma_{exc} \gg \sigma_g$).

- ii) Lifetimes in the microsecond time range and a large population in the triplet state.
- iii) Rapid intersystem crossing in order to populate the triplet state.
- iv) Optical stability, to minimize degradation of the optical limiting material under laser irradiation.
- v) Good processibility (Dini et al. 2003, Hanack et al. 2001, Dini et al. 2005, Dini and Hanack 2003, Dini et al. 2001 and Chen et al. 2005).

The detailed experimental procedure of optical power limiting is mentioned in section 2.3.2. Optical limiting experiments were carried out by placing the metal-organic samples at the focus of the Gaussian laser beam and by measuring the transmitted energy for different input laser energies. Figure 3.33 to 3.36 show the optical power limiting response of the palladium complexes PdL1, PdL2, PdL3 and PdL4 in solution form. The palladium complexes in film form have also been studied for optical power limiting properties. Figures 3.37 to 3.40 show the optical power limiting behavior of palladium complexes PdL1, PdL2, PdL3 and PdL4 in film form. The optical limiting threshold and clamped output energy of palladium complexes PdL1, PdL2, PdL3 and PdL4 in solution and film form are tabulated in Tables 3.9 and 3.10.

Among the four investigated palladium complexes the PdL4 exhibits better optical limiting property. This may be due to the presence of dimethoxy group in the terminal of palladium complex which has strong electron donating ability. Optical limiting data also shows that, as the doping concentration increases, the clamping level decreases. This is because at higher concentration more absorptive centers are created in the solution and film samples. Thus, the palladium complexes studied by us seem to emerge as promising candidates for making optical power limiting devices.

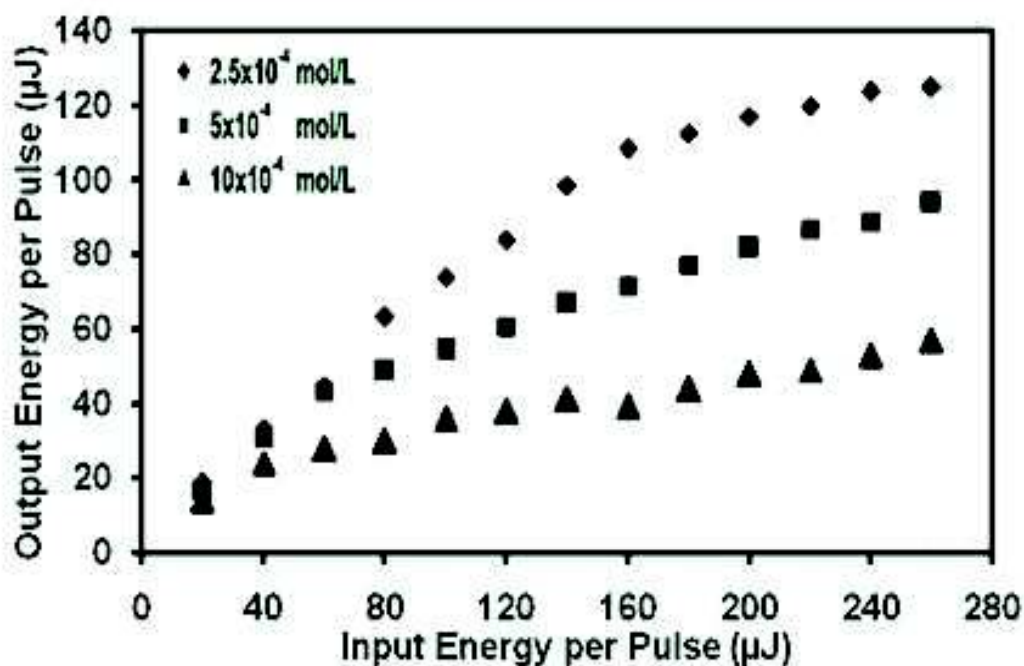


Figure 3.33 Optical power limiting behavior of palladium complex PdL1 in solution form at various concentrations indicated in the inset

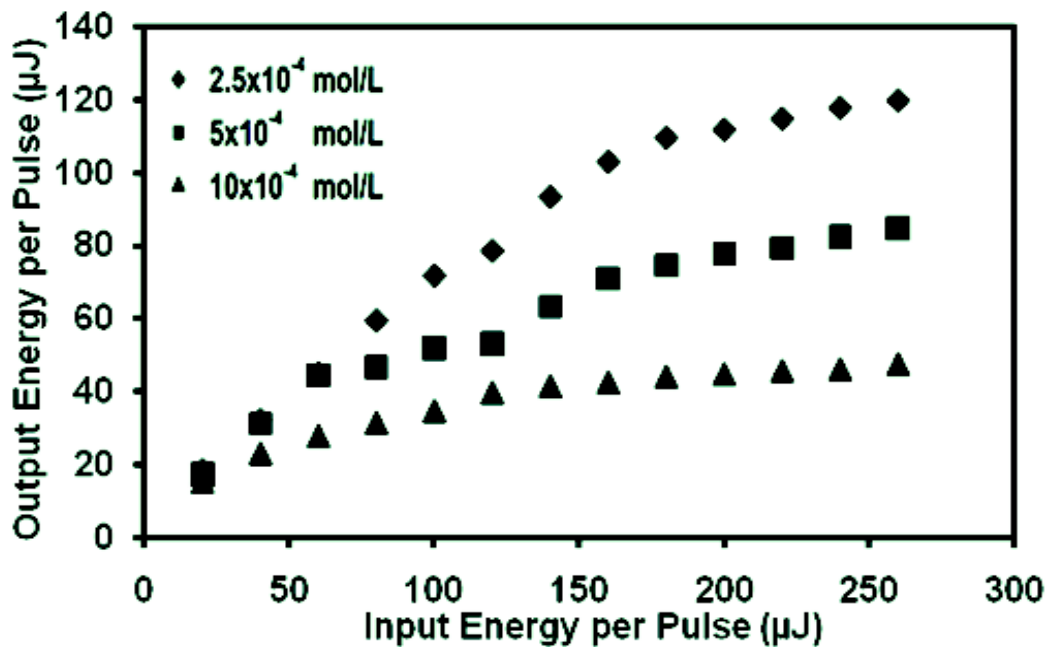


Figure 3.34 Optical power limiting behavior of palladium complex PdL2 in solution form at various concentrations indicated in the inset

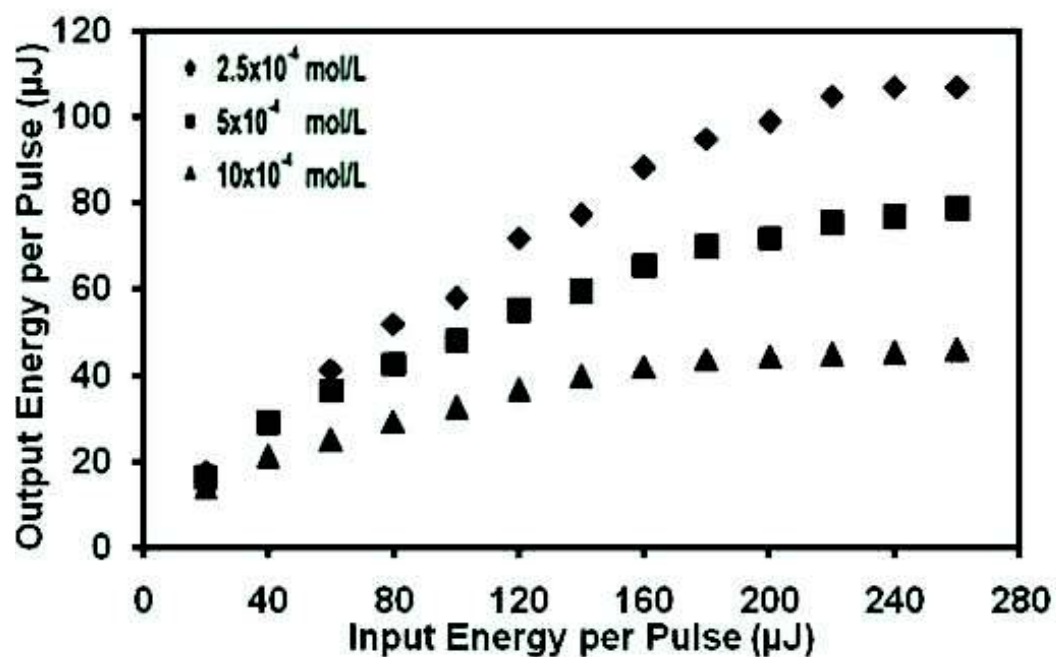


Figure 3.35 Optical power limiting behavior of palladium complex PdL3 in solution form at various concentrations indicated in the inset

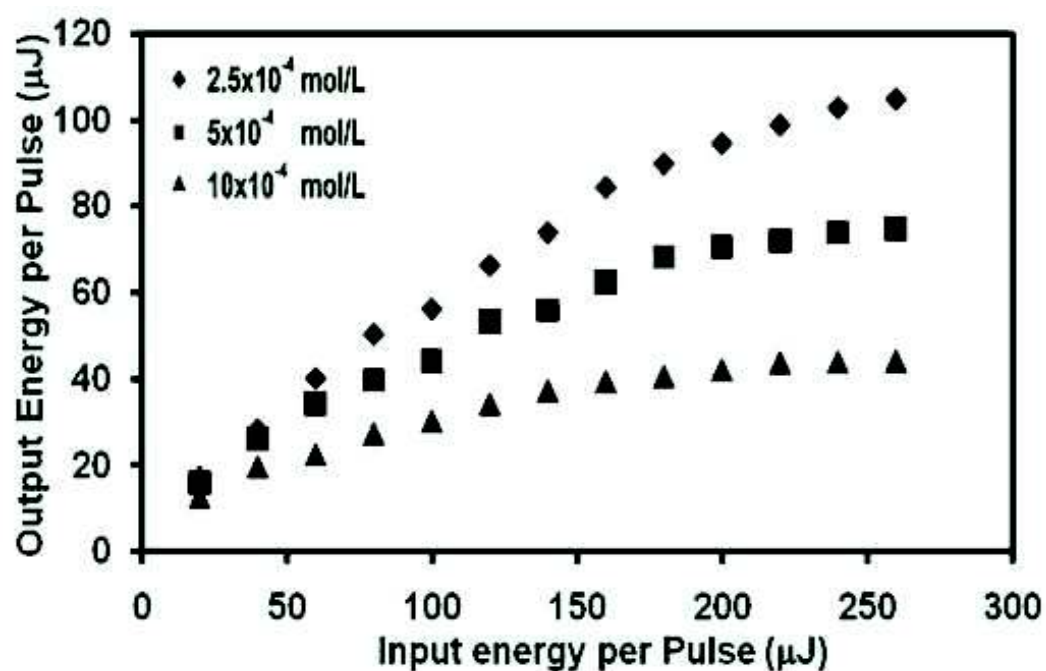


Figure 3.36 Optical power limiting behavior of palladium complex PdL4 in solution form at various concentrations indicated in the inset

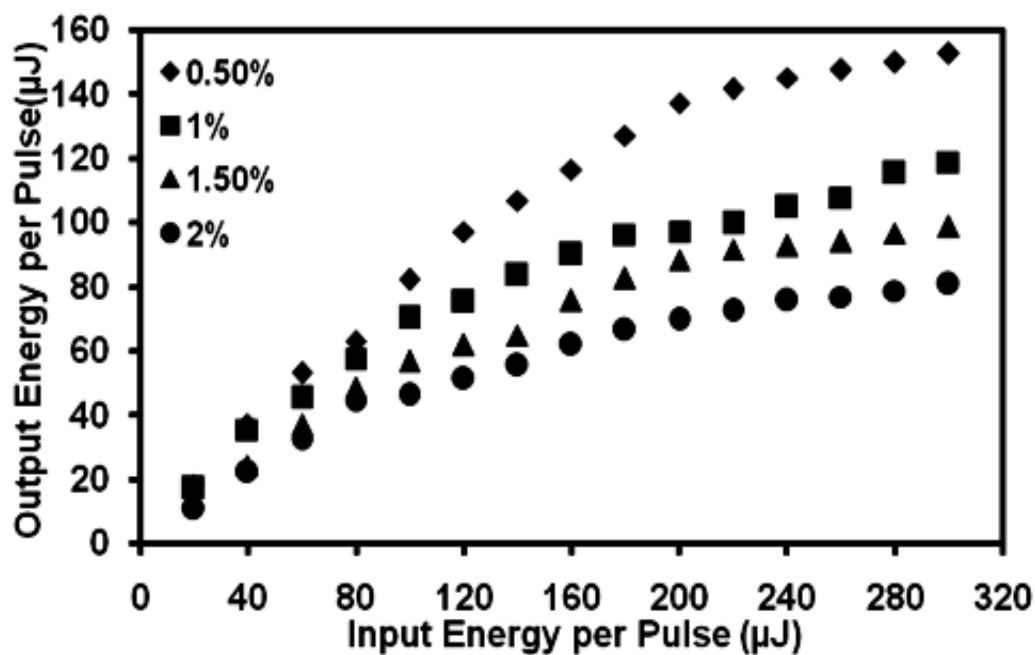


Figure 3.37 Optical power limiting behavior of palladium complex PdL1 in film form at various concentrations indicated in the inset

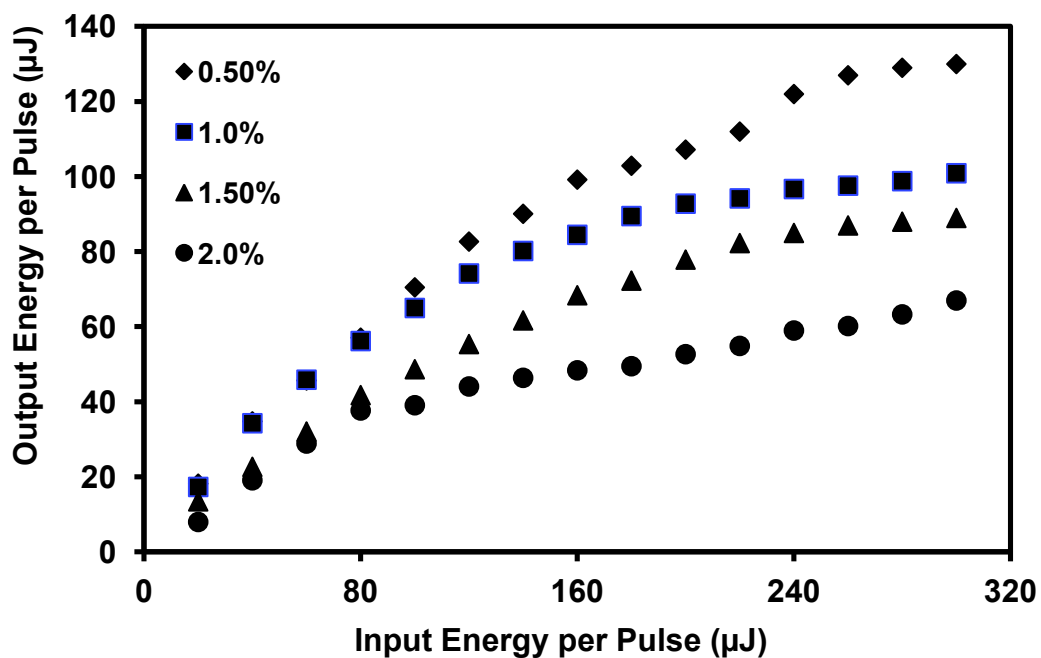


Figure 3.38 Optical power limiting behavior of palladium complex PdL2 in film form at various concentrations indicated in the inset

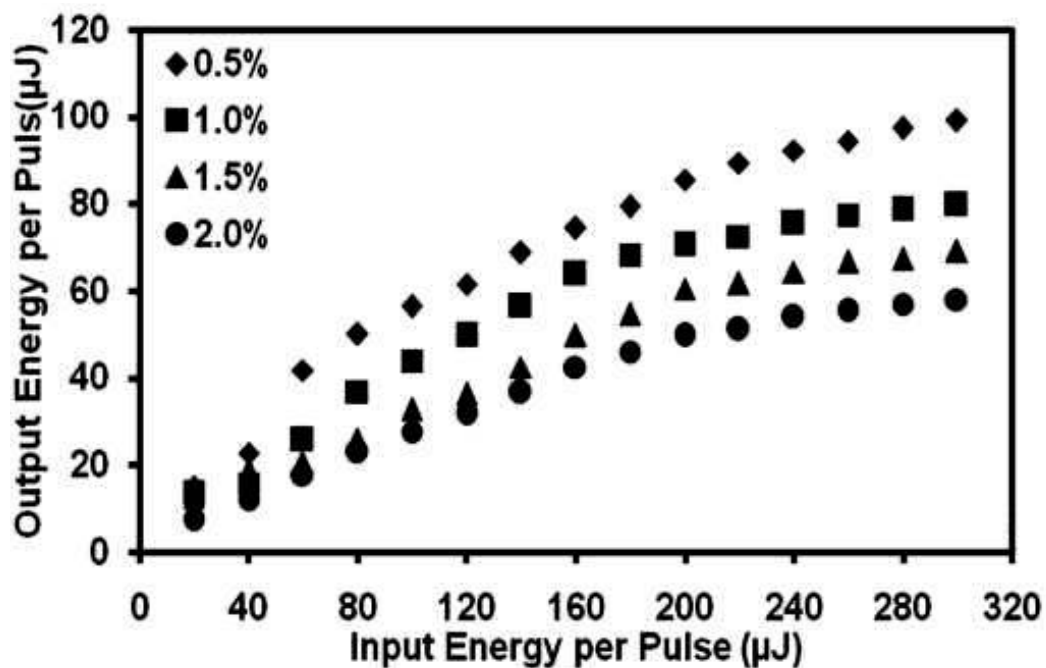


Figure 3.39 Optical power limiting behavior of palladium complex PdL3 in film form at various concentrations indicated in the inset

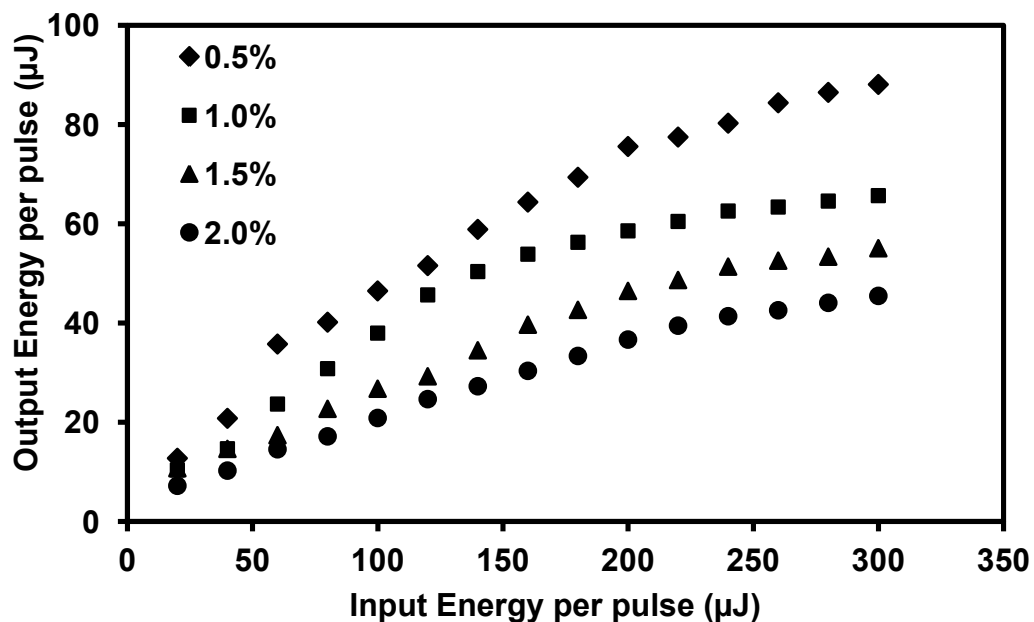


Figure 3.40 Optical power limiting behavior of palladium complex PdL4 in film form at various concentrations indicated in the inset

Table 3.9 Optical limiting threshold and clamped output energy of the palladium complexes in solution form at different concentrations

Sample	Concentrations (x 10⁻³ mol/L)	Optical limiting threshold (μJ)	Clamped output energy (μJ)
PdL1	0.25	190	120
	0.5	170	92
	1	140	55
PdL2	0.25	180	115
	0.5	160	83
	1	150	48
PdL3	0.25	180	107
	0.5	150	78
	1	130	45
PdL4	0.25	160	103
	0.5	120	73
	1	100	43

Table 3.10 Optical limiting threshold and clamped output energy of the palladium complexes doped in film form at different dopant concentrations

Sample	Dopant Concentrations (wt.%)	Optical limiting threshold (μJ)	Clamped output energy (μJ)
PdL1	0.5	240	150
	1.0	200	115
	1.5	190	98
	2.0	180	80
PdL2	0.5	220	128
	1.0	190	96
	1.5	170	88
	2.0	150	65
PdL3	0.5	200	96
	1.0	180	78
	1.5	160	68
	2.0	140	57
PdL4	0.5	200	87
	1.0	160	64
	1.5	140	55
	2.0	100	45

3.8 CONCENTRATION DEPENDENCE OF THIRD ORDER NONLINEARITY

Z-scan measurements were performed on solutions and films of different concentration to study the effect of concentration of the dopant on third-order NLO parameters. Figures 3.41 and 3.42 show the dependence of nonlinear absorption (β_{eff}) on the concentration for PdL1 and PdL4 in solution and film form, respectively. Nonlinear absorption coefficient varies linearly with sample concentration. The study reveals that there is a relationship between nonlinear response and concentration of the solute/dopants. Hence, the nonlinear absorption arises mainly from doped NLO chromophores PdL1, PdL2, PdL3 and PdL4.

This result also tallies with Tables 3.1 and 3.2, whereas NLO parameters are seen to increase with concentrations.

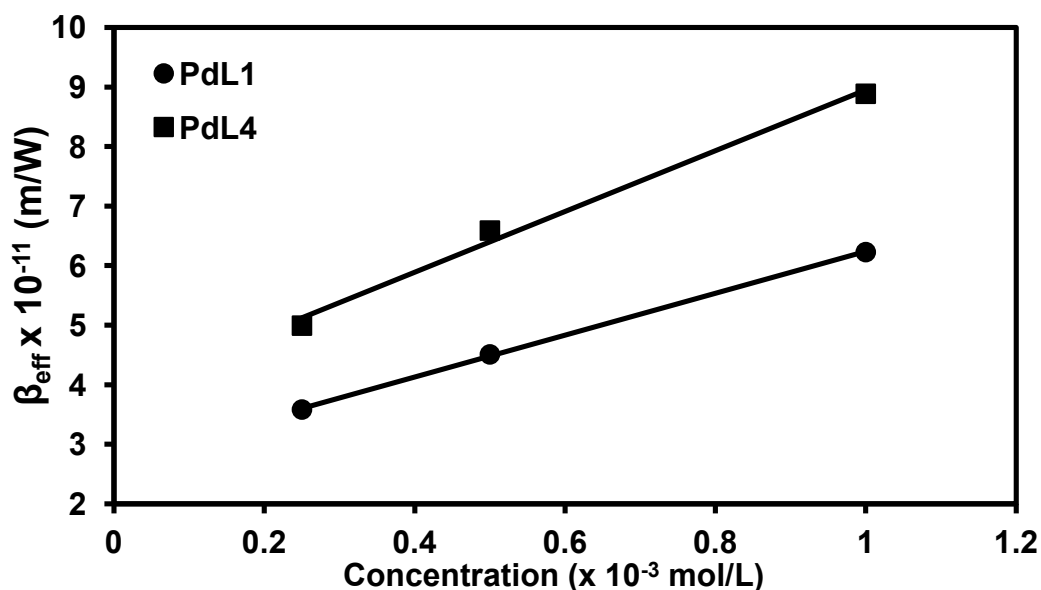


Figure 3.41 Concentration dependent nonlinear absorption coefficient (β_{eff}) of PdL1 and PdL4 in solution form

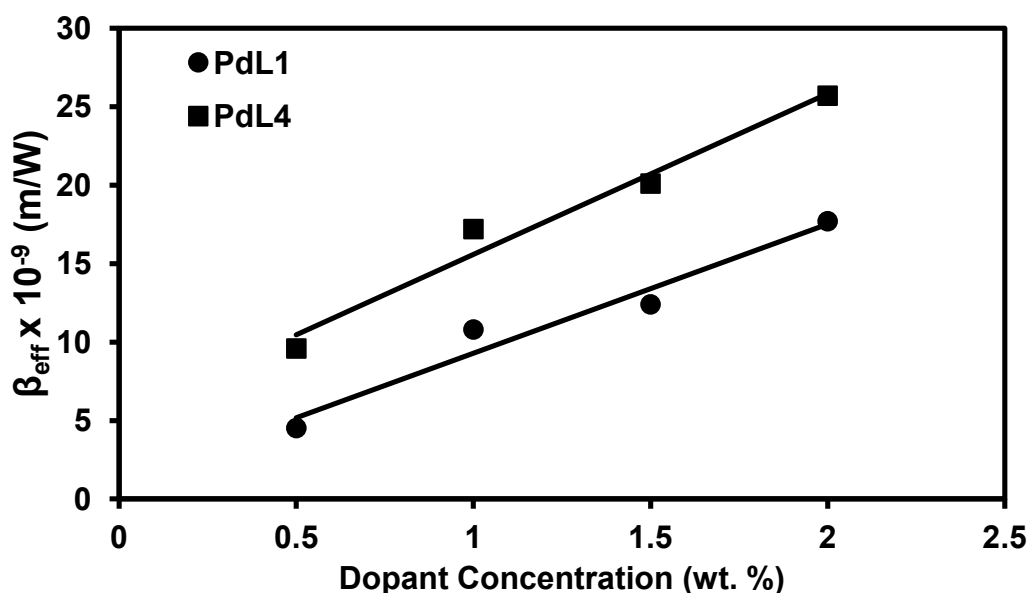


Figure 3.42 Concentration dependent nonlinear absorption coefficient (β_{eff}) in PdL1 and PdL4 film form

Results indicate that palladium complexes in film form possess large NLO properties, and the values of $\chi^{(3)}$ are of the order of 10^{-11} esu. This is simply due to the fact that the number density of palladium molecules in film form is much more than that in the solution form, resulting in a larger number of absorbing centers to be present in the film than in the solution (Tekin et al. 2010).

3.9 ALL-OPTICAL SWITCHING STUDIES OF PALLADIUM COMPLEXES

We now discuss the all-optical switching behavior of palladium complexes based on excited state absorption. The laser pulse shapes recorded in the pump-probe experiments on switching action of our sample films are shown in Figure 3.43 for PdL1. When the pump pulse is turned off, the output probe beam regains its full intensity (ON-state). Thus, the CW He-Ne laser beam passing through the sample film can be switched ON and OFF by the 7 ns Q-switched Nd: YAG laser of 532 nm wavelength (Abdeldayem et al. 2003). The upper curves are the pulse shape of pump beam at different intensities (a) 5 GW/cm², (b) 10 GW/cm² and (c) 15 GW/cm² whereas lower curves show the output signal shape of probe beam at corresponding pump intensities.

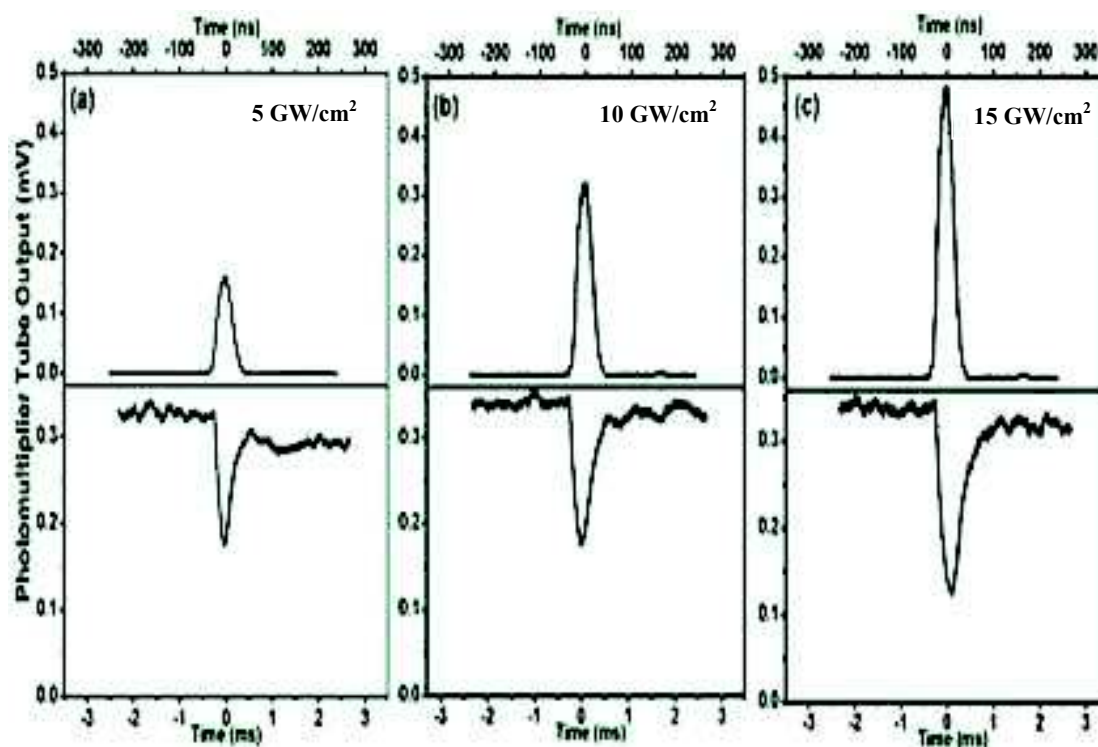


Figure 3.43 All-optical switching signal for PdL1 (Conc. 1.0 wt.%) with varying pump beam intensities 5 GW/cm² (a), 10 GW/cm² (b) and 15 GW/cm² (c). The upper curves show the pulse shape of the Nd: YAG laser beam used, whereas the lower curves show the signal wave form of the probe He-Ne laser beam.

The physical mechanism responsible for all-optical switching is primarily based on ESA. When the pump pulse passes through the sample, the population of the triplet state, T_1 increases, which results in strong absorption of the probe He-Ne beam, thereby reducing its transmission. After the pump pulse crosses the sample, the population of the triplet state drops drastically and the He-Ne laser output intensity regains its original value. At higher pump beam intensities the increased population of the excited state causes increase in the probe beam absorption. The modulation of the probe intensity calculated for palladium complexes are given in Table 3.9. The strength of modulation of the probe increases as the intensity of pump beam increases due to the increase in the population of triplet state (Singh et al. 2005). The switching times, seen to be in the range of few micro seconds, are given in Table 3.11. The relaxation of the triplet state to the ground state is forbidden, resulting in slow switching time of the molecules (Henari 2001). Similar all-optical switching curves

were obtained for other investigated palladium metal-organic complexes PdL2, PdL3 and PdL4 with different response time and modulation of probe beam are listed in Table 3.9.

Table 3.11 Fall time, rise time, FWHM and modulation of probe beam of PdL1, PdL2, PdL3 and PdL4 at different pump intensities.

Sample	Intensity (GW/cm ²)	Fall Time (T _f) (μs)	Rise Time (T _r) (μs)	FWHM (μs)	Modulation of probe beam %
PdL1	5	142	336	323	46
	10	206	373	398	49
	15	224	533	490	64
PdL2	5	199	221	311	32
	10	311	476	415	40
	15	306	340	449	54
PdL3	5	160	225	288	41
	10	175	312	468	46
	15	260	359	594	49
PdL4	5	100	185	237	50
	10	180	411	437	56
	15	225	549	536	62

3.10 CONCLUSIONS

In summary, the third-order nonlinear optical properties, optical power limiting and all-optical switching performance of the palladium metal-organic series in both solution and in film forms were studied using nanosecond Z-scan technique at 532 nm wavelength. Films possess the third-order nonlinear optical susceptibility of the order of 10^{-11} esu which is two orders of magnitude higher than that for the PdL

solution. Further, our experiments indicate that the nonlinear absorption is due to RSA. Palladium complex films exhibit good optical power limiting behavior for nanosecond laser pulses. The complex shows all-optical switching behavior. Among the four palladium metal-organic complexes investigated here, PdL4 exhibits the best NLO properties for nanosecond laser pulses compared to the other three molecules PdL1, PdL2 and PdL3. This is due to the presence of strong electron donating groups in the molecule. Increasing the strength of electron donating ability of the complex i.e. $\text{NO}_2 < \text{Cl} < \text{H} < \text{OCH}_3$, resulted in increase in the third-order nonlinear optical parameters, which shows that the structure and NLO property in the molecule are correlated. With these NLO properties, it is concluded that the metal-organic material investigated herein are a promising materials for new photonic devices.

CHAPTER 4

CHAPTER 4

THIRD-ORDER NONLINEAR OPTICAL STUDIES OF RUTHENIUM METAL-ORGANIC COMPLEXES CONTAINING DMIT LIGAND

Abstract

This chapter reports the results of Z-scan, DFWM, optical power limiting and all-optical switching experiments on two ruthenium complexes containing dmit ligand. The effect of π -conjugation and delocalization on third-order nonlinear optical properties is discussed. The concentration dependence of third-order nonlinear optical properties of these metal-organic complexes is also presented.

4.1 INTRODUCTION

Recently exciting new developments have occurred in the domain of photonic devices due to the synthesis of several novel materials possessing large and ultrafast nonlinear optical responses which has led to the fabrication of ultrafast optical switching and processing devices (Halvorson et al. 1994, Marder et al. 1997, Slepko et al. 2002, Chen et al. 2003, Gu et al. 2004). For such applications, a variety of materials including semiconductors, polymers, nanomaterials and inorganic materials have been researched. In recent years, π -conjugated organic materials have received considerable interest since they possess high nonlinear optical (NLO) properties and fast response time (Gomes et al. 1996). The exciting thing about such organic materials is the possibility of enhancing their third-order nonlinearity by incorporating metals into molecules. Organometallic and coordination chemistry offers a very large variety of NLO materials differing in metal nd configuration, oxidation state and spin state. Such materials are also seen to have good optical transparency and thermal stability. The central metal atom of organometallic and coordination complexes can readily coordinate with conjugated ligands and undergo metal-ligand orbital overlap, facilitating effective electronic transport and electronic transitions between the metal

ion and the ligand, leading to large changes in the dipole moment between the excited states (Deng et al. 2000).

Metal complexes with sulfur-containing chelating ligands have attracted attention of several researchers due to their unique physical and chemical properties (Matsubayashi et al. 2002). Among such ligands, dithiolate ligands have been studied most extensively (Karlin and Stiefel 2004). Oxidation of dianionic complexes $[M(S_2C_2R^1R^2)_2]^{2-}$ leads to neutral compounds (Schrauzer and Mayweg 1962) in which sulfur-containing ligands may have dithiocarbonyl or dithiolate structure depending on the different oxidation states of the metal atom. High degree of electron delocalization, strong mixing of orbitals of the ligand and metal ion and the possibility of stabilization of metal complexes in different oxidation states are key factors responsible for unique properties of these compounds. Specially, π -electron conjugated systems like 2-thioxo-1,3-dithiole-4,5-dithiolate (dmit) and related ligands have been used in the synthesis of good electrically conducting radical anion salts and charge-transfer complexes. Recently several investigations have been carried out on potential applications of dithiolene complexes to study their magnetic, electrical and non-linear optical properties (Kato 2004, Karlin and Stiefel 2004, Fourmigue 2004, Davison et al. 1963 and Williams et al. 1966). The nature of electronic structure of dithiolene metal complexes leads to a variety of important photonic devices.

With the above facts in mind, we have synthesized and investigated two new ruthenium complexes focusing on their third-order nonlinear optical, optical power limiting and all-optical switching properties. The correlation between the values of the NLO parameters and the molecules is also discussed.

4.2 SYNTHESIS AND CHARACTERIZATION OF RUTHENIUM COMPLEXES BASED DMIT LIGAND

4.2.1 Materials and methods

We used analytic grade chemicals for synthesizing the new compounds. Solvents were purified and dried according to the standard procedures (Vogel 1989). $[RuCl_2(PPh_3)_2]$ and $[RuCl_2(PPh_3)_2]$ were synthesized as per the reported procedure

(Stephenson and Wilkinson 1966). The C, H, O and S contents of the complex were determined by Thermoflash EA1112 series elemental analyzer. Magnetic susceptibility measurement was recorded on a Sherwood Scientific instrument (UK). Thermal analysis was carried out (EXSTAR-6000) from room temperature to 700°C at a heating rate of 10°C/min. The electronic spectrum of the complex was measured on a GBC Cintra 101 UV–Vis double beam spectrophotometer using DMF in the 200–800 nm wavelength range. FT-IR spectrum was recorded on a Thermo Nicolet Avatar FTIR spectrometer in the range 400–4000 cm^{-1} . ^1H NMR and ^{31}P NMR spectra were recorded in Bruker AV 400 instrument using TMS and H_3PO_4 as internal standards, respectively. Electrochemical study was performed using Versa STAT-3 in 0.005 M dichloromethane solutions of $[(\text{n-C}_4\text{H}_9)_4\text{N}]\text{ClO}_4$ (TBAP) as a supporting electrolyte. Coupling reactions were monitored by gas chromatography (Shimadzu GC2014).

4.2.2 Synthesis of complex $[\text{RuCl}_2\text{C}_3\text{S}_5](\text{H}_2\text{O})(\text{AsPh}_3)_2$ (RuL1)

Complex (1) was prepared under strictly anhydrous conditions. To a methanol (20 ml) solution containing CS_2 (0.2 ml, 3 mmol) and sodium metal, was added ruthenium complex, $[\text{RuCl}_2(\text{AsPh}_3)_2]$ (695 mg, 1 mmol) with constant stirring. The mixture was refluxed for 4 h. The dark brown precipitate obtained was filtered, washed with methanol, petroleum ether (60–80 °C) and dried in vacuo.

4.2.3 Synthesis of complex $[\text{RuCl}(\text{C}_3\text{S}_5)(\text{H}_2\text{O})(\text{PPh}_3)_2]$ (RuL2)

Complex (2) was prepared by a procedure similar to that used for complex 1. To methanol (20 ml) solution containing CS_2 (0.2 ml, 3 mmol) and sodium metal, we added ruthenium complex, $[\text{RuCl}_2(\text{PPh}_3)_2]$ (735 mg, 1 mmol) with constant stirring. The mixture was refluxed for 4 h. The dark brown precipitate obtained was filtered, washed with methanol, petroleum ether (60–80 °C) and dried in vacuo. The characterization data are given in Table 4.1.

Table 4.1 Yield, CHNS, IR and NMR data of ruthenium complexes (RuL1 and RuL2)

Ruthenium complex	CHNS (%) found (Calculated)	IR (KBr, cm ⁻¹)	¹ H NMR (DMSO, δ ppm)	³¹ P NMR (DMSO, δ ppm)
RuL1 <i>C₃₉H₃₂ClOAs₂RuS₅</i> Yield: 75%	C: 54.86 (54.54); H: 4.62 (4.22); O: 2.89 (2.11); S: 19.26 (19.42).	1433.1(s), 1296 (m), 998.8 (m), 925.3 (m), 619.8 (m), 3350.1 (s), 787.5 (s), 651.1 (m) and 531 (m).	δ 7.08–7.23 (due to triphenyl groups attached to arsenic)	49.55 (referenced with respect to H ₃ PO ₄).
RuL2 <i>C₃₉H₃₂ClOP₂RuS₅</i> Yield: 72%.	C: 52.86 (53.50); H: 3.62 (3.68); O: 1.89 (1.83); S: 18.26 (18.31)	1431(s), 1226 (m), 1053 (m), 972.9 (m), 619 (m), 3383.6 (s), 747 (s), 691.7 (m) and 511 (m)	δ 7.08–7.23 (due to triphenyl groups attached to phosphorous)	50.28 (referenced with respect to H ₃ PO ₄)

4.3 MOLECULAR STRUCTURES AND UV-VISIBLE SPECTRA OF RUTHENIUM COMPLEXES CONTAINING DMIT LIGAND

The molecular structure of RuL1 and RuL2 is shown in Figures 4.1 and 4.2. The UV-Vis spectra of two ruthenium complexes in solution as well as complexes in film form are shown in Figure 4.3 and 4.4. The molecular formulas for the two molecules are:

- [Ru (dmit) (triphenylarsine) (H₂O) (Cl)] {dmit=1, 3 – dithiole – 2 – thione - 4, 5-dithiolate} **[RuL1]**.

2. [Ru (dmit) (triphenylphosphine) (H₂O) (Cl)] {dmit=1,3 – dithiole – 2 – thione - 4, 5-dithiolate} [RuL2].

In these complexes ruthenium acts as a central metal ion surrounded by two organic π -conjugated ligands (1,3-dithiole-2-thione-4,5-dithiolate (dmit) and triphenylarsine / triphenylphosphine). The bands appearing in the region 230-350 nm are assigned to intraligand charge transfer transitions (ILCT) and less intense bands in the range 390–500 nm corresponds to the d-d forbidden transitions (Dileep and Bhat 2010). The small absorption tails at 532 nm give linear absorption coefficient (α_0) for all samples, which are tabulated in Table 4.6

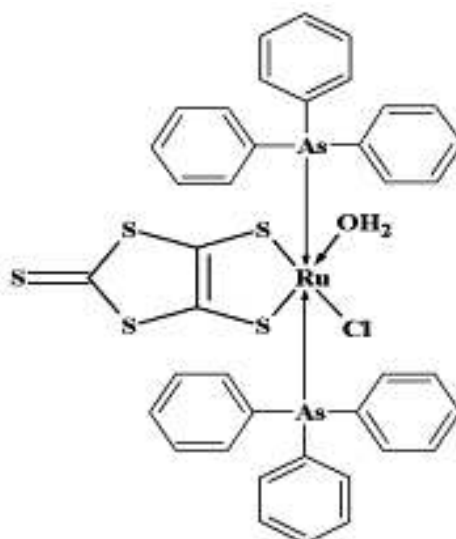


Figure 4.1 Molecular structure of [Ru (dmit) (triphenylarsine) (H₂O) (Cl)] {dmit=1, 3 – dithiole – 2 – thione - 4, 5-dithiolate} [RuL1]

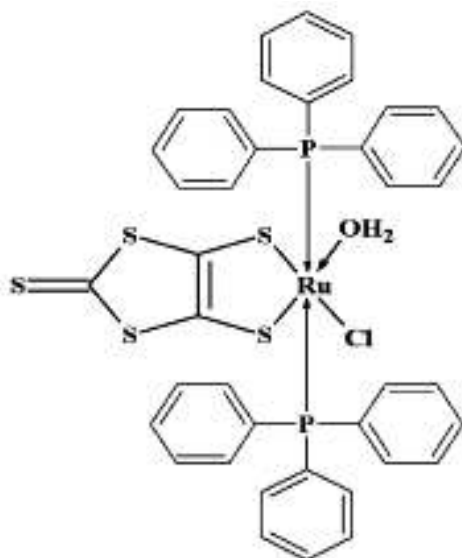


Figure 4.2 Molecular structure of [Ru (dmit) (triphenylphosphine) (H₂O) (Cl)] {dmit=1,3 – dithiole – 2 – thione - 4, 5-dithiolate} [RuL2]

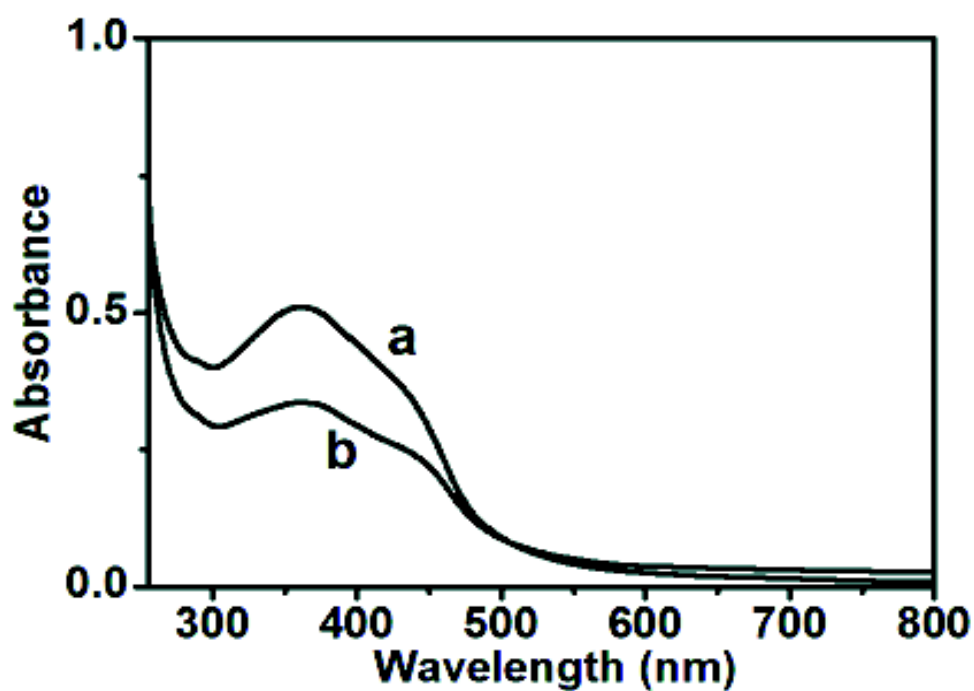


Figure 4.3 UV-Visible absorption Spectrum of the ruthenium complex RuL1 in both solution (a) and film form (b), (Absorbance (A) = $-\ln(I/I_0)$, where I – transmitted intensity and I_0 – incident intensity)

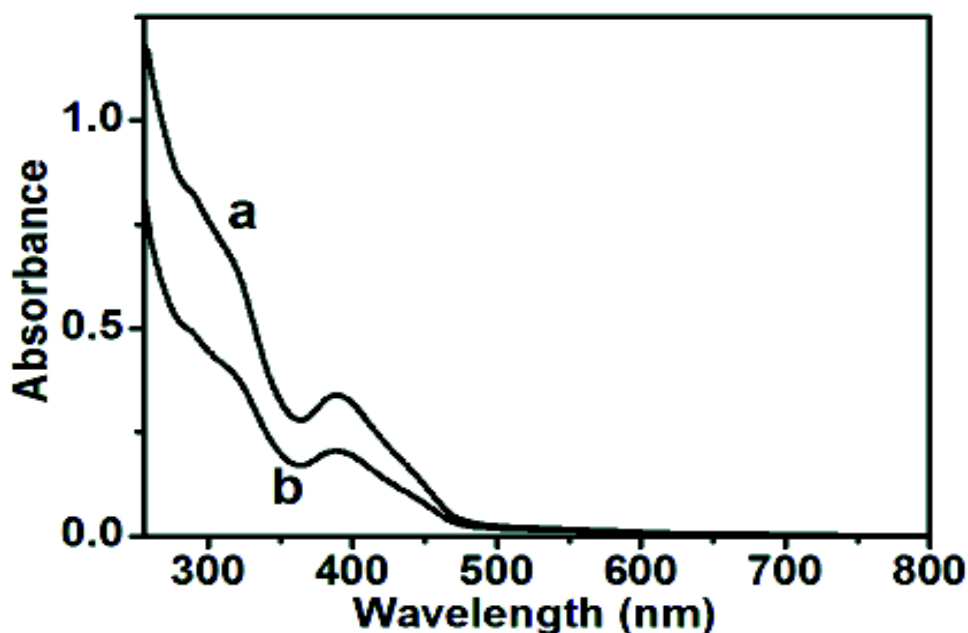


Figure 4.4 UV-Visible absorption Spectrum of the ruthenium complex RuL2 in both solution (a) and film form (b), (Absorbance (A) = $-\ln(I/I_0)$, where I – transmitted intensity and I_0 – incident intensity)

4.4. Z-SCAN STUDIES OF RUTHENIUM COMPLEXES CONTAINING DMIT LIGANDS

Z-scan measurement, described in section 2.1.5, was performed on RuL1 and RuL2 in solution and in film form at different concentrations and sample preparation, described in section 2.5. The scan was obtained at pulse energy of 50 μJ which corresponds to an intensity of 1.2 GW/cm^2 . The normalized open aperture Z-scan traces of the RuL1 and RuL2 in solution form at the concentration of 1×10^{-3} mol/L are shown in Figures 4.5 (a) and 4.6 (a), respectively. Figures 4.7 (a) to 4.10 (a) show normalized open aperture Z-scan traces of the RuL1 and RuL2 in film form at the dopant concentrations of 0.5 and 2.0 wt. %. It is seen that the transmission is symmetric with respect to the focus ($z = 0$) where it has a minimum. The corresponding normalized transmission as a function of sample position in open aperture set-up is given by (Bahae et al. 1990 and O'Flaherty et al. 2003),

$$T(z) = 1 - \left(q_0 / 2\sqrt{2} \right) \text{ for } |q_0| < 1 \quad (4.1)$$

where $q_0 = \beta_{\text{eff}} I_0 L_{\text{eff}} / (1 + z^2/z_0^2)$, β_{eff} is the nonlinear absorption coefficient of the sample, I_0 is the intensity of the laser beam at the focus, z_0 is the Rayleigh range for

the lens used for focusing the laser beam. $L_{eff} = [1 - \exp(-\alpha_0 L)] / \alpha_0$ is the effective sample thickness for a sample of actual thickness L and α_0 is the linear absorption coefficient. Nonlinear absorption coefficient of the ruthenium complex is obtained by fitting the experimental data using Equation (4.1). The imaginary part of $\chi^{(3)}$ for the ruthenium complex i.e. $(\text{Im } \chi^{(3)})$, is determined using Equation 2.26. Similarly, open aperture Z-scan curves were also obtained for other concentrations of ruthenium metal-organic complexes in solution and film form. The calculated β_{eff} and $\text{Im } \chi^{(3)}$ values of RuL1 and RuL2 are tabulated in Tables 4.2 and 4.3.

The closed aperture curves for RuL1 and RuL2 in solution form at the concentrations of 1×10^{-3} mol/L are shown in Figures 4.5 (b) and 4.6 (b), respectively. Figures 4.7 (b) to 4.10 (b) show closed aperture Z-scan traces of the RuL1 and RuL2 in film form at the dopant concentrations of 0.5 and 2.0 wt.%. In the case of closed aperture Z-scan, nonlinear refraction (NLR) is accompanied by significant amount of nonlinear absorption (NLA). This aspect is reflected by the reduced peak and enhanced valley seen in Figure 4.5 (b). Division method (Bahae et al. 1990) is used to discriminate NLR from NLA and is used in the present study to obtain pure nonlinear refraction curve. Accordingly, the closed aperture data is divided by corresponding open aperture data resulting in a pure NLR curve. Figures 4.5 (c) to 4.10 (c) show the NLR curves for RuL1 and RuL2 in both solution (1×10^{-3} mol/L) and film form (0.5 and 2.0 wt. %), respectively. Similar curves were also obtained for other concentrations.

The peak-valley configuration of the pure nonlinear refraction curve shown in Figures 4.5 (c) to 4.10 (c) clearly indicates that the compound possesses large negative refractive nonlinearity. Similar closed aperture and pure nonlinear refraction Z-scan curves were also obtained for other concentrations of ruthenium metal-organic complexes in solution and film form. The estimated values of NLO coefficients obtained through a best fit of data are tabulated in Tables 4.2 and 4.3.

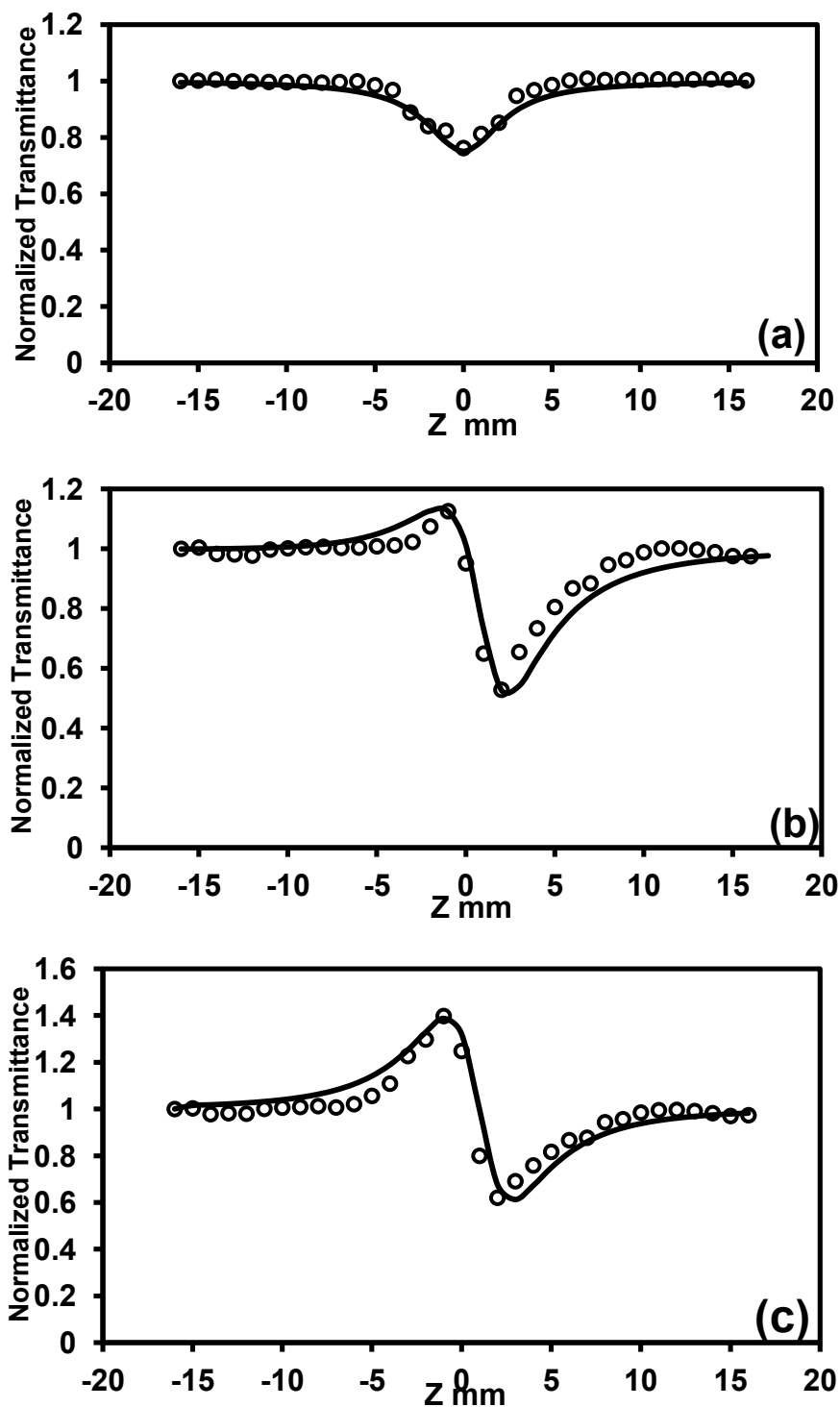


Figure 4.5 Plots of Open aperture (a), Closed aperture (b) and Pure nonlinear refraction (c) curves for RuL1 in solution form (1×10^{-3} mol/L). Solid line is a theoretical fit to the experimental data

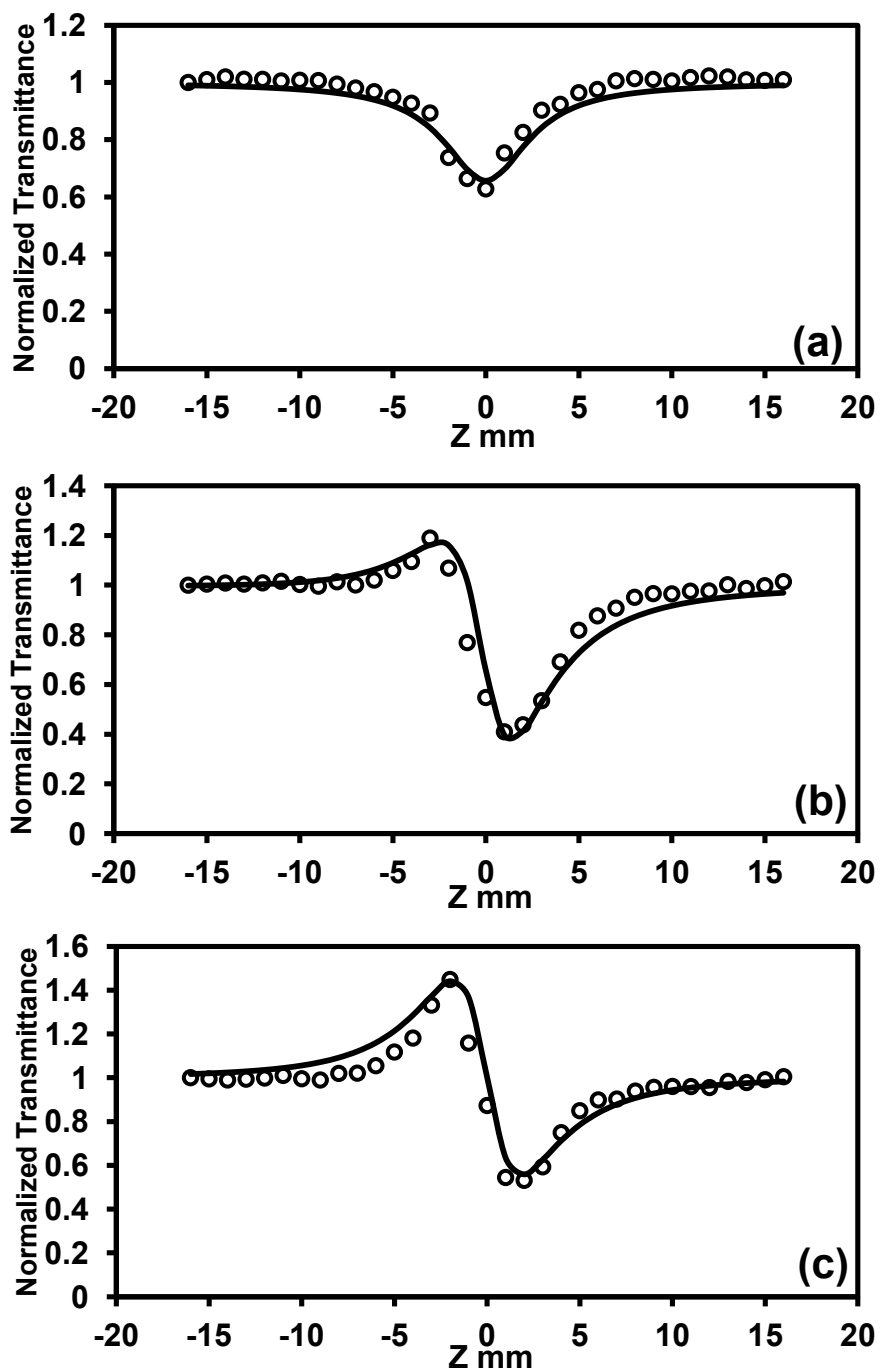


Figure 4.6 Plots of Open aperture (a), Closed aperture (b) and pure nonlinear refraction (c) curves for RuL2 in solution form (1×10^{-3} mol/L). Solid line is a theoretical fit to the experimental data

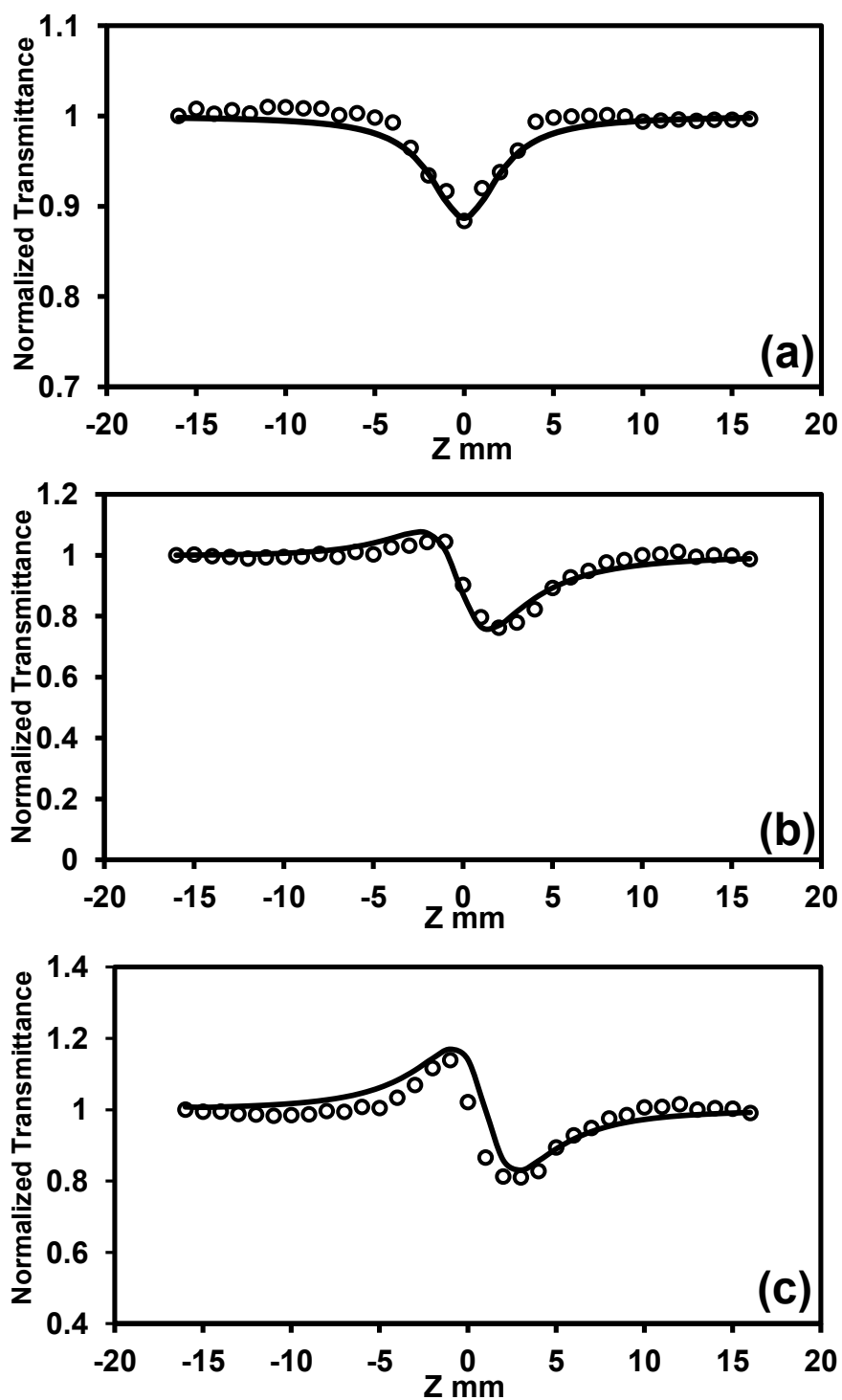


Figure 4.7 Plots of Open aperture (a), Closed aperture (b) and Pure nonlinear refraction (c) curves for RuL1 in film form (0.5 wt.%). Solid line is a theoretical fit to the experimental data

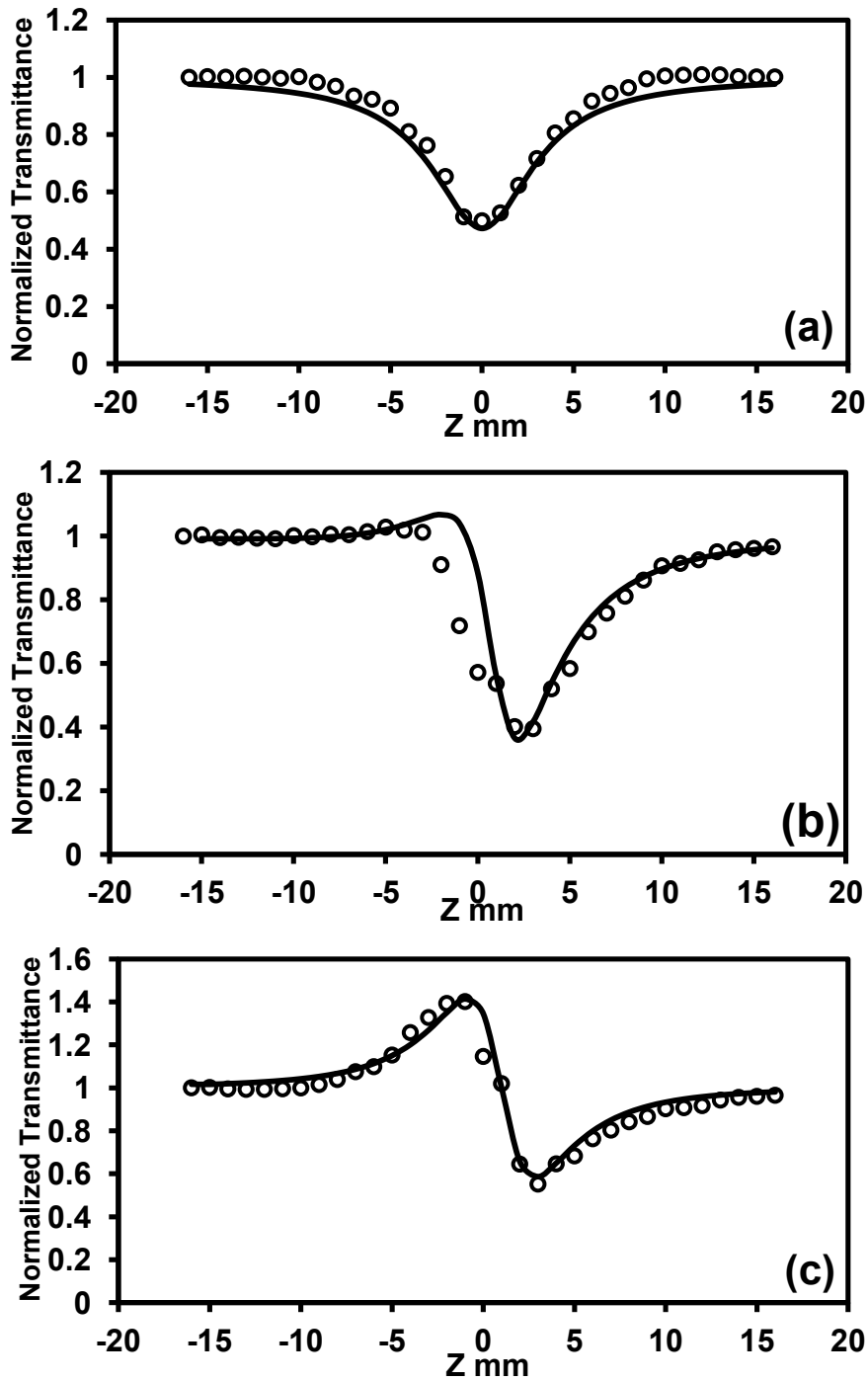


Figure 4.8 Plots of Open aperture (a), Closed aperture (b) and Pure nonlinear refraction (c) curves for RuL1 in film form (2.0 wt.%). Solid line is a theoretical fit to the experimental data

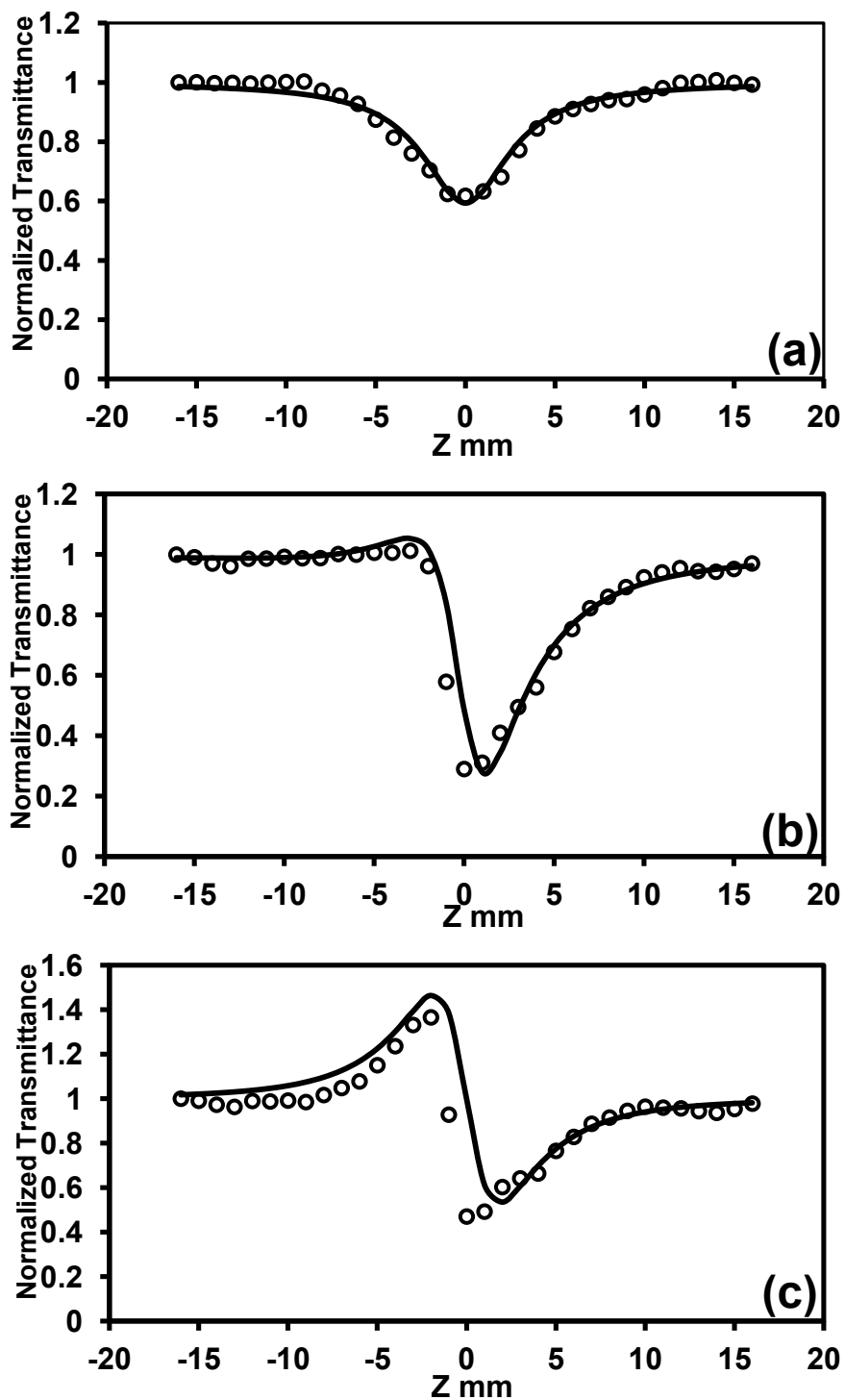


Figure 4.9 Plots of Open aperture (a), Closed aperture (b) and Pure nonlinear refraction (c) curves for RuL2 in film form (0.5 wt.%). Solid line is a theoretical fit to the experimental data

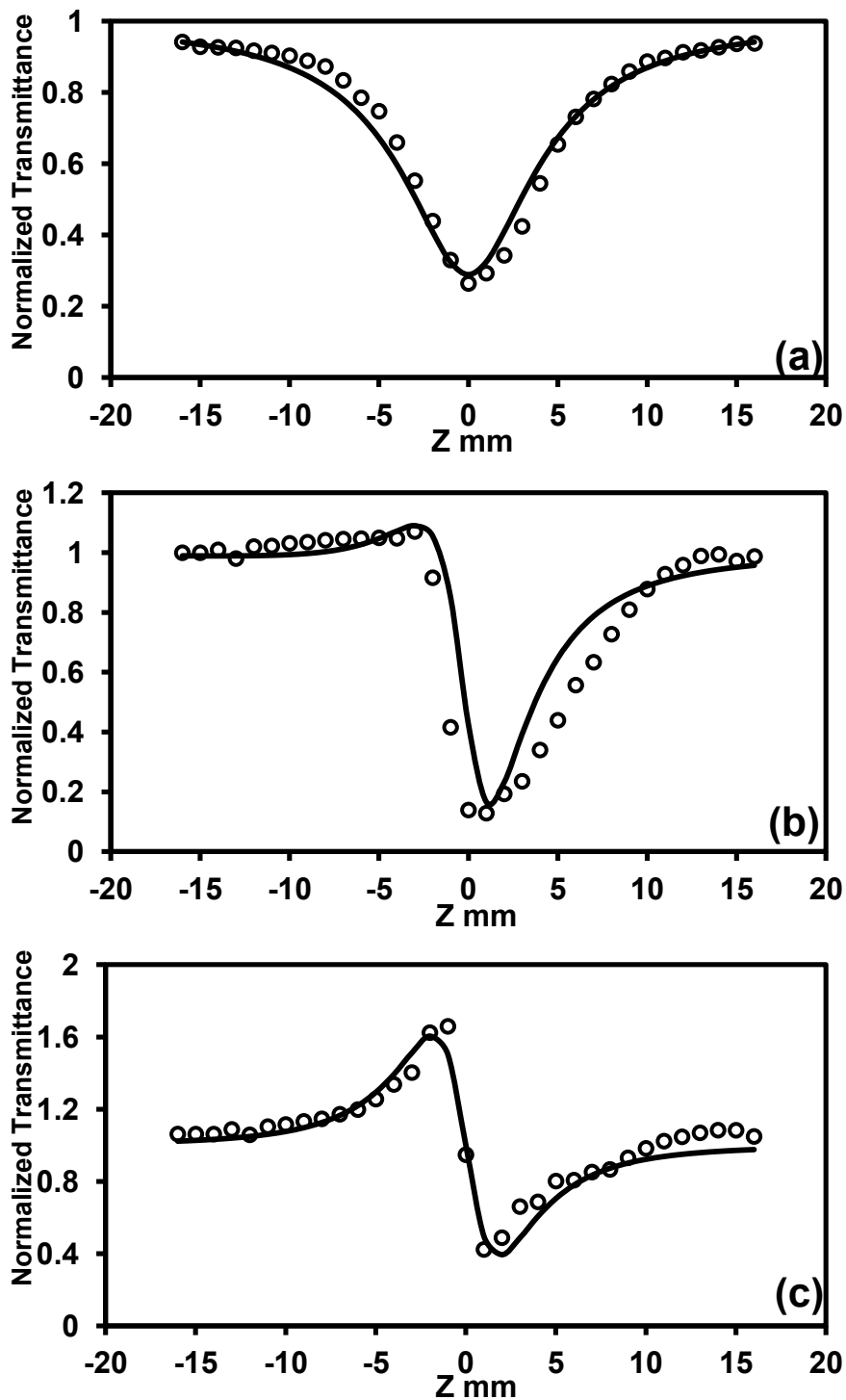


Figure 4.10 Plots of Open aperture (a), Closed aperture (b) and Pure nonlinear refraction (c) curves for RuL2 in film form (2.0 wt.%). Solid line is a theoretical fit to the experimental data

Table 4.2 Third-order nonlinear optical parameters of ruthenium complexes in solution form at different concentrations at the input laser intensity of 1.2 GW/cm².

Sample	Concentration (x10 ⁻³ mol/L)	β_{eff} (m/W) x10 ⁻¹¹	Im $\chi^{(3)}$ (esu) x10 ⁻¹³	n_2 (esu) x10 ⁻¹¹	Re $\chi^{(3)}$ (esu) x10 ⁻¹³
RuL1	0.25	2.73	0.42	-1.65	-1.77
	0.5	3.98	0.61	-3.61	-3.85
	1	5.72	0.88	-4.50	-4.80
RuL2	0.25	5.11	0.77	-3.30	-3.49
	0.5	6.74	1.02	-4.79	-5.06
	1	9.56	1.44	-5.89	-6.22

Table 4.3 Third-order nonlinear optical parameters of the ruthenium complexes at different dopant concentrations in film form at the input laser intensity of 1.2 GW/cm².

Sample	Concentration (wt.%)	β_{eff} (m/W) x10 ⁻⁹	Im $\chi^{(3)}$ (esu) x10 ⁻¹¹	n_2 (esu) x10 ⁻⁹	Re $\chi^{(3)}$ (esu) x10 ⁻¹¹
RuL1	0.50	3.24	0.71	-2.60	-3.52
	1.00	9.51	2.10	-4.88	-6.63
	1.50	11.35	2.50	-5.92	-8.10
	2.00	13.95	3.10	-6.70	-9.11
RuL2	0.50	10.83	2.38	-7.18	-9.76
	1.00	18.94	4.17	-8.89	-12.08
	1.50	21.65	4.77	-10.29	-13.94
	2.00	27.77	6.11	-12.93	-17.58

Second order hyperpolarizability (γ_h) of a molecule is related to the third-order bulk susceptibility through Equation (2.42) as shown in chapter 2. The calculated values of γ_h for RuL1 and RuL2 are 1.064×10^{-30} esu and 2.625×10^{-30} esu, respectively.

The Mechanism of nonlinear absorption is generally explained by a five-level model which was described in chapter 3. The excited-state absorption cross-section σ_{exc} of the ruthenium complex samples were obtained by fitting the open aperture data using the equation available in literature (Henari 2001 and Henari et al. 1997). The ground-state absorption cross-section σ_g was calculated using the relation $\sigma_g = \alpha/N_a C$, where N_a is the Avogadro's number and C is the concentration in mol/L. The values of σ_g and σ_{exc} for RuL1 and RuL2 in solution form is given in Table 4.4 and in film form in Table 4.5. The larger value of σ_{exc} as compared to σ_g indicates that the observed nonlinear absorption is due to RSA (Henari 2001, Henari et al. 1997, Sun et al. 1999 and Przhonska et al. 1998). Further, Figures 4.15 and 4.16 show that the value of β_{eff} decreases with increasing on-axis intensity I_0 , which confirms the RSA mechanism (Guo et al. 2003 and Auger et al. 2003). For TPA mechanism β_{eff} is independent of I_0 (Guo et al. 2003 and He et al. 1998).

Table 4.4 Ground state absorption cross-section and excited state absorption cross-section of the ruthenium complexes in solution form at different concentrations

Sample	Concentrations ($\times 10^{-3}$ mol/L)	σ_g ($\times 10^{-19}$ cm ²)	σ_{exc} ($\times 10^{-18}$ cm ²)
RuL1	0.25	7.68	1.22
	0.5	7.20	1.43
	1	6.80	2.61
RuL2	0.25	8.73	1.91
	0.5	8.05	2.25
	1	7.51	4.39

Table 4.5 Ground state absorption cross-section and excited state absorption cross-section of the ruthenium complexes in film form at different dopant concentrations

Sample	Dopant Concentrations (wt. %)	σ_g ($\times 10^{-17} \text{ cm}^2$)	σ_{exc} ($\times 10^{-16} \text{ cm}^2$)
RuL1	0.5	2.65	2.28
	1.0	2.13	3.01
	1.5	1.86	3.43
	2.0	1.46	3.66
RuL2	0.5	6.02	2.47
	1.0	4.82	3.29
	1.5	4.69	4.50
	2.0	4.42	5.36

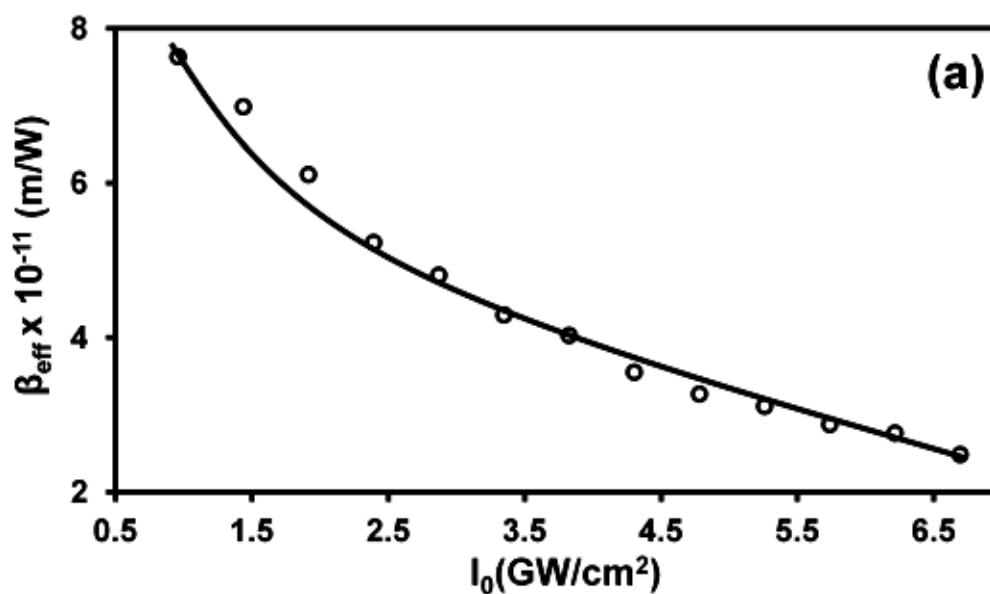


Figure 4.11(a) Nonlinear absorption coefficient (β_{eff}) versus on-axis input intensity I_0 for RuL1 in solution ($1 \times 10^{-3} \text{ mol/L}$)

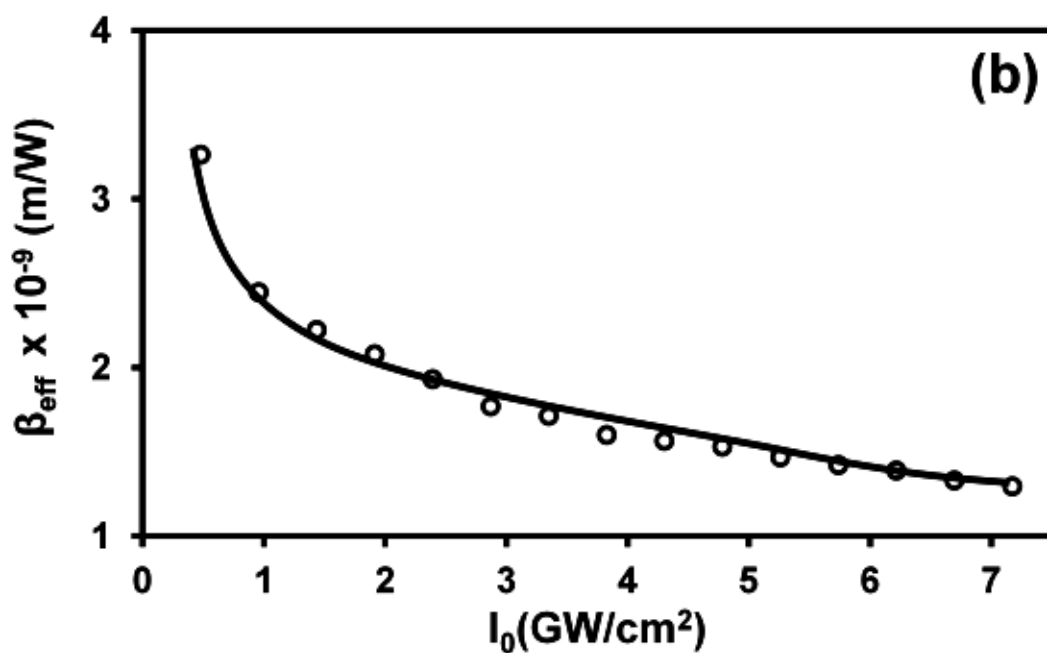


Figure 4.11 (b) Nonlinear absorption coefficient (β_{eff}) versus on-axis input intensity I_0 for RuL1 in film form (1.0 wt.%)

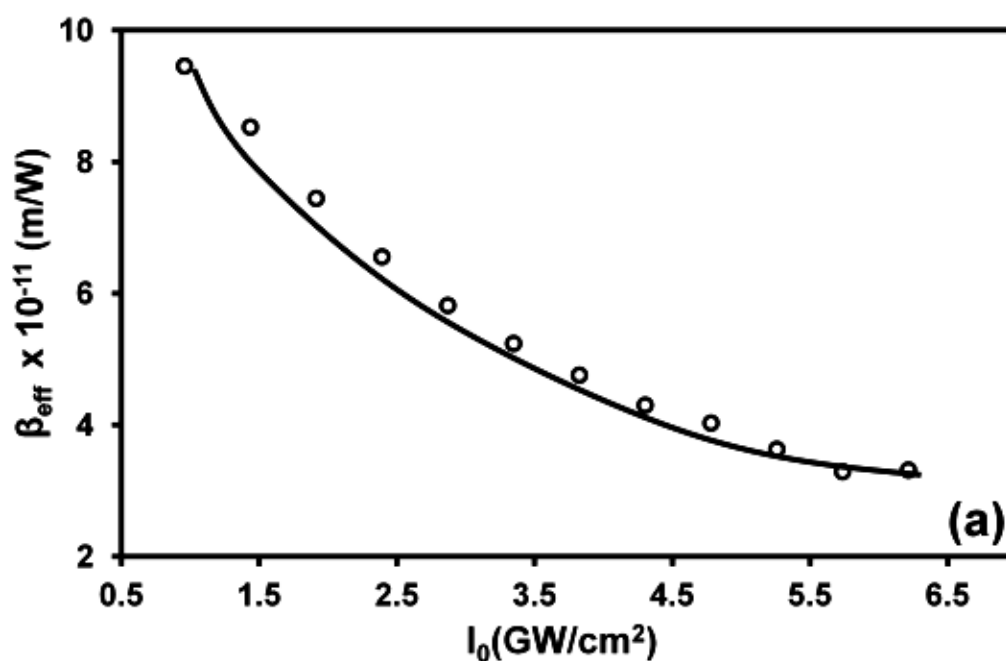


Figure 4.12 (a) Nonlinear absorption coefficient (β_{eff}) versus on-axis input intensity I_0 for RuL2 in solution (1×10^{-3} mol/L)

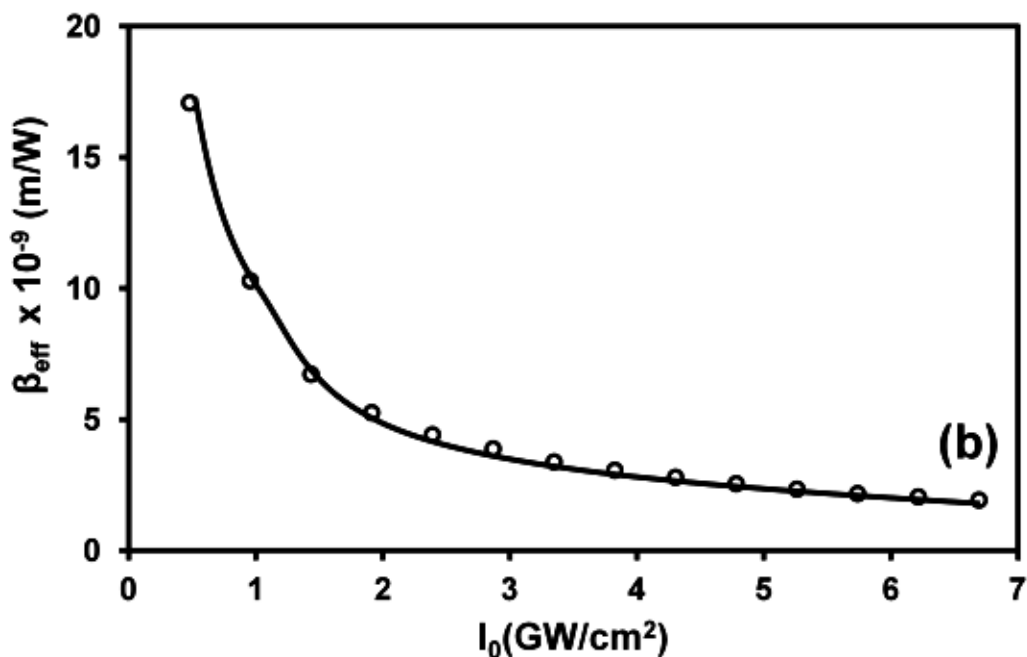


Figure 4.12 (b) Nonlinear absorption coefficient (β_{eff}) versus on-axis input intensity I_0 for RuL2 in film form (1.0 wt.%)

4.5 DEGENERATE FOUR WAVE MIXING STUDIES

Figures 4.13 and 4.14 show the variation of DFWM signal with input laser energy for ruthenium complex RuL1 and RuL2 at the concentrations of 1×10^{-3} mol/L, respectively. The cubic dependence of DFWM signal with respect to input energy is observed in all samples. The signal is proportional to the cubic power of the input intensity as given by the Equation 2.35. This behaviour of the DFWM signal indicates that the optical nonlinearity is third order in nature.

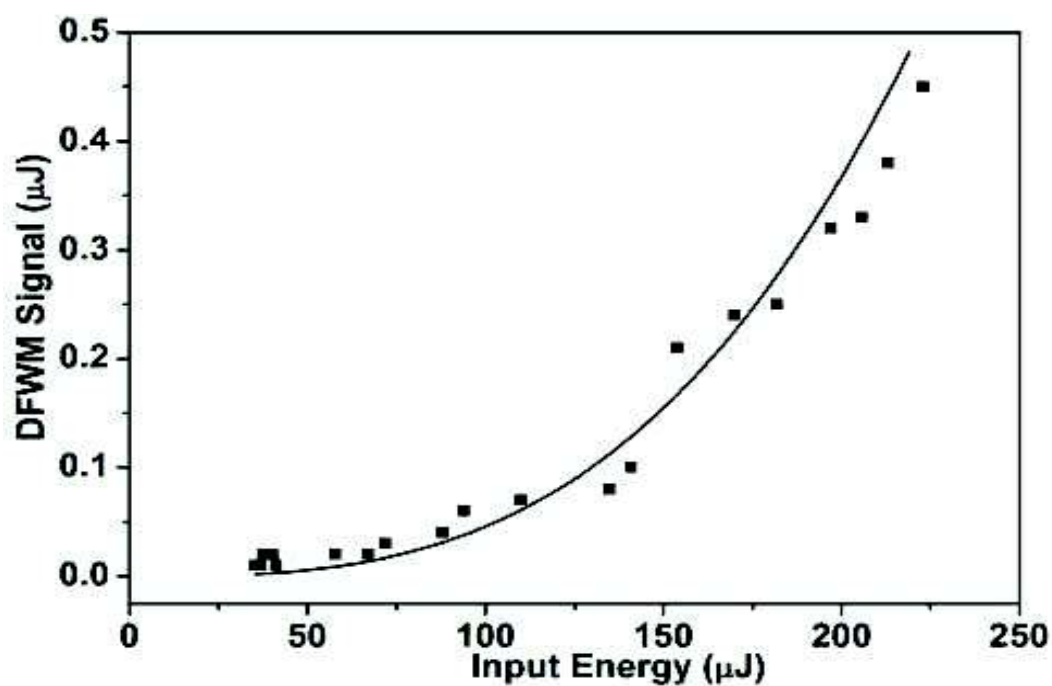


Figure 4.13 DFWM signal of RuL1 at the concentration of 1×10^{-3} mol/L. Squares are data points while the solid curve is a cubic fit to the data

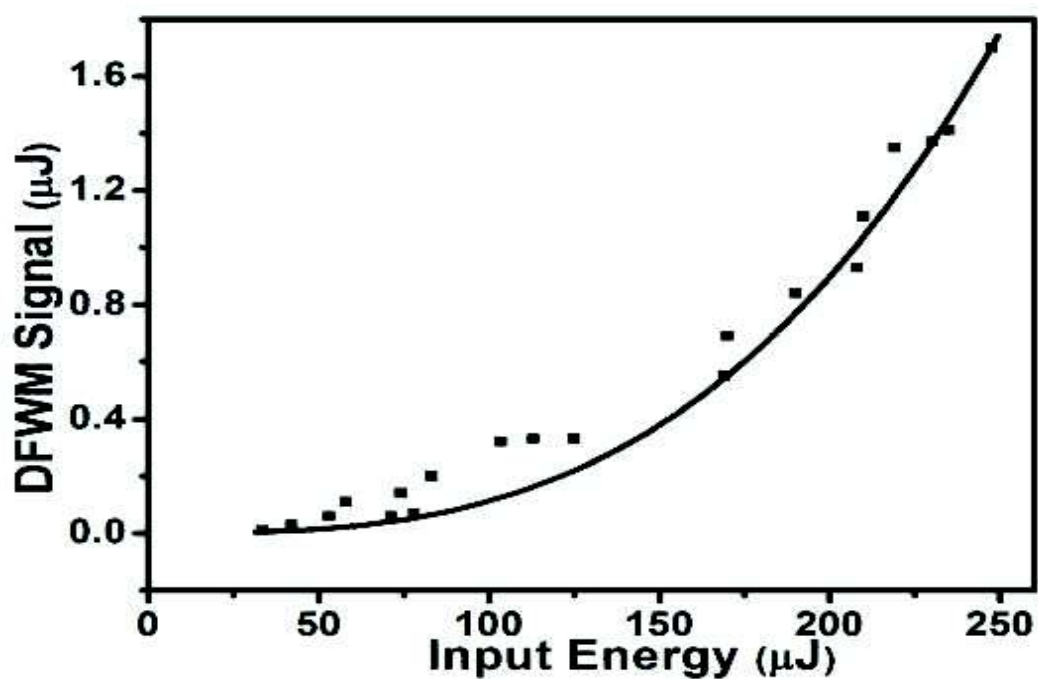


Figure 4.14 DFWM signal of RuL2 at the concentration of 1×10^{-3} mol/L. Squares are data points while the solid curve is a cubic fit to the data

The measured values of third-order nonlinear optical susceptibility $|\chi^{(3)}|$, second-order hyperpolarizability γ_h are given in the Table 4.6.

Table 4.6 Linear absorption coefficient α_0 , third-order nonlinear optical susceptibility $|\chi^{(3)}|$, second-order hyperpolarizability γ_h of different ruthenium complexes measured by DFWM technique.

Sample	α_0 (cm ⁻¹)	$ \chi^{(3)} $ (x 10 ⁻¹³ esu)	γ_h (x 10 ⁻³¹ esu)
RuL1	0.314	4.453	2.324
RuL2	0.473	6.401	3.398

4.6 STRUCTURE-PROPERTY RELATIONSHIP WITH THIRD-ORDER NONLINEAR OPTICAL PARAMETERS IN RUTHENIUM METAL-ORGANIC COMPLEXES

The experimental results show that the ruthenium complex containing dmit exhibits large third-order NLO properties at 532 nm. Such a large nonlinearity originates in these compounds due to the effective electronic communication between π -conjugated dmit ligand and triphenylphosphine ligand through central ruthenium atom and also because of effective overlapping of metal orbitals with the ligand orbitals. Combining the conjugated triphenylphosphine ligand with its electron accepting character (d to σ^*) (Orpen and Connelly 1985 and Pacchioni and Bagus 1992), facilitates effective electronic communication and CT transitions between metal and ligands leading to large dipole moment changes between the excited states (Liyanage et al. 2003) and also makes circulation of electrons throughout the distorted inorganic octupolar center. Several reports on complexes containing phosphine and dmit ligands (Cheng et al. 1990, Whittal et al. 1996, Whittal et al. 1997 and McDonagh et al. 2000) exhibit large nonlinear coefficient and absorption coefficient. The existence of strong intramolecular CT excitations in a noncentrosymmetric molecular environment is the key to the NLO activity. The first criterion can be satisfied by considering a polarizable molecular system (e.g. π -conjugated pathway) having an uneven or asymmetric charge distribution. The simplest way to achieve this

is to have a donor (D) – acceptor (A) system with a bridge (D– π –A) which can help the electronic communication between donor and the acceptor. Most metal complexes can be assumed within an above mentioned D– π –A system, in which donor and/or acceptor, or the bridge moieties are selectively replaced by an organometallic group. This is because metal complexes possess intense, low energy MLCT, LMCT, or intraligand charge transfer (ILCT) excitations. Therefore they can effectively behave as donor and/or acceptor groups of the D– π –A system, or as constituents of the polarisable bridge (Liyanage et al. 2003). Metal ions make an important contribution to the NLO properties. The strength of the NLO properties can be altered by the π -back-donation capacity of the metal ions to the ligands, and the increased π -back donation capacity of the metal ions to the ligands may enhance the extension of the electronic π system and improve the NLO properties (Chao et al. 1999). For example, in the reported polymers $[\text{Co}(\text{bbbt})_2(\text{NCS})_2]_n$, $[\text{Mn}(\text{bbbt})_2(\text{NCS})_2]_n$ and $[\text{Cd}(\text{bbbt})_2(\text{NCS})_2]_n$, $[\text{Co}(\text{bbbt})_2(\text{NCS})_2]_n$ possesses the strongest NLO properties just because the electronic π back-donation capacity of Co^{2+} is the largest among the three kinds of ions (Hou et al. 2002). This phenomenon is also observed in other reported compounds of chromium, zinc, cadmium, lead, molybdenum and tungsten (Meng et al. 2003, Fan et al. 2004 and Mata et al. 1998). From these results it is clear that the resonance and structural effects which determine the electronic polarization properties will modulate the observed nonlinearity. Among two metal complexes, one with triphenylphosphine as ligand shows better nonlinear response. This is because triphenylphosphine is a good back π -bonding ligand compared to triphenylarsine. The strength of the NLO properties can be altered by the π -back-donation capacity of the metal ions to the ligands, and the increased π -back donation capacity of the metal ions to the ligands may enhance the extension of the electronic π system and improve the NLO properties. Moreover, phosphine is a better electron acceptor than arsenic.

4.7 OPTICAL POWER LIMITING STUDIES

Optical power limiting is an area of growing interest due to its applications in eye and sensor protection against intense light (Perry et al. 1996 and Ganeev et al. 2002). The nonlinear optical mechanisms that cause optical limiting have different

origins such as two-photon absorption, free carrier absorption, reverse saturable absorption, excited-state absorption and nonlinear scattering (Tutt and Boggess 1993)

The ruthenium complexes RuL1 and RuL2 studied by us show good optical power limiting performance because of the large nonlinear absorption due to RSA. Figures 4.15 and 4.16 show the optical power limiting of RuL1 and RuL2, respectively, in the solution form. Figures 4.17 and 4.18 show the optical power limiting of RuL1 and RuL2 in film form. The optical limiting threshold and clamped output energy of ruthenium complexes RuL1 and RuL2 in solution and film form are given in Tables 4.7 and 4.8. As the concentration increases the clamping level decreases. The ruthenium complexes investigated by us exhibit good optical power limiting for nanosecond laser pulses. Thus, RuL1 and RuL2 would be promising materials for making optical power limiting devices.

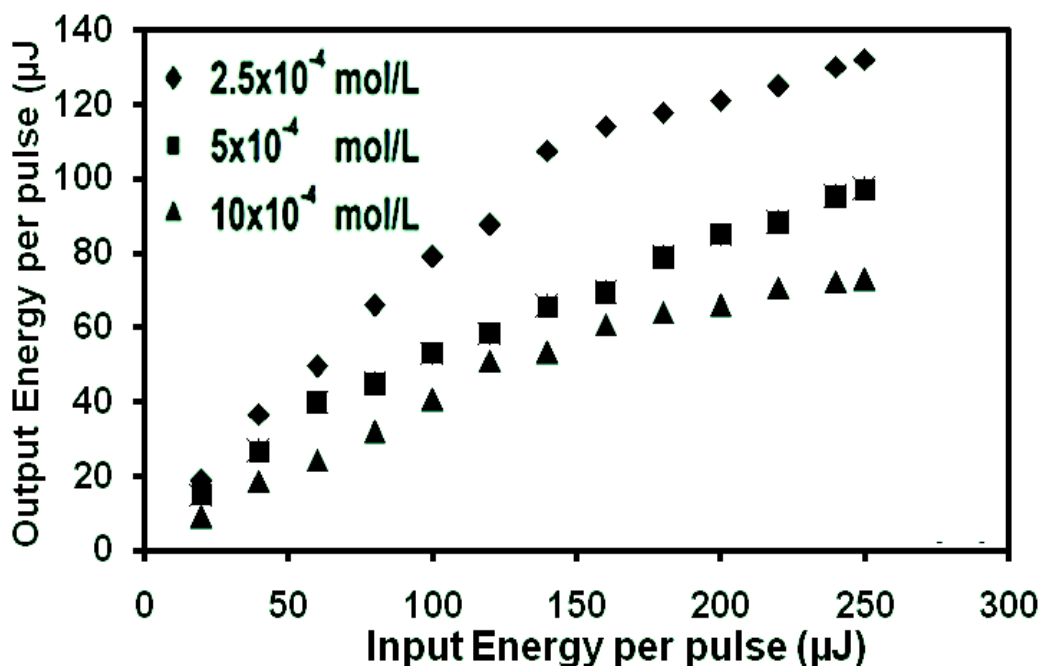


Figure 4.15 Optical power limiting behaviour of ruthenium complex RuL1 in solution form at various concentrations indicated in the inset

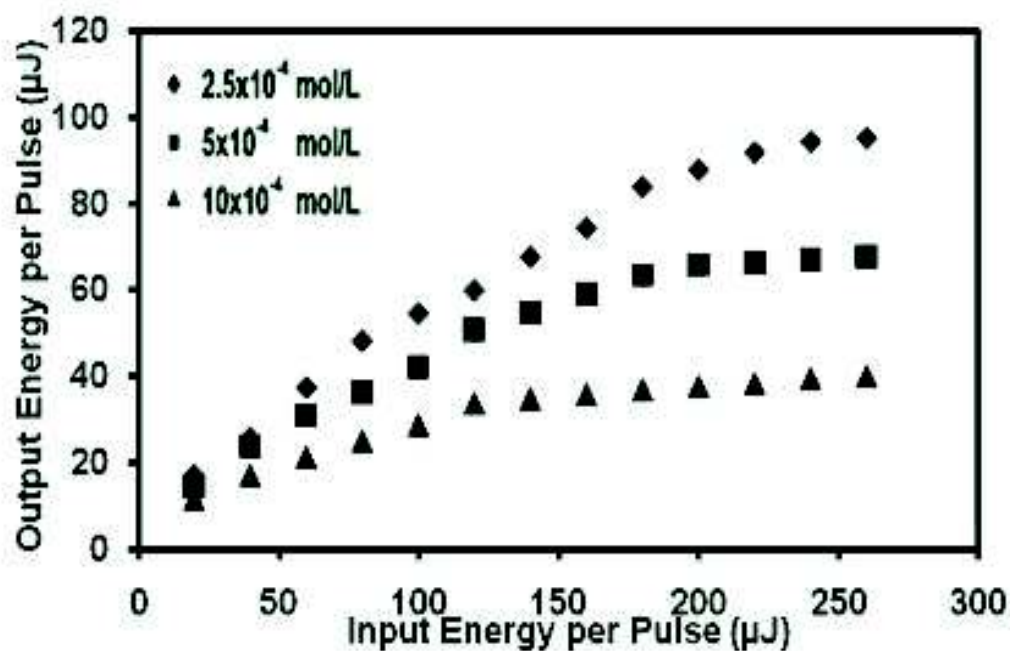


Figure 4.16 Optical power limiting behavior of ruthenium complex RuL2 in solution form at various concentrations indicated in the inset

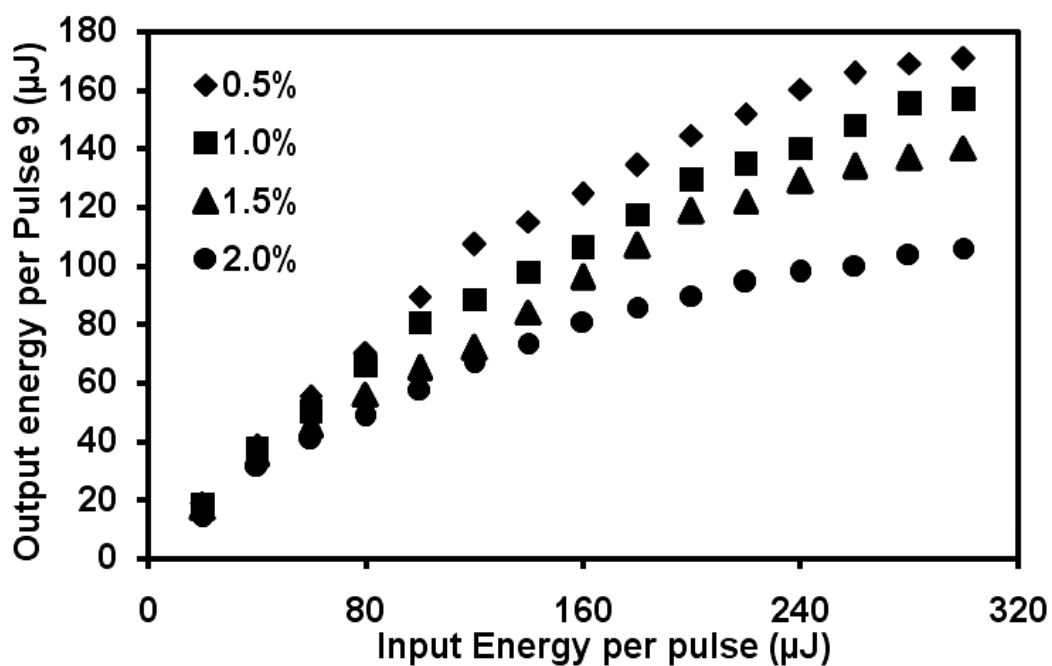


Figure 4.17 Optical power limiting behavior of ruthenium complex RuL1 in film form at various concentrations indicated in the inset

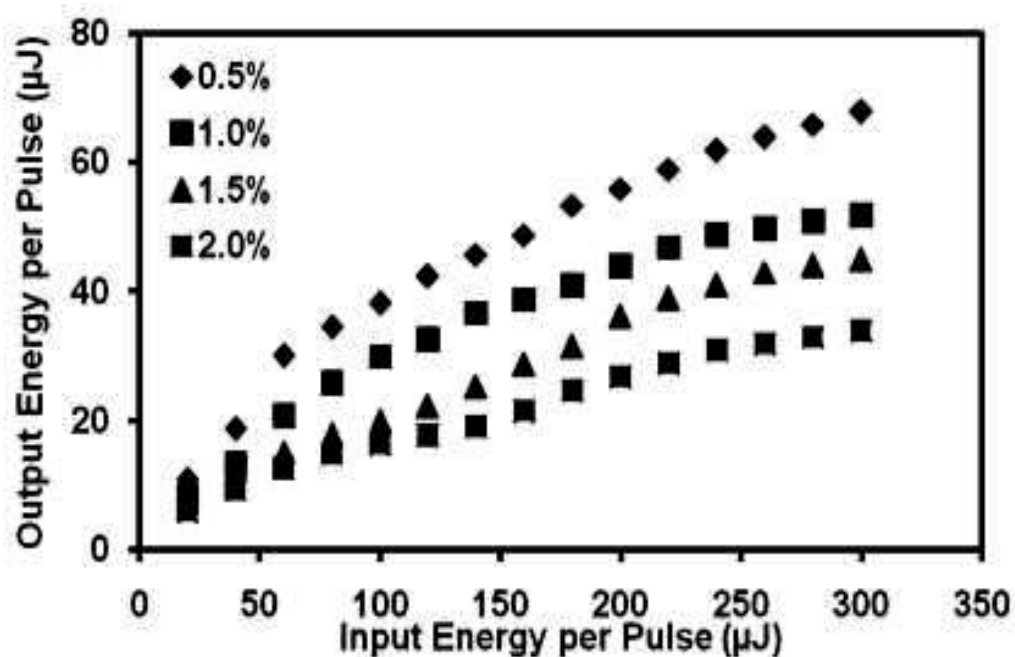


Figure 4.18 Optical power limiting behavior of ruthenium complex RuL2 in film at various concentrations indicated in the inset

Table 4.7 Optical limiting threshold and clamped output energy of the ruthenium complexes in solution form at different concentrations

Sample	Concentrations ($\times 10^{-3}$ mol/L)	Optical limiting threshold (μJ)	Clamped output energy (μJ)
RuL1	0.25	200	125
	0.5	180	95
	1	160	70
RuL2	0.25	160	95
	0.5	140	66
	1	110	40

Table 4.8 Optical limiting threshold and clamped output energy of the ruthenium complexes doped in film form at different dopant concentrations

Sample	Dopant Concentrations (wt.%)	Optical limiting threshold (μJ)	Clamped output energy (μJ)
RuL1	0.5	250	170
	1.0	230	155
	1.5	200	138
	2.0	180	105
RuL2	0.5	90	66
	1.0	80	50
	1.5	60	45
	2.0	50	34

4.8 CONCENTRATION DEPENDENCE OF THIRD ORDER NONLINEARITY

The concentration of compounds prepared as films was varied and Z-scans were repeated on the samples in order to study the dependence of nonlinearity of samples on their concentrations. This will help us in extracting information on NLO properties of solute in the solution and solid film.

Figures 4.19 and 4.20 show the dependence of nonlinear absorption (β_{eff}) on the concentration of RuL1 and RuL2 in solution form and in film form, respectively. The NLA coefficient β_{eff} varies almost linearly with sample concentration. The nonlinear absorption as well as the nonlinear refraction decreased as the concentration in solution decreased from 1×10^{-3} mol/L to 0.25×10^{-3} mol/L and in solid film from 2.0 wt.% to 0.5 wt.%. Thus, the observed decrease in the NLO response is directly correlated to concentration of the organic samples in solution and film form. Optical power limiting behavior of RuL1 and RuL2 at different concentration in solution and

in film is shown in Figures 4.15 to 4.18. It was observed that the limiting action became poor as the concentration of compound in solution and in solid film decreased, which correlates with the reduced NLA coefficients at lower concentrations.

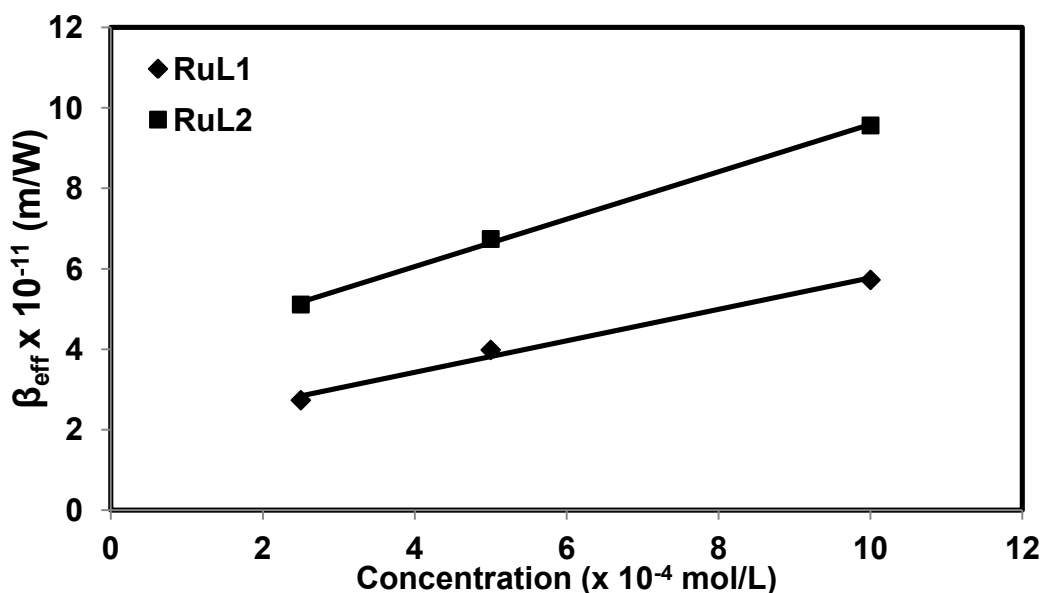


Figure 4.19 Concentration dependent nonlinear absorption coefficients (β_{eff}) of RuL1 and RuL2 in solution form

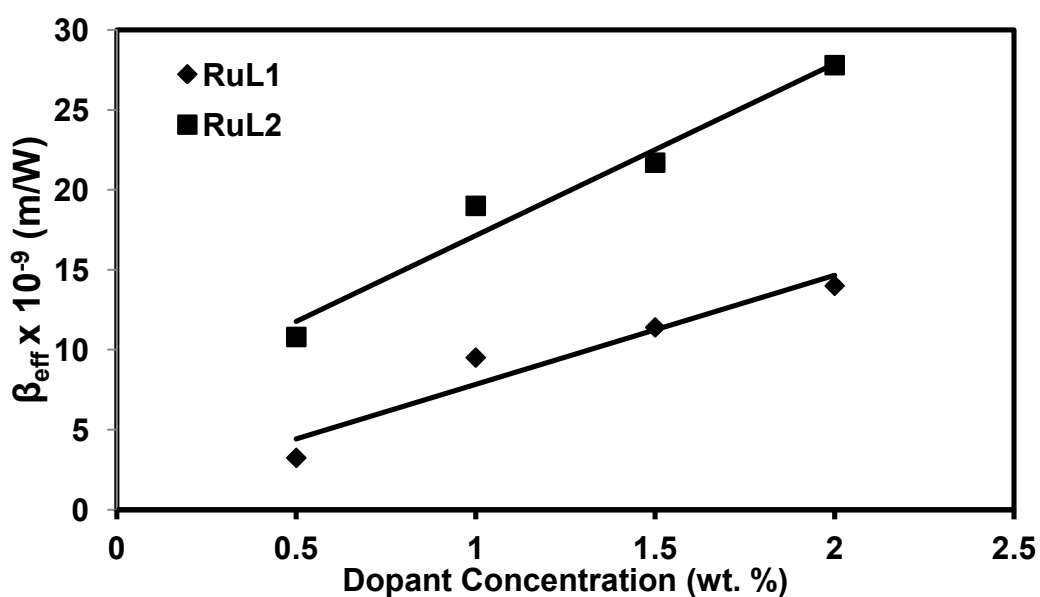


Figure 4.20 Concentration dependent nonlinear absorption coefficient (β_{eff}) in RuL1 and RuL2 in film form

4.9 ALL-OPTICAL SWITCHING STUDIES OF RUTHENIUM COMPLEXES

The nonlinear absorption induced in the samples can be exploited to modulate the transmission of a second CW laser beam. In our experiments, 7 ns duration laser pulses at 532 nm wavelength from the Nd-YAG laser was used as the pump and a low power (2 mW) continuous laser beam from a He-Ne laser (633 nm wavelength) was used as the probe. The pulsed nature of the pump beam resulted in a pulsed output signal at 633 nm at the same pulse repetition rate as that of the Nd-YAG laser (Pump) (Abdeldayem et al. 2003). This aspect is clearly seen in Figures 4.21 and 4.22. The upper curves are the pulse shape of pump beam at different intensities (a) 5 GW/cm², (b) 10 GW/cm² and (c) 15 GW/cm² whereas lower curves show the output signal shape of probe beam at corresponding pump intensities. The same experiment was performed on pure PMMA film and we did not observe any transmission modulation.

In fact, the observed optical switching indicates that one can fabricate an optical inverter or NOT gate using the new materials studied by us. The modulation of the probe intensity calculated for ruthenium complexes are given in Table 4.9. The higher probe modulation at higher intensity of pump beam may be ascribed to the increase in the population of triplet state (Singh et al. 2005). The switching response times were in the range of a few micro seconds. The relaxation of the triplet state to the ground state is forbidden, resulting in slow switching time shown by the molecules (Henari 2001).

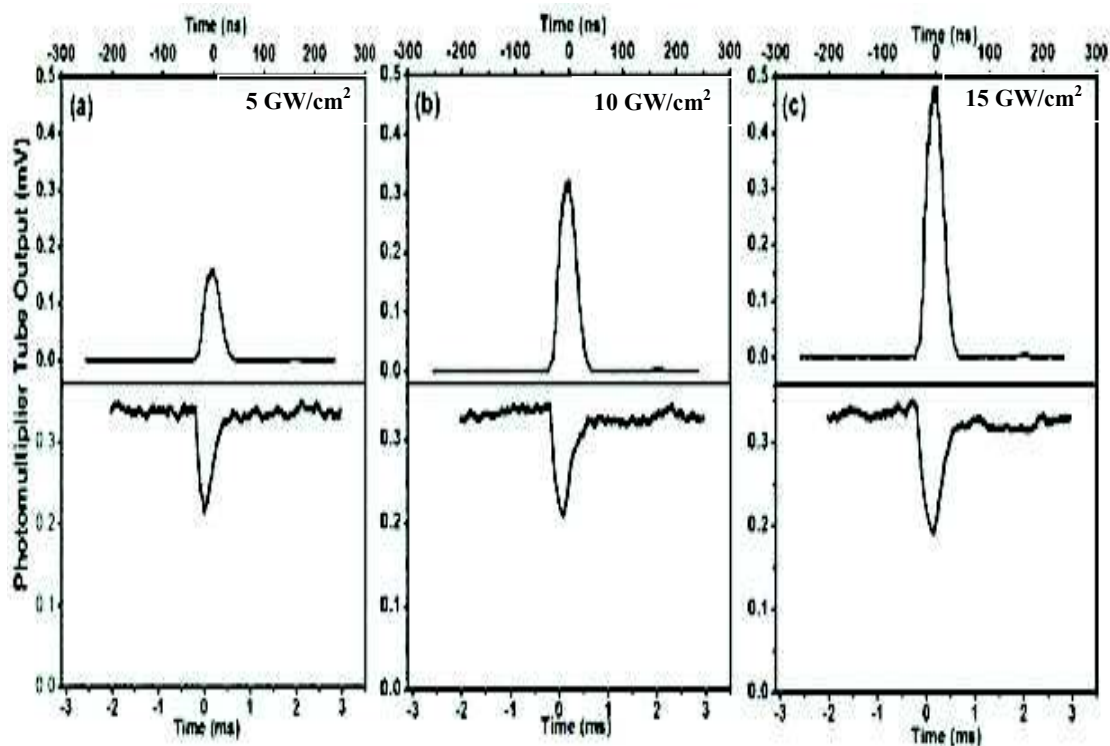


Figure 4.21 All-optical switching signal for RuL1 (Conc. 1.0 wt.%) with varying pump beam intensities (a) 5 GW/cm^2 , (b) 10 GW/cm^2 and (c) 15 GW/cm^2 . The upper curves show the pulse shape of the Nd: YAG laser beam used, whereas the lower curves show the signal wave form of the probe He-Ne laser beam.

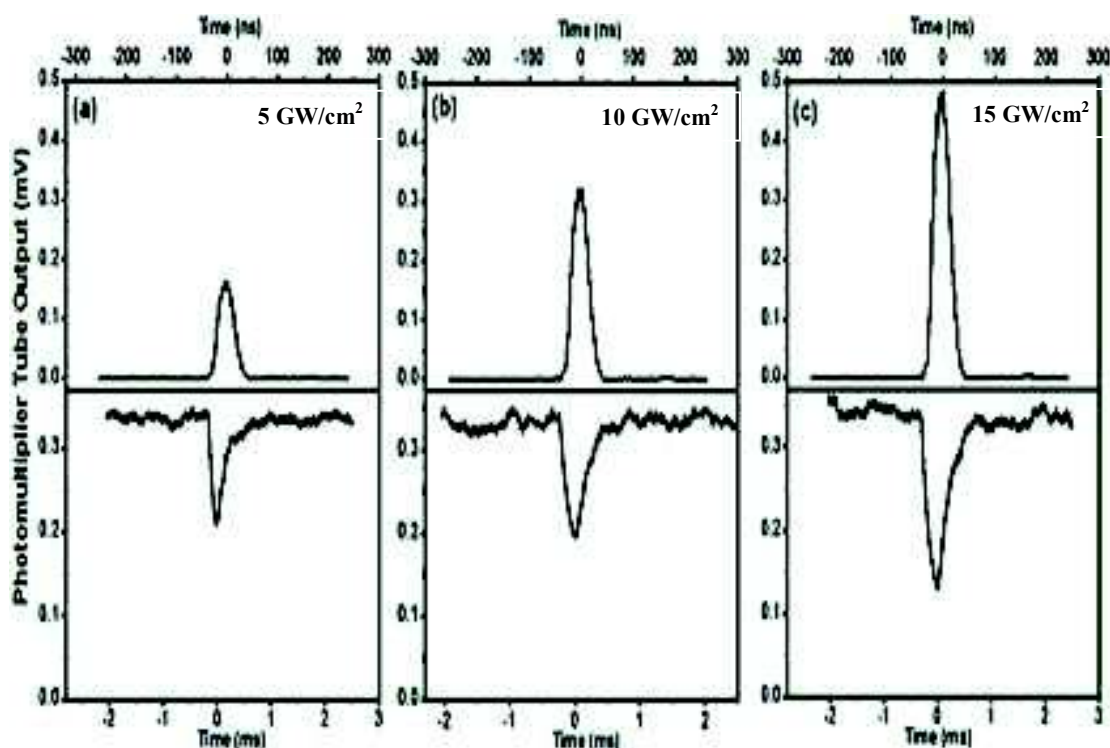


Figure 4.22 All-optical switching signal for RuL2 (Conc. 1.0 wt.%) with varying pump beam intensities (a) 5 GW/cm², (b) 10 GW/cm² and (c) 15 GW/cm². The upper curves show the pulse shape of the Nd: YAG laser beam used, whereas the lower curves show the signal wave form of the probe He-Ne laser beam.

Table 4.9 Fall time, rise time, FWHM and modulation of probe beam of RuL1 and RuL2 at different pump intensities in optical switching experiments

Sample	Intensity (GW/cm ²)	Fall Time (T _f) (μs)	Rise Time (T _r) (μs)	FWHM (μs)	Modulation of probe beam %
RuL1	5	140	268	344	35
	10	172	393	369	39
	15	222	313	443	44
RuL2	5	98	224	246	38
	10	154	292	305	43
	15	210	469	407	62

4.10 CONCLUSIONS

In summary, the third-order nonlinearity of novel ruthenium complexes has been investigated by Z-scan and DFWM techniques using 7 ns pulses at 532 nm. We have shown that the ruthenium complexes exhibit RSA and self-defocusing character. These materials show optical power limiting capability. The all-optical switching of the ruthenium complexes was demonstrated using the pump-probe technique. The five-level model provides a good understanding of the observed nonlinearity and all-optical switching. Hence, the investigated ruthenium complexes are potential candidates for new photonic device applications.

CHAPTER 5

CHAPTER 5**THIRD-ORDER NONLINEAR OPTICAL STUDIES OF
RUTHENIUM COMPLEXES CONTAINING SALEN AND
SALOPHENE*****Abstract***

This chapter focuses on the results of Z-scan, DFWM, optical power limiting and all-optical switching experiments on two ruthenium complexes containing salen and salophene ligands. The effect of π -conjugation and delocalization on third-order nonlinear optical properties is discussed. The concentration dependence of third-order nonlinear optical properties of these metal-organic complexes is also presented.

5.1 INTRODUCTION

In the previous chapter we have presented the investigation of the third order NLO characteristics of ruthenium complexes containing dmit ligands. One of the attractive features of organic materials is the possibility of altering the molecular structure slightly in order to obtain desirable NLO properties. With this in mind, we carried out the investigation on ruthenium complexes having salen and salophene ligands in place of dmit ligands. Among metal-organic compounds, one of the first studies reported was on the NLO properties of a ferrocene derivative (Green et al. 1987). It was seen that these compounds possess good NLO properties and that a ferrocenyl conjugated system possesses efficient electronic transport between terminal subunits, which is of particular interest for device applications (Mata et al. 2001 and Mata et al. 2001). The incorporation of transition metal ions introduces more sublevels into the energy hierarchy, thus permitting more allowed electronic transitions and giving larger NLO effects (Chao et al. 1999). Metal ions being excellent templates, can gather organic one dimensional dipolar chromophores around to form predetermined two or three dimensional NLO-phores with various symmetries and charge-transfer dimensions by virtue of which the coordinated metal center as

well as the presence of polarisable *d* orbital electrons would contribute to the larger nonlinear activity (Long 1995 and Evans and Lin 2002).

The N₂O₂ Schiff-base ligands derived from salicylaldehyde and diamines (generically named as salen and salophene ligands) can be used as alternative building blocks for the design/preparation of NLO compounds owing to their synthetic versatility relative to the introduction of electron donor/acceptor functionalities and creation of extensive π -delocalization to induce large electron asymmetry (Freire and de Castro 1998 and Freire and de Castro 1998). Furthermore, they can also coordinate several transition metal cations in different oxidation states which can additionally fine-tune the NLO responses. The NLO properties of metal complexes with salen and salophene ligands, functionalized with electron donor and acceptor groups with a D- π -A structure, have been extensively studied (Bella et al. 1995, Bella et al. 1996, Bella et al. 1997, Lacroix 2001, Bella and Fragala 2000 and Bella 2001). The NLO responses of salen and salophene-type complexes were related to the presence of intense low-energy metal-to-ligand, ligand-to-metal charge transfer and intraligand transitions. Inclusion of metal centres in Schiff-base ligands was always accompanied by an enhancement of NLO responses compared to that of the free ligands. The role of the metal centre could be twofold as it could act as both, the donor of the D- π -A structure, and/or as part of the π -bridging moiety (Lacroix 2001, Bella 2001 and Gaudry et al. 2000).

In this chapter, we report synthesis and experimental studies on NLO properties of ruthenium metal-organic complexes with salen and salophene ligands. We have also investigated the optical power limiting and all-optical switching behaviors of these samples.

5.2 SYNTHESIS AND CHARACTERIZATION OF RUTHENIUM COMPLEXES CONTAINING SALEN AND SALOPHENE

5.2.1 Materials and methods

All the chemicals used were of analytical grade. Solvents were purified and dried according to standard procedure (Vogel 1989). Ruthenium (III) chloride trihydrate and all other reagents were procured from Sigma Aldrich Chemicals, and

were used without further purification. The two Schiff base ligands were prepared in 85-95% yield by condensation reactions of 1,2-diaminoethane (H_2L^1) and 1, 2-diaminobenzene (H_2L^2) with salicylaldehyde, respectively, in methanolic media (Amirnasr et al. 2001).

The electronic spectra of the complexes in N, N-dimethylformamide solution were recorded on GBC UV-Vis double beam Spectrophotometer in 200 – 800 nm wavelength range. FT-IR spectra were recorded on a Thermo Nicolet Avatar FT – IR Spectrometer as KBr powder in the frequency range 400 – 4000 cm^{-1} . The C, H, N and S contents were determined by Thermoflash EA1112 series elemental analyzer. 1H NMR spectra were recorded on a Bruker AMX 400 instrument using TMS as internal standard. Magnetochemical measurement was recorded on a Sherwood Scientific instrument.

5.2.2 Synthesis of ligand

The Schiff base ligands salen H_2L^1 and salphen H_2L^2 were prepared (Amirnasr et al. 2001) by condensation of salicylaldehyde with 1,2-diaminoethane and 1,2-diaminobenzene, respectively, in a 2:1 mole ratio. The H_2L^2 : 1H NMR spectrum in (DMSO- d_6) showed a singlet at δ 8.55 for the imino proton and a broad singlet at δ 13.59 for the hydroxyl proton, respectively. IR spectrum (cm^{-1} , KBr): 2998m, 1579m, 1468s, 1327m, 1251s, 1135m, 1083m, 961m, 819s cm^{-1} . UV-Vis : λ_{max} (nm) 353, 262. H_2L^2 : The 1H NMR spectrum of in (DMSO- d_6) showed a singlet at δ 8.911 for the imino proton and a broad singlet at δ 12.95 for the hydroxyl proton, respectively. IR (cm^{-1} , KBr) : 3310m, 2954m, 1611vs, 1465s, 1402m, 1252s, 1204m, 1099m, 971m, 737s cm^{-1} . UV-vis λ_{max} (nm) 336, 281, 239.

5.2.3 General procedure for synthesis of complexes

The complexes were prepared following a reported procedure (Tedim et al. 2006, Booth et al. 1971, Lacroix et al. 1996 and Lenoble et al. 1998). Refluxing ethanol solution of $RuCl_3 \cdot 3H_2O$ and the respective ligands in a 1:1 molar ratio for 2 hours yielded the corresponding complexes. The complexes were filtered, washed

with the mother liquor and then with hexane and dried in vacuo. The formation of the complex was checked by TLC. The yield was about 70 – 80%.

(a) [Ru (salen) (H₂O) (Cl)] {salen = N, N'- disalicylidene - 1,2-ethylenediimine dianion}

The Ru(II) Schiff base complexes, RuL¹ was prepared in high yield via the interaction of the free Schiff base, H₂L¹, with RuCl₃.3H₂O in a 1:1 mole ratio in refluxing absolute ethanol for 12 h. RuL¹: ¹H NMR (DMSO-*d*₆): δ 8.40 (s, 2H, HC=N), 6.77-6.74 (m, 8H, ArH), 6.33 (t, 2H, ArH) and 3.71 (s, 4H, -NCH₂CH₂N-). IR (cm⁻¹, KBr): 3281 m, 1660 s, 1471 s, 1445 s, 1399 m, 1239 s, 1170 m, 978 m, 728 s cm⁻¹.

(b) [Ru (salophene) (H₂O) (Cl)] {salophene = N, N'-disalicylidene-1,2-ethylendiimine dianion}

The Ru(II) Schiff base complexes, RuL² was prepared in high yield via the interaction of the free Schiff base, H₂L², with RuCl₃.3H₂O in a 1:1 mole ratio in refluxing absolute ethanol for 12 h. RuL²: ¹H NMR (DMSO-*d*₆): δ 8.40 (s, 2H, HC=N), 7.88-7.86 (m, 2H, ArH), 7.37-7.34 (m, 2H, ArH), 7.03 (d, *J* 7.6 Hz, 2H, ArH), 6.86 (d, *J* 7.6 Hz, 2H, ArH) and 6.44 (t, *J* 7.6 Hz, 2H, ArH). IR (cm⁻¹, KBr): 3314 m, 1613 s, 1585 s, 1540 s, 1467 s, 1444 s, 1389 m, 1238 s, 1193 s, 1107 m, 975 m, 737 s.

5.3 MOLECULAR STRUCTURES AND UV-VISIBLE SPECTRA OF RUTHENIUM COMPLEXES CONTAINING SALEN AND SALOPHENE LIGAND

Figures 5.1 and 5.2 show the molecular structure of RuL₃ and RuL₄. The UV-Vis spectra of the two ruthenium complexes dissolved in solution as well as in film form are shown in Figures 5.3 to 5.4.

In our present study we used following two metal complexes of ruthenium (Ru) containing salen/salophene ligand,

1. [Ru (salen) (H₂O) (Cl)] {salen = N, N'- disalicylidene - 1,2-ethylenediimine dianion} **[RuL₃]**

2. [Ru (salophene) (H₂O) (Cl)] {salophene = N, N'-disalicylidene-1,2-ethylenediimine dianion} [RuL4].

The salen and salophene are Schiff base ligands which form cyclic coordination compounds with metals using its four donor atoms (O, O, N and N). In salen ligand, ethylene forms a bridge between two adjacent phenyl groups, whereas in salophene ligand the phenyl ring forms a bridge between two adjacent phenyl groups. The bands appearing in the region 230-350 nm are assigned to intraligand charge transfer transitions (ILCT) and less intense bands in the range 390–500 nm corresponds to the d-d forbidden transitions (Dileep and Bhat 2010). The small absorption tails at 532 nm give linear absorption coefficient (α_0) for all samples, which are tabulated in Table 5.5.

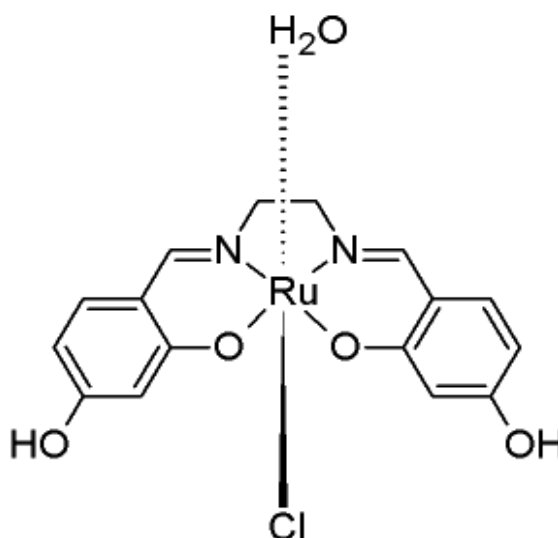


Figure 5.1 Molecular structure of [Ru (salen) (H₂O) (Cl)] {salen = N, N'-disalicylidene - 1,2-ethylenediimine dianion} [RuL3]

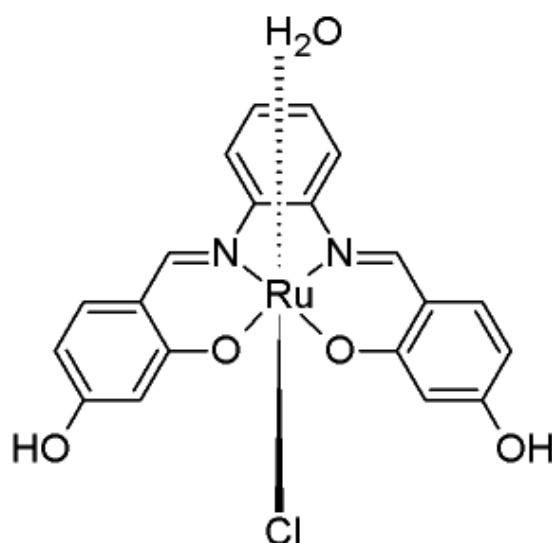


Figure 5.2 Molecular structure of [Ru (salophene) (H₂O) (Cl)] {salophene = N, N'-disalicylidene-1,2-ethylenediimine dianion} [RuL4]

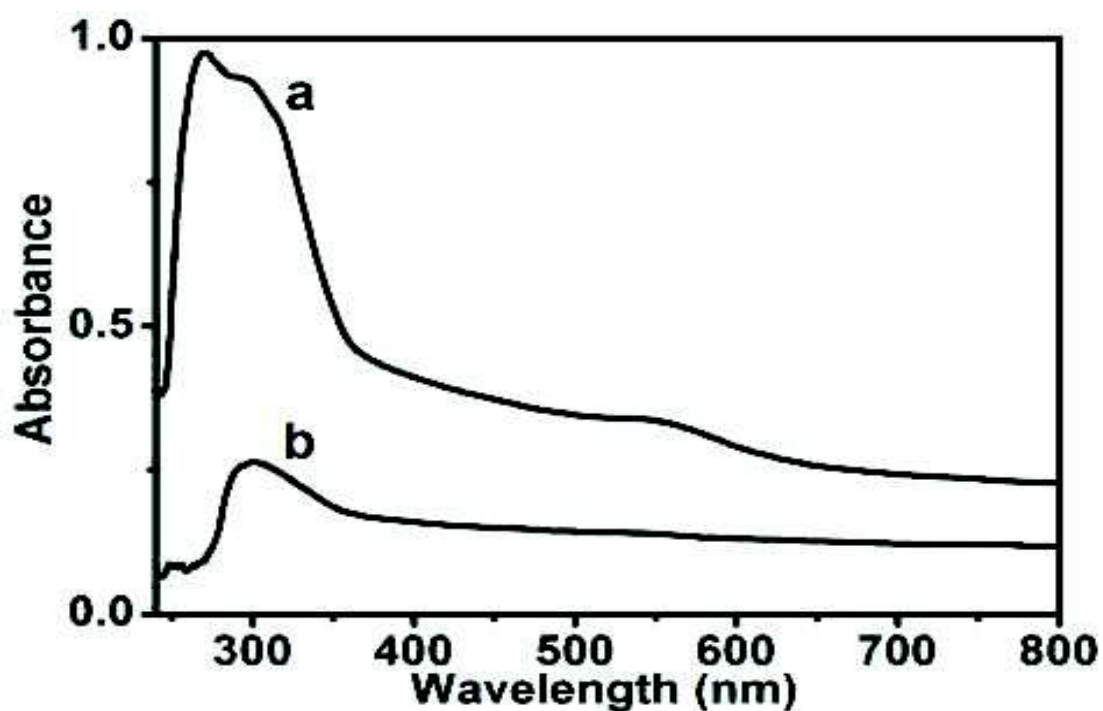


Figure 5.3 UV-Visible absorption Spectrum of the ruthenium complex RuL3 in both solution (a) and film form (b), (Absorbance (A) = $-\ln(I/I_0)$, where I – transmitted intensity and I_0 – incident intensity)

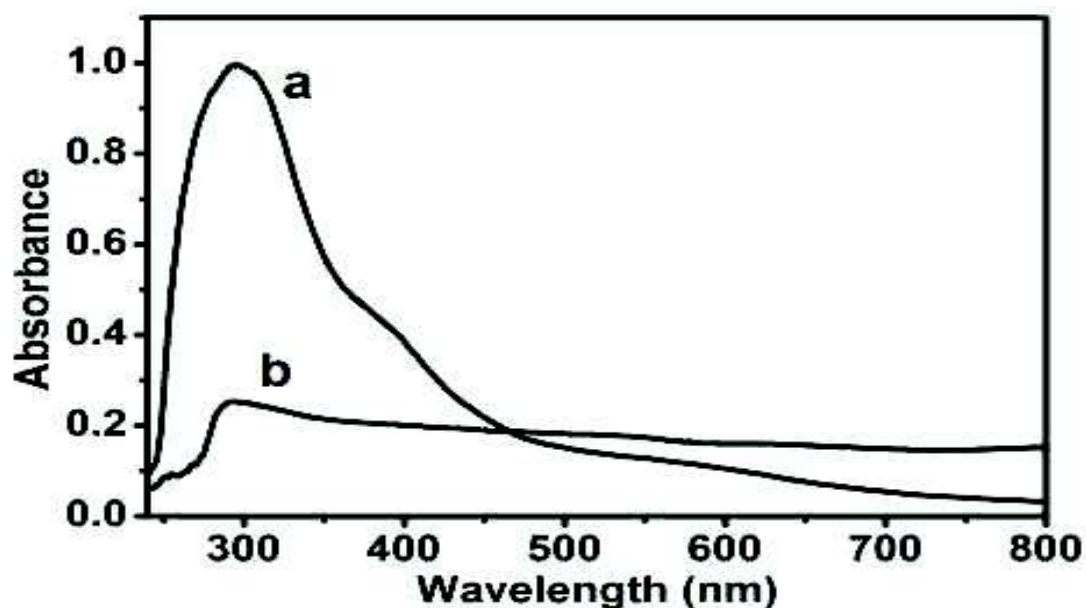


Figure 5.4 UV-Visible absorption Spectrum of the ruthenium complex RuL4 in both (a) solution (a) and film form (b), (Absorbance (A) = $-\ln(I/I_0)$, where I – transmitted intensity and I_0 – incident intensity)

5.4. Z-SCAN STUDIES OF RUTHENIUM COMPLEXES CONTAINING SALEN AND SALOPHENE LIGANDS

The Z-scan experiment was performed using 7 ns laser pulses at pulse energy of 50 μJ which corresponds to a peak irradiance of 1.2 GW/cm^2 . The magnitude of nonlinear absorption coefficient β_{eff} of the metal-organic complexes was estimated by performing the open aperture Z-scan. Figures 5.5 (a) to 5.10 (a) show the open aperture Z-scan traces of RuL3 and RuL4 in solution and in film form at various dopant concentrations. The transmission is symmetric about the focus ($z=0$) where it has a minimum transmission. Thus an intensity dependent absorption effect is observed. Nonlinear absorption was found to be strong in all the complexes.

Figures 5.5 (b) to 5.10 (b) depict closed aperture curves and Figures 5.5 (c) to 5.10 (c) show pure nonlinear refraction curves obtained through division method, for RuL3 and RuL4. The closed aperture Z-scan signature indicates a strong negative refractive nonlinearity of the metal-organic complexes. Similar Z-scan curves were obtained for complexes with different concentrations in solution and film form.

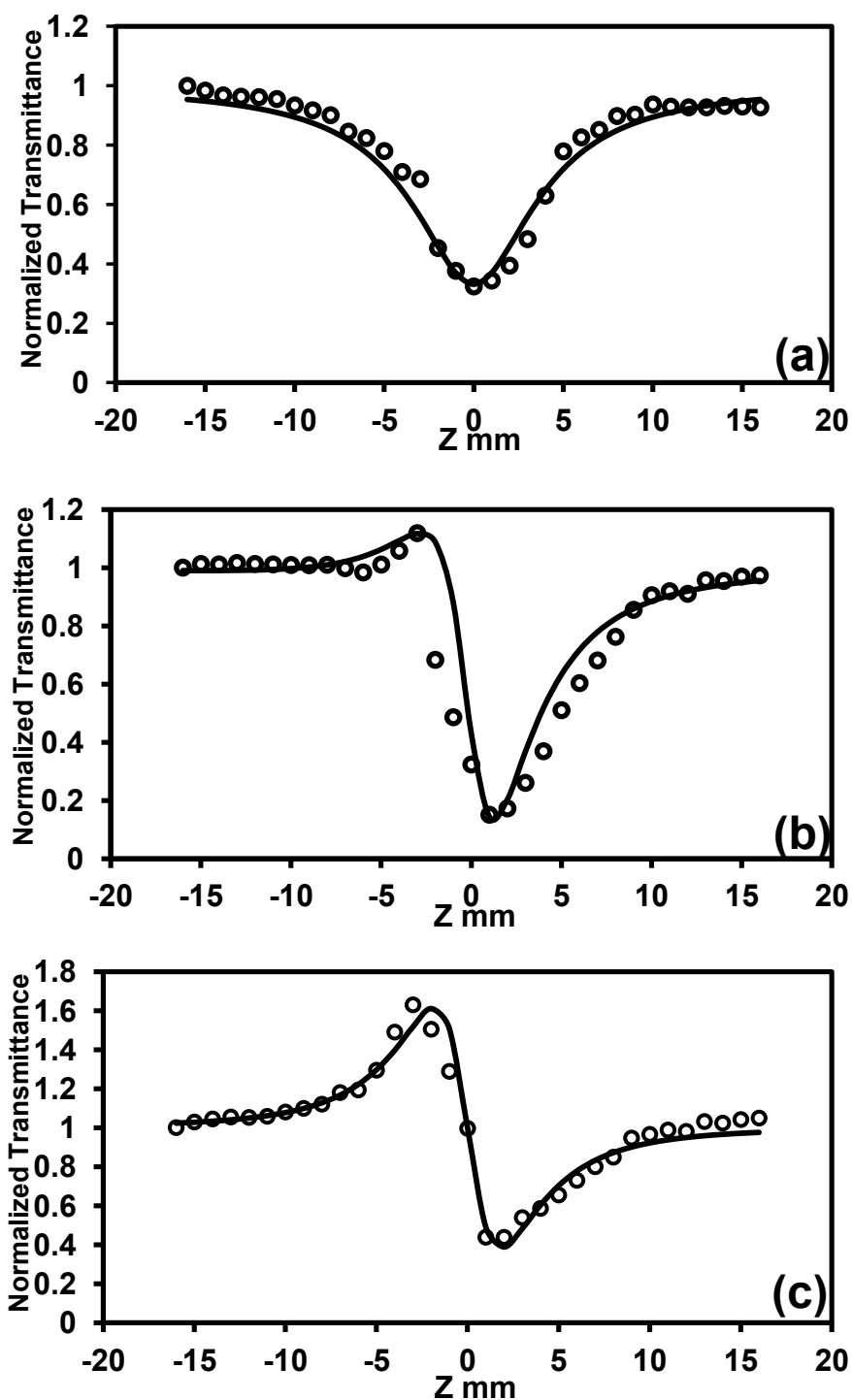


Figure 5.5 Plots of Open aperture (a), Closed aperture (b) and Pure nonlinear refraction (c) curves for RuL3 in solution form (1×10^{-3} mol/L). Solid line is a theoretical fit to the experimental data.

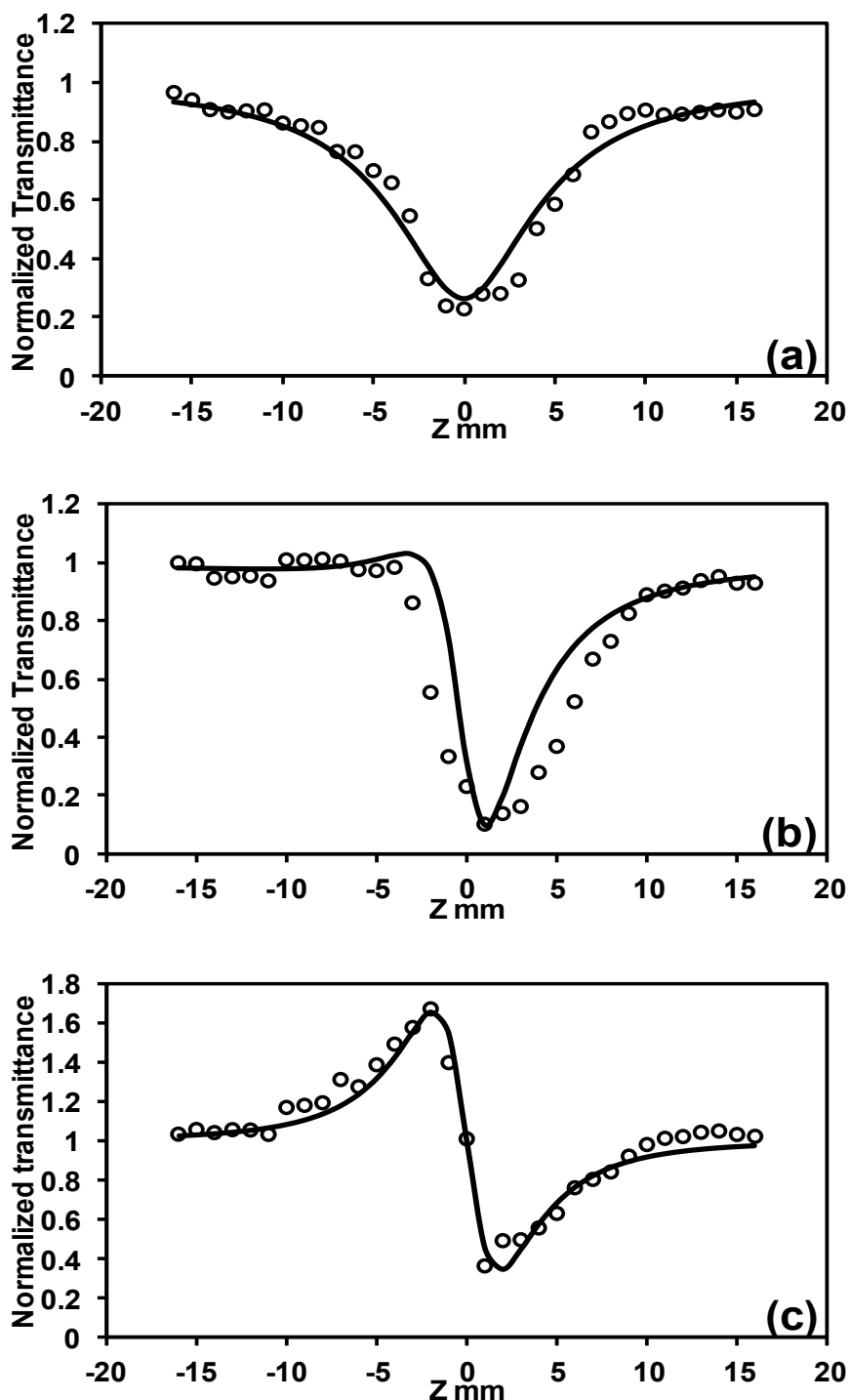


Figure 5.6 Plots of Open aperture (a), Closed aperture (b) and pure nonlinear refraction (c) curves for RuL4 in solution form (1×10^{-3} mol/L). Solid line is a theoretical fit to the experimental data.

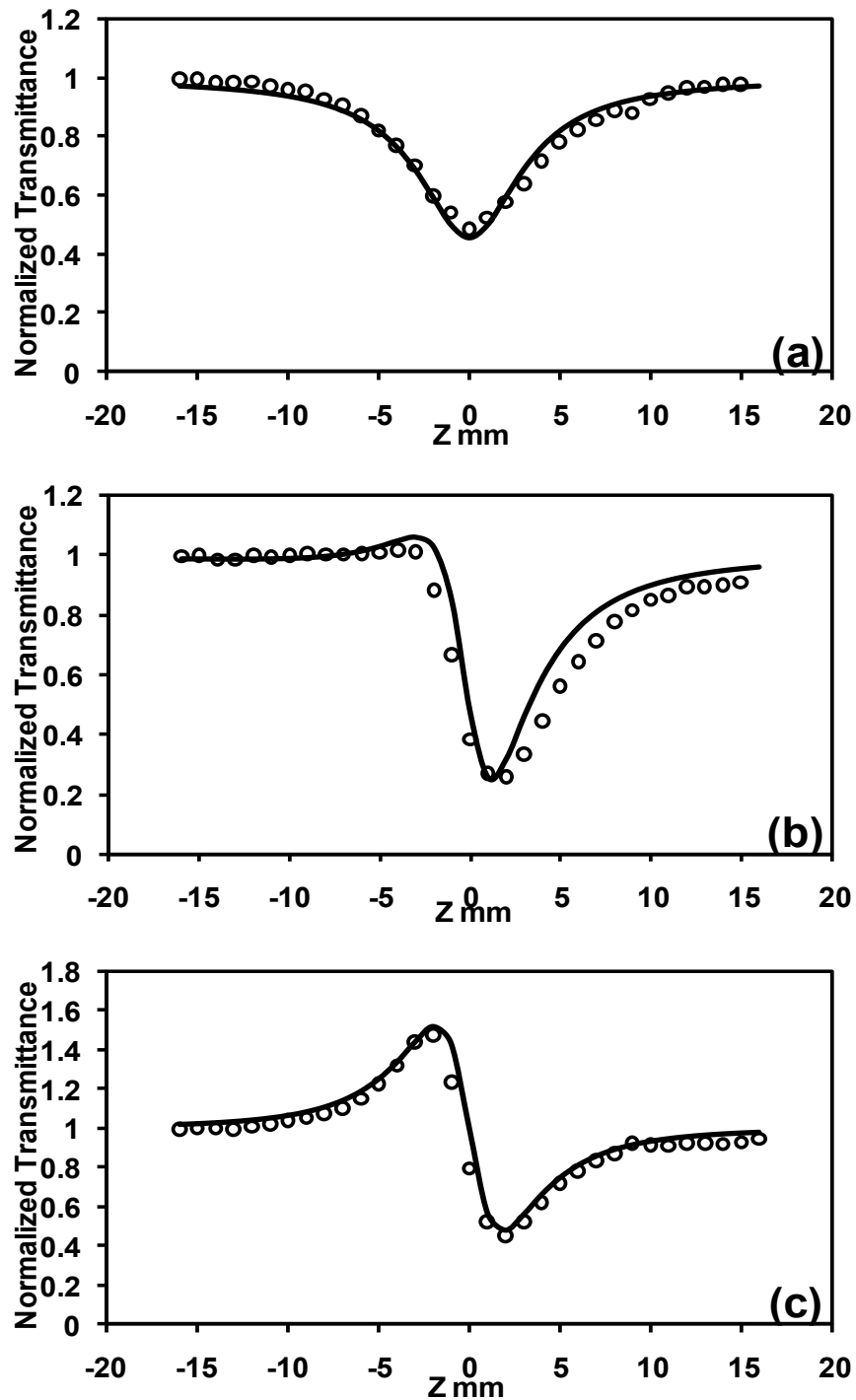


Figure 5.7 Plots of Open aperture (a), Closed aperture (b) and Pure nonlinear refraction (c) curves for RuL3 in film form (0.5 wt.%). Solid line is a theoretical fit to the experimental data

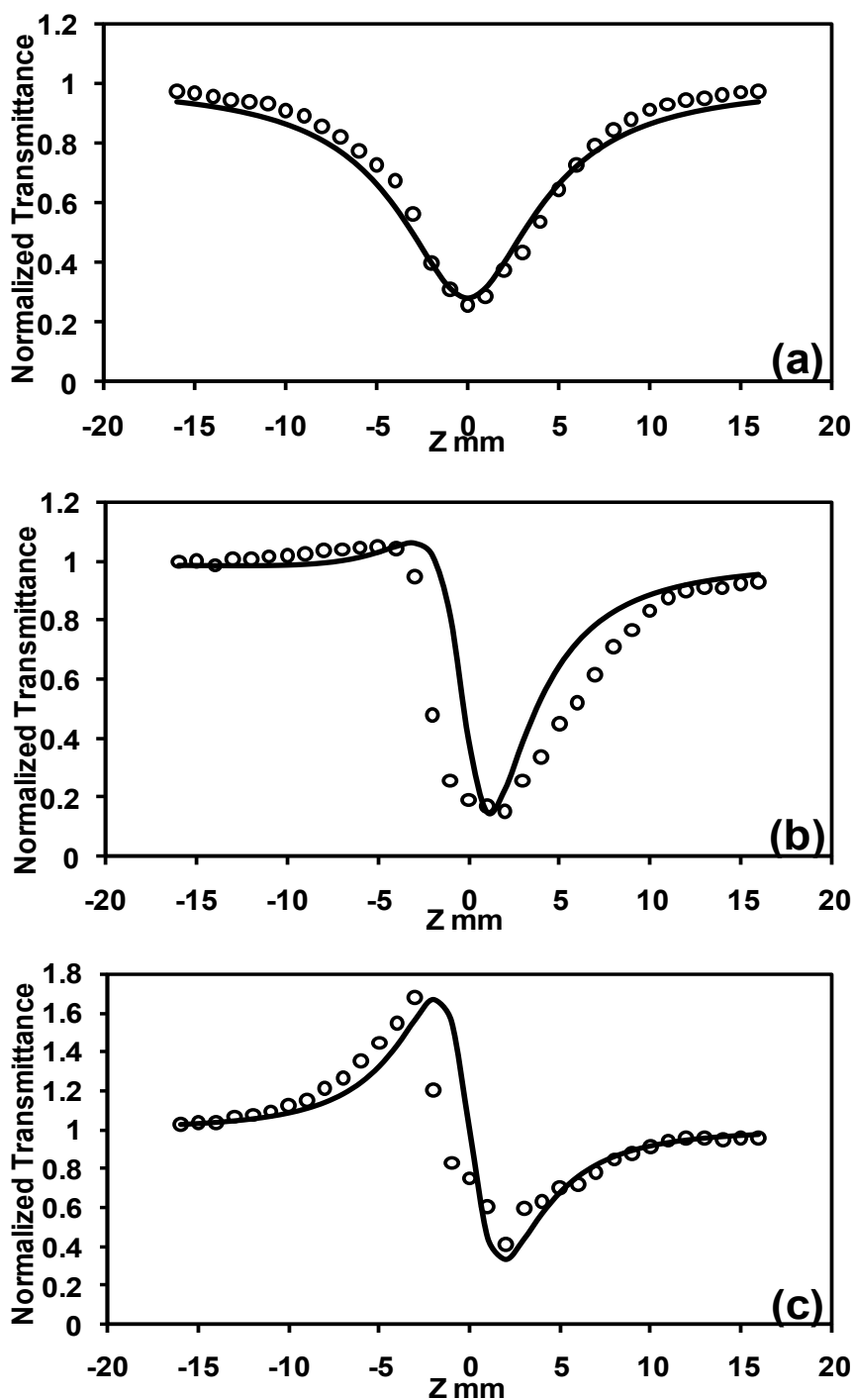


Figure 5.8 Plots of Open aperture (a), Closed aperture (b) and Pure nonlinear refraction (c) curves for RuL3 in film form (2.0 wt.%). Solid line is a theoretical fit to the experimental data

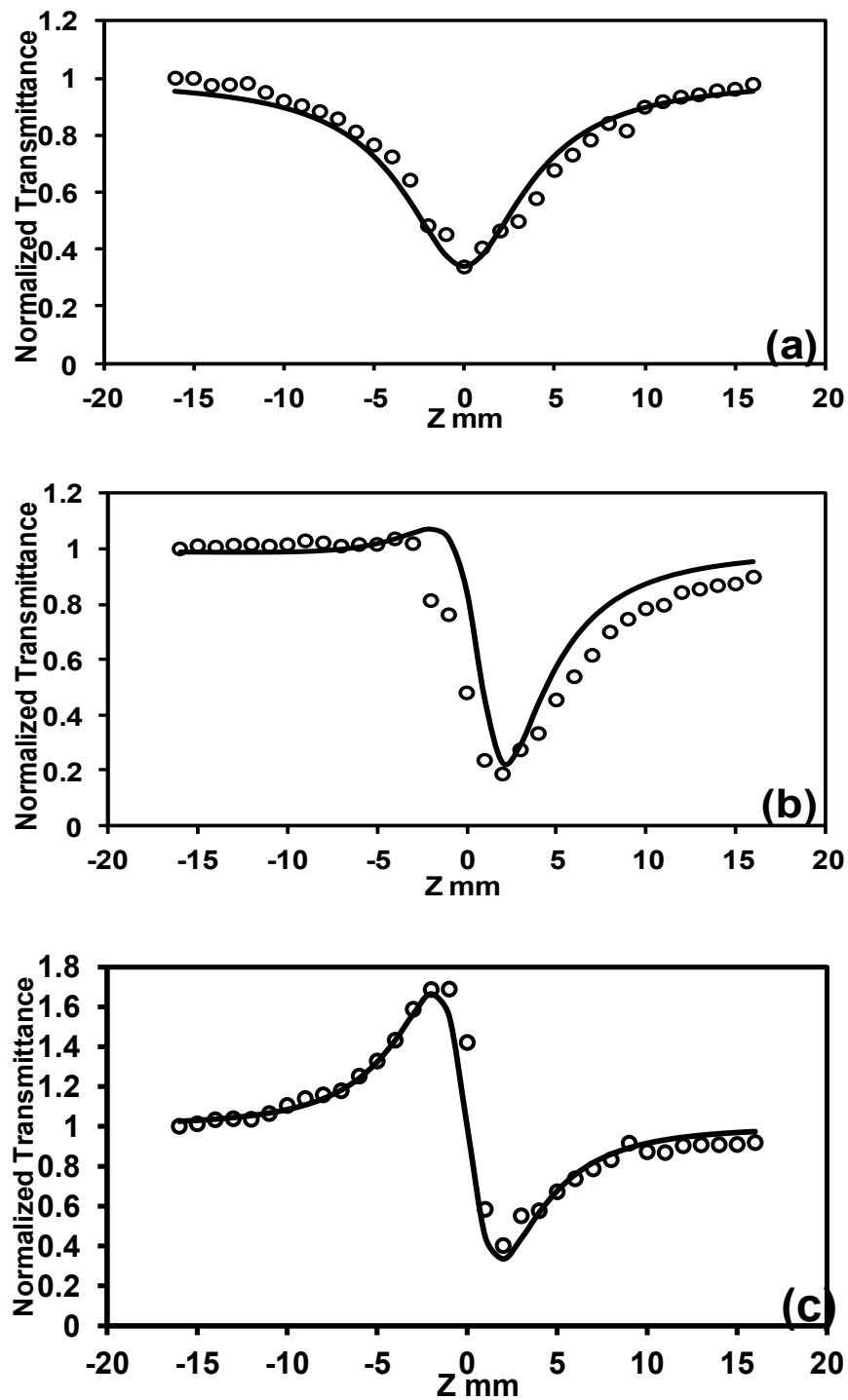


Figure 5.9 Plots of Open aperture (a), Closed aperture (b) and Pure nonlinear refraction (c) curves for RuL4 in film form (0.5 wt.%). Solid line is a theoretical fit to the experimental data

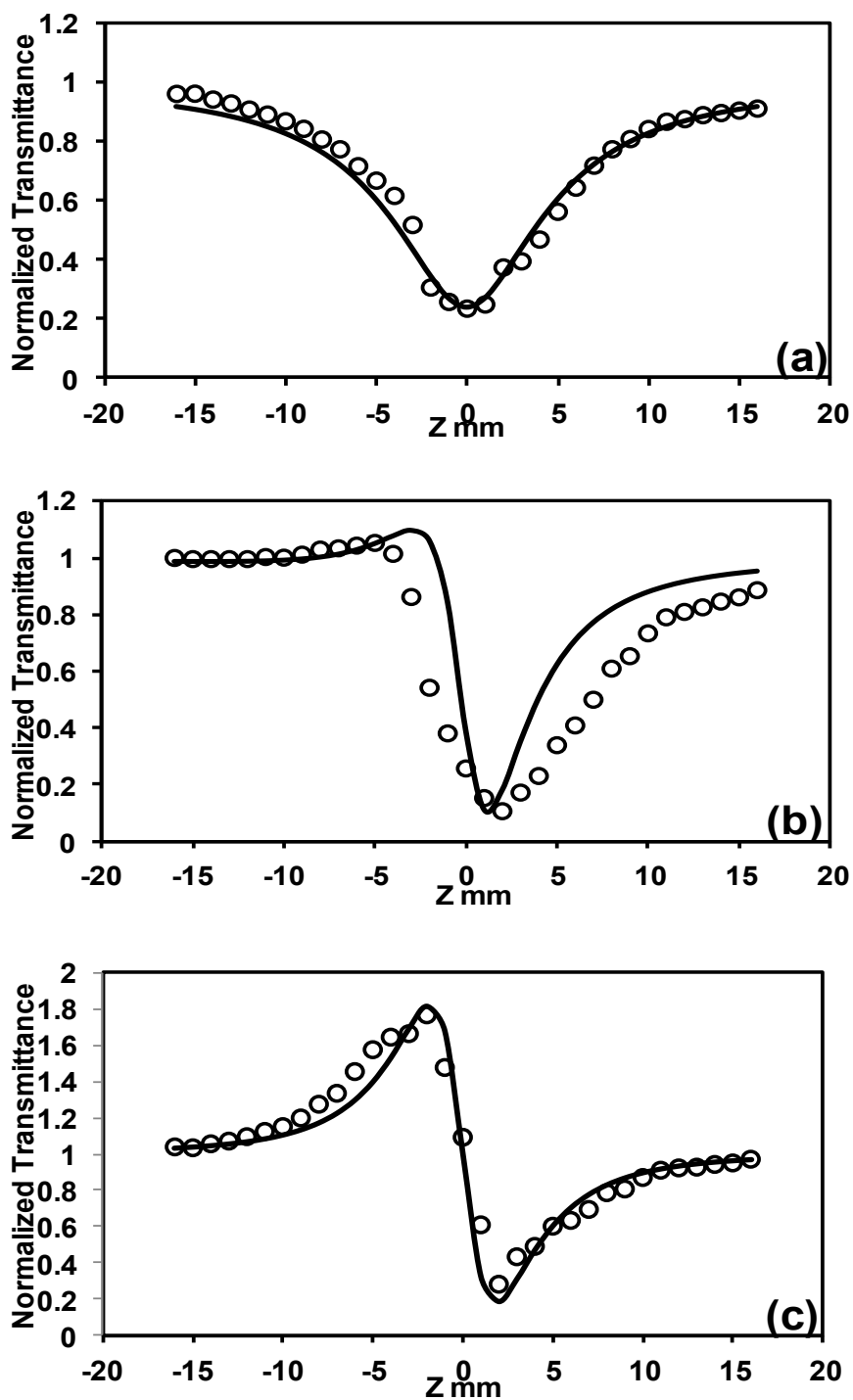


Figure 5.10 Plots of Open aperture (a), Closed aperture (b) and Pure nonlinear refraction (c) curves for RuL3 in film form (2.0 wt.%). Solid line is a theoretical fit to the experimental data

The third-order nonlinear optical parameters of RuL3 and RuL4 in solution and solid film obtained through Z-scan measurements are tabulated in Tables 5.1 and 5.2.

Table 5.1 Third-order nonlinear optical parameters of ruthenium complexes in solution form at different concentrations at the input laser intensity of 1.2 GW/cm².

Sample	Concentration (x10 ⁻³ mol/L)	β_{eff} (m/W) x10 ⁻¹¹	Im $\chi^{(3)}$ (esu) x10 ⁻¹³	n_2 (esu) x10 ⁻¹¹	Re $\chi^{(3)}$ (esu) x10 ⁻¹³
RuL3	0.25	9.119	1.372	-4.569	-4.822
	0.5	11.596	1.745	-5.853	-6.177
	1	21.717	3.267	-9.563	-10.092
RuL4	0.25	11.574	1.741	-5.895	-6.221
	0.5	17.052	2.565	-7.503	-7.918
	1	32.648	4.912	-13.852	-14.618

Table 5.2 Third-order nonlinear optical parameters of the ruthenium complexes at different dopant concentrations in film form at the input laser intensity of 1.2 GW/cm².

Sample	Concentration (wt. %)	β_{eff} (m/W) x10 ⁻⁹	Im $\chi^{(3)}$ (esu) x10 ⁻¹¹	n_2 (esu) x10 ⁻⁹	Re $\chi^{(3)}$ (esu) x10 ⁻¹¹
RuL3	0.50	15.888	3.497	-8.998	-12.237
	1.00	22.375	4.925	-10.945	-14.885
	1.50	25.519	5.617	-12.409	-16.876
	2.00	34.113	7.509	-17.089	-23.241
RuL4	0.50	20.778	4.574	-11.408	-15.515
	1.00	25.103	5.526	-13.727	-18.670
	1.50	27.003	5.944	-14.856	-20.203
	2.00	38.884	8.560	-20.324	-27.640

Second order hyperpolarizability (γ_h) of a molecule is related to the third-order bulk susceptibility through Equation (2.42) as given in chapter 2. The calculated values of γ_h for RuL3 and RuL4 are 1.725×10^{-30} esu and 2.368×10^{-30} esu, respectively.

The excited state cross-section σ_{exc} can be measured from the normalized open aperture Z-scan data (Henari et al. 1997). Molecules are optically excited from the ground state to the singlet-excited state. The molecules from this state relax either to the ground state or the triplet state when excited state absorption occurs from the triplet to the higher triplet state.

The change in the intensity of the laser beam as it passes through the material is given by

$$\frac{dI}{dz} = -\alpha_0 I - \sigma_{exc} N(t) I \quad (5.1)$$

where I is the intensity and N is the density of molecules in the excited state. The excited state density of molecules arises as a result of a nonlinear absorption process whose intensity dependence can be obtained from the following equation

$$\frac{dN}{dz} = \frac{\sigma_{exc} I}{h\omega} \quad (5.2)$$

where ω is the angular frequency of the laser. Combining the above two equations and solving for the fluence of the laser and over the spatial extent of the beam gives the normalized transmission for open aperture as

$$T = \ln \left(1 + \frac{q_0}{1+x^2} \right) \bigg/ \frac{q_0}{1+x^2} \quad (5.3)$$

where $x=z/z_0$, $q_0 = \frac{\sigma_{exc} F_0 L_{eff}}{2h\omega}$, F_0 is the fluence of the laser at the focus and

$L_{eff} = (1 - \exp^{-\alpha_0 L}) / \alpha_0$. A fit of Equation (5.3) to the open aperture data at 532 nm yields σ_{exc} for RuL3 and RuL4 and are given in Tables 5.3 and 5.4. The ground state absorption cross-section, σ_g is calculated from $\alpha_0 = \sigma_g N_a C$, where N_a is Avogadro's

number and C is the concentration in moles/cm³ for RuL3 and RuL4. The values obtained are tabulated in Tables 5.3 and 5.4.

Table 5.3 Ground state absorption cross-section and excited state absorption cross-section of the ruthenium complexes in solution form at different concentrations

Sample	Concentrations (x 10 ⁻³ mol/L)	σ_g (x 10 ⁻¹⁹ cm ²)	σ_{exc} (x 10 ⁻¹⁸ cm ²)
RuL3	0.25	15.577	3.410
	0.5	13.853	4.336
	1	11.252	7.120
RuL4	0.25	19.770	4.328
	0.5	17.514	6.376
	1	15.184	12.208

Table 5.4 Ground state absorption cross-section and excited state absorption cross-section of the ruthenium complexes doped in film form at different dopant concentrations

Sample	Dopant Concentrations (wt. %)	σ_g (x 10 ⁻¹⁷ cm ²)	σ_{exc} (x 10 ⁻¹⁶ cm ²)
RuL3	0.5	8.827	3.626
	1.0	5.698	4.683
	1.5	5.442	5.824
	2.0	4.687	7.785
RuL4	0.5	9.643	4.742
	1.0	6.393	5.729
	1.5	5.759	6.162
	2.0	4.978	8.874

The calculated values of σ_{exc} are greater than σ_g for all investigated complexes, which is the required condition for reverse saturable absorption to occur. Generally, reverse saturable absorption occurs in a molecule when excited state cross-section is larger than the ground state cross-section.

A plot of absorption coefficient β_{eff} versus I_0 , the input laser intensity, enables us to identify the mechanism responsible for nonlinear absorption. Figures 5.11 and 5.12 shows a plot of β_{eff} versus I_0 for two ruthenium metal-organic complexes RuL3 and RuL4 in solution and film form.

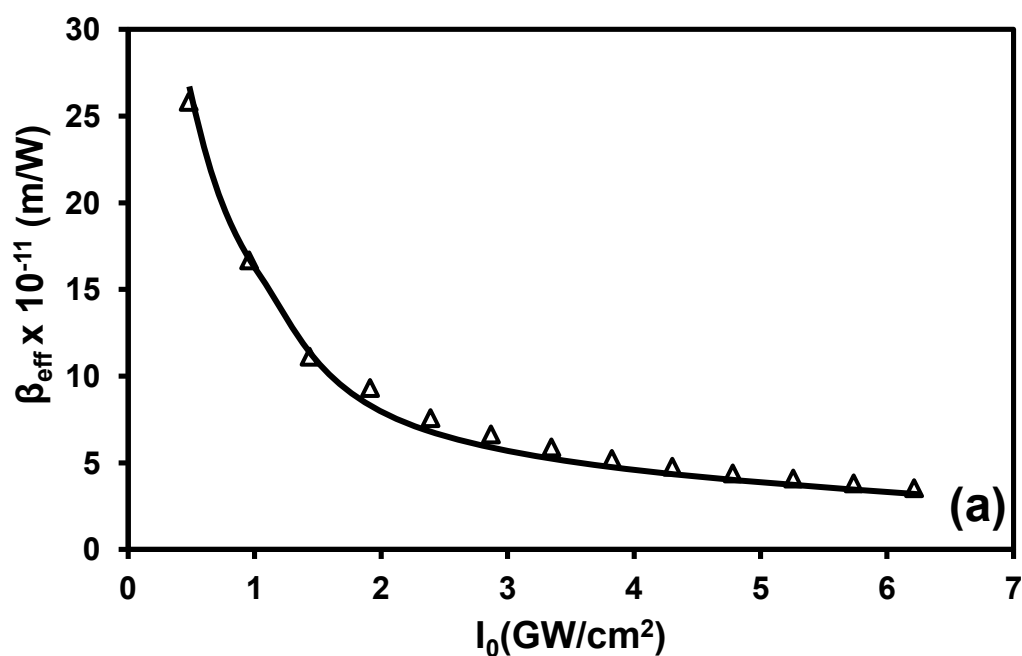


Figure 5.11 (a) Nonlinear absorption coefficient (β_{eff}) versus on-axis input intensity I_0 for RuL3 in solution (1×10^{-3} mol/L)

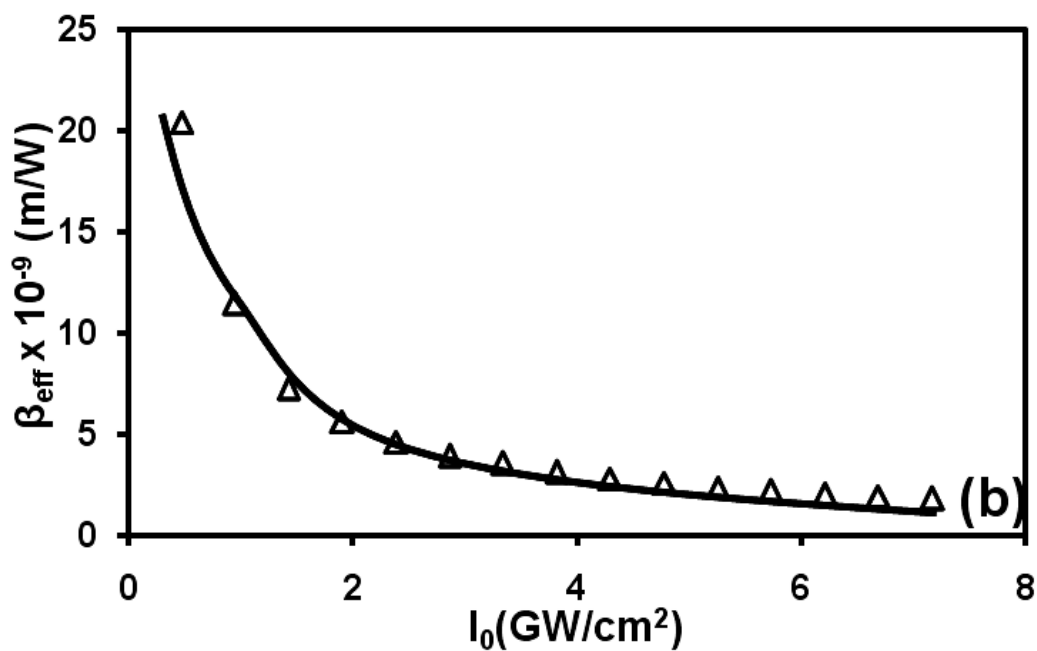


Figure 5.11 (b) Nonlinear absorption coefficient (β_{eff}) versus on-axis input intensity I_0 for RuL3 in film form (1 wt.%)

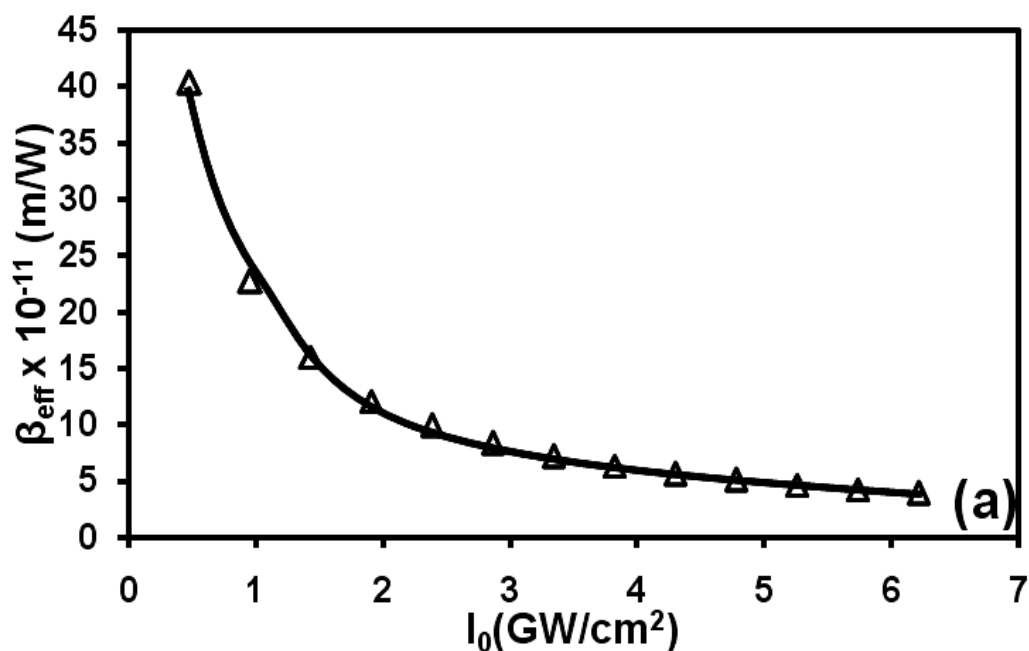


Figure 5.12 (a) Nonlinear absorption coefficient (β_{eff}) versus on-axis input intensity I_0 for RuL4 in solution ($1 \times 10^{-3} \text{ mol/L}$)

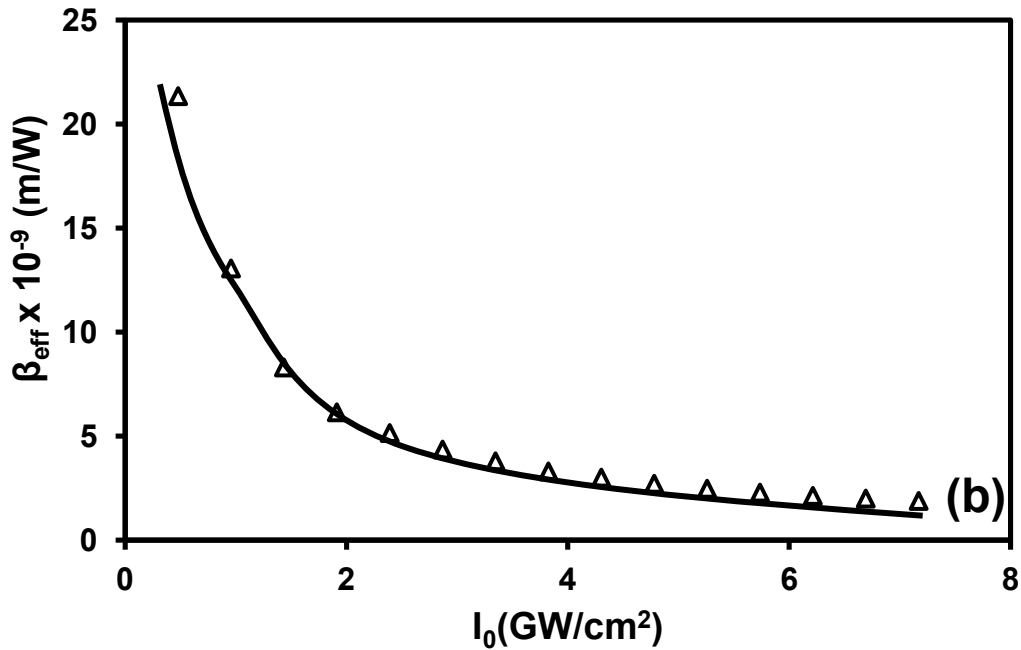


Figure 5.12 Nonlinear absorption coefficient (β_{eff}) versus on-axis input intensity I_0 for RuL4 in film form (1 wt.%) (b)

Generally, NLA can be caused by free carrier absorption, saturated absorption, direct multiphoton absorption, or excited state absorption. If the mechanism belongs to the simple two-photon absorption, β should be a constant that is independent of the on-axis irradiance I_0 . If the mechanism is the direct three-photon absorption, it should be a linear increasing function of I_0 and intercepts on the vertical axis should be nonzero (Guo et al. 2003).

Figures 5.11 and 5.12 show that β_{eff} is decreasing with increasing I_0 . The fall of β_{eff} with increasing I_0 is a consequence of the reverse saturable absorption (Auger et al. 2003). A small linear absorption at 532 nm and the measured σ_{exc} values indicate that there is a contribution from excited state absorption to the observed NLA. Therefore, we attribute this NLA to reverse saturable absorption.

5.5 DFWM STUDIES OF RUTHENIUM COMPLEXES CONTAINING SALEN AND SALOPHENE LIGANDS

Figures 5.13 and 5.14 show the DFWM signal versus input energy graphs of ruthenium complex RuL3 and RuL4 at the concentrations of 1×10^{-3} mol/L, respectively. The cubic dependence of DFWM signal with respect to input energy is observed in all samples. The signal is proportional to the cubic power of the input intensity as given by the Equation 2.35. Cubic behavior of the DFWM signal indicates the third-order nature of the NLO process as well as the absence of saturation of nonlinearity in the measurements.

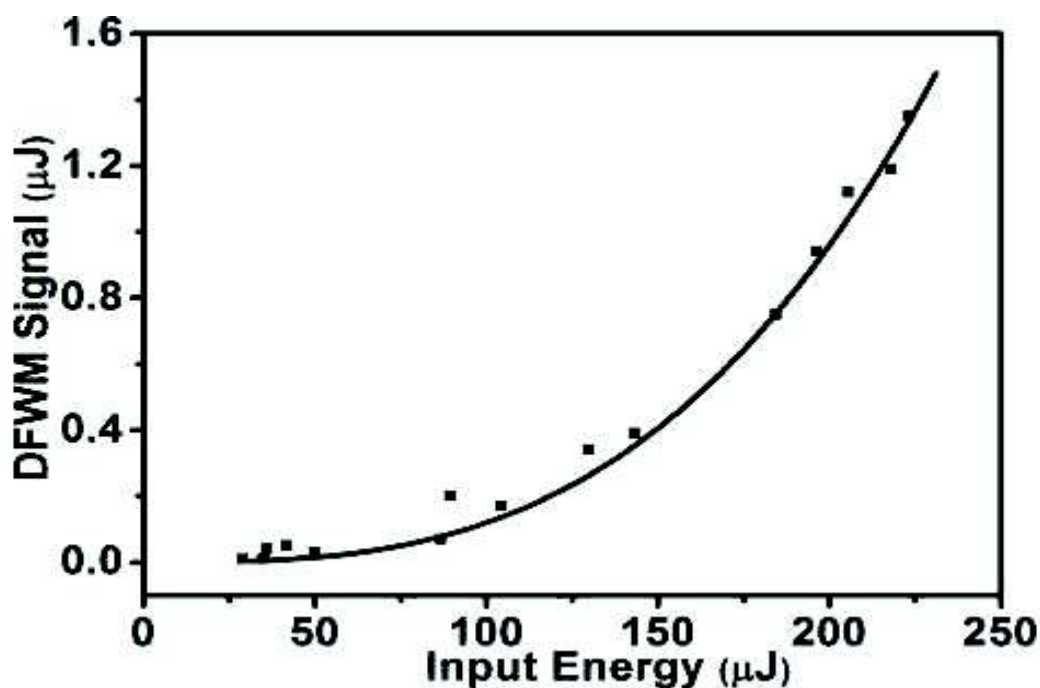


Figure 5.13 DFWM signal of RuL3 at the concentration of 1×10^{-3} mol/L. Squares are data points while the solid curve is a cubic fit to the data

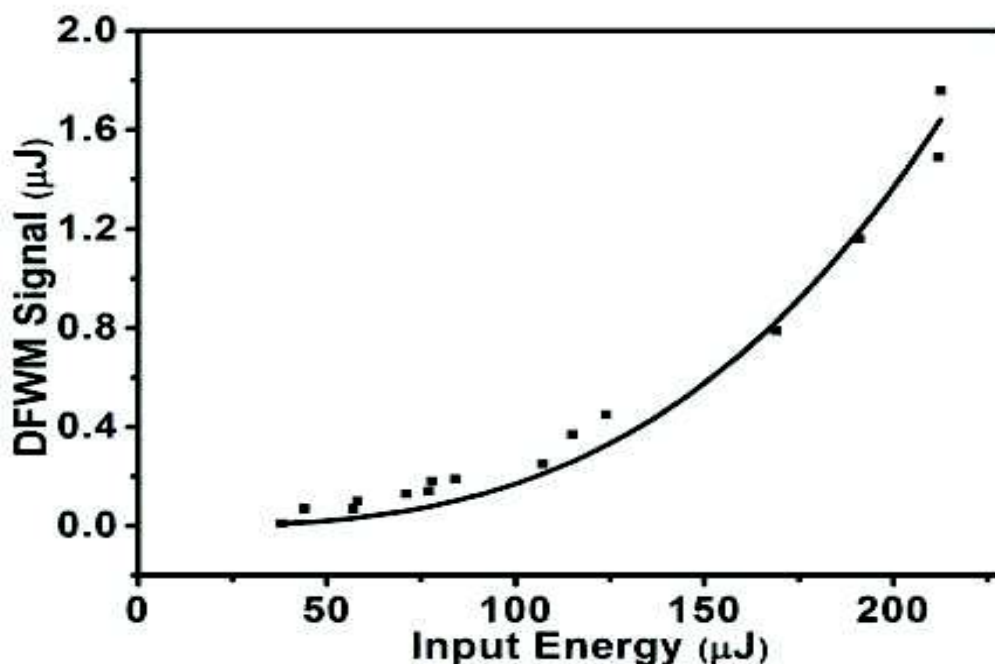


Figure 5.14 DFWM signal of RuL4 at the concentration of 1×10^{-3} mol/L. Squares are data points while the solid curve is a cubic fit to the data

Table 5.5 Linear absorption coefficient α_0 , third-order nonlinear optical susceptibility $|\chi^{(3)}|$, second-order hyperpolarizability γ_h of different ruthenium complexes measured in DFWM technique.

Sample	α_0 (cm ⁻¹)	$ \chi^{(3)} $ (x 10 ⁻¹³ esu)	γ_h (x 10 ⁻³¹ esu)
RuL3	0.648	10.146	5.402
RuL4	1.298	14.865	7.917

5.6 STRUCTURE-PROPERTY RELATIONSHIP WITH THIRD-ORDER NONLINEAR OPTICAL PARAMETERS IN RUTHENIUM METAL-ORGANIC COMPLEXES WITH SALEN AND SALOPHENE

The absorption between 240 and 380 nm can be assigned to the π to π^* transitions of the Schiff base ligands. The photophysical properties of the Schiff base complexes can be fine-tuned by changing the linkage between the two Schiff base units or the electronic properties of the substituents on the flanking phenyl rings. By

extension of the conjugation either through the spacer or substituents, the absorption and emission spectra of the complexes is red shifted.

Among transition-metal complexes, those with porphyrins and their derivatives exhibit great potential application due to their two dimensional structures and unique electronic properties. The N_2O_2 Schiff-base ligands derived from salicylaldehyde and diamines (generically named as salen ligands) can be used as alternative building blocks for the design/preparation of NLO compounds owing to their synthetic versatility relative to the introduction of electron donor/acceptor functionalities and creation of extensive π -delocalisation to induce large electron asymmetry. Furthermore, they can also coordinate several transition metal cations in different oxidation states which can additionally fine-tune the NLO responses.

The second-order NLO properties of metal complexes with salen-type ligands functionalized with electron donor and acceptor groups with a D- π -A structure have been extensively studied by Bella and Lacroix and some important conclusions have been presented on the relationship between complex molecular structure and second-order NLO properties. It has been shown that second-order NLO responses of salen-type complexes were related to the presence of intense low-energy metal-to-ligand, ligand-to-metal charge transfer and intraligand transitions. The importance of the metal centre in these complexes was shown in the surveys carried out by the same authors and others. Inclusion of metal centres in Schiff-base ligands was always accompanied by an enhancement of second-order NLO responses compared to that of the free ligands and the role of the metal centre could be twofold as it could act as both the donor of the D- π -A structure and/or as part of the π -bridging moiety (Bella et al. 1995, Bella et al. 1996, Bella et al. 1997, Lacroix 2001, Bella and Fragala 2000 and Bella 2001).

The linear and nonlinear optical properties of the Ru (II) complexes with salen and salophen ligands have been investigated as a function of the different combination of aliphatic and aromatic diimine bridges. These N_2O_2 tetradentate ligands with delocalized π -systems impart strong ligand fields leading to almost square-planar geometries and low-spin ground states for the metal complexes (for those that have more than one spin ground state), inducing high degrees of covalence/delocalisation within the metal–ligand bonds. The presence of these electronic properties are

important in the design of molecules with high nonlinear optical properties. Between Ru(salen) and Ru(salophen) complexes with the same aldehyde part, those complexes with aromatic diimine bridge show higher NLO parameters, indicating that, besides the presence of D-A electron groups within the ligand, NLO responses can also be fine tuned by the extending π -conjugation through metal (Lacroix 2001 and Bella 2001).

5.7 OPTICAL POWER LIMITING STUDIES

Based on the strong reverse saturable absorption, a good optical limiting property can be expected for RuL3 and RuL4.

Optical power limiting measurements were carried out by placing the samples at the focus of the Gaussian laser beam and by measuring the transmitted energy for different input laser energies. Figures 5.15 and 5.16 show the optical power limiting of RuL3 and RuL4 in solution form, respectively. Figures 5.17 and 5.18 show the optical power limiting of RuL3 and RuL4 in film form. The optical limiting threshold and clamped output energy of ruthenium complexes RuL3 and RuL4 in solution and film form are tabulated in Tables 5.6 and 5.7. As the concentration increases the clamping level is decreased. The ruthenium complexes containing salen and salophene ligands, investigated here, exhibits good optical power limiting for nanosecond laser pulses. Thus, RuL3 and RuL4 are seen to be promising materials for making optical power limiting devices.

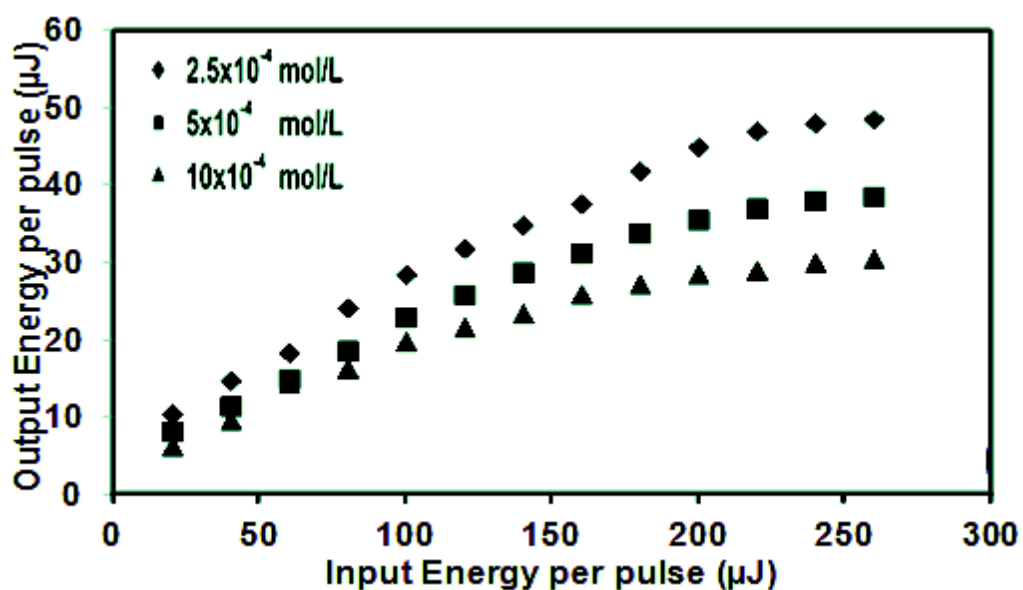


Figure 5.15 Optical power limiting behavior of ruthenium complex RuL3 in solution form at various concentrations indicated in the inset

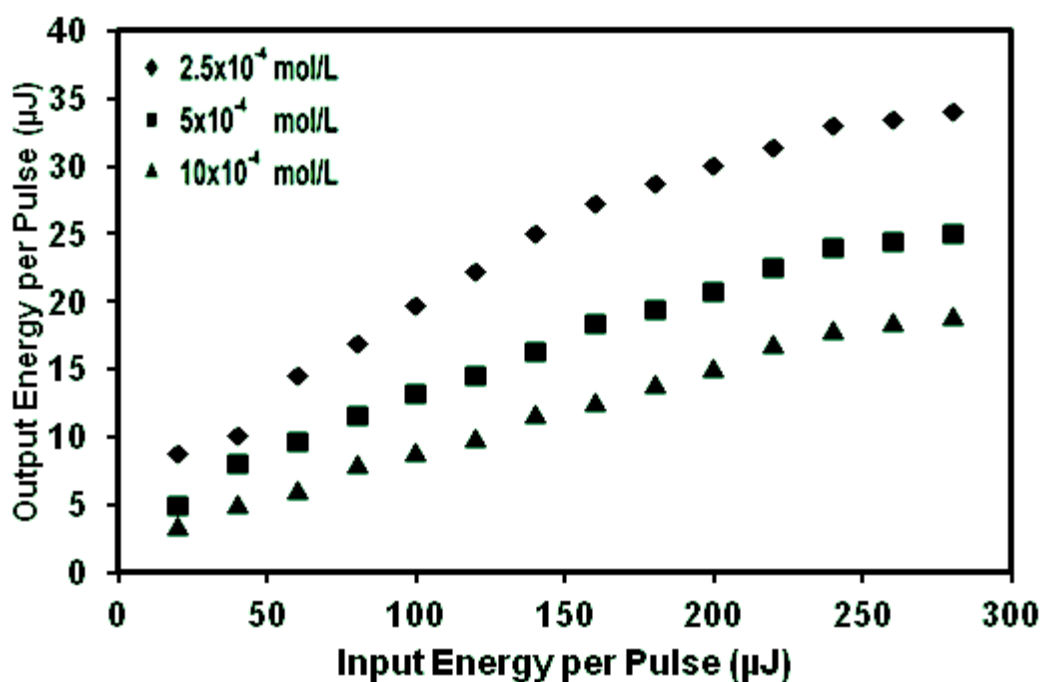


Figure 5.16 Optical power limiting behavior of ruthenium complex RuL4 in solution form at various concentrations indicated in the inset

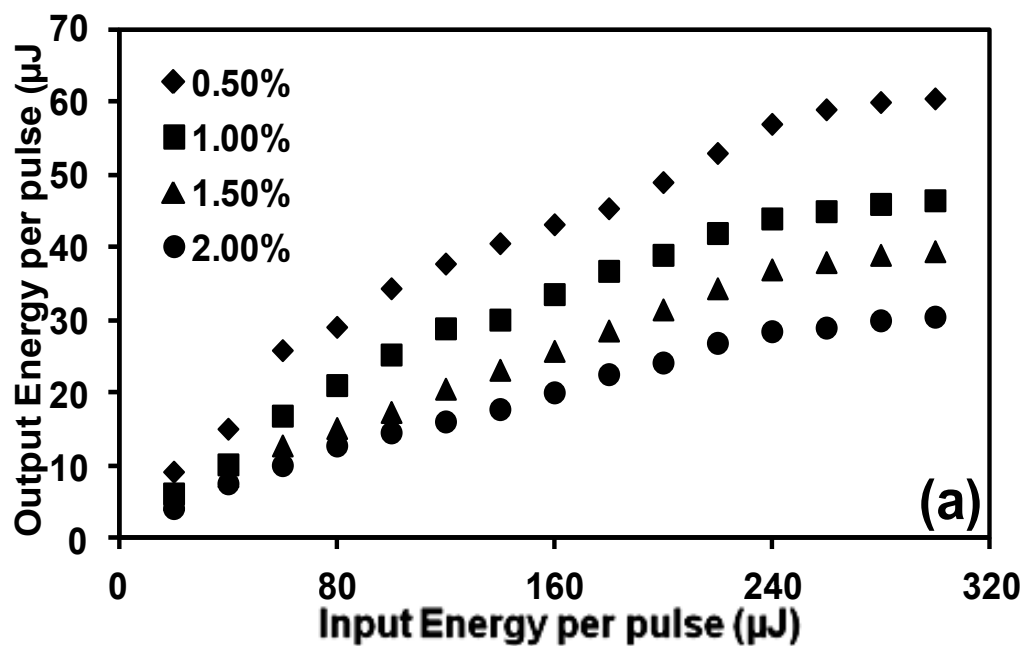


Figure 5.17 Optical power limiting behavior of ruthenium complex RuL3 in film form at various concentrations indicated in the inset

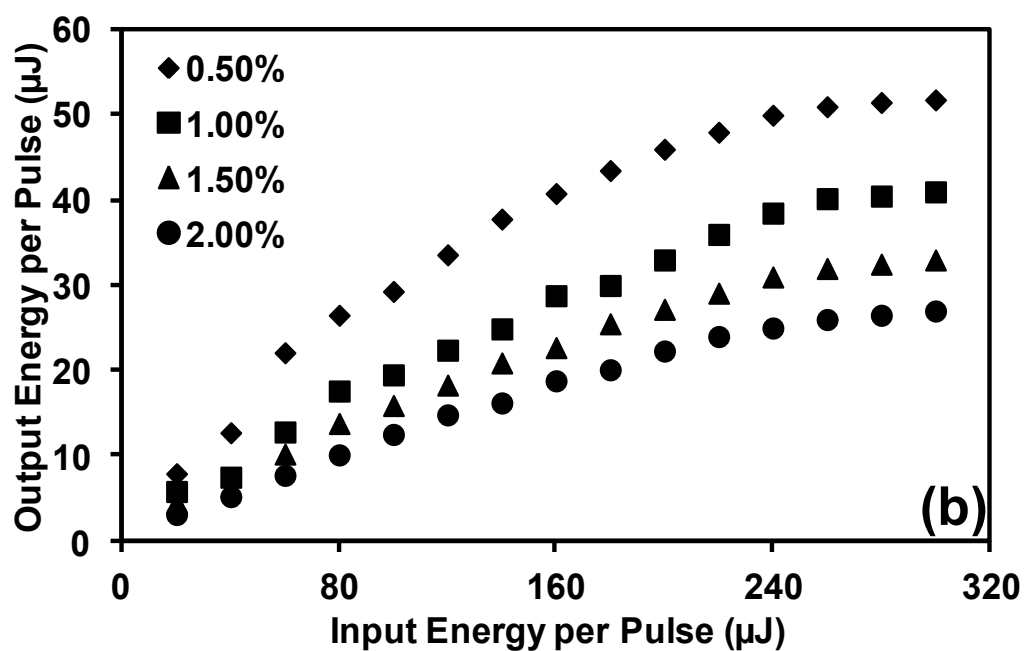


Figure 5.18 Optical power limiting behavior of ruthenium complex RuL4 in film form at various concentrations indicated in the inset

Table 5.6 Optical limiting threshold and clamped output energy of the ruthenium complexes in solution form at different concentrations

Sample	Concentrations (x 10 ⁻³ mol/L)	Optical limiting threshold (μJ)	Clamped output energy (μJ)
RuL3	0.25	135	48
	0.5	120	38
	1	110	30
RuL4	0.25	120	34
	0.5	100	24
	1	80	18

Table 5.7 Optical limiting threshold and clamped output energy of the ruthenium complexes doped in film form at different dopant concentrations

Sample	Dopant Concentrations (wt.%)	Optical limiting threshold (μJ)	Clamped output energy (μJ)
RuL3	0.5	100	60
	1.0	80	46
	1.5	60	39
	2.0	40	30
RuL4	0.5	80	52
	1.0	80	41
	1.5	60	32
	2.0	40	26

5.8 CONCENTRATION DEPENDENCE OF THIRD-ORDER NONLINEARITY

Concentration dependence of β_{eff} can be analyzed to extract information on the NLO properties of the solute. The concentrations of the two complexes in solution and film were varied and Z-scan and optical power limiting were repeated on solutions and films at each concentration to study the variation of nonlinear response and power limiting ability. Figures 5.19 and 5.20 show the dependence of nonlinear absorption (β_{eff}) on the concentration of RuL3 and RuL4 in solution and film form. The NLA decreased as the concentration in solution decreased from 1×10^{-3} mol/L to 0.25×10^{-3} mol/L in solution form and 2.0 wt.% to 0.5 wt.% in film form. Thus the observed decrease in the nonlinear response has direct correlation with the concentration of the organic samples.

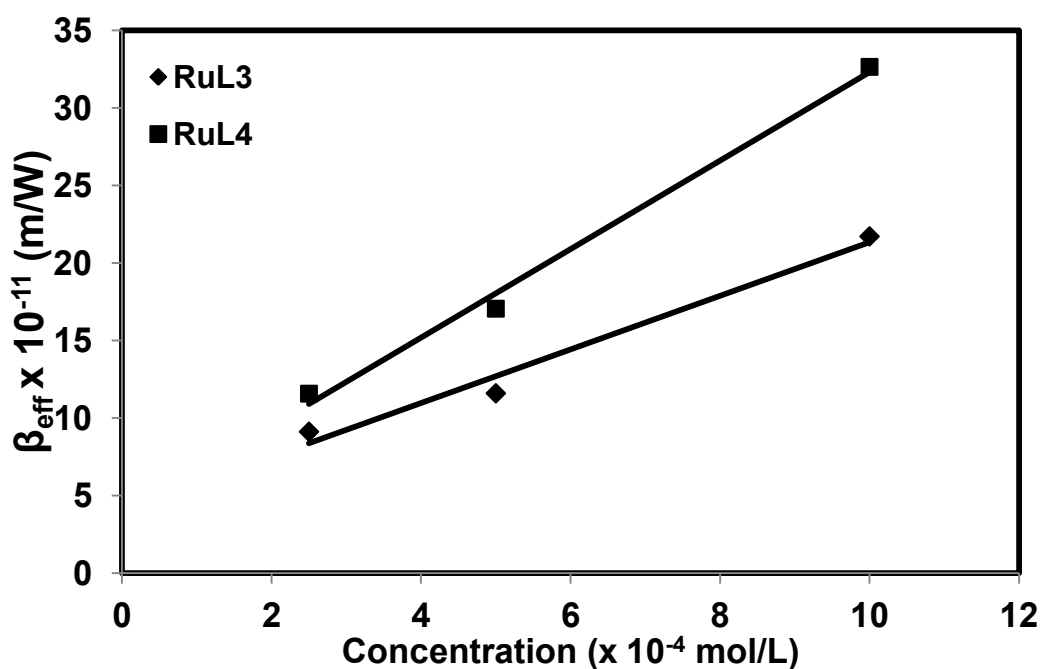


Figure 5.19 Concentration dependent nonlinear absorption coefficient (β_{eff}) of RuL3 and RuL4 in solution form

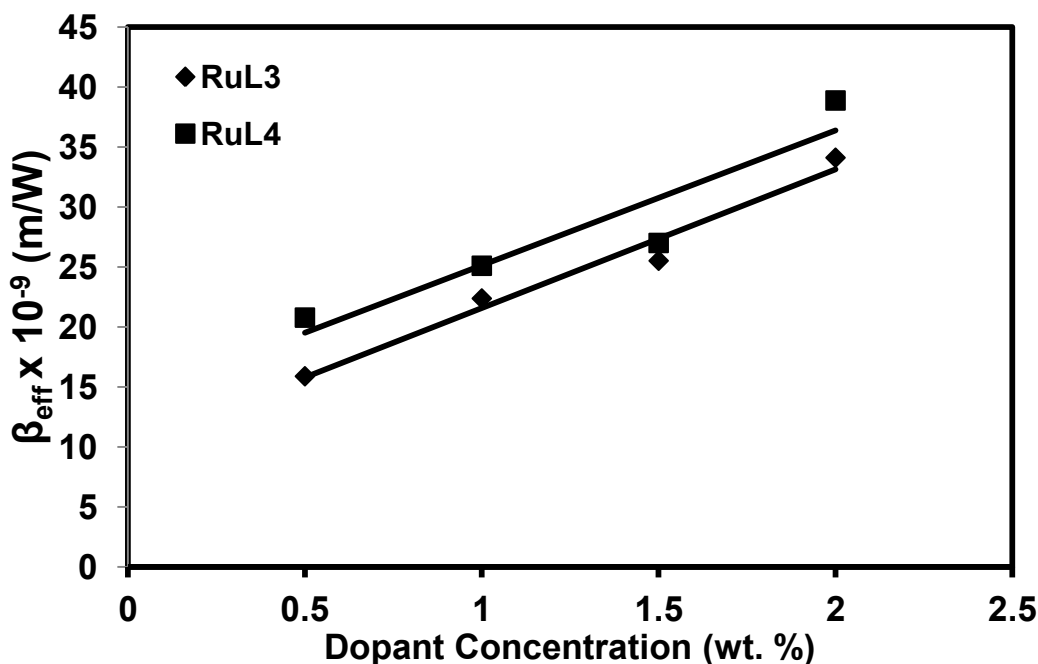


Figure 5.20 Concentration dependent nonlinear absorption coefficient (β_{eff}) in RuL3 and RuL4 film form

5.9 ALL-OPTICAL SWITCHING STUDIES OF RUTHENIUM COMPLEXES

The laser pulse shapes recorded in the pump-probe experiments on switching action of our sample films are shown in Figures 5.21 and 5.22. The upper curves are the pulse shape of pump beam at different intensities (a) 5 GW/cm², (b) 10 GW/cm² and (c) 15 GW/cm² whereas lower curves show the output signal shape of probe beam at corresponding pump intensities. When the pump pulse from the Nd: YAG laser passes through the sample, the output intensity of the probe beam from the He-Ne laser gets reduced drastically (OFF-state). When the pump pulse is turned off, the output probe beam regains its full intensity (ON-state). Thus, the CW He-Ne laser beam passing through the sample film can be switched ON and OFF by the 7 ns Q-switched Nd: YAG laser of 532 nm wavelength (Abdeldayem et al. 2003).

The physical mechanism responsible for all-optical switching is that, when the pump pulse passes through the sample, the population of the triplet state T_1 increases, which results in strong absorption of the probe He-Ne beam thereby, reducing its transmission. After the pump pulse crosses the sample, the population of the triplet

state drops drastically and the He-Ne laser output regains the original transmission value. The modulation of the probe intensity calculated for ruthenium complexes are given in Table 5.8. The strength of modulation of the probe increases as the intensity of the pump beam increases, which is due to the increase in the population of triplet state (Singh et al. 2005). The switching times are seen to be in the range of few microseconds. The relaxation of the triplet state to the ground state is forbidden, resulting in slow switching time of the molecules (Henari 2001).

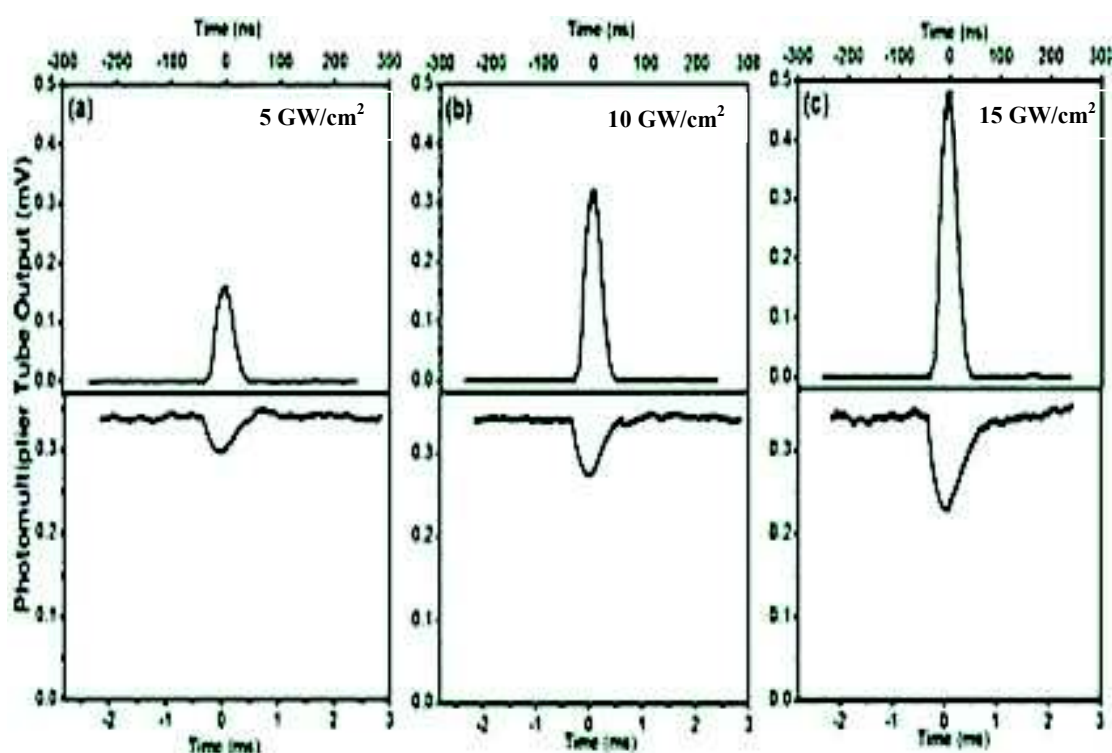


Figure 5.21 All-optical switching signal for RuL3 (Conc. 1.0 wt.%) with varying pump beam intensities (a) 5 GW/cm², (b) 10 GW/cm² and (c) 15 GW/cm². The upper curves show the pulse shape of the Nd: YAG laser beam used, whereas the lower curves show the signal wave form of the probe He-Ne laser beam.

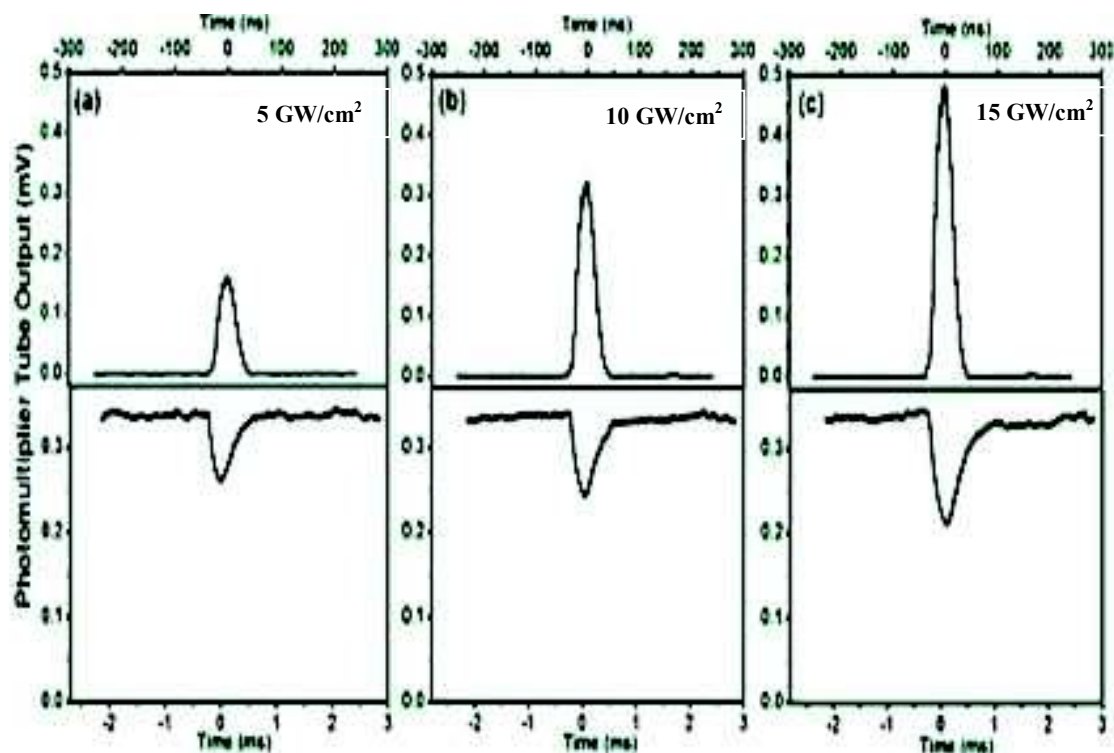


Figure 5.22 All-optical switching signal for RuL4 (Conc. 1.0 wt.%) with varying pump beam intensities (a) 5 GW/cm², (b) 10 GW/cm² and (c) 15 GW/cm². The upper curves show the pulse shape of the Nd: YAG laser beam used, whereas the lower curves show the signal wave form of the probe He-Ne laser beam.

Table 5.8 Fall time, rise time, FWHM and modulation of probe beam of RuL3 and RuL4 at different pump intensities

Sample	Intensity (GW/cm ²)	Fall Time (T _f) (μs)	Rise Time (T _r) (μs)	FWHM (μs)	Modulation of probe beam %
RuL3	5	181	388	491	12
	10	197	367	499	20
	15	205	488	608	33
RuL4	5	136	389	354	23
	10	177	395	425	29
	15	212	485	515	38

5.10 CONCLUSIONS

In summary, the third-order nonlinear optical properties of the ruthenium metal-organic complexes were investigated by employing the nanosecond Z-scan and DFWM technique. Z-scan results indicate that the ruthenium complexes possess negative nonlinear refraction. The operating nonlinear mechanism, leading to optical power limiting, was found to be reverse saturable absorption. The real and imaginary parts of third-order nonlinear optical susceptibility were of the order of 10^{-11} esu. Results indicate that the complexes exhibit good optical power limiting and switching behavior of nanosecond laser pulses at 532nm wavelength. The reverse saturable absorption was the leading mechanism of optical power limiting and all-optical switching. Among the investigated ruthenium complexes, RuL4 exhibits good NLO response compared to other ruthenium complex RuL3. Hence, the ruthenium metal-organic complexes investigated here are potential candidates for new photonic and optoelectronic applications.

CHAPTER 6

CHAPTER 6

SUMMARY AND CONCLUSIONS

6.1 SUMMARY AND CONCLUSIONS

We have investigated third-order nonlinear optical characteristics, optical power limiting and all-optical switching properties of novel organo-metallic complexes containing (i) palladium and (ii) ruthenium metal ions; over all 8 complexes have been studied. Z-scan and DFWM experiments were performed to determine third-order nonlinear optical susceptibility of these metal complexes. The optical power limiting properties of the metal complexes were evaluated by measuring the transmission of laser light as a function of the laser power. All-optical switching capability of these metal complexes was investigated using the standard pump-probe technique.

The compounds synthesised for our studies have some distinct advantages. The substitution of heavy metal (Pd and Ru) into the π -conjugated structure of ligand, significantly improves the electron donor-acceptor strength of palladium and ruthenium metal complexes. These metal-organic complexes are easy to synthesise. They are nonreactive with PMMA matrix and the solvent used for preparing solution. Hence, they can be easily doped into solid PMMA films. We find that these materials are suitable for making optical devices in the solid state film form.

6.1.1 Palladium metal-organic complexes

Four different palladium metal-organic complexes were synthesized and their NLO properties were studied. The nonlinear optical properties of the complexes with varying functional group were also studied. It is observed that as the electron donor strength of the complex increases, the nonlinearity also increases. The NLO results also show that the complex, with donor substituent, shows better NLO activity compared to the complex with acceptor substituent. The strength of NLO response is

least for complex with NO₂, and increases progressively for Cl (electron acceptor), H (electron donor) and OCH₃ (electron donor). This indicates the influence of molecular structure on the observed NLO properties.

The observed nonlinear absorption is explained using five-level model. Large nonlinear absorption due to reverse saturable absorption (RSA). Consequently, these samples exhibit good optical power limiting property. All-optical switching behaviour was observed with these complexes using nanosecond pump beam. The concentration dependence of third-order NLO properties of palladium complexes has also been studied.

Among the four investigated palladium metal-organic complexes, complex with strong donor (OCH₃) exhibited largest NLO properties. The $\chi^{(3)}$ and γ_h values of palladium complexes are two order larger than those of orthogonal-tetrathiafulvalene-based Pd complex (Iliopoulos et al. 2010) and also are well comparable with those of Schiff-base derived Pd complex (Zhang 2011).

6.1.2 Ruthenium metal-organic complexes

The four ruthenium metal-organic complexes with different substituents were synthesized and their NLO properties were investigated. The different substituents resulted in changes in π -conjugation length and electron delocalization. Third-order NLO properties of the complexes were studied for the different ligand environments. Ruthenium complexes show RSA as the mechanism for nonlinearity. Large nonlinear absorption leads to strong optical power limiting of nanosecond laser pulses at 532 nm wavelength. All-optical switching behavior was observed in these complexes using nanosecond pump beam. The variation of third order NLO properties of these complexes with dopant concentration was also studied. The large optical nonlinearities observed in these materials is ascribed to the nature of bonding of ruthenium and coordinated ligands. The correlation of the molecular structure and π -conjugation with NLO properties is also discussed.

From the present study we concluded that the nature of charge-transfer in the metal-organic materials determines the magnitude of their NLO response. The magnitude of $\chi^{(3)}$ is of the order of 10^{-11} esu. The excited state absorption cross-

section (σ_{exc}) was seen to be greater than ground state absorption cross-section (σ_{g}) for all investigated samples indicating that the operating mechanism for optical nonlinearity is reverse saturable absorption. We, therefore conclude that these metal-organic complexes exhibit all-optical switching and optical power limiting of 7 ns laser pulses at 532 nm wavelength due to reverse saturable absorption mechanism. The values of $\chi^{(3)}$ varied from 9.4×10^{-11} esu for RuL1 to 2.8×10^{-10} esu for RuL4. The magnitude of nonlinear refractive index n_2 varied from 2.6×10^{-9} esu for RuL1 to 1.1×10^{-8} esu for RuL4.

Amongst the metal-organic complexes investigated, the sample RuL4 exhibited better NLO and optical power limiting properties compared to the other metal-organic complexes investigated by us. The magnitude of the nonlinear refractive index n_2 was of the order of 10^{-9} esu and nonlinear absorption β_{eff} was of the order of 10^{-9} m/W which is two orders larger than that of the zinc-phthalocyanines in polymeric matrix (Ostuni et al. 2007), a widely studied material. The threshold input energy for onset of optical limiting for RuL4 is 40 μJ and the clamped output energy value for it is 22 μJ . As the concentration increases the limiting threshold and clamping levels decrease for all the investigated metal-organic complexes.

Clearly the palladium and ruthenium metal-organic compounds investigated by us are promising materials for new photonic devices.

6.2 SCOPE FOR FUTURE WORK

The present research investigations can be further extended in the following directions,

- Present measurements were performed using the nanosecond laser pulses regime. This can be extended to picosecond and femtosecond laser pulses.
- Current NLO and optical power limiting measurements were carried out using pulsed lasers. One can study the optical power limiting property using continuous wave lasers (CW-lasers).
- The studies presented here were limited to PMMA as a host material and palladium and ruthenium-metal organics were the guest molecules. This can

extended to the other host systems such as PUA, PVA, epoxy compound, glass etc. The most appropriate host material could be identified.

- Palladium and ruthenium-metal organics were studied at the wavelength of 532 nm. The measurements can be performed at different wavelengths to examine their suitability for devices at wavelengths.
- Optimization of the material and physical characteristics should be carried out to arrive at best devices performance.

In summary, the field of Nonlinear Optics has been a very active area for many researchers and continues to attract the interest of many more. As stated in the beginning, the present century is expected to be the era of Photonics. We look forward to making further contributions to make this dream comes true.

REFERENCES

REFERENCES

- Abdeldayem, H., Frazier, D. O. and Paley, M. S. (2003). "An all-optical picosecond switch in polydiacetylene." *Appl. Phys. Lett.*, 82(7), 1120–1122.
- Akhmanov, S. A. and Khokhlov, R. V. (1972). *Problems of Nonlinear Optics*. Gordon and Breach, New York.
- Almeida, V. R., Barrios, C. A., Panepucci, R. R. and Lipson, M. (2004). "All-optical control of light on a silicon chip." *Nature*, 431(7012), 1081–1084.
- Amirnasr, M., Schenk, K. J., Gorji, A. and Vafazadeh, R. (2001). "Synthesis and spectroscopic characterization of [CoIII(salophen)(amine)₂]ClO₄ (amine=morpholine, pyrrolidine, and piperidine) complexes. The crystal structures of [CoIII(salophen)(morpholine)₂]ClO₄ and [CoIII(salophen)(pyrrolidine)₂]ClO₄." *Polyhedron*, 20(7), 695-702.
- Asma, A., Badshah, S., Ali, M., Sohail, M., Fettouhi, S. Ahmad. and Malik, A. (2006). "Synthesis, Characterization of Mixed Ligand Palladium(II) Complexes of Triphenylphosphine and Anilines and their Enzyme Inhibition Studies against β -glucuronidase. The Crystal Structure of *trans* -dichloro-(*m*-chloroaniline) (triphenylphosphine) palladium(II)." *Transition Met. Chem.*, 31, 556-559.
- Auger, A., Blau, W. J., Burnham, P. M., Chambrier, I., Cook, M. J., Isare, B., Nekelson, F. and O'Flaherty, S. M. (2003). "Nonlinear absorption properties of some 1,4,8,11,15,18,22,25-octaalkylphthalocyanines and their metallated derivatives." *J. Mater. Chem.*, 13(5), 1042-1047.
- Bahae, S M., Said, A.A., and Vanstyland, E.W. (1989). "High-sensitivity, single-beam n₂ measurements." *Opt. Lett.*, 14(17), 955-957.
- Bahae, S. M. and Hasselbeck, M. P. (2000). "Third-order optical nonlinearities." *Handbook of Optics, Optical Society of America*.

- Bahae, S. M., Said, A.A., Wei, T.H., Hagan, D.J and Vanstynland, E.W. (1990). "Sensitive Measurement of Optical Nonlinearities Using a Single Beam." *IEEE J. Quantum Electron.*, 26(4), 760-769.
- Bahtiar, A., Koynov, K., Mardiyati, Y. Horhold, H. H. and Bubeck, C. (2009). "Slab waveguides of poly (p-phenylenevinylene) s for all-optical switching: impact of side-chain substitution." *J. Mater. Chem.*, 19 (40), 7490-7497.
- Band, Y. B., Harter, D. J. and Bavli, R. (1986). "Optical pulse compressor composed of saturable and reverse saturable absorbers." *Chem. Phys. Lett.*, 126(3), 280-284.
- Bass, M., Enoch, J.M., Stryland, E.W.V. and Wolfe, W.L. (2001). "Handbooks of Optics IV, Fiber Optics and Nonlinear Optics", 2nd ed. *McGraw-Hill*, New York.
- Bella S. D., Fragalà, I., Ledoux, I. and Marks, T. J. (1995). "Role of Metal Electronic Properties in Tuning the Second-Order Nonlinear Optical Response of Coordination Complexes. A Combined Experimental and Theoretical Investigation of a Homologous Series of (N, N'-Disalicylidene-1,2-phenylenediaminato)M(II) (M = Co, Ni, Cu) Complexes." *J. Am. Chem. Soc.*, 117(37), 9481–9485.
- Bella, S. D. (2001). "Second-order nonlinear optical properties of transition metal complexes." *Chem. Soc. Rev.*, 30(6), 355–366.
- Bella, S. D. and Fragalà, I. (2000). "Synthesis and second-order nonlinear optical properties of bis(salicylaldiminato)M(II) metalloorganic materials." *Synth. Met.*, 115(1), 191–196.
- Bella, S. D., Fragalà, I., Ledoux, I., Diaz-Garcia, M. A. and Marks, T. J. (1997). "Synthesis, Characterization, Optical Spectroscopic, Electronic Structure, and Second-Order Nonlinear Optical (NLO) Properties of a Novel Class of Donor–Acceptor Bis(salicylaldiminato)nickel(II) Schiff Base NLO Chromophores." *J. Am. Chem. Soc.*, 119(40), 9550–9557.

- Bella, S. D., Fragalà, I., Marks, T. J. and Ratner, M. A. (1996). "Large Second-Order Optical Nonlinearities in Open-Shell Chromophores. Planar Metal Complexes and Organic Radical Ion Aggregates." *J. Am. Chem. Soc.*, 118(50), 12747–12751.
- Benson, M. T., Cundari, T. R., Lim, S. J., Nguyen, H. D. and Beaver, K. P., (1994). "An Effective Core Potential Study of Transition-Metal Chalcogenides. 1. Molecular Structure." *J. Am. Chem. Soc.*, 116 (9), 3955–3966.
- Blau, M., Hales, J., Hagan, D. J. and Van Stryland, E. W. (2004). "White-light continuum z-scan technique for nonlinear materials characterization," *Opt. Express*, 12 (16), 3820-3826.
- Blau, W. J., Byrne, H. J., Cardin, D. J. and Davey, A. P. (1991). "Non-linear optical properties of Group 10 metal alkynyls and their polymers." *J. Mater. Chem.*, 1, 245-249.
- Bloembergen N. (1964). *Nonlinear Optics*. Benjamin, New York.
- Bloembergen, N. (1980). "Conservation laws in nonlinear optics." *J. Opt. Soc. Am.*, 70(12), 1429-1436.
- Bogdan, A. R., Prior, Y. and Bloembergen, N. (1981). "Pressure-induced degenerate frequency resonance in four-wave light mixing." *Opt. Lett.*, 6(2), 82-83.
- Booth, J., Craig, P. J., Dobbs, B., Pratt, J. M., Randall, G. L. P. and Williams, A. G. (1971). "Macrocyclic Derivatives of Cobalt including Some New Organometallic Complexes." *J. Chem. Soc. (A)*, 1964-1968.
- Butcher, P. N. and Cotter, D. (1990). *The elements of nonlinear optics*. Cambridge University Press, Cambridge.
- Caro, R. G. and Gower, M. C. (1982). "Phase conjugation by degenerate four-wave mixing in absorbing media." *IEEE J. Quantum Electron.*, 18(9), 1376-1380.

- Cassano, T., Tommasi, R., Meacham, A. P. and Ward, M. D. (2005). "Investigation of the excited-state absorption of a Ru dioxolene complex by the Z-scan technique." *J. Chem. Phys.*, 122, 154507.
- Casstevens, M. K., Samoc, M., Pflieger, J. and Prasad, P. N. (1990). "Dynamics of third-order nonlinear optical processes in Langmuir–Blodgett and evaporated films of phthalocyanines." *J. Chem. Phys.*, 92(3), 2019-2024.
- Chandrasekhar, V., Azhakar, R., Murugesapandian, B., Senapati, T., Bag, P., Pandey, M. D., Maurya, S. K. and Goswami, D. (2010). "Synthesis, Structure, and Two-Photon Absorption Studies of a Phosphorus-Based Tris Hydrazone Ligand (S)P[N(Me)N=CH-C₆H₃-2-OH-4-N(CH₂CH₃)₂]₃ and Its Metal Complexes." *Inorg. Chem.*, 49(9), 4008–4016.
- Chao, H., Li, R. H., Ye, B. H., Li, H., Feng, X. L., Cai, J. W., Zhou, J. Y. and Ji, L. N. (1999). "Syntheses, characterization and third order non-linear optical properties of the ruthenium(II) complexes containing 2-phenylimidazo[4,5-*f*][1,10]phenanthroline derivatives." *Chem. Soc., Dalton Trans.*, (21), 3711-3717.
- Chapple, P. B., Staromlynska, J., Hermann, J. A., Mckay, T. J. and Mcduff, R. G. (1997). "Single-Beam Z-Scan: Measurement Techniques and Analysis", *J. Nonlinear Opt. Phys. Mater.*, 6(3), 251-293.
- Charas, A., Mendonça, A. L., Clark, J., Bazzana, L., Nocivelli, A., Lanzani, G. and Morgado, J. (2011). "Stimulated emission and ultrafast optical switching in a ter(9,9'-spirobifluorene)-co-methylmethacrylate copolymer." *J. Polym. Sci., B, Polym. Phys.*, 49(1), 52–61.
- Chemla, D. S. and Zyss, J. (1987). *Nonlinear Optical Properties of Organic Molecules and Crystals*, Academic Press, New York.
- Chen, J., Ren, Q., Wang, X., Li, T., Yang, H., Zhang, J. and Li., G. (2012). "Third order nonlinear optical properties of ethyltriphenylphosphonium bis(2-thioxo-1,3-dithiole-4,5-dithiolato)aurate (III)." *Optik*, 123(19), 1761-1764.

- Chen, Q., Kuang, L., Sargent, E. H. and Wang, Z. Y. (2003). "Ultrafast nonresonant third-order optical nonlinearity of fullerene-containing polyurethane films at telecommunication wavelengths." *Appl. Phys. Lett.*, 83(11), 2115-2117.
- Chen, Y. -C., Raravikar, N. R., Schadler, L. S., Ajayan P. M., Zhao, Y. -P., Lu, T. -M., Wang, G. -C., Wang and Zhang, X. -C. (2002). "Ultrafast optical switching properties of single-wall carbon nanotube polymer composites at 1.55 μm ." *Appl. Phys. Lett.*, 81(6), 975-977.
- Chen, Y., Hanack, M., Araki, Y. and Ito, O. (2005). "Axially modified gallium phthalocyanines and naphthalocyanines for optical limiting." *Chem. Soc. Rev.*, 34(6), 517-529.
- Cheng, L. T., Tam, W., Meredith, G. R. and Marder, S. R. (1990). "Quadratic Hyperpolarizabilities of Some Organometallic Compounds." *Mol. Cryst. Liq. Cryst.*, 189(1), 137-153.
- Cheng, W. -D., Wu, D. -S., Zhang, H. and Chen, J. -T. (2001). "Electronic structure and spectrum third-order nonlinear optics of the metal phthalocyanines $\text{PcM}(\text{M}=\text{Zn}, \text{Ni}, \text{TiO})$." *Phys. Rev. B*, 64, 125109-125120.
- Cifuentes, M. P. and Humphrey, M. G. (2004). "Alkynyl compounds and nonlinear optics." *J. Organomet. Chem.*, 689(24), 3968–3981.
- Costes, J. C., Lamère, J. F., Lepetit, C., Lacroix, P. G. and Dahan, F. (2005). "Synthesis, Crystal Structures, and Nonlinear Optical (NLO) Properties of New Schiff-Base Nickel(II) Complexes. Toward a New Type of Molecular Switch?" *Inorg. Chem.*, 44 (6), 1973–1982.
- Cui, Y., Zhao, M., He, G. S. and Prasad, P. N. (1991). "Dynamic characteristics of coherent and population grating processes in resonant degenerate four-wave mixing." *J. Phys. Chem.*, 95(18), 6842-6848.
- Dai, J., Bian, G. Q., Wang, X., Xu, Q. F. and Zhou, M. Y. (2000). "A New Method to Synthesize Unsymmetrical Dithiolene Metal Complexes of 1, 3-Dithiole-2-

- thione-4,5-dithiolate for Third-Order Nonlinear Optical Applications.” *J. Am. Chem. Soc.*, 122(44), 11007- 11008.
- Das, S. Nag, A., Goswami, D. and Bharadwaj, P. K. (2006). "Zinc(II)- and Copper(I)- Mediated Large Two-Photon Absorption Cross Sections in a Bis-cinnamaldiminato Schiff Base." *J. Am. Chem. Soc.*, 128(2), 402–403.
- Dasari, R. R., Sartin, M. M., Cozzuol, M., Barlow, S., Perry, J. W. and Marder, S. R. (2011). “Synthesis and linear and nonlinear absorption properties of dendronised ruthenium(II) phthalocyanine and naphthalocyanine.” *Chem. Commun. (Camb.)*, 47(15), 4547–4549.
- Davison, A., Edelstein, N., Holm, R. H. and Maki, A. H. E. (1963). “The Toluenedithiolate and Maleonitriledithiolate Square-Matrix Systems.” *J. Am. Chem. Soc.*, 85(13), 2029-2030.
- Deng, Y., Xu, Y., Lin, L., Qian, W., Xia, Z., Teo, B. K. and Zou, Y. (2000). “Heterodyned femtosecond optical Kerr effect of silver phenylacetylide complex.” *J. Mater. Sci. Lett.*, 19(7), 549-551.
- Dileep, R. and Bhat, B. R. (2010). “Palladium – Schiff base – triphenylphosphine catalyzed oxidation of alcohols.” *Appl. Organometal. Chem.*, 24(9), 663–666.
- Dini, D. and Hanack, M. (2003). “Physical properties of phthalocyanine-based materials.” *The Porphyrin Handbook: Phthalocyanines: Properties and Materials*, K.M. Kadish, K.M. Smith and R. Guilard, eds., Academic Press, New York.
- Dini, D., Barthel, M. and Hanack, M. (2001). “Phthalocyanines as Active Materials for Optical Limiting.” *Eur. J. Org. Chem.*, 2001(20), 3759-3769.
- Dini, D., Barthel, M., Schneider, T., Ottmar, M., Verma, S. and Hanack, M. (2003). “Phthalocyanines and related compounds as switchable materials upon strong

- irradiation: the molecular engineering behind the optical limiting effect.”*Solid State Ionics*, 165(1), 289-303.
- Dini, D., Hanack, M. and Meneghetti, M. (2005). “Nonlinear Optical Properties of Tetrapyrazinoporphyrazinato Indium Chloride Complexes Due to Excited-State Absorption Processes.” *J. Phys. Chem. B.*, 109(26), 12691-12696.
- Eichler, H. J. (1977). “Laser-induced Grating Phenomena.” *Opt. Acta.*, 24(6), 631-642.
- Eichler, H. J., Gunter, P. and Pohl, D. W. (1986). *Laser-induced Dynamic grating*, Springer, Berlin.
- Eimerl, D. (1987). "Electro-optic, linear, and nonlinear optical properties of KDP and its isomorphs." *Ferroelectrics*, 72(1), 95-139.
- Erlacher, A., Miller, H. and Ullrich, B. (2004). “Low-power all-optical switch by superposition of red and green laser irradiation in thin-film cadmium sulfide on glass.” *J. Appl. Phys.*, 95, 2927-2929.
- Espinoza, E. G. M., Sanchez-Montes, K. E., Klimova, E., Klimova, T., Lijanova, I. V., Maldonado, J. L., Ramos-Ortíz, G., Hernández-Ortega, S. and Martínez-García, M. (2010). “Dendrimers Containing Ferrocene and Porphyrin Moieties: Synthesis and Cubic Non-Linear Optical Behavior.” *Molecules*, 15(4), 2564-2575.
- Evans, O. R. and Lin, W. (2002). "Crystal Engineering of NLO Materials Based on Metal–Organic Coordination Networks." *Acc. Chem. Res.*, 35 (7), 511–522.
- Eyring, G. and Fayer, M. D. (1984). “A picosecond holographic grating approach to molecular dynamics in oriented liquid crystal films.” *J. Chem. Phys.*, 81(10), 4314-4321.
- Fan, Y. T., Xue, D. X., Li, G., Hou, H. W., Du, C. X. and Lu, H. J. (2004). “Synthesis, crystal structures, and third-order nonlinear optical properties of two

- novel complexes of H₄edbbp with Zn(II), Cd(II).” *J. Mol. Struct.*, 707 (1) 153-160.
- Feuvrie, C., Maury, O., Bozec, H. L., Ledoux, I., Morrall, J. P., Dalton, G. T., Samoc, M. and Humphrey, M. G. (2007). “Nonlinear Optical and Two-Photon Absorption Properties of Octupolar Tris(bipyridyl) metal Complexes.” *J. Phys. Chem. A.*, 111, 8980-8985.
- Fisher, R. (1983). *Optical Phase Conjugation*, Academic Press, New York.
- Fourkas, J. T., Trebino, R. and Fayer, M. D. (1992). “The grating decomposition method: A new approach for understanding polarization-selective transient grating experiments. I. Theory.” *J. Chem. Phys.*, 97(1), 69-77.
- Fourkas, J. T., Trebino, R. and Fayer, M. D. (1992). “The grating decomposition method: A new approach for understanding polarization-selective transient grating experiments. II. Applications.” *J. Chem. Phys.*, 97(1), 78-85.
- Fourmigue, M. (2004). “Paramagnetic Cp/Dithiolene Complexes as Molecular Hinges: Interplay of Metal/Ligand Electronic Delocalization and Solid-State Magnetic Behaviour.” *Acc. Chem. Res.* 37(3), 179-186.
- Franken, P. A., Hill, A. E., Peters, C. W. and Weinreich, G. (1961). “Generation of Optical Harmonics.” *Phys. Rev. Lett.*, 7(4), 118–119.
- Frazier, C. C., Guha, S., Chen, W. P., Cockerham, M. P. and Porter, P. L. (1987). “Third-order optical non-linearity in metal-containing organic polymers.” *Polymer*, 28(4), 553–555.
- Freire, C. and de Castro, B. (1998). “Epr characterisation of nickel (III) complexes with N₂O₂ Schiff base ligands derived from naphthaldehyde and their pyridine adducts.” *Polyhedron*, 17(23), 4227–4235.

- Freire, C. and de Castro, B. (1998). "Spectroscopic characterisation of electrogenerated nickel(III) species. Complexes with N₂O₂ Schiff-base ligands derived from salicylaldehyde." *J. Chem. Soc., Dalton Trans.*, (9), 1491–1498.
- Friberg, S. R. and Smith, P. W. (1987). "Nonlinear *Optical* Glasses for Ultrafast *Optical Switches*." *IEEE J. Quantum Electron.*, QE-23, 2089–2094.
- Ganeev, R. A., Ryasnyansky, A.I., Kodirov, M. K., Kamalov, S. R., Tugushev, R. I. and Usmanov, T. (2002). "Optical limiting in cobalt-doped polyvinylpyrrolidone." *Appl. Phys. B: Lasers Opt.*, 74(1), 47-51.
- Garcia M. A. D, Cabrera, J. M., Agullo'-Lo'pez, F., Duro, J. A., de la Torre, G., Torres, T., Ferna'ndez-La'zaro, F., Delhaes, P. and Mingotaud, C. (1996). "Third-order nonlinear optical susceptibilities of the Langmuir–Blodgett films of octa-substituted metallophthalocyanines." *Appl. Phys. Lett.*, 69 (3), 293-295.
- Gatri, R., Fillaut, J. -L., Mysliwicz, J., Szukalski, A., Bartkiewicz, S., El-Ouazzani, H., Guezguez, I., Khammar, F. and Sahraoui, B. (2012). "Synthesis and characterization of azo-containing organometallic thin films for all optical switching applications." *Chem. Phys. Lett.*, 535, 106-110.
- Gaudry, J. -B., Capes, L., Langot, P., Marcén, S., Kollmannsberger, M., Lavastre, O., Freysz, E., Létard, J. -F. and Kahn, O. (2000). "Second-order non-linear optical response of metallo-organic compounds: towards switchable materials." *Chem. Phys. Lett.*, 324(5), 321–329.
- Ghosal, S., Samaoc, M., Prasad, P.N. and Tufariello, J.J. (1990). "Optical nonlinearities of organometallic structures: aryl and vinyl derivatives of ferrocene." *J.Phys. Chem.*, 94, 2847-2851.
- Ghoshal, S. K., Chopra, P., Singh, R. P., Swiatkiewicz, J. and Prasad, P. N. (1989). "Picosecond degenerate four-wave mixing study of nonlinear optical properties of the poly-*N*-vinyl carbazole: 2,4,7-trinitrofluorenone composite polymer photoconductor." *J. Chem. Phys.*, 90(9), 5078- 5081.

- Giuliano, C. and Hess, L. (1967). "Nonlinear absorption of light: Optical saturation of electronic transitions in organic molecules with high intensity laser radiation." *IEEE J. Quantum Electron.*, 3(8), 358-367.
- Goeppert-Mayer, M. (1931). "Über Elementarakte mit zwei Quantensprüngen." *Ann. Physik*, 9, 273-295.
- Gomes, A. S. L., Demenicis, L., Petrov, D.V., de Araújo, C. B., de Melo, C. P. and Maior, R. S. (1996). "Time-resolved picosecond optical nonlinearity and all-optical Kerr gate in poly (3-hexadecylthiophene)." *Appl. Phys. Lett.*, 69 (15), 2166-2168.
- Gong, Q., Sun, Y., Xia, Z., Zou, Y.H., Gu, Z., Zhou, X. and Qiang, D. (1992). "Nonresonant third-order optical nonlinearity of all-carbon molecules C₆₀." *J. Appl. Phys.*, 71, 3025-3026.
- Green, K. A., Cifuentes, M. P., Samoc, M. and Humphrey, M. G. (2011). "Metal Alkynyl Complexes as Switchable NLO Systems." *Coord. Chem. Rev.*, 255(21), 2530-2541.
- Green, M. L. H., Marder, S. R., Thompson, M. E., Bandy, J. A., Bloor, D., Kolinsky, P. V. and Jones, R. J. (1987). "Synthesis and structure of (cis)-[1-ferrocenyl-2-(4-nitrophenyl)ethylene], an organotransition metal compound with a large second-order optical nonlinearity." *Nature*, 330(6146), 360-362.
- Gu, B., Wang, Y. H., Peng, X. C., Ding, J. P., He, J. L. and Wang, H. T. (2004). "Giant optical nonlinearity of a Bi₂Nd₂Ti₃O₁₂ ferroelectric thin film." *Appl. Phys. Lett.*, 85 (17), 3687-3689.
- Gu, B., Yan, J., Wang, Q., He, J. L. and Wang H. T. (2004). "Z-scan technique for characterizing third-order optical nonlinearity by use of quasi-one-dimensional slit beams." *J. Opt. Soc. Am. B*, 21(5), 968-972.

- Guo, S. L., Xu, L. I., Wang, H. -T., You, X. -Z. and Ming, N.B. (2003). "Investigation of optical nonlinearities in Pd(po)₂ by Z-scan technique." *Optik*, 114(2), 58-62.
- Hache A. and Bougeois, M. (2000). "Ultrafast all-optical switching in a silicon-based photonic crystal." *Appl. Phys. Lett.*, 25, 4089–4092.
- Hagan, D. (2001). "Optical limiting." *Handbook of Optics: Fiber Optics and Nonlinear Optics*, M. Bass, eds., McGraw-Hill, New York.
- Hales, J. M. and Perry, J. W. (2008). "Organic and polymeric third-order nonlinear optical materials." *Introduction to organic electronic and optoelectronic materials and devices*, S.-S. Sun and L.R. Dalton, eds., CRC Press, Boca Raton, Florida.
- Hales, J. M., Matichak, J., Barlow, S., Ohira, S., Yesudas, K., Brédas, J. L., Perry, J. W. and Marder, S. R. (2010). "Design of polymethine dyes with large third-order optical nonlinearities and loss figures of merit." *Science*, 327(5972), 1485–1488.
- Hales, J. M., Zheng, S., Barlow, S., Marder, S. R. and Perry, J. W. (2006). "Bisdioxaborine polymethines with large third-order nonlinearities for all-optical signal processing." *J. Am. Chem. Soc.*, 128, 11362–11363.
- Halvorson C., Hays, A., Kraabel, B., Wu, R., Wudl, F. and Heeger, A. J. (1994). "A 160-Femtosecond Optical Image Processor Based on a Conjugated Polymer." *Science*, 265(5176), 1215-1216.
- Hanack, M., Schneider, T., Barthel, M., Shirk, J.S., Flom, S. R. and Pong, R. G. S. (2001). "Indium phthalocyanines and naphthalocyanines for optical limiting." *Coord. Chem. Rev.*, 219, 235-258.
- Haque S. A. and Nelson J. (2010). "Toward organic all-optical switching." *Science*, 327(5972), 1466–1467.

- Harbold, J. M., Ilday, F. O., Wise, F. W., Sanghera, J. S., Nguyen V. Q., Shaw, L. B. and Aggarwal I. D. (2002). "Highly nonlinear As-S-Se glasses for all-optical switching." *Opt. Lett.*, 27 (2), 119-121.
- Hari, M., Mathew, S., Nithyaja, B., Joseph, S. A., Nampoori, V. P. N. and Radhakrishnan, P. (2012). "Saturable and reverse saturable absorption in aqueous silver nanoparticles at off-resonant wavelength." *Opt. Quantum Electron.*, 43(1), 49–58.
- Hauer, J., Buckup, T. and Motzkus, M. (2007). "Pump-Degenerate Four Wave Mixing as a Technique for Analyzing Structural and Electronic Evolution: Multidimensional Time-Resolved Dynamics near a Conical Intersection." *Phys. Chem. A.*, 111(42), 10517-10529.
- He, G. S., Weder, C., Smith, P. and Prasad, P. N. (1998). "Optical power limiting and stabilization based on a novel polymer compound." *IEEE J. Quantum Electron.*, 34(12), 2279-2285.
- He, G., Zhu, J., Baev, A., Samoć, M., Frattarelli, D., Watanabe, N., Facchetti, A., Agren, H., Marks, T. and Prasad, P. N. (2011). "Twisted π -System Chromophores for All-Optical Switching." *J. Am. Chem. Soc.*, 133 (17), 6675-6680.
- He, G.S., Tan, L. S., Zheng, Q. and Prasad, P.N. (2008). "Multiphoton Absorbing Materials: Molecular Designs, Characterizations, and Applications." *Chem. Rev.*, 108 (4), 1245–1330.
- Henari, F. Z. (2001). "Optical switching in organometallic phythalocyanine." *J. Opt. A: Pure Appl. Opt.*, 3(3), 188–190.
- Henari, F. Z. and Cassidy, S. (2012). "Non-linear optical properties and all-optical switching of congo red in solution." *Optik*, 123(8), 711-714.

- Henari, F. Z., Blau, W. J., Milgrom, L. R., Yahioğlu, G., Philips, D. and Lacey, J. A. (1997). "Third-order optical non-linearity in Zn(II) complexes of 5,10,15,20-tetraarylethynyl-substituted porphyrins." *Chem. Phys. Lett.*, 267(3), 229-233.
- Hermann, J. A. (1984). "Beam propagation and optical power limiting with nonlinear media." *J. Opt. Soc. Am. B.*, 1(5), 729-736.
- Hiroiyuki S. (2002). *Hyper-structured molecules III: chemistry, physics and applications*, CRC Press.
- Hou, H. W., Meng, X. R., Song, Y. L., Fan, Y. T., Zhu, Y., Lu, H. J., Du, C. X. and Shao, W. H. (2002). "Two-Dimensional Rhombohedral Grid Coordination Polymers $[M(\text{bbbt})_2(\text{NCS})_2]_n$ (M = Co, Mn, or Cd; bbbt = 1,1'-(1,4-butanediyl) bis-1*H*-benzotriazole): Synthesis, Crystal Structures and Third-Order Nonlinear Optical Properties." *Inorg. Chem.*, 41(15), 4068-4075.
- Hrozhyk, U. A., Serak, S. V., Tabiryán, N. V., Hoke, L., Steeves, D. M. and Kimball, B. R. (2010). "Azobenzene liquid crystalline materials for efficient optical switching with pulsed and/or continuous wave laser beams." *Opt. Express*, 18(8), 8697-8704.
- Hu, L., Qin, J., Zhou, N., Meng, Y. -F., Xu, Y., Zuo, J. -L. and You, X. -Z. (2012). "Synthesis, characterization and optical properties of new metal complexes with the multi-sulfur 1,2-dithiolene ligand." *Dyes and Pigments*, 92(3), 1223-1230.
- Hu, X., Jiang, P., Ding, C., Yang, H. and Gong, Q. (2008). "Picosecond and low-power all-optical switching based on an organic photonic bandgap microcavity." *Nat. Photonics*, 2(3), 185-189.
- Hu, X., Wang, Y., Liu, Y., Cheng, B. and Zhang, D. (2004). "An optical switching in two dimensional Ce:BaTiO₃ nonlinear photonic crystal." *Opt. Commun.*, 237(4), 371-377.

- Huang, T., Hao, Z., Gong, H., Liu, Z., Xiao, S., Li, S., Zhai, Y., You, S., Wang, Q. and Qin, J. (2008). "Third order nonlinear optical properties of a new copper coordination compound: A promising candidate for all optical switching." *Chem. Phys. Lett.*, 451, 213-217.
- Huang, Y., Wu, S. -T. and Zhao, Y. (2004). "All-optical switching characteristics in bacteriorhodopsin and its applications in integrated optics." *Opt. Express*, 12(5), 895-906.
- Hughes, S. and Burzler, J. M. (1997). "Theory of Z-scan measurements using Gaussian-Bessel beams." *Phys. Rev. A.*, 56(2), R1103–R1106.
- Humphrey, J. and Kuciauskas, D. (2004). "Charge-Transfer States Determine Iron Porphyrin Film Third-Order Nonlinear Optical Properties in the near-IR Spectral Region." *J. Phys. Chem. B*, 108, 12016 -12023.
- Hursthouse, M. B., Karaulov, A. I., Oliver, S. N. and Kershaw, S. V. (1995). "Preparation, properties and crystal structures of new nickel(II) complexes of 1,2-asymmetrically substituted dithiolenes for third-order non-linear optical applications." *J. Chem. Soc., Dalton Trans.*, (4), 587-594.
- Hutchings, D. C. and Van Stryland, E.W. (1992). "Nondegenerate two-photon absorption in zinc blende semiconductors." *Opt. Soc. Am. B.*, 9(11), 2065-2074.
- Ikeda, T., Tsutsumi, O. and Sasaki, T. (1996). "Optical Switching and Image Storage by Means of Nematic Liquid Crystals and Ferroelectric Liquid Crystals." *Synth. Met.*, 81, 289-296.
- Iliopoulos, K., Czaplicki, R., El-Ouazzani, H., Balandier, J.Y., Chas, M., Goeb, S., Sallé, M., Gindre, D., Sahraoui, B (2010). "Physical origin of the third order nonlinear optical response of orthogonal pyrrolo-tetrathiafulvalene derivatives." *Appl. Phys. Lett.*, 97, 101104(1)- 101104(3).

- Jin, Z. J., Lan, Z. G., Xue, G. Y., Ping, L. X. and Ju, C. W. (2007). "All-optical switching and nonlinear optical properties of HBT in ethanol solution." *Chinese Phys.* 16(4), 1047-1051.
- Joseph, S. A., Sharma, G., Hari, M., Mathew, S., Radhakrishnan, P. and Nampoore, V. P.N. (2010). "Laser-induced Bessel beams can realize fast all-optical switching in gold nanosol prepared by pulsed laser ablation." *J. Opt. Soc. Am. B*, 27, 577-581.
- Kaiser, W. and Garret, C. G. B. (1961). "Two-Photon Excitation in $\text{CaF}_2: \text{Eu}^{2+}$." *Phys. Rev. Lett.*, 7(6), 229-231.
- Kamada, K., Sugino, T., Ueda, M., Tawa, K., Shimizu, Y. and Ohta, K. (1999). "Femtosecond optical Kerr study of heavy-atom effects on the third-order optical non-linearity of thiophene homologues: electronic hyperpolarizability of tellurophene." *Chem. Phys. Lett.*, 302(5), 615-620.
- Kamata, T., Fukaya, T., Kozasa, T., Matsuda, H., Mizukami, F., Tachiya, M., Ishikawa, R., Uchida, T. and Yamazaki, Y. (1995). "Third Harmonic Generation Measurements on Evaporated Thin Films of Coordination Compounds." *Nonlinear Opt.*, 13, 31-40.
- Kar, A.K., (2000). "Organic materials for optical switching." *Polym. Adv. T.*, 11(8-12), 553-559
- Karlin, K. D. and Stiefel, E. I. (2004). Eds., "Dithiolene Chemistry: Synthesis, Properties, and Applications." *Progress in Inorganic Chemistry Series*, Wiley, New York, vol. 52.
- Kato, R. (2004). "Conducting Metal Dithiolene Complexes: Structural and Electronic Properties" *Chem. Rev.*, 104(11), 5319-5346.
- Kershaw, S. (1998). "Two-photon absorption, In: Characterization Techniques and Tabulations for Organic Nonlinear Optical Materials.", M. G. Kuzyk, C. W. Dirk, Eds., *Marcel Dekker*, New York.

- Khoo, I. C., Park, J. H. and Liou, J. (2007). "All-optical switching of continuous wave, microsecond lasers with a dye-doped nematic liquid crystal." *Appl. Phys. Lett.*, 90, 151107-151109.
- Kobayashi, T., Terasaki, A., Hattori, T. and Kurokawa, K. (1988). "The application of incoherent light for the study of femtosecond-picosecond relaxation in condensed phase." *Appl. Phys. B.*, 47(2), 107-125.
- Krishna, M. B., Venkatramaiah, M., N., Venkatesan, R. and Rao, N. D. (2012). "Synthesis and structural, spectroscopic and nonlinear optical measurements of graphene oxide and its composites with metal and metal free porphyrins." *J. Mater. Chem.*, 22, 3059-3068.
- Kühlke, D. (1984). "Transient orientational grating technique for investigations of fast molecular relaxation processes." *Appl. Phys. B.*, 34(3), 129-137.
- Kürüm, U., Ceyhan, T., Elmali, A. and Bekaroğlu, Ö. (2009). "Optical limiting response by embedding copper phthalocyanine into polymer host." *Opt. Commun.*, 282(12), 2426-2430.
- Lacroix, P. G. (2001). "Second-Order Optical Nonlinearities in Coordination Chemistry: The Case of Bis(salicylaldiminato)metal Schiff Base Complexes." *Eur. J. Inorg. Chem.*, 2001(2), 339-348.
- Lacroix, P. G., Bella, S. D. and Ledoux, I. (1996). "Synthesis and Second-Order Nonlinear Optical Properties of New Copper(II), Nickel(II), and Zinc(II) Schiff-Base Complexes. Toward a Role of Inorganic Chromophores for Second Harmonic Generation." *Chem. Mater.*, 8(2), 541-545.
- Laubereau, A., von der Linde, D. and Kaiser, W. (1973). "Direct observation of the lifetime of a polariton mode in gallium phosphide." *Opt. Commun.*, 7(3), 173-175.

- Lee, H. -K., Doi, K., Kanazawa, A., Shiono, T., Ikeda, T., Fujisawa, T., Aizawa, M. and Lee, B. (2000). "Light-scattering-mode optical switching and image storage in polymer/liquid crystal composite films by means of photochemical phase transition." *Polymer*, 41, 1757–1763.
- Lenoble, G., Lacroix, P. G., Daran, J. C., Bella, S. D. and Nakatani, K. (1998). "Syntheses, Crystal Structures, and NLO Properties of New Chiral Inorganic Chromophores for Second-Harmonic Generation." *Inorg. Chem.*, 37(9), 2158–2165.
- Li, C., Zhang, L., Wang, R., Song, Y. and Wang, Y. J. (1994). "Dynamics of reverse saturable absorption and all-optical switching in C60." *J. Opt. Soc. Am. B.*, 11(8), 1356–1360.
- Li, C., Zhang, L., Yang, M., Wang, H. and Wang, Y. (1994). "Dynamic and steady-state behaviors of reverse saturable absorption in metallophthalocyanine." *Phys. Rev. A.*, 49(2), 1149–1157.
- Liu, M.O., Tai, C.-H., Hu, A. T. and Wei, T.-H. (2004). "Reverse saturable absorption of lanthanide bisphthalocyanines and their application for optical switches." *J. Organomet. Chem.* 689, 2138–2143.
- Liu, X., Guo, S., Wang, H. and Hou L. (2001). "Theoretical study on the closed aperture Z-scan curves in the materials with nonlinear refraction and strong nonlinear absorption." *Opt. Commun.*, 197(4), 431-437.
- Liu, Y., Pu, J. and Qi, H. (2008). "Investigation on z-scan experiment by use of partially coherent beams." *Opt. Commun.*, 281(2), 326–330.
- Liyanage, P. S., de Silva, R. M. and de Silva, K. M. N. (2003). "Nonlinear optical (NLO) properties of novel organometallic complexes: high accuracy density functional theory (DFT) calculations." *J. Mol. Struct. THEOCHEM*, 639(1), 195-201.

- Long, N. J.(1995). "Organometallic compounds for nonlinear optics - the search for en-light-enment." *Angew. Chem. Int. Edit.*, 34, 21-38.
- Luo, Y., She, W., Wu, S., Zeng, F. and Yao, S. (2005). "Improvement of all-optical switching effect based on azobenzene-containing polymer films." *Appl. Phys. B*, 80, 77–80.
- MacKenzie, H., Hagan, D. and Al-Attar, H. (1986). "Four-wave mixing in indium antimonide." *IEEE J. Quantum. Electron.*, 22(8), 1328-1340.
- Maksymov, I. S., Marsal, L. F., Pallares, J. (2007). "Modeling of two-photon absorption in nonlinear photonic crystal all-optical switch." *Opt. Commun.*, 269, 137–141.
- Marder, S. R., Torruellas, W. E., Blanchard-Desce, M., Ricci, V., Stegeman, G. I., Gilmour, S., Br´edas, J. L., Li, J., Bublitz, G. U. and Boxer, S. G. (1997). "Large molecular third-order optical nonlinearities in polarized carotenoids." *Science*, 276 (5316), 1233–1236.
- Mata, J. A.; Peris, E.; Asselberghs, I.; Van Boxel, R.; Persoons, A. (2001). "Syntheses, characterization and second-order nonlinear optical behavior of new ferrocenyl-terminated phenylethenyl oligomers with a pendant nitro group." *New J. Chem.*, 25, 299-304.
- Mata, J. A.; Peris, E.; Asselberghs, I.; Van Boxel, R.; Persoons, A. (2001). "Large second-order NLO properties of new conjugated oligomers with a pendant ferrocenyl and an end-capped pyridine." *New J. Chem.* 2001, 25, 1043-1046.
- Mata, J., Uriel, S., Peris, E., Llusar, R., Houbrechts, S. and Persoons, A. (1998). "Synthesis and characterization of new ferrocenyl heterobimetallic compounds with high NLO responses." *J. Organomet. Chem.*, 562(2), 197-202.
- Matsubayashi, G., Nakano, M. and Tamura, H. (2002). "Structures and properties of assembled oxidized metal complexes with C₈H₄S₈ and related sulfur-rich dithiolate ligands." *Coord. Chem. Rev.*, 226(1), 143-151.

- McDonagh, A. M., Lucas, N. T., Cifuentes, M. P., Humphrey, M. G., Houbrechts, S. and Persoons, A. (2000). "Organometallic complexes for nonlinear optics: Part 20. Syntheses and molecular quadratic hyperpolarizabilities of alkynyl complexes derived from (E)-4,4'-HC=CC₆H₄N=NC₆H₄NO₂." *J. Organomet.Chem.*, 605(2), 193-201.
- Meng, X. R., Song, Y. L., Hou, H. W., Fan, Y. T., Li, G. and Zhu, Y. (2003). "Novel Pb and Zn Coordination Polymers: Synthesis, Molecular Structures and Third-Order Nonlinear Optical Properties." *Inorg. Chem.*, 42(4), 1306-1315.
- Mingaleev S. F., Miroshnichenko, A. E., Kivshar, Y. S. and Busch, K. (2006). "All-optical switching, bistability and slow-light transmission in photonic crystal waveguide-resonator structures." *Phys. Rev. E.*, 74(4), 046603-046617.
- Miroshnichenko, A. E., Brasselet, E. and Kivshar, Y. S. (2008), "All-optical switching and multistability in photonic structures with liquid crystal defects." *Appl. Phys. Lett.*, 92, 253306(1)-253306(3).
- Myers, L. K., Langhoff, C. and Thompson, M. E. (1992). "Cubic nonlinear optical properties of Group 4 metallocene halide and acetylide complexes." *J. Am. Chem. Soc.*, 114 (19), 7560–7561.
- Nalwa, H. S. (1991). "Organometallic materials for nonlinear optics." *Appl. Organomet. Chem.*, 5(5), 349–377.
- Nalwa, H. S. and Miyata, S. (1997). "Nonlinear Optics of Organic Molecules and Polymers." CRC Press, Boca Raton, Florida.
- O'Flaherty, S. M., Hold, S.V., Cook, M.J., Torres, T., Chen, Y., Hanack, M. and Blau, W.J. (2003). "Molecular Engineering of Peripherally And Axially Modified Phthalocyanines for Optical Limiting and Nonlinear Optics." *Adv. Mat.*, 15(1), 19–32.

- Orpen, A. G. and Connelly, N. G. (1985). "Structural evidence for the participation of P–X σ^* orbitals in metal–PX₃ bonding." *J. Chem. Soc., Chem. Commun.*, (19), 1310-1311.
- Ostuni, R., Larciprete, M.C., Leahu, G., Belardini, A., Sibilia, C. Bertolotti M. (2007). "Optical limiting behavior of zinc phthalocyanines in polymeric matrix." *J. Appl. Phys.* 101, 033116-033120.
- Pacchioni, G. and Bagus, P. S. (1992). "Metal-phosphine bonding revisited. .sigma.-Basicity, .pi.-acidity, and the role of phosphorus d orbitals in zerovalent metal-phosphine complexes." *Inorg. Chem.*, 31(21) 4391-4398.
- Padilha, L. A., Neves, A. A. R., Rodriguez, E., Cesar, C. L., Barbosa, L. C. and Cruz, C. H. B., (2005). "Ultrafast optical switching with CdTe nanocrystals in a glass matrix." *Appl. Phys. Lett.*, 86, 161111(1)- 161111(3).
- Pang, Y., Samoc, M. and Prasad, P. N. (1991). "Third-order nonlinearity and two-photon-induced molecular dynamics: Femtosecond time-resolved transient absorption, Kerr gate, and degenerate four-wave mixing studies in poly (*p*-phenylene vinylene)/sol-gel silica film." *J. Chem. Phys.*, 94(8), 5282-5290.
- Pepper, D. M. (1982). "Nonlinear optical phase conjugation," *Opt. Eng.* 21, 156-183.
- Perry, J. W. (1997). "Organic and metal-containing reverse saturable absorbers for optical limiters," *Nonlinear Optics of Organic Molecules and Polymers*, H.S. Nalwa and S. Miyata, eds., CRC Press, Boca Raton.
- Perry, J. W., Mansour, K., Lee, I. -Y. S., Wu, X. -L., Bedworth, P. V., Chen, C. -T., Ng, D., Marder, S.R., Miles, P., Wada, T., Tian, M. and Sasabe, H. (1996). "Organic Optical Limiter with a Strong Nonlinear Absorptive Response." *Science*, 273(5281), 1533-1536.
- Perry, J. W., Stiegman, A. E., Marder, S. R. and Coulter, D. R. (1989). *Organic Materials for Nonlinear Optics*, The Royal Society of Chemistry, London.

- Philip, R., Ravikanth, M. and Ravindra Kumar G. (1999). "Studies of third order optical nonlinearity in iron (III) phthalocyanine μ -oxo dimers using picosecond four-wave mixing, *Opt. Commun.*, 165(1), 91-97.
- Piccione, B., Cho, C. -H., Vugt, L. K. V. and Agarwal, R. (2012). "All-optical active switching in individual semiconductor nanowires." *Nat. Nanotechnol.*, 7, 640-645.
- Polin, J. (1994). "*Molecular Electronics and Molecular Electronic Devices.*" K. Sienicki, eds. CRC Press, Boca Raton, Florida.
- Poornesh, P., Pramod K. H., Umesh, G., Manjunatha, M. G., Manjunatha, K. B. and Adhikari, A. V. (2010). "Nonlinear optical and optical power limiting studies on a new thiophene-based conjugated polymer in solution and solid PMMA matrix." *Opt. Laser Technol.*, 42(1), 230-236.
- Poornima, S., Liyanage, Rohini, M., de Silva, Nalin de Silva, K.M. (2003). "Nonlinear optical (NLO) properties of novel organometallic complexes: high accuracy density functional theory (DFT) calculations." *J. Mol. Struct. (Theochem)*, 639(1-3), 195-201.
- Powell, C. E., Morrall, J. P., Ward, S. A., Cifuentes, M. P., Notaras, E. G. A., Samoc, M. and Humphrey, M. G. (2004). "Dispersion of the Third-Order Nonlinear Optical Properties of an Organometallic Dendrimer." *J. Am. Chem. Soc.*, 126, 12234-12235.
- Prasad, P.N. and Williams, D. J. (1992). *Introduction to Nonlinear Optical Effects in Molecules and Polymers*, Wiley, New York.
- Przhonska, O. V., Lim, J., Hagan, D. J. and Van Stryland, E. W. (1998). "Nonlinear light absorption of polymethine dyes in liquid and solid media." *J. Opt. Soc. Am. B.*, 15(2), 802-809.

- Qian, Y., Cai, M., Wang, S., Yi, Y., Shuai, Z. and Yang, G. (2010). "Synthesis and third-order optical nonlinearities of nickel complexes of 8-hydroxyquinoline derivatives." *Opt. Commun.*, 283(10), 2228–2233.
- Rhee, B. K., Byun, J. S. and Van Stryland, E.W. (1996). "Z scan using circularly symmetric beams." *J. Opt. Soc. Am. B.*, 13(12), 2720–2723.
- Rojo, G., Fernando Agulló-López, José A. Campo, José V. Heras, and Mercedes Cano. (1999). "Third-Order Nonlinear Optical Properties of Donor–Acceptor Organometallic Compounds in Films and Solution." *J. Phys. Chem. B.*, 103 (50), 11016–11020.
- Roy, S. and Yadav, C. (2011). "All-optical ultrafast logic gates based on saturable to reverse saturable absorption transition in CuPc-doped PMMA thin films," *Opt. Commun.*, 284(19), 4435–4440.
- Roy, S., Prasad, M. Topolancik, J. and Vollmer, F. (2010), "All-optical switching with bacteriorhodopsin protein coated microcavities and its application to low power computing circuits." *J. Appl. Phys.* 107, 053115(1) - 053115(9).
- Roy, S., Sharma, P., Dharmadhikari, A.K., Mathur, D. (2004). "All-optical switching with bacteriorhodopsin." *Opt. Commun.*, 237(4–6), 251-256.
- Samoc, A., Samoc, M., Woodruff, M. and Luther-Davies, B. (1995). "Tuning the properties of poly(*p*-phenylenevinylene) for use in all-optical switching." *Opt. Lett.*, 20(11), 1241-1243.
- Samoc, M. and Prasad, P. N. (1989). "Dynamics of resonant third-order optical nonlinearity in perylene tetracarboxylic dianhydride studied by monitoring first- and second-order diffractions in subpicosecond degenerate four-wave mixing." *J. Chem. Phys.*, 91(11), 6643- 6649.
- Samoc, M., Corkery, T.C., McDonagh, A. M., Cifuentes, M. P. and Humphrey, M. G. (2011), "Organometallic Complexes for Non-linear Optics. 49.* Third-Order

- Non-linear Optical Spectral Dependence Studies of Arylalkynylruthenium Dendrimers." *Aust. J. Chem.*, 64(9), 1269-1273.
- Samoc, M., Dalton, G. T., Gladysz, J. A., Zheng, Q., Velkov, Y., Ågren, H., Norman, P. and Humphrey, M.G. (2008). "Cubic Nonlinear Optical Properties of Platinum-Terminated Polyynediyl Chains." *Inorg. Chem.*, 47(21), 9946–9957.
- Samoc, M., Samoc, A., Dalton, G., Cifuentes, M., Humphrey, M., Fleitz, P. (2012). "Two-photon Absorption Spectra and Dispersion of the Complex Cubic Hyperpolarizability γ in Organic and Organometallic Chromophores." *Multiphoton Processes in Organic Materials and Their Application*, Rau, I. and Kajzar, F., eds., *Old City Publishing Inc.*, Philadelphia.
- Sampath Kumar, H. C., Bhat, B. R. Rudresha, B. J., Ravindra, R. and Philip, R. (2010). "Synthesis, characterization of N,N'-bis(2-hydroxynaphthalidene)phenylene-1,2-diamine with M(II)(M = Ni, Zn and Fe) Schiff-base complexes and their non-linear optical studies by Z-scan technique." *Chem. Phys. Lett.*, 494(1), 95-99.
- Schmid, W., Vogtmann, T. and Schwoerer, M. (1995). "A modulation technique for measuring the optical susceptibility $\chi^{(5)}$ by degenerate four-wave mixing." *Opt. Commun.*, 121(1), 55-62.
- Schrauzer, G. N. and Mayweg, V. (1962). "Reaction of Diphenylacetylene with Nickel Sulfides." *J. Am. Chem. Soc.*, 84(16), 3221.
- Schwich, T., Cifuentes, M. P., Gugger, P. A., Samoc, M. and Humphrey, M. G. (2011). "Electronic, Molecular Weight, Molecular Volume, and Financial Cost-Scaling and Comparison of Two-Photon Absorption Efficiency in Disparate Molecules. A Response to "Correspondence on "Organometallic Complexes for Nonlinear Optics. 45. Dispersion of the Third-Order Nonlinear Optical Properties of Triphenylamine-Cored Alkynylruthenium Dendrimers." Increasing the

-
- Nonlinear Response by Two Orders of Magnitude.” *Adv. Mat.*, 23 (12), 1433-1435.
- Sharma, P., Roy, S. and Singh, C. P. (2005). “Dynamics of all-optical switching in polymethine dye molecules.” *Thin Solid Films*, 477(1), 42–47.
- Shen, Y. (1986). “Basic considerations of four-wave mixing and dynamic gratings.” *IEEE J. Quantum. Electron.*, 22(8), 1196-1203.
- Shen, Y. R. (1984). *The principle of nonlinear optics*, Wiley, New York.
- Shirk, J. S., Lindle, J. R., Bartoli, F. J. and Boyle, M. E. (1992). “Third-order optical nonlinearities of bis(phthalocyanines).” *J. Phys. Chem.*, 96(14), 5847-5852.
- Singh, B. P., Prasad, P. N. and Karasz, F. E. (1988). “Third-order non-linear optical properties of oriented films of poly(p-phenylene vinylene) investigated by femtosecond degenerate four wave mixing.” *Polymer*, 29(11), 1940-1942.
- Singh, B. P., Samoc, M., Nalwa, H. S. and Prasad, P. N. (1990). “Resonant third-order nonlinear optical properties of poly(3-dodecylthiophene).” *J. Chem. Phys.*, 92(5), 2756-2771.
- Singh, C. P., Bindra, K. S., Jain, B. and Oak, S. M. (2005). “All-optical switching characteristics of metalloporphyrins.” *Opt. Commun.*, 245(1), 407–414.
- Singh, C.P., Kulshrestha, K. and Roy,S. (2006). “High-contrast all-optical switching with Pt:ethynyl complex.” *Optik*, 117, 499–504.
- Sio, L. D., Veltri, A., Umeton, C., Serak, S. and Tabiryan, N. (2008). “All-optical switching of holographic gratings made of polymer-liquid crystal-polymer slices containing azo-compounds.” *Appl. Phys. Lett.*, 93, 181115(1)-181115(2).

- Slepkov A. P., Hegmann, F. A., Zhao, Y., Tykwinski, R. R. and Kamada, K. (2002). Ultrafast optical Kerr effect measurements of third-order nonlinearities in cross-conjugated *iso*-polydiacetylene oligomers." *J. Chem. Phys.*, 116 (9), 3834-3840.
- Soto, F. C., Martinez, A., Garcia, J., Ramos, F., Sanchis, P., Blasco, J., Marti, J. (2004). "All-optical switching structure based on a photonic crystal directional coupler." *Opt. Express*, 12(1), 161-167.
- Stephenson, T. A. and Wilkinson, G. (1966). "New complexes of ruthenium (II) and (III) with triphenylphosphine, triphenylarsine, trichlorostannate, pyridine and other ligands." *J. Inorg. Nucl. Chem.*, 28(4), 945-956.
- Sun, W., Byeon, C. C., McKerns, M. M., Lawson, C. M., Dong, S. and Wang, D. (1999). "Characterization of the third-order nonlinearity of $[(\text{CH}_3\text{-TXP})\text{Cd}]\text{Cl}$." *Proc.SPIE*, 3798, 107-116.
- Sun, W., Wu, Z. X., Yang, Q. Z., Wu, L. Z. and Tung, C. H. (2003). "Reverse saturable absorption of platinum ter/bipyridyl polyphenylacetylide complexes." *Appl. Phys. Lett.*, 82, 850 -852.(2003).
- Sun, Y. P. and Riggs, J. E. (1999). "Organic and inorganic optical limiting materials. From fullerenes to nanoparticles." *Int. Rev. Phys. Chem.* 18, 43-90.
- Sutherland, R. L. (2003). *Handbook of nonlinear optics*, Marcel Dekker, New York.
- Sutherland, R.L., Brant, M.C., Heinrichs, J., Rogers, J.E., Slagle, J.E., McLean, D.G., and Fleitz, Paul A. (2005). "Excited-state characterization and effective three-photon absorption model of two-photon-induced excited-state absorption in organic pushpull charge-transfer chromophores." *J. Opt. Soc. Am. B.*, 22(9), 1939-1948.
- Tedim, J., Patrício, S., Bessada, R., Morais, R., Sousa, C., Marques, M. B. and Freire, C. (2006). "Third-Order Nonlinear Optical Properties of DA-salen-Type Nickel (II) and Copper (II) Complexes." *Eur. J. Inorg. Chem.*, 17, 3425-3433.

- Tekin, S., Kürüm, U., Durmuş, U. M., Yaglioglu, H. G., Nyokong, T. and Elmali, A. (2010). "Optical limiting properties of zinc phthalocyanines in solution and solid PMMA composite films." *Opt. Commun.*, 283(23), 4749-4753.
- Terazima, M., Shimizu, H. and Osuka, A. (1997). "The third-order nonlinear optical properties of porphyrin oligomers." *J. Appl. Phys.*, 81, 2946-2951.
- Tian, Y. P., Zhang, M. L., Hu, Z. J., Hu, H. M., Wu, J. Y., Zhang, X. J. and Zhang, S. Y. (2005). "Synthesis, crystal structure and NLO properties of a novel ruthenium(II) complex with unusual coordination mode." *Transition Met. Chem.*, 30(7), 778-785.
- Trebino, R., Gustafson, E. K. and Siegman, A. E. (1986). "Fourth-order partial-coherence effects in the formation of integrated-intensity gratings with pulsed light sources." *J. Opt. Soc. Am. B.*, 3(10), 1295-1304.
- Tsigaridas, G., Fakis, M., Polyzos, I., Tsibouri, M., Persephonis, P. and Giznnetad, V. (2003). "Z-scan analysis for near-Gaussian beams through Hermite–Gaussian decomposition." *J. Opt. Soc. Am. B.*, 20(4), 670–676.
- Tutt L. W. and Boggess T. F. (1993). "A review of optical limiting mechanisms and devices using organics, fullerenes, semiconductors and other materials." *Prog. Quantum Electron.*, 17(4), 299-338.
- Van Stryland E. W., Vanherzeele, H., Woodall, M. A., Soileau, M. J., Smirl, A. L., Guha, S. and Boggess, T. F. (1985). "Two photon absorption, nonlinear refraction, and optical limiting in semiconductors." *Opt. Eng.*, 24, 613-623.
- Van Stryland, E. W. and Sheik-Bahae, M. (1998). "Z-scan measurements of optical nonlinearities," *Characterization techniques and tabulations for organic nonlinear materials*, M. Kuzyk and C. Dirk, eds. Marcel Dekker Inc., New York.
- Villaverde, A.B. (1980). "Saturable absorption and self-focusing effects in molecular iodine vapour." *J. Phys. B: At. Mol. Phys.*, 13(9), 1817-1822.

- Vivas, M.G. Piovesan, E. Silva, D.L. Cooper, T.M., Boni, L. D. and Mendonca, C. R. (2011). "Broadband three-photon absorption spectra of platinum acetylide complexes." *Opt. Mater. Express*, 1(4), 700-710.
- Vlcek Jr., A. (2000). "The life and times of excited states of organometallic and coordination compounds." *Coordin. Chem. Rev.*, 200, 933-977.
- Vogel, A. I. (1989). *Textbook of Practical Organic Chemistry*, 5th ed., Longman, London.
- Walser, A. D., Coskun, G. and Dorsinville, R. (1998). *Electrical and Optical Polymer Systems*, D.L. Wise, G.E. Wnek, D.J. Trantolo, T.M. Cooper and J.D. Gresser, Marcel Deccer Inc., New York.
- Wang, H., Su, H., Qian, H., Wang, Z., Wang, X. and Xia, A. (2010). "Structure-dependent all-optical switching in graphene-nanoribbon-like molecules: fully conjugated tri(perylene bisimides)." *J. Phys. Chem. A.*, 114(34), 9130-9135.
- Wang, S., Huang, W., Zhang, T., Yang, H. Gong, Q., Okuma, Y., Horikiri, M. and Miura, Y.F. (1999). "Third-order nonlinear optical properties of didodecyldimethylammonium-Au(dmit)₂." *Appl. Phys. Lett.*, 75(13), 1845-1847.
- Wang, X. Q., Ren, Q., Sun, J., Fan, H. L., Li, T. B., Liu, X. T., Zhang, G. H., Zhu, L. Y. and Xu, D. (2011). "Preparation, crystal growth, characterization, thermal and third-order nonlinear optical properties of ethyltriphenylphosphonium bis(2-thioxo-1,3-dithiole-4,5-dithiolato)aurate(III) for all-optical switching." *J. Cryst. Growth*, 324(1), 124-129.
- Weaire, D., Wherrett, B. S., Miller, D. A. B. and Smith, S. D. (1974). "Effect of low-power nonlinear refraction on laser-beam propagation in InSb." *Opt. Lett.*, 4(10), 331-333.

- Wherrett, B., Smirl, A. and Boggess, T. (1983). "Theory of degenerate four-wave mixing in picosecond excitation-probe experiments." *IEEE J. Quantum. Electron.*, 19(4), 680-690.
- Whittall, I. R., Cifuentes, M. P., Humphrey, M. G., Luther-Davies, B., Samoc, M., Houbrechts, S., Persoons, A., Heath, G. A. and Bogsanyi, D. (1997). "Organometallic Complexes for Nonlinear Optics 11. Molecular Quadratic and Cubic Hyperpolarizabilities of Systematically Varied (Cyclopentadienyl) (triphenylphosphine) nickel σ -Arylacetylides." *Organometallics*, 16(12), 2631-2637.
- Whittall, I. R., Humphrey, M. G., Persoons, A. and Houbrechts, S. (1996). "Organometallic Complexes for Nonlinear Optics 3. Molecular Quadratic Hyperpolarizabilities of Ene-, Imine-, and Azo-Linked Ruthenium σ -Acetylides: X-ray Crystal Structure of Ru(*E*)-4,4'-C \equiv CC₆H₄CH=CHC₆H₄NO₂(PPh₃)₂(η -C₅H₅)." *Organometallics*, 15(7), 1935-1941.
- Whittall, I. R., McDonagh, A. M., Humphrey, M. G. and Samoc, M. (1999). "Organometallic complexes in nonlinear optics II: Third-order nonlinearities and optical limiting studies." *Adv. Organomet. Chem.*, 43, 349-405.
- Whittall, I. R., McDonagh, A. M., Humphrey, M. G. and Samoc, M. (1998). "Organometallic complexes in nonlinear optics I: Second-order nonlinearities." *Adv. Organomet. Chem.*, 42, 291-362.
- Williams, R., Billig, E., Waters, J. H. and Gray, H. B. (1966). "The Toluenedithiolate and Maleonitriledithiolate Square-Matrix Systems." *J. Am. Chem. Soc.*, 88(1), 43-50.
- Williams, S., Rahn, L. A. and Zare, R. N. (1996). "Effects of different population, orientation, and alignment relaxation rates in resonant four wave mixing." *J. Chem. Phys.*, 104(11), 3947-3955.

- Winter, C.S., Oliver, S.N. and Rush, J.D. (1988). "n₂ Measurements on various forms of ferrocene." *Opt. Commun.*, 69(1), 45-48.
- Wood, G.L., Miller, M.J., and Mott, A.G. (1995). "Investigation of tetrabenzporphyrin by the Z-scan technique." *Opt. Lett.*, 20 (9), 973-976.
- Wu, S., Lu, M., She, W., Yan, K. and Huang, Z. (2004). "All-optical switching effect in PVK-based optoelectronic composites." *Mater. Chem. Phys.*, 83, 29–33.
- Wu, S., Luo, S., She, W., Luo, D. and Wang, H. (2003). "All-optical switching effects in poly(methyl methacrylate) composites." *React. Funct. Polym.*, 56, 83–88.
- Wu, S., Yao, S., She, W., Luo, D. and Wang, H. (2003). "All-optical switching properties of poly(methylmethacrylate) azobenzene composites." *J. Mater. Sci.*, 38, 401–405.
- Xia, T., Hagan, D. J., Sheik-Bahae, M. and Van Stryland, E. W. (1994). "Eclipsing Z-scan measurement of $\lambda/10^4$ wave-front distortion." *Opt. Lett.*, 19(5), 317–319.
- Xu, H. Y., Guang, S. Y., Xu, D., Yuan, D. Y., Bing, Y. H. and Jiang, M. H. (1996). "All-optical switching a new polydiacetylene." *Mater. Res. Bull.*, 31(4), 351-354.
- Xu, T., Chen, G., Zhang, C., Hao, Z., Xu, X. and Tian, J. (2008). "All-optical switching characteristics of ethyl red doped polymer film." *Opt. Mater.*, 30, 1349–1354.
- Xu, T., Zhang, C., Lin, Y. and Qi, S. (2008). "Study on all-optical switching characteristics of ethyl orange-doped polymer film." *Optik*, 119, 643–647.
- Yang, M., Li Y. and Hiller M. (2003). "Third-order optical nonlinearity of novel π -conjugated soluble palladium-polyynes polymers." *J. Mater. Sci. Lett.*, 22(9), 707–708.
- Yang, M., Zhang, L., Lei, Z., Ye, P., Si, J., Yang, Q. and Wang, Y. (1998). " π -conjugated soluble nickel–polyynes copolymer: Synthesis and third-order optical nonlinearity." *J. Appl. Polym. Sci.*, 70(6), 1165–1172.

- Yariv, A. (1978). "Phase conjugate optics and real-time holography." *IEEE J. Quantum Electron.*, 14(9), 650-660.
- Yariv, A. and Pepper, D. M. (1977). "Amplified reflection, phase conjugation, and oscillation in degenerate four-wave mixing." *Opt. Lett.*, 1(1), 16-18.
- Yariv, A., (1989). "*Quantum electronics.*" Wiley, New York.
- Yim, S. H., Lee, D. R., Rhee, B. K. and Kim, D. (1998). "Nonlinear absorption of Cr⁴⁺:YAG studied with lasers of different pulsewidths." *Appl. Phys. Lett.*, 73(22), 3193-3195.
- Yin, M., Li, H. P., Tang, S. H. and Ji, W. (2000). "Determination of nonlinear absorption and refraction by single Z-scan method." *Appl. Phys. B.*, 70(4), 587-591.
- YiZhong, Y., ZhenRong, S. and ZuGeng, W. (2008). "Structural dependences of the η^6 complexes of 3-amino-9-ethylcarbazole with chromium tricarbonyl fragment on third-order optical nonlinearities." *Chin. Sci. Bull.*, 53(10), 1473-1478.
- Zang, W. P., Tian, J. G., Liu, Z. B., Zhou, W. Y., Zhang, C. P. and Zhang, G.Y. (2003). "Variational analysis of Z-scan of thick medium with an elliptic Gaussian beam." *Appl. Opt.* 42(12), 2219-2225.
- Zhang, F. J., Guo, W. F., Sun, X. B., Ren, Q., Gao, Y., Yang, H. L., Zhang, G. H., Chow, Y. T. and Xu, D. (2007). "Nonlinear optical absorption of [(C₂H₅)₄N]₂Cu(dmit)₂ irradiated by picosecond and nanosecond laser pulses." *Laser Phys. Lett.*, 4(3), 230-233.
- Zhang, K., Li, J., Wang, W., Xiao, J., Yin, W. and Yu, L. (2011). "Enhancing the linear absorption and tuning the nonlinearity of TiO₂ nanowires through the incorporation of Ag nanoparticles." *Opt. Lett.*, 36 (17), 3443-3445

- Zhang, P. (2011). “Comparative Studies on the Third-Order Nonlinear Optical Properties of Three Metal-Organic Compounds” *J. Nonlinear Opt. Phys. Mater.*, 20, 229–236.
- Zhang, W. and Kuzyk, M. G. (2006). “Effect of a thin optical Kerr medium on a Laguerre–Gaussian beam.” *Appl. Phys. Lett.*, 89(10), 101103-101105.
- Zhao, M. -T., Singh, B. P. and Prasad, P. N. (1988). “A systematic study of polarizability and microscopic third-order optical nonlinearity in thiophene oligomers.” *J. Chem. Phys.*, 89(9), 5535-5541.
- Zhao, M., Cui, Y., Samoc, M., Prasad, P. N., Unroe, M. R. and Reinhardt, B. A. (1991). “Influence of two-photon absorption on third-order nonlinear optical processes as studied by degenerate four-wave mixing: The study of soluble didecyloxy substituted polyphenyls.” *J. Chem. Phys.*, 95(6), 3991-4001.
- Zhao, W. and Palffy-Muhoray, P. (1993). “Z-scan technique using top-hat beams.” *Appl. Phys. Lett.*, 63(12), 1613–1615.
- Zhu, Y. Elim, H. I., Foo, Y.-L., Yu, T., Liu, Y., Ji, W., Lee, J.-Y., Shen, Z., Wee, A. T. S., Thong, J. T. L. and Sow, C. H. (2006). “Multiwalled Carbon Nanotubes Beaded with ZnO Nanoparticles for Ultrafast Nonlinear Optical Switching.” *Adv. Mater.*, 18(5), 587–592.
- Zidan, H. M. (2003). “Electron spin resonance and ultraviolet spectral analysis of UV-irradiated PVA films filled with $MnCl_2$ and CrF_3 .” *J. Appl. Polym. Sci.*, 88(1), 104-111.

PUBLICATIONS

PUBLICATIONS**(A) Research papers in International Journals**

1. **Manjunatha K.B.**, Dileep R., G. Umesh, M. N. Satyanarayan and B. Ramachandra Bhat (2014). “All Optical Nonlinear and Switching Characteristics of a Novel Ruthenium Complex Optical Materials.” *Opt. Mater.* (Accepted).
2. **Manjunatha K.B.**, Vikas M. Shelar, Dileep R., G. Umesh, M. N. Satyanarayan and B. Ramachandra Bhat (2014). “Third-Order Nonlinear Optical, Optical Power Limiting and All-Optical Switching Studies on Palladium Complexes.” *Synth. React. Inorg. Met.-Org. Chem.*, 44(2), 282-290.
3. **Manjunatha K.B.**, Dileep R., G. Umesh and B. Ramachandra Bhat (2013). “Nonlinear optical and all-optical switching studies of novel ruthenium complex.” *Opt. Laser Technol.*, 52, 103–108.
4. **Manjunatha K. B.**, R. Dileep, G. Umesh and B. Ramachandra Bhat (2013). “Study of third-order nonlinear optical and all-optical switching properties of palladium metal–organic complex.” *Opt. Mater.*, 35, 1366–1372.
5. **Manjunatha K. B.**, R. Dileep, G. Umesh and B. Ramachandra Bhat (2013). “Nonlinear Optical and All-Optical Switching Studies of Palladium (II) Complex.” *Mater. Lett.*, 105, 173-176.
6. Laxminarayana Kamath, **Manjunatha K. B.**, Seetharam Shettigar, G. Umesh, B. Narayana, S.Samshuddin and B.K.Sarojini (2014). “Investigation of Third-Order Nonlinear and Optical Power Limiting Properties of Terphenyl Derivatives.” *Opt. Laser Technol.*, 56, 425-429.
7. Y.L.N. Murthy, K.P. Suhasini, V. Veeraiah, G. Umesh, **Manjunatha K.B.**, V. Christopher (2013). “Synthesis, characterization and evaluation of the photophysical and nonlinear optical behaviour of novel 4-substituted arylidene-2-[5-(2,6-dichlorophenyl)-3-methyl-1,2-oxazol-4-yl]-1,3-oxazol-5-ones.” *Dyes Pigments*, 99(3), 713-719.
8. Rudresha B.J., **Manjunatha K.B.**, G. Umesh and Ramachandra Bhat B. (2012). “Octupolar metal complexes for third order nonlinear optical studies.” *Chem. Phys. Lett.*, 542, 159-163.

(Note: Sl. no. 6-8 not included in the thesis)

(B) Research papers in Conference Proceedings

1. **Manjunatha K. B.**, Seetharam Shettigar, Ravindra R., G. Umesh and B. Ramachandra Bhat (2012). “Investigation of Nonlinear Optical and All-Optical Switching Properties of Novel Ruthenium Complex.” *Photonics – 2012, Optical Society of America*, TPO-45.
2. **Manjunatha K.B.**, Dileep R., Shelar Vikas M., G. Umesh, M. N. Satyanarayan and B. Ramachandra Bhat (2011). “Third-order nonlinear optical properties and optical switching of Palladium (I) Complex.” *AIP Conf. Proc., 1391, 706-708*.

(C) Research Papers presented in Conferences

1. **Manjunatha K. B.**, Seetharam Shettigar, Ravindra R., G. Umesh and B. Ramachandra Bhat (2012). “Investigation of Nonlinear Optical and All-Optical Switching Properties of Novel Ruthenium Complex.” *Photonics – 2012, International Conference on Fiber Optics and Photonics, 09-12, December, IIT Madras, Chennai*.
2. **Manjunatha K.B.**, Dileep R., Shelar Vikas M., G. Umesh, M. N. Satyanarayan and B. Ramachandra Bhat (2011). “Third-order nonlinear optical properties and optical switching of palladium (I) complex”, *Optics’11, 23-25, May, Calicut*.
3. **Manjunatha K.B.**, Dileep R., Shelar Vikas M., Hidayath Ulla, G. Umesh, M. N. Satyanarayan and B. Ramachandra Bhat (2010). “Nonlinear refractive index and reverse saturable absorption of thiolato complexes of ruthenium”, *Photonics – 2010, International Conference on Fiber Optics and Photonics, 11-15, December, IIT Guwahati, Guwahati*.
4. **Manjunatha K.B.**, Dileep R., Shelar Vikas M., G. Umesh, M. N. Satyanarayan and B. Ramachandra Bhat (2010). “Third-order nonlinear optical properties of palladium (I) complex”, *Photonics – 2010, International Conference on Fiber Optics and Photonics, 11-15, December, IIT Guwahati, Guwahati*.
5. **Manjunatha K.B.**, Dileep R., Shelar Vikas M., G. Umesh, M. N. Satyanarayan and B. Ramachandra Bhat (2010). “Nonlinear optical properties of thiolato complex of ruthenium in solution and PMMA matrix using single beam Z-scan technique” *NLS-19, Dec. 1-4, December, RRCAT, Indore*.

CURRICULUM VITAE

CURRICULUM VITAE

MANJUNATHA K.B.

Lecturer

E-mail: manjukb15@yahoo.com

Department of Physics

Mobile: +91- 9986190099

NMAM Institute of Technology

Nitte – 574 110

INDIA

OBJECTIVE

To seek a position which can give me an opportunity to serve the organization in achieving excellence, unleash my potentials and replenish a good learning experience.

EDUCATION

☉ **Ph.D in Physics (Lasers and Nonlinear optics) [2014]**

Title: “Investigation of Third-Order Nonlinear Optical and All-Optical Switching Properties of Metal-Organic Materials”

Institute: National Institute of Technology Karnataka, Surathkal, INDIA.

Advisor: Prof. G. Umesh

☉ **M.Sc. Physics with specialization in Condensed Matter Physics [2003 - 05]**

Mangalore University, Mangalore, INDIA.

☉ **B.Sc. Physics, Mathematics and Computer Science [2000 - 03]**

F.M.K.M.C. College, Madikeri, INDIA.

RESEARCH EXPERIENCE

☉ **Senior Research Fellow** [August 2011 – July 2012], Department of Physics, National Institute of Technology Karnataka, Surathkal, INDIA.

☉ **Project Scientist** [May 2007 - July 2007], Surface Engineering Division, National Aerospace Laboratories, Bangalore - 560 017, INDIA.

☉ **Project Graduate Trainee** [May 2006 - April 2007], Surface Engineering Division, National Aerospace Laboratories, Bangalore - 560 017, INDIA.

TEACHING EXPERIENCE

- **Lecturer** [August 2012-Till date], Department of Physics, NMAM Institute of Technology, Nitte, Karkala, Karnataka, INDIA.
- **Worked as PGT for Pre-University students** [June 2005 - April 2006], Bharatiya Vidya Bhavan Kodagu Vidyalaya, Madikeri, Karnataka, INDIA.
- **Taught Engineering Physics Laboratory for B.Tech students** [August 2007 - April 2010], National Institute of Technology Karnataka, Surathkal, Mangalore, Karnataka, INDIA.
- **Taught Physics Laboratory for M.Sc students** [August 2008 - April 2010], National Institute of Technology Karnataka, Surathkal, Mangalore, Karnataka, INDIA.

PRACTICAL EXPERIENCE

- Familiar in handling Q-Switched Nd: YAG Laser, He-Ne laser and skilled in setting up optical experiments using optical table and performing experiments.
- Extensive experience in setting up and performing Z-scan, DFWM and pump-probe experiments.
- Good in interfacing instruments to computer and data collection.
- Good experience in characterization of Third-Order Nonlinear Optical Materials in solution/films using Z-scan and Degenerate Four Wave Mixing technique.
- Significant experience in characterizing All-optical switching behavior of organometallics using Pump-probe technique.
- Led an effort to characterize various organic nonlinear materials for optical limiting applications.
- Involved in identifying the Second Harmonic Generation in Nonlinear Optical Crystals.
- Experience in handling vacuum coating unit, spin coating unit, pulsed laser deposition, magnetron sputtering and thermal vapor deposition.
- Experience in depositing thin films using Pulsed laser deposition and Magnetron sputtering.

- Involved in Laser Shock Peening Technique for Surface Treatment of Welded Stainless Steels using Nd-YAG laser.
- Extensive knowledge and experience in utilizing various instruments including oscilloscopes, UV-Vis spectrometer, power meters, Photomultiplier tube (PMT), optical microscope, Monochromators and Imaging Spectrometer.
- Sound knowledge in Origin, MS Word, Excel and PowerPoint.

PUBLICATIONS IN INTERNATIONAL JOURNALS

1. **Manjunatha K.B.**, Dileep R., G. Umesh, M. N. Satyanarayan and B. Ramachandra Bhat (2014). "All Optical Nonlinear and Switching Characteristics of a Novel Ruthenium Complex Optical Materials." *Opt. Mater.* (Accepted).
2. **Manjunatha K.B.**, Vikas M. Shelar, Dileep R., G. Umesh, M. N. Satyanarayan and B. Ramachandra Bhat (2014). "Third-Order Nonlinear Optical, Optical Power Limiting and All-Optical Switching Studies on Palladium Complexes." *Synth. React. Inorg. Met.-Org. Chem.*, 44(2), 282-290.
3. **Manjunatha K. B.**, R. Dileep, G. Umesh and B. Ramachandra Bhat (2013). "Study of third-order nonlinear optical and all-optical switching properties of palladium metal–organic complex." *Opt. Mater.*, 35, 1366–1372.
4. **Manjunatha K. B.**, R. Dileep, G. Umesh and B. Ramachandra Bhat (2013). "Nonlinear Optical and All-Optical Switching Studies of Palladium (II) Complex." *Mater. Lett.*, 105, 173-176.
5. **Manjunatha K.B.**, Dileep R., G. Umesh and B. Ramachandra Bhat (2013). "Nonlinear optical and all-optical switching studies of novel ruthenium complex." *Opt. Laser Technol.*, 52, 103–108.
6. **Manjunatha K.B.**, Dileep R., Shelar Vikas M., G. Umesh, M. N. Satyanarayan and B. Ramachandra Bhat (2011). "Third-order nonlinear optical properties and optical switching of Palladium (I) Complex." *AIP Conf. Proc.*, 1391, 706-708.
7. Laxminarayana Kamath, **Manjunatha K. B.**, Seetharam Shettigar, G. Umesh, B. Narayana, S.Samshuddin and B.K.Sarojini (2014). "Investigation of Third-Order Nonlinear and Optical Power Limiting Properties of Terphenyl Derivatives." *Opt. Laser Technol.*, 56, 425-429.

8. Y.L.N. Murthy, K.P. Suhasini, V. Veeraiah, G. Umesh, **Manjunatha K.B.**, V. Christopher (2013). "Synthesis, characterization and evaluation of the photophysical and nonlinear optical behaviour of novel 4-substituted arylidene-2-[5-(2,6-dichlorophenyl)-3-methyl-1,2-oxazol-4-yl]-1,3-oxazol-5-ones." *Dyes Pigments*, 99(3), 713-719.
9. Rudresha B.J., **Manjunatha K.B.**, G. Umesh and Ramachandra Bhat B. (2012). "Octupolar metal complexes for third order nonlinear optical studies." *Chem. Phys. Lett.*, 542, 159-163.
10. K. Naseema, **Manjunatha K.B.**, K.V. Sujith, G. Umesh, Balakrishna Kalluraya, Vijayalakshmi Rao (2012). "Third order optical nonlinearity and optical limiting studies of propane hydrazides." *Opt. Mater.*, 34, 1751-1757.

PRESENTATIONS IN CONFERENCES

1. **Manjunatha K. B.**, Seetharam Shettigar, Ravindra R., G. Umesh and B. Ramachandra Bhat (2012). "Investigation of Nonlinear Optical and All-Optical Switching Properties of Novel Ruthenium Complex." *Photonics – 2012, International Conference on Fiber Optics and Photonics, 09-12, December, IIT Madras, Chennai.*
2. **Manjunatha K.B.**, Dileep R., Shelar Vikas M., G. Umesh, M. N. Satyanarayan and B. Ramachandra Bhat (2011). "Third-order nonlinear optical properties and optical switching of palladium (I) complex", *Optics'11, 23-25, May, Calicut.*
3. **Manjunatha K.B.**, Dileep R., Shelar Vikas M., Hidayath Ulla, G. Umesh, M. N. Satyanarayan and B. Ramachandra Bhat (2010). "Nonlinear refractive index and reverse saturable absorption of thiolato complexes of ruthenium", *Photonics – 2010, International Conference on Fiber Optics and Photonics, 11-15, December, IIT Guwahati, Guwahati.*
4. **Manjunatha K.B.**, Dileep R., Shelar Vikas M., G. Umesh, M. N. Satyanarayan and B. Ramachandra Bhat (2010). "Third-order nonlinear optical properties of palladium (I) complex", *Photonics – 2010, International Conference on Fiber Optics and Photonics, 11-15, December, IIT Guwahati, Guwahati.*

5. **Manjunatha K.B.**, Dileep R., Shelar Vikas M., G. Umesh, M. N. Satyanarayan and B. Ramachandra Bhat (2010). “Nonlinear optical properties of thiolato complex of ruthenium in solution and PMMA matrix using single beam Z-scan technique” *NLS-19*, Dec. 1-4, December, RRCAT, Indore.

WORKSHOPS AND SEMINARS ATTENDED

- Attended one day symposium on “Recent Advances in Photonics”, March 29, 2011. CAMP, Manipal University, Manipal, INDIA.
- Participated the “Workshop on Experimental Techniques in Nonlinear Optics”, January 19-20, 2011, Raman Research Institute, Bangalore, INDIA.
- Attended one day symposium on “Laser Technology and Photonics”, March 20, 2010. CAMP, Manipal University, Manipal, INDIA.
- Participated the annual photonics workshop on “Quantum Optics”, February 27-28, 2010, CUSAT, Kochi, INDIA.
- Attended one day discussion meeting on “Recent Advances in Photonics”, April 11, 2009. CAMP, Manipal University, Manipal, INDIA.
- Participated the national seminar on “Photonic Polymers: Materials, Devices and Applications”, April 3-4, 2008, BITS, Pilani, INDIA.

PERSONAL INFORMATION

Gender : Male
Marital Status : Married
Date of Birth : 15.11.1982
Residential Address : Door No. 13/117, Lakshmi Nilaya, Gowli Street,
Madikeri – 571201, Karnataka, INDIA.

DECLARATION

I hereby declare that all the above details are true to the best of knowledge and belief.

Place: NITK, Surathkal

Yours faithfully

Date: 28-2-2014

(Manjunatha K.B.)

REFERENCES

1. **Prof. G. Umesh**, Department of Physics, National Institute of Technology Karnataka, Surathkal (NITK), Mangalore -575025, INDIA. Email: umesh52@gmail.com Phone No. 9901184376.
2. **Dr. Harish C. Barshilia**, Scientist G, Surface Engineering Division, National Aerospace Laboratories (NAL), Kodihalli campus, Bangalore - 560 017, INDIA. Email: harish@nal.res.in Phone No. +91- 80 - 25086494.
3. **Dr. M. N. Satyanarayan**, Associate Professor, Department of Physics, National Institute of Technology Karnataka (NITK), Surathkal, Mangalore - 575025, INDIA. Email: mn.satyanarayan@gmail.com Phone No. 9686146138.